Molecular weight effects on crystallization of polypropylene

By

Ismael Amer

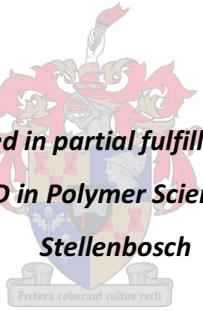

Dissertation is presented in partial fulfillment of the requirements for the degree of PhD in Polymer Science at the University of Stellenbosch

Promoter: Prof A.J. van Reenen

Department of Chemistry and Polymer Science

March 2011

Stellenbosch University http://scholar.sun.ac.za

DECLARATION

I, the undersigned hereby declare that the work in this thesis is my own original work and that I have not previously in its entirety or in part submitted it at any university for a degree.

Signature:……

Date:…….

Stellenbosch University http://scholar.sun.ac.za

Abstract

The crystallization of polyolefins is an important parameter in determining the properties of such materials. The crystallization phenomenon generally depends on the molecular symmetry (tacticity) and molecular weight of the material. In this study, a series of polypropylenes was prepared using heterogeneous $MgCl_2$-supported Ziegler catalysts with two different external donors, diphenyldimethoxysilane (DPDMS) and methyl-phenyl-dimethoxysilane (MPDMS), and two different homogeneous metallocene catalysts, *rac*-ethylene-bis(indenyl) zirconium dichloride, $Et(Ind)_2ZrCl_2$ (EI), and *rac*-ethylene-bis(4,5,6,7-tetrahydro-1-indenyl) zirconium dichloride, $Et(H4Ind)_2ZrCl_2$ (EI(4H)). Molecular hydrogen was used as terminating agent.

In order to establish a correlation between the molecular weight and the crystallization of these polymers, fractionation of the materials according to crystallizability was performed by means of temperature rising elution fractionation (TREF). This affords the opportunity of blending materials of different molecular weights but similar symmetry.

These materials were characterized using various analytical techniques: differential scanning calorimetry (DSC), wide-angle X-ray diffraction (WAXD), ^{13}C nuclear magnetic resonance spectroscopy (^{13}C-NMR), high temperature gel permeation chromatography (HT-GPC) and Fourier-transform infrared spectroscopy (FT-IR).

DSC was used to study the bulk crystallization of different polypropylene blends, most of which showed only one melting peak. The latter is usually associated with a high degree of cocrystallization. Turbidity analysis of the different polypropylene polymers, obtained using solution crystallization analysis by laser light scattering (SCALLS), provided good crystallization information – similar to that provided by crystallization analysis fractionation (CRYSTAF) and TREF. It was also possible to differentiate between polypropylenes with similar chemical structure but different tacticity and molecular weight. SCALLS results also showed that the blends of different isotactic polypropylene polymers were miscible and cocrystallization had occurred, whereas, the blends of syndiotactic polypropylene and different isotactic polypropylenes were not miscible and some interaction between phases had occurred.

Optical microcopy (OM) and scanning electronic microscopy (SEM) were used to study the morphological properties of different isotactic polypropylenes. Results revealed a well-defined and large spherulitic morphology of mixed $\alpha 1$ (disordered) and $\alpha 2$ (ordered) crystal

Stellenbosch University http://scholar.sun.ac.za

form structures. OM and SEM images also clearly showed an effect of molecular weight and tacticity on the crystal structure of the different polypropylene samples.

Finally, various homopolymers and blends were studied to investigate the effect of molecular weight on the mechanical properties of these materials. This was done using microhardness testing and dynamic mechanical analysis.

Stellenbosch University http://scholar.sun.ac.za

Opsomming

Die kristallisasie van poliolefiene is ‘n belangrike faktor wat die eienskappe van hierdie tipe materiale bepaal. In die algemeen hang kristallisasie af van die molekulêre simmetrie (taktisiteit) en molekulêre massa van die materiaal. ‘n Reeks polipropilene is berei deur gebruik te maak van heterogene $MgCl_2$-ondersteunde Ziegler-kataliste met twee verskillende elektron donors, difenieldimetoksisilaan (DPDMS) en metielfenieldimetoksisilaan (MPDMS), en twee verskillende homogene metalloseenkataliste, *rac*-etileen-bis(indeniel) sirkoniumdichloried, $Et(Ind)_2ZrCl_2$ (EI), en *rac*-etileen-bis(4,5,6,7-tetrahidro-1-indeniel) sirkoniumdichloried, $Et(H4Ind)_2ZrCl_2$ (EI(4H)). Molekulêre waterstof is gebruik as termineringssagent.

Ten einde ‘n verband te bepaal tussen die molekulêre massa en kristallisasie van hierdie polimere is hulle gefraksioneer op die basis van hulle kristallisseerbaarheid deur gebruik te maak van temperatuurstyging-elueringsfraksionering (TREF). Deur hierdie tegniek verkry ons materiale van verskillende molekulêre massa maar met dieselfde taktisiteit wat ons kan vermeng.

Verskeie tegnieke is gebruik om hierdie materiale te karakteriseer: differensiële skandeerkalorometrie (DSC), wyehoek X-straal diffraksie (WAXS), ^{13}C-kernmagnetiese resonansspektroskopie (^{13}C-KMR), hoë-temperatuur gelpermeasiechromotagrafie (HT-GPC) en Fourier-transform-infrarooispektroskopie (FT-IR).

DSC is gebruik om die vaste-toestand kristallisasie van verskeie vermengde polipropilene te bestudeer., en net een smeltpunt is in meeste gevalle waargeneem. Laasgenoemde word gewoonlik verbind met ‘n hoë mate van kokristallisasie. Oplossingkristallisasie analise, dmv laserligverstrooiing (SCALLS), is gebruik om die turbiditeit van die verskillende polipropileen kopolimeervermengings te bepaal. Goeie inligting aangaande die kristallisasie in oplossing – soortgelyk aan dié wat dmv die kristallisasie-analise-fraksioneringstegniek (CRYSTAF) en TREF bepaal is, is verkry. Dit was ook moontlik om te onderskei tussen polipropilene met soortgelyke chemiese strukture maar verskillende taktisiteit en molekulêre massas. SCALLS data het ook getoon dat die vermengings van verskeie isotaktiese polipropileen polimere versoenbaar was en dat kokristallisasie plaasgevind het, terwyl vermengings van sindiotaktiese polipropileen en verskeie isotaktiese polipropilene nie versoenbaar was nie en dat ‘n mate van fase-skeiding plaasgevind het.

Optiese mikroskopie (OM) en skandeer-elektronmikroskopie (SEM) is gebruik om die morfologiese eienskappe van verskillende isotaktiese polipropilene te bepaal. Goed gedefineerde

Stellenbosch University http://scholar.sun.ac.za

en groot sferulitiese morfologie van gemengde $\alpha 1$ (onordelike struktuur) en $\alpha 2$ (ordelike struktuur) kristal-strukture is waargeneem.

OM en SEM beelde het ook gewys dat molekulêre massa en taktisiteit ‘n effek het op die kristalstruktuur van die verskillende polipropileenmonsters.

Laastens is die meganiese eienskappe van ‘n verskeidenheid homopolimere en vermengde materiale bestudeer, deur gebruik te maak van mikro-hardheid metings en dinamies-meganiese analise (DMA).

Stellenbosch University http://scholar.sun.ac.za

Dedicated to:

My Mother, Aisha

and

My Father, Salem

For their love, support and encouragement and
for giving me the opportunities they didn't have.

Stellenbosch University http://scholar.sun.ac.za

ACKNOWLEDGEMENTS

I would like to thank Allah/God for giving me strength, health, opportunity and courage to face my reality. I thank him also for blessing me.

I cordially appreciate my study leader, Prof. Albert J. Van Reenen for his support, advice, and guidance throughout this work. I really appreciate his time and concern.

I sincerely thank the International Centre for Macromolecular Chemistry and Technology in Libya for financial support and encouragement.

I am grateful to Dr. M. J. Hurndall, for her assistance and advice on the proofreading of this thesis.

I also would like to express my thanks to all the members of our polyolefins research group at Institute of Polymer Science in Stellenbosch University for their friendship, fellowship, assistance, helpful suggestions, support and encouragement.

My appreciation also extended to the people who kindly did my measurements and analysis.

Lastly and most of all, there are not enough words to thank my family for their continuous love, strong support and unlimited encouragement that I have received over the years. Without them none of this would have been possible. My appreciation is also expressed to all my dear and wonderful friends for their friendship, help and support.

Stellenbosch University http://scholar.sun.ac.za

List of contents

Stellenbosch University http://scholar.sun.ac.za

CHAPTER 3: Fractionation and crystallization of isotactic polypropylenes prepared using a heterogeneous transition metal catalysts

Stellenbosch University http://scholar.sun.ac.za

CHAPTER 4: Fractionation and crystallization of isotactic polypropylenes prepared using homogenous metallocene catalysts

Stellenbosch University http://scholar.sun.ac.za

CHAPTER 5: Use of DSC and SCALLS for studying the bulk and solution crystallization of different polypropylenes

Stellenbosch University http://scholar.sun.ac.za

CHAPTER 6: Morphological and mechanical properties of polypropylene and polypropylene blends

CHAPTER 7: Synopsis and conclusions

Stellenbosch University http://scholar.sun.ac.za

List of figures

CHAPTER 2

CHAPTER 3

Stellenbosch University http://scholar.sun.ac.za

Stellenbosch University http://scholar.sun.ac.za

Stellenbosch University http://scholar.sun.ac.za

CHAPTER 4

Stellenbosch University http://scholar.sun.ac.za

CHAPTER 5

Stellenbosch University http://scholar.sun.ac.za

CHAPTER 6

Stellenbosch University http://scholar.sun.ac.za

Stellenbosch University http://scholar.sun.ac.za

List of tables

CHAPTER 2

CHAPTER 3

CHAPTER 4

Stellenbosch University http://scholar.sun.ac.za

CHAPTER 5

CHAPTER 6

Stellenbosch University http://scholar.sun.ac.za

List of schemes

CHAPTER 2

Stellenbosch University http://scholar.sun.ac.za

List of publications

- Fractionation and Crystallization of Isotactic Poly(propylenes) Prepared with a Heterogeneous Transition Metal Catalysts (Ismael Amer, Albert van Reenen/ Macromol. Symp. 2009, 282, 33–40)

- An investigation of the effect of chain length on stereo-regulation with C2 symmetric metallocene catalysts (I. Amer and A. van Reenen/ Submitted to Polymer Bulletin, 2010)

- Use of a Turbidity Analyzer for Studying the Solution Crystallization of Different Polypropylenes (Ismael Amer, Albert Van Reenen, Margaretha Brand/ Submitted to Polymer, 2010)

Stellenbosch University http://scholar.sun.ac.za

List of abbreviations

AlR_3	alkyl aluminium
BHT	2,6-di-tert-butyl-4-methylphenol
B_z	benzene
CEF	crystallization elution fractionation
Cp	cyclopentadienyl
CRYSTAF	crystallization analysis fractionation
DMA	dynamic mechanical analysis
DSC	differential scanning calorimetry
DPDMS	diphenyldimethoxysilane
d_w	down
E′	Storage modulus
E″	loss modulus
ED	external donor
EI	*rac*-ethylene-bis(indenyl) zirconium dichloride
EI(4H)	*rac*-ethylene-bis(4,5,6,7-tetrahydro-1-indenyl) zirconium dichloride
$Fe(Cp)_2$	ferrocene
FT-IR	fourier-transform infrared spectroscopy
g	gauche
GC	gas chromatography
HDPE	high density polyethylene
HT-GPC	high-temperature gel permeation chromatography
K_p	propagation constant rate
L	left-handed
MAO	methylaluminoxane
MDSC	modulated differential scanning calorimetry
MH	microhardness
MH_1 and MH_2	hardness of the single components
MH_b	hardness of the blend
$\overline{M_n}$	number average molecular weight
mmmm %	pentad mole percentage
MPDMS	methyl-phenyl-dimethoxysilane
Mt	metal
$\overline{M_w}$	weight average molecular weight
MWD	molecular weight distribution
NC	nitrocellulose
NMR	nuclear magnetic resonance spectroscopy
NR	natural rubber
OM	optical microscopy
p-TREF	preparative temperature rising elution fractionation
PVC	polyvinyl chloride
R	right-handed
SCALLS	crystallization analysis by laser light scattering
SCBD	short chain branching distribution

Stellenbosch University http://scholar.sun.ac.za

SEC	size exclusion chromatography
SEM	scanning electron microscopy
SPP	syndiotactic polypropylene
t	helix trans
Tan δ	damping coefficient or damping ratio
T_c	crystallisation temperature
TCB	trichlorobenzene
T_e	elution temperature
TEA	triethylaluminium
T_g	glass transition temperature
T_m	melting temperature
TMA	trimethylaluminium
TREF	temperature rising elution fractionation
WAXD	wide angle X-ray diffraction
$W_i\%/\Delta T$	differential weight fraction to temperature
W_t	weight fraction
$W_i\%$	weight fraction percentage
$X_c\%$	crystallinity percentage
α	alpha phase
α_1	disordered alpha phase
α_2	ordered alpha phase
β	beta phase
ΔH_f^o	heat of fusion
ΔT	difference in temperature
γ	gama phase
ϕ	weight fraction of component
$\Sigma W_i\%$	accumulative weight fraction
2θ	bragg angle

Stellenbosch University http://scholar.sun.ac.za

CHAPTER 1

Introduction and objectives

1.1 General introduction

During the past two decades, isotactic polypropylenes have received increasing attention due to their attractive physical, mechanical and, more importantly, cost-effective properties. The characteristics of isotactic polypropylenes depend greatly on the type of catalyst used in the polymerization of the propylene monomer. The most common catalysts used in the polymerization are the Zigler-Natta and metallocene types. The heterogeneous Ziegler-Natta catalyst was developed in the early 1950s.[1,2] Polypropylene is formed by insertion of the monomer at the transition metal-carbon bonds after initial coordination of the monomer by the transition metal. The recently developed metallocene type catalyst is a combination of stereorigid metallocenes of the transition metals with methylaluminoxane (MAO).[3] Metallocene type catalysts have single active sites leading to better control of molecular weight distribution as opposed to multiple catalytic sites in Ziegler-Natta catalysts.[1,2] Isotactic polypropylenes made using metallocenes display narrower molecular weight and have fewer defects than the polymers made using Ziegler-Natta type catalysts.

The crystallization of polyolefins is an important parameter determining the properties of the material. For stereoregular isotactic polypropylenes the most important factor affecting crystallization and melting behaviour arises from their subtle structural differences. The effects of molecular weight,[4-6] molecular weight distribution[7] and tacticity[8-10] on the crystallization have been investigated by several authors. Results indicate that the linear growth rate of crystals markedly decreases with increasing molecular weight,[5] but the overall crystallization rate might increase because an increasing number of intramolecular folded-chain nuclei could result in a higher nucleation density.[6] For samples with similar molecular weights and different tacticities the linear crystal growth rate might increase by three orders of magnitude when the isotacticiy (*mmmm* %) of isotactic polypropylene increases from 78.7 to 98.8%.[9,11] The degree of crystallinity of isotactic polypropylene is commonly in the range of 40 to 70%.[12] Atactic polypropylene, on the other hand, is considered uncrystallizable, since the chain structure lacks regularity. Isotactic polypropylene can crystallize in three different crystal forms, depending on the polymer structure and the crystallization conditions: the α-

Stellenbosch University http://scholar.sun.ac.za

form with a monoclinic, the γ-form with an orthorhombic, and the β-form with a hexagonal unit cell.[13]

Most commercial isotactic polypropylenes can, for practical purposes, be regarded as blends of materials differing with respect to molecular weight, molecular weight distribution and tacticity.[14-16] The molecular make-up of isotactic polypropylenes will differ, which will, in turn, affect the crystallization and melting behaviour of these polymers. The use of preparative temperature rising elution fractionation (p-TREF) allows the characterization of a given isotactic polypropylene in terms of molecular make-up.[17] The use of p-TREF also allows for the isolation of fairly well-defined isotactic polypropylene fractions of a given molecular weight and tacticity, which, in turn, allows for the more detailed study of, for example, crystallization behaviour of such materials.

1.2 Objectives

This study mainly focuses on the effect of molecular weight on the crystallization of polypropylenes produced using different types of catalysts, and under different reaction conditions:

- Polypropylene produced by $MgCl_2$-supported Ziegler-Natta catalysts with two different external donors, diphenyldimethoxysilane (DPDMS) and methyl-phenyl-dimethoxysilane (MPDMS).
- Polypropylene produced by two different types of isospecific C_2 symmetric metallocene catalysts, *rac*–ethylene–bis(indenyl) zirconium dichloride, $Et(Ind)_2ZrCl_2$ (EI), and *rac*–ethylene–bis(4,5,6,7-tetrahydro-1-indenyl) zirconium dichloride, $Et(H4Ind)_2ZrCl_2$ (EI(4H)).
- Molecular hydrogen was used to control the molecular weight during these polymerization reactions.

In order to establish a correlation between the molecular weight and the crystallization of these polymers, the following were carried out. First, fractionation of the materials according to their crystallizability was performed by means of temperature rising elution fractionation (TREF), which affords the opportunity for blending materials of differing molecular weights but similar symmetry.

Second, blending studies of these fractions with respect to the similarities and the differences in their structure (molecular weight and tacticities) were performed. Third, the bulk and solution crystallization behaviour of the blends were investigated using differential scanning

Stellenbosch University http://scholar.sun.ac.za

calorimetry (DSC) and solution crystallization analysis by laser light scattering (SCALLS) analyses respectively. Finally, morphology and mechanical properties on different homopolymers and blends were investigated to determine the effect of the molecular structure on these properties.

1.3 References

1. K. Ziegler, E. Holzkamp, H. Breil, H. Martin, *Angew. Chem*. **1954**, 67, 541.
2. G. Natta, P. Corradini, *Macromol. Chem*. **1955**, 16, 213.
3. H. Sinn, W. Kaminsky, H. Vollmer, R. Woldt, *Angew. Chem., Int. Ed*. **1980**, 19, 390.
4. J. D. Hoffman, R. L. Miller, *Macromolecules* **1988**, 21, 3038.
5. S. Z. Cheng, J. J. Janimak, A. Zhang, *Macromolecules* **1990**, 23, 298.
6. B. D. Carvalho, R. E. Bretas, *J. Appl. Polym. Sci*. **1998**, 68, 1159.
7. P. J. Phillips, N. Vatansever, *Macromolecules* **1987**, 20, 2138.
8. S. Z. Cheng, J. J. Janimak, A. Zhang, *Polymer* **1991**, 32, 648.
9. J. J. Janimak, S. Z. Cheng, P. A. Giust, E. T. Hsieh, *Macromolecules* **1991**, 24, 2253.
10. J. J. Janimak, S. Z. Cheng, A. Zhang, *Polymer* **1992**, 33, 728.
11. L. Hongbin, Q. Jinliang, X. Yibin, Y. Yuliang, *J. Appl. Polym. Sci*. **2002**, 85, 333.
12. E. P. Moore, Jr. *Polypropylene Handbook*, Hanser Publishers. Munich, **1996**.
13. S. Bruckner, S. Meille, V. Petraccone, B. Pirizzi, *Prog. Polym. Sci*. **1991**, 16, 361.
14. H. Kawamura, T. Hayashi, Y. Inoue, R. Chujo, *Macromolecules* **1989**, 22, 2181.
15. G. Morini, E. Albizzati, G. Balbontin, I. Mingozzi, C. M. Sacchi, F. Forlini, I. Tritto, *Macromolecules* **1996**, 29, 5770.
16. R. Zacur, G. Goizueta, N. Capiati, *Polym. Eng. Sci*. **1999**, 39, 921.
17. J. B. Soares, A. E. Hamielec, *Polymer* **1995**, 36, 1639.

Stellenbosch University http://scholar.sun.ac.za

CHAPTER 2

Historical and theoretical background

2.1 Polypropylene

2.1.1 History

Polypropylene was discovered in the early 1950s. In 1953 Ziegler discovered that polyethylene could be prepared using a mixture of metal salts and transition metal salts.[1] Giulio Natta succeeded in preparing polypropylene using the Ziegler catalyst and was able to obtain and characterize isotactic polypropylene by fractionation. In 1957 polypropylene was taken into commercial production.[2-4] Since then major developments in the production and applications of polypropylenes have occurred. The polymer yield of the catalyst (the so-called Ziegler-Natta catalyst) has increased enormously from 0.8 kg/gram catalyst to more than 100 kg/gram catalyst, along with a significant increase in isotacticity, over four different generations of the Ziegler-Natta catalyst system. Moreover, polypropylene proved to be not only highly isotactic, but also highly syndiotactic, perfectly atactic, and even as a divertissement hemiisotactic.[5,6]

2.1.2 Polypropylene configurations

Polypropylene is a very common semi-crystalline polymer that is finding increasing use in modern technological applications. The polypropylene chain resulting from the head-to-tail addition of propylene monomers can have three different configurations: the regular isotactic, the regular syndiotactic and the irregular atactic configurations, which are classified based on the arrangement of the methyl groups with respect to the polymer backbone. In the extended isotactic polypropylene chain all methyl groups are on the same side of the plane formed by the main chain carbon atoms. In the syndiotactic polypropylene the methyl groups are arranged alternating on both sides of the plane. In the atactic configuration the methyl groups are positioned randomly on both sides along the polymer chain.[7] The three configurations of the polypropylene are illustrated in Figure 2.1.

Stellenbosch University http://scholar.sun.ac.za

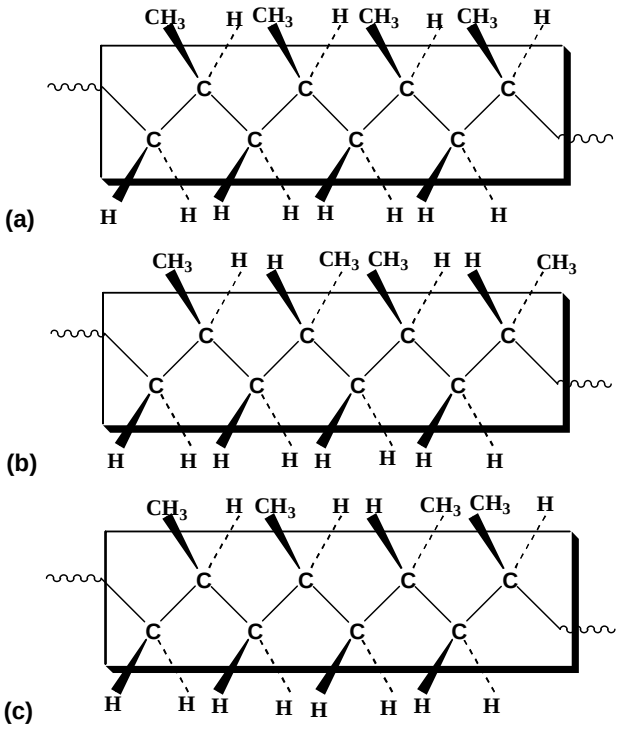

Figure 2.1: Schematic illustration of the stereochemical configurations of polypropylene: a) isotactic, b) syndiotactic, c) atactic.

2.1.3 Polypropylene conformations and crystal structures

None of the configurations of polypropylene exist in an extended conformation. The chain assumes a helical structure in order to relieve the steric hinderance, which is caused as a result of the presence of methyl groups along the chain backbone, in order to achieve an energy minimum.

The polymer chain of isotactic polypropylene adapts the conformation of a three-folded chain 2x3/1 helix trans(t)-gauche(g), with a repeat distance of 6.5 Å. This conformation leads to the lowest intramolecular interaction energy of the methyl groups attached to the polypropylene chain.[8] The isotactic polypropylene helix exhibits four different chiralities. Both right-handed (R) and left-handed (L) helices are based on the helix direction, which can be up or down, depending on the methyl group orientation. Figure 2.2 illustrates the four possible chain conformations of isotactic polypropylene.[9] Syndiotactic polypropylene exhibits three different chain conformations: the planar zigzag chain (tt), the (4x2/1) helix $(t_2g_2)2$ (where t and g indicate bonds in *trans* and *gauche* conformation, respectively) and the $(t_6g_2t_2g_2)$ conformation, which is an intermediate between the planar zigzag and the helix form. The

Stellenbosch University http://scholar.sun.ac.za

helix conformation leads to the lowest interaction energy between the methyl groups.[7] Atactic polypropylene with a random arrangement of the methyl groups along the polymer chain leads to random conformations.

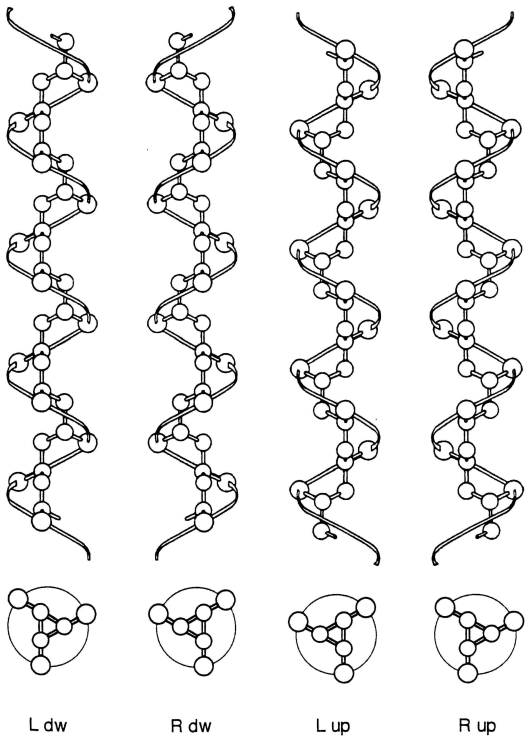

Figure 2.2: Chain conformations of isotactic polypropylene. Right (R)- and left (L)-handed helices in their up (up) and down (dw) configurations.[9]

2.1.4 Crystallinity and polymer structure

Both the crystallization behaviour and crystal form of the polymer are strongly affected by the configuration (tacticity) and conformational structure of the polypropylene chain. Isotactic and syndiotactic polypropylene can crystallize. The degree of crystallinity is usually in the range 40–70% and depends on the level of the tacticity of the polymer.[4] Atactic polypropylene is considered as uncrystallizable, since the chain structure lacks regularity. The syndiotactic polypropylene chains form either an orthorhombic unit cell if they have a $(t_2g_2)2$ or a planar zigzag conformation and triclinic unit cell with the $(t_6g_2t_2g_2)$ conformation.[7] Isotactic polypropylene can crystallize in three different crystal forms depending on the polymer structure and the crystallization conditions: the α-form with a monoclinic, the γ-form

Stellenbosch University http://scholar.sun.ac.za

with an orthorhombic and the β-form with a hexagonal unit cell.[10,11]

2.2 The crystalline structure of isotactic polypropylene

2.2.1 The α-phase of isotactic polypropylene

The most common crystal form in isotactic polypropylene is the α-phase, which has a monoclinic crystal structure. The α-phase was the first to be discovered and characterized.[12,13] This crystalline form is observed for both melt and solution crystallized samples prepared under atmospheric pressure.

The α-phase of isotactic polypropylene is described by an alternation, in the b-axis direction, of layers parallel to the ac-plane and composed of only left-handed (L) or right-handed (R) helices, indicated in Figure 2.3 by white and gray triangles, respectively. The location of the methyl groups in both the left- or right-handed helix can be placed 'up' or 'down' (up or dw) (see Figure 2.2 for a helix with 'dw' position of the methyl groups). Due to the possibility of the chains to be positioned 'up' or 'down', two limiting α-phases (α1: disordered, α2: ordered) are formed (see Figure 2.3). The ordered α2-phase (Figure 2.3, right) can be obtained by recrystallizing or annealing.[14] These two forms can be distinguished via detailed X-ray analysis at high diffraction angles.[15] Samples existing essentially in the α1 form show a double melting peak upon slow heating in DSC experiments.[15,16] In contrast, a sample near the α2 form only displays a narrow single melting peak. The double melting can be explained as a disorder-order transition if the heating rate allows partial melting of the material.[17] The partial melting is needed for recrystallization of the α1- into the α2- phase. In highly stereoregular samples the double melting is also associated with the melting of the daughter and the mother lamellae, respectively.[18]

The monoclinic unit cell has the following parameters: a = 6.65 Å, b = 20.96 Å, c = 6.5 Å and β = 9.62°.[19,20] The overall density is 0.946 g/mol (room temperature).[20] The value of the thermodynamic equilibrium melting point ($T_m°$) of the α-phase has been studied by many researchers.[10] $T_m°$ was found to be between 185 and 209 °C. The variation of $T_m°$ is related to the different techniques used to measure it. The results of the heat of fusion ($\Delta H_f°$) measurements are also scattered. Data obtained from calorimetry show values of $\Delta H_f° = 8.7 \pm 0.8$ kJ/mol, while the values obtained from the melting point depression by diluents is $\Delta H_f° = 9.1 \pm 1.6$ kJ/mol. Recently, a value of $\Delta H_f° = 8.7$ kJ/mol was adopted.[10]

Stellenbosch University http://scholar.sun.ac.za

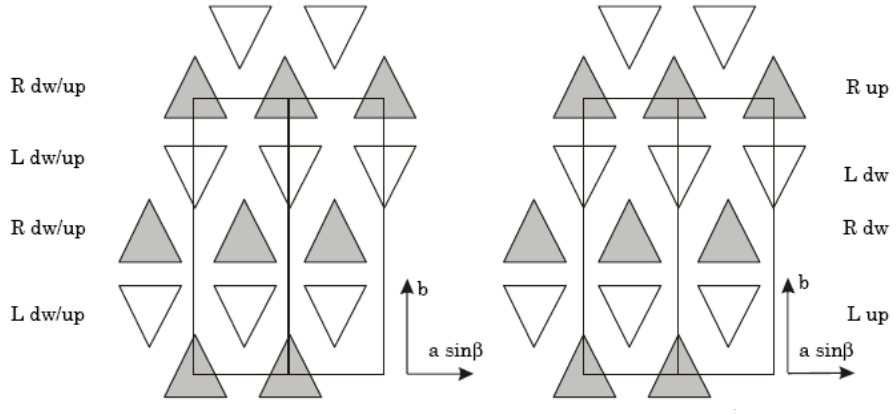

Figure 2.3: Two limiting forms of the α-phase. Left: α1; Right: α2. The horizontal arrows indicate the projection of the a-axis, the vertical arrow indicates the b-axis. The c-axis is perpendicular to the plane of view.[21]

2.2.2 The β-phase of isotactic polypropylene

The β-form of isotactic polypropylene was first reported by Padden and Keith in 1959.[22] Under suitable crystallization conditions (shear, large temperature gradients, or use of β-nucleating agents like quinacridone,[23] the anhydrous calcium salt of suberic acid,[24] and other agents), polypropylene samples with a high content of the β-phase can be obtained.[23-25] In samples that have been subjected to high shear in the melt the β-phase can also be found.[23] The β-phase has a trigonal unit cell (see Figure 2.4) with lattice parameters a = b = 11.0 Å, c = 6.5 Å, β = 120° and α = β = 90°.[19,24,26-28]

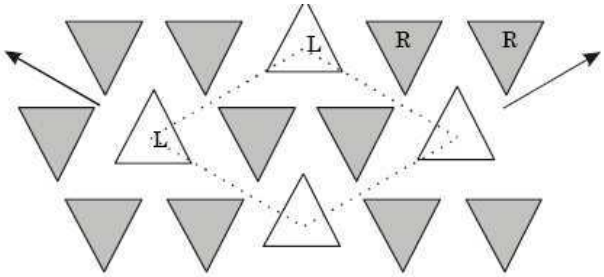

Figure 2.4: Schematic representation of the arrangement of isotactic polypropylene helices in the β-phase. The arrows indicate the b-axes. The c-axis is perpendicular to the plane of view.

Stellenbosch University http://scholar.sun.ac.za

The thermodynamic properties of the β-phase have not been as comprehensively studied as those of the α-phase. The β-phase is metastable relative to the α-phase ($T_m \cong 155$ °C versus 180 °C). The equilibrium melting temperature of the crystals ($T_m°$) ranges from 170 to 200 °C.[7] The values of $\Delta H_f°$ vary from 4.76 to 7.45 kJ/mol.[4,7]

2.2.3 The γ-phase of isotactic polypropylene

The γ-phase is usually associated with the α-phase, although individual single crystals of the γ-phase have also been observed.[29] The γ-modification may be formed in degraded, low molecular weight isotactic polypropylene and in samples crystallized under high pressures.[30-32] Significant amounts of the γ-modification were also obtained under atmospheric pressure, both in systems with low tacticity or polymers made by homogeneous metallocene catalysts.[25,33] The value of the thermodynamic equilibrium melting point, $T_m°$, of the γ-phase is 187.2 °C and the value of the heat of fusion $\Delta H_f° = 6.1$ kJ/mol.[33]

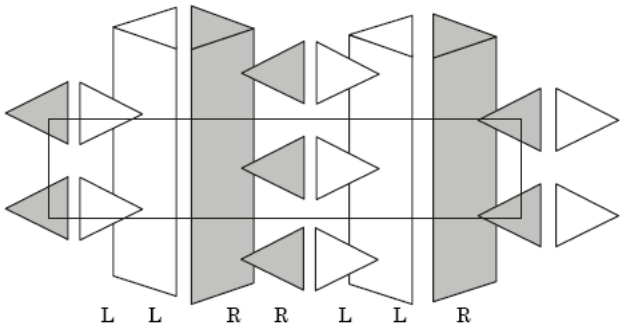

Figure 2.5: Schematic representation of the arrangement of isotactic polypropylene helices in the γ-phase.[32-34]

The crystalline structure of the γ-modification was first denoted as triclinic.[25,35] It was shown that the structure is orthorhombic, with parameters a = 8.54 Å, b = 9.93 Å and c = 42.41 Å,[32] with the above-mentioned triclinic cell as a sub-cell.[36] The structure is composed of sheets of parallel chains, in which the molecular orientation in adjacent sheets is inclined to one another at an 80° angle.[37] In this unit cell the c-axis is not parallel to chain axis direction.

Stellenbosch University http://scholar.sun.ac.za

2.3 The crystalline structure of syndiotactic polypropylene

Syndiotactic polypropylene was first synthesized in the early 1960s by Natta *et al.*[38,39] using Ziegler-Natta catalysts, but the resulting polymer contained a large number of regio-defects (e.g., head to head/tail to tail type defects), even when a fair level of syndiotactic content was obtained. A much better syndiotactic polypropylene was successfully synthesized in 1988 by Ewen *et al.*[40] using a new metallocene catalyst. The new catalyst systems made it possible to produce syndiotactic polypropylene with much improved purity and yields, which led to renewed interest in scientific research and industrial applications.[41,42] Syndiotactic polypropylene has a very complex crystal structure. The studies performed in the early 1960s on regioirregular and poorly syndiotactic polypropylene samples prepared with the vanadium-based Ziegler-Natta catalysts had already shown the existence of polymorphism.[38,43-46] Two different crystalline forms, characterized by macromolecular chains having different conformations, were described at that time. Generally, the most stable form is when the chains present a two-fold helical conformation, with s(2/1)2 symmetry[46-49] (the sequence of torsion angles along the backbone is $(ttgg)_n$).[38,43,44,46] The less stable form is characterized by chains in trans-planar conformation and t*cm* symmetry, with a sequence of torsion angles of the kind $(tttt)_n$.[47] The two-fold helical and trans-planar conformations of syndiotactic polypropylene chains are shown in the Figure 2.6.

Four different polymorphic crystalline forms (shown in Figure 2.7) and a disordered mesomorphic form have been found so far. They have been called forms I, II, III and IV, despite the chronology of their discovery, but only considering that form I is the most stable and common form (even though it was discovered a while after form II),[50] while forms III and IV are the less stable forms observed only in oriented fibers.[45,51,52] This nomenclature has been proposed by De Rosa *et al.*[53] and is nowadays commonly accepted. Form I and form II are characterized by chains in s(2/1)2 helical conformation packed in different orthorhombic crystalline lattices (Figure 2.7 A and B, respectively), form III presents polymer chains in the trans-planar conformation with t*cm* symmetry (Figure 2.7 C) and, finally, form IV is characterized by chains in $t_6g_2t_2g_2$ conformation (Figure 2.7 D).

Stellenbosch University http://scholar.sun.ac.za

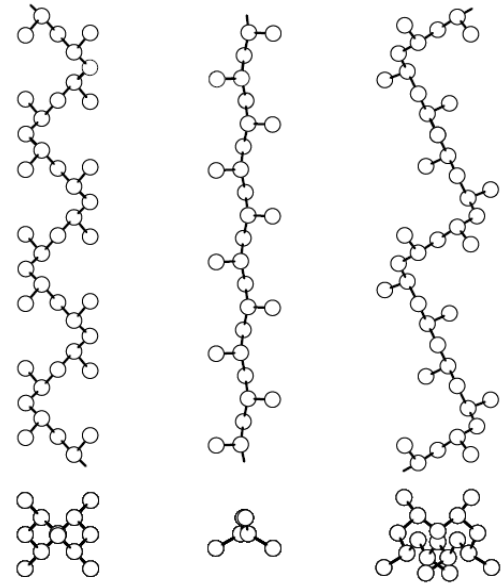

Figure 2.6: Conformations of chains of syndiotactic polypropylene in the different crystalline polymorphic forms. Helical $(ttgg)_n$ conformation with s(2/1)2 symmetry (A), trans-planar conformation with t*cm* symmetry (B) and $t_6g_2t_2g_2$ conformation with t2 symmetry (C).[54]

2.4 Molecular weight effects on crystallization

The molecular parameters that are commonly considered to characterize polypropylene and largely determine its physico-chemical and processing properties are molecular weight, molecular weight distribution, and tacticity.[56] The effect of molecular weight on the crystallization during the fractionation has been largely disregarded in the past. Burfield *et al*.[57] found correlations between both crystallization, and melting properties and isotacticity, in the same study. Molecular weight also had some influence on crystallization and melting temperatures, especially melting temperature, which increased with increasing molecular weight. Wild *et al*.[58] studied the possibility of molecular weight effects on TREF seperations. It was found that at low molecular weights (<10 000 g/mol) there is a significant molecular weight dependence on separation. According to Martuscelli *et al*.[59,60] molecular weight distribution affected the crystallization rate. However, tacticity was one of the main factors determining this property. Later, Janimak and others[61-64] utilized polypropylene fractions with similar molecular weights and molecular weight distributions but different isotacticities to examine the influence of isotacticity on the crystallization behaviour.

Stellenbosch University http://scholar.sun.ac.za

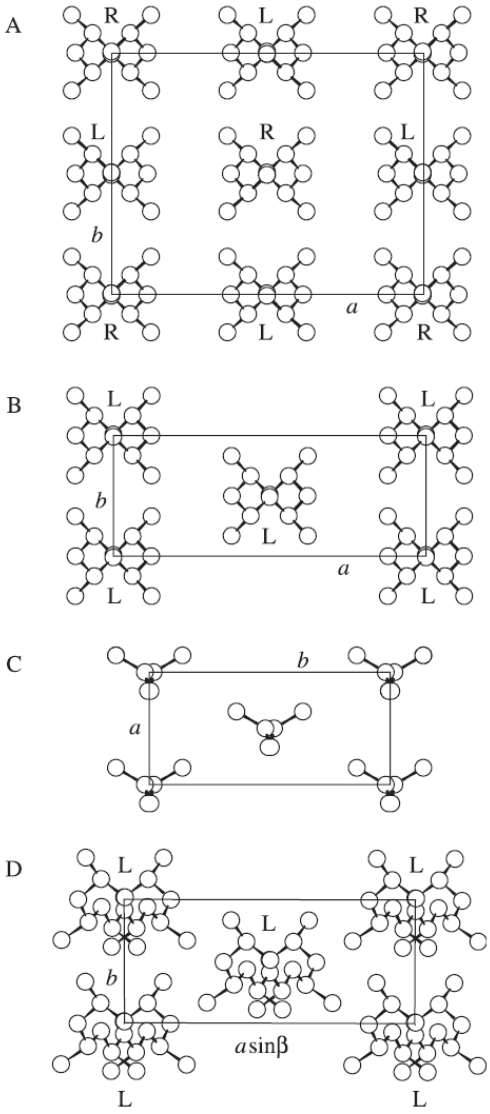

Figure 2.7: Limit ordered models of packing of form I (A), form II (B), form III (C) and form IV (D) of syndiotactic polypropylene. R:right-handed helix, L:left-handed helix.[55]

Solvent/non-solvent systems are also used in fractionation experiments. Lehtinen and Paukkeri[65] investigated the fractionation of isotactic polypropylene and polyethylene by solvent/non-solvent systems. Fractionation, when using a xylene/ethylene glycol monoethyl ether solvent/non-solvent system, occurred due to molecular weight for polyethylene. Polypropylene was fractionated according to isotacticity first, and when a constant tacticity was reached, was separated according to molecular weight. Fractionation occurred only according to molecular weight when ethylene glycol monobutyl ether/diethylene glycol monobutyl ether was used as a solvent/non-solvent system. Xu and Feng[66] studied the

Stellenbosch University http://scholar.sun.ac.za

characterization of isotactic polypropylene produced using a supported metallocene catalyst by TREF and various other techniques. TREF fractionates according to crystallinity and both molecular weight and isotacticity influence crystallinity. It was observed that the viscosity-average molecular weight of the fractions obtained by TREF increased with increasing elution temperature. The melting temperature, on the other hand, only increased in the first seven fractions and remained constant for the last six fractions. ^{13}C-NMR showed that the isotacticity increased in the first seven fractions but remained constant for the last six fractions. Consequently, it was concluded that the main factor influencing fractionation in the first seven fractions was isotacticity. However, as soon as tacticity remained constant, as in the case of the last six fractions, molecular weight became the main factor influencing crystallinity and thus the fractionation. Recently, Arranz-Andrés *et al.*[67] studied the effect of isotacticity and molecular weight on the properties of isotactic polypropylene made using metallocene catalysts. They concluded that the most important factors affecting the structure and properties of these polymers are those that lead to an increase of crystallinity. Accordingly, they found that the isotacticity degree has a greater effect on the crystallinity than the molecular weight effect. In contrast, a clear molecular weight effect has been found for the sample with lowest molecular weight.

2.5 Ziegler-Natta catalysts

2.5.1 Background

Since the 1950s, polyolefins have been produced using Ziegler-Natta catalysts. These catalysts are based on the work of Karl Ziegler and Guilio Natta, which jointly won them the Nobel Prize for Chemistry in 1963. These catalyst systems allow for the production of specific polyolefins, such as linear unbranched polyethylene and isotactic polypropylene. Free radical vinyl polymerizations can only produce branched polyethylene and can not be used in the production of propylene.[2,68] The Ziegler-Natta catalyst has joined the ranks of conventional cationic, anionic and radical initiators as one of the common methods available to initiate polymerizations, and it is doubtful that it can be challenged by any other catalyst for its versatility. Ziegler-Natta catalysts became prominent in a special period in the history of polymer science, a period that not only produced many new commercial polymers but also improved our basic knowledge of polymer properties and structure as well as polymerization processes.[2] Using these catalysts Natta and coworkers polymerized propylene to isotactic polypropylene. They discovered the principles of the regio- and stereospecific polymerization

Stellenbosch University http://scholar.sun.ac.za

of 1-alkenes.[69,70] The process used to synthesize isotactic polypropylene was transferred into a industrial process within a few years because polymers with new properties were obtainable.[71] These catalysts can also be used for the copolymerization of ethylene and propylene to produce ethylene–propylene elastomers–again, these were new polymers.[72]

The evolution of Ziegler-Natta catalysts can be categorized into four main generations as tabulated in Table 2.1. A large increase in productivity results from the use of generation III catalysts, (catalysts supported on a support). The optimizations of supporting protocols have led to a largely experimental understanding of these systems. The developed catalysts have multiple types of titanium sites, yielding ill-defined materials. The mechanisms and structure-property relationships are not well understood. Furthermore, these catalysts are not able to polymerize functional monomers.[73]

Table 2.1: Development of Ziegler-Natta catalyst systems

Generation	Time range	Catalyst	Productivity (kg PP/g Ti)	Isotacticity
I	1950-1970	$TiCl_3/AlEt_2Cl$	5	90
II	1950-1970	$TiCl_3$/isoamyl ether/$AlCl_3/AlEt_2Cl$	15	95
III	1970-1990	$MgCl_2$/ester/$TiCl_4/AlEt_3$/ester	300	92
IV	1990-	$MgCl_2$/ester/$TiCl_4/AlEt_3/PhSi(OEt)_3$	600	98

2.5.2 Ziegler-Natta catalyst systems

Ziegler-Natta catalyst systems are generally based on a titanium chloride complex, for example titanium trichloride ($TiCl_3$) or titanium tetrachloride ($TiCl_4$), and an alkyl aluminium species, such as triethylaluminum. One of the main difficulties associated with these systems is the determination of the exact active species. It does appear certain the active catalytic sites are not simple coordination adducts formed from the titanium halide and the alkylaluminum. An “activation” period, in which the titanium and aluminum species are mixed together before the addition of monomer, is often needed before the system reaches its highest activity. A number of complex reactions are proposed to take place during this activation period, resulting in the formation of a highly active species. Among these reactions contain an exchange of substituent groups between the two metals to form titanium-carbon bonds, such as shown in Equations A and B. The organotitanium complexes formed in this stage are

Stellenbosch University http://scholar.sun.ac.za

unstable and can undergo further reductive decomposition processes, as can be seen in Equations C and D. Radicals formed during theses processes might be removed by combination, disproportionation, or reaction with solvent.

$$AlR_3 + TiCl_4 \rightleftharpoons R_2AlCl + RTiCl_3 \quad (A)$$

$$R_2AlCl + TiCl_4 \rightleftharpoons RAlCl_2 + RTiCl_3 \quad (B)$$

$$RTiCl_3 \rightleftharpoons R^{\bullet} + TiCl_3 \quad (C)$$

$$R_2TiCl_2 \rightleftharpoons R^{\bullet} + RTiCl_2 \quad (D)$$

The exact mechanism for olefin addition is still not completely understood. Two general mechanisms have been proposed; one involves the coordination of the olefin to a vacant site on the transition metal and the other one suggests participation by both the transition metal and the aluminum species.

A problem of the early Ziegler-Natta systems was their low productivity. Large amounts of catalyst were necessary to achieve acceptable yields of polymer. It was however found that by impregnating a solid support (such as $MgCl_2$ or MgO), the activities of the system were considerably increased. The exact mechanism for this increase is not entirely clear. It is presumed the support maximizes the number of active sites on the surface. Researchers have shown that increasing the number of surface defects in the magnesium support increases the activity of the resulting catalyst.[73] It has been suggested that the active titanium chloride species “sits” in small crevices and cracks in the surface, whereas the inactive species are more likely to be bound to the surface.[73]

2.5.3 Lewis donors in Ziegler-Natta catalyst systems

Over the years, Ziegler-Natta catalysts have evolved from simple $TiCl_3$ crystals into the $MgCl_2/TiCl_4$/donor systems used today, where the donor is a Lewis base that can be added during catalyst preparation (the so-called internal donor).[4,74] Among donors, 1,3-diethers,[75] aromatic esters (benzoates and phthalates in particular)[76] and, recently, aliphatic esters (succinates in particular) have been shown to be particularly effective.[77] Catalyst activation requires the addition of alkylating reducing species ($AlEt_3$ is generally used), possibly mixed

Stellenbosch University http://scholar.sun.ac.za

with a second electron donor (the so-called external donor (ED)), usually an alkoxysilane or, more recently, a succinate. The resulting active system is of extreme chemical complexity, and the polypropylenes obtained present very different properties.[77] The nature of the added Lewis bases is fundamental in terms of catalyst performance, since it can effectively modify the tacticity and molecular weight distribution of the produced polypropylenes.[78-87] It has been suggested that the Lewis bases stabilize small primary crystallites of $MgCl_2$ and/or to influence the amount and distribution of $TiCl_4$ in the final catalyst. The donor has to compete with $TiCl_4$ to coordinate on the $MgCl_2$ surfaces, possibly inducing formation of the more stereoselective sites.

2.6 Metallocene catalysts

2.6.1 Historical background

The discovery in the 1980s of effective homogeneous transition metal catalysts for olefin polymerization is probably one of the most significant advances in polymer synthesis. The development of group 4 metallocene catalysts not only improved the control over the properties of polyolefins but also made it possible to synthesize new types of polyolefins. Numerous studies have been carried out on the structure and properties of the polyolefins resulting from the advances in catalyst technology.[88] The first metallocene was discovered in 1951 in the form of ferrocene, $Fe(Cp)_2$,[2,89] as is shown in Figure 2.8. The sandwich structure of ferrocene was formulated in 1952 by Wilkinson *et al.*[90] and a number of other metallocenes were synthesized soon after this discovery.[91]

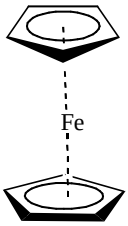

Figure 2.8: Structure of ferrocene.

In 1953 Karl Ziegler and coworkers[92] discovered catalyst systems based on transition metal compounds (zirconium and titanium halides), which were used for the polymerization of α-olefins.[93] In the presence of aluminum alkyl activators these catalyst systems were able to polymerize ethylene to yield high density polyethylene (HDPE) at low pressure, but could not

Stellenbosch University http://scholar.sun.ac.za

polymerize propylene. In 1954 Natta reported the successful polymerization of propylene using the same catalyst system.[94] After characterization of the resulting polymer, he was able to define the three stereo conformations of polypropylene: isotactic, syndiotactic, and atactic polypropylene. In 1957 titanocene dichloride was found to be active in olefin polymerization.[95,96] In these experiments aluminium alkyls were used as activators but only low polymerization activities were obtained when using metallocene catalysts.

It was not until 1973 that the true potential of group 4 metallocene catalysts was recognized it was observed that controlled addition of water into the titanocene/aluminium alkyl system increased the catalytic activity significantly.[97] The increase in activity was found to arise from the formation of aluminoxanes, e.g. methyl aluminoxane (the general structure of it is shown in Figure 2.9), which can be obtained from the reaction of trimethylaluminium (TMA) and water.[98]

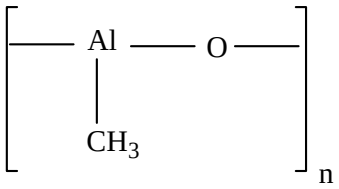

Figure 2.9: Simplified representation of methyl aluminoxane.

Many research groups proceeded to develop new metallocene complexes once the potential of metallocenes was established. One major advance was the synthesis of bridged zirconocene dichlorides with C_2-symmetry by Brintzinger and coworkers.[99] Soon after this, Kaminsky and Arndt produced isotactic polypropylene with these bridged zirconocenes.[100] Their success spurred efforts to find more active and stereoselective catalysts for the polymerization of a wide range of monomers.[101] Presently, MAO-activated metallocene catalysts are currently still the subject of extensive research.[100,102] Although group 4 metallocene based catalysts are already being employed in the polyolefin industry, much work remains to be done in the field of catalyst design to produce cheaper, and more robust catalysts.

2.6.2 Metallocene catalyst systems

Metallocene catalyst systems result from the reaction of metallocenes and a cocatalyst, which is generally an organoaluminium compound. These catalysts play an important role in the polymerization of olefins, dienes and styrene. Today a significant part of the chemical

Stellenbosch University http://scholar.sun.ac.za

industry uses these catalysts to produce increasing amounts of plastic materials. Metallocene catalysts are soluble in hydrocarbons, show only one type of active site and their chemical structures can be easily changed. These properties allow one to accurately predict the properties of the resulting polyolefins. Molecular weight and distribution, comonomer content and tacticity can be controlled by careful selection of the catalyst and reaction conditions. In addition, the catalytic activity of the metallocene catalysts is 10–100 times higher than that of the typical Ziegler-Natta system.[103]

Metallocene catalyst systems can be conveniently divided into two categories. In the first, an aluminoxane, an alkylaluminum, or a combination of aluminoxane and alkylaluminium, is used to activate the metallocene catalyst. In the second category, an ion exchange compound is combined with the metallocene catalyst, forming what is generally called a cationic metallocene catalyst. It is now generally accepted that the catalytic active species for metallocene/aluminoxane/alkylaluminium systems is cationic in nature.[104]

Remarkable features of metallocene catalyst systems, and their uses, in preference to other catalyst systems, include the following:

1. Very uniform homo- and copolymers with narrow molecular weight distributions, with $M_w/M_n = 2$, are typical for catalysts with only one type of active site ('single-site' catalysts).
2. Excellent control of molecular weight, end groups, stereochemistry, long- and short-chain branching is achieved.
3. Molecular weight-independent comonomer incorporation, including the less reactive comonomers such as long-chain α-olefins and styrenes, is possible.
4. Cyclo-olefins can be polymerized.
5. Morphology can be controlled, and there is potential for production of reactor blends using metallocene catalysts.
6. New catalysts can be introduced into old plants to produce new polymers ('drop-in' technology).
7. Polymers that are easier to recycle can be produced.
8. Only small quantities of catalyst are required.

Stellenbosch University http://scholar.sun.ac.za

2.6.3 General structure of metallocene catalysts

The general structure of a group 4 metallocene catalyst precursor such as is used in olefin polymerization is presented in Figure 2.10. The most remarkable feature of these catalysts is that their molecular structure can be designed to create active centers to produce polymers with entirely novel properties.[105]

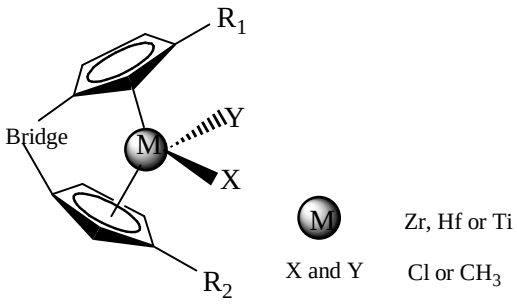

Figure 2.10: General structure of a bridged group 4 metallocene catalyst precursor.

The carbon atoms of the cyclopentadiene (Cp) ligands can bear hydrogen or other substituents, such as alkyl, aryl or silyl groups. Up to 10 different substituents are possible on a metallocene. Different substituents change not only the size and shape of the Cp ligands but also the Cp-Mt-Cp distances and angles, and that affects the activity of the metallocenes and the properties of the polymers produced by these catalysts.[6]

Metallocenes used in olefin polymerization have been classified on the basis of their symmetry (see Figure 2.11). In class I two η^5-cyclopentadienyl ligands (represented by shaded rectangles) can be bridged or not; in the other classes they are bridged. In classes I and II, the two sites occupied by the η^5-ligands are bisected by a horizontal mirror plane and are therefore achirotopic; they are related by a twofold rotation axis in class III and are homotopic (equal). In class IV the two sites are related by a vertical mirror plane and are enantiotopic (mirror images of each other). No symmetry elements are present in class V, and the two sites are diastereotopic (different).[106-110]

Stellenbosch University http://scholar.sun.ac.za

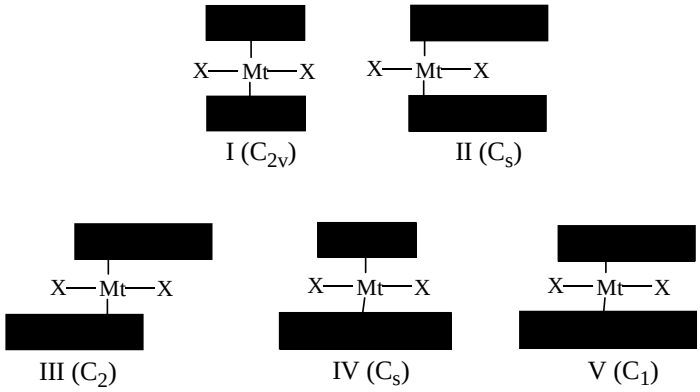

Figure 2.11: Classification of metallocene catalysts according to their symmetry.[107-110]

2.6.4 Mechanism of propylene polymerization using metallocene catalyst systems

The polymerization reaction of propylene using metallocenes is initiated by active centers of the metallocene catalysts. Active species (chain initiators) are ionic pairs containing cationic species, like Cp_2M^+–R. These species are either synthesized or are formed in the reaction between metallocene complexes, such as Cp_2ZrMe_2 or Cp_2ZrCl_2 and MAO.[111,112] The mechanism of propylene polymerization using metallocenes can be summarized by a number of reaction steps, which are initiation reactions, propagation reactions and transfer reactions.

2.6.4.1 Initiation reactions

The polymerization reaction starts when a propylene monomer coordinates to the transitional metal atom bearing a positive charge, and subsequently inserts into the Zr-Me bond (probably by Me migration), as shown in Scheme 2.1

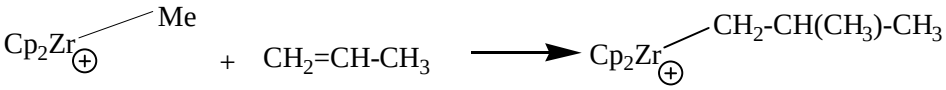

Scheme 2.1: Insertion of a propylene monomer to a Zr-Me bond.

2.6.4.2 Propagation reactions

The insertion of a propylene monomer in the metal carbon bond may take place in two different ways, as shown in Scheme 2.2.

Stellenbosch University http://scholar.sun.ac.za

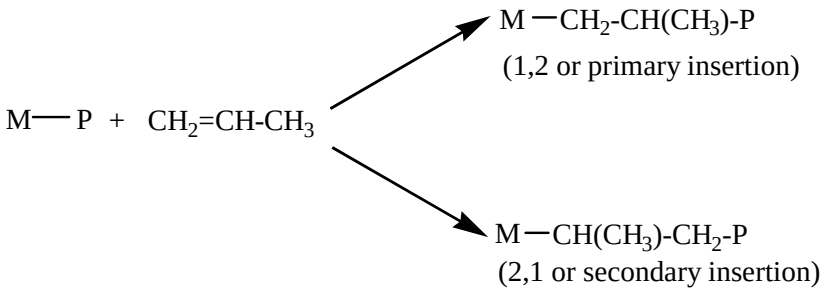

Scheme 2.2: Primary and secondary insertion of a propylene monomer in the metal-carbon bond.

It was proved by chain end-group analysis that the 1,2-insertion mode is predominant in isospecific polymerization of olefins using both heterogeneous[113,114] and metallocene-based[115,116] catalysts and in the syndiospecific polymerization of propylene using the homogeneous $Me_2C(Cp,F)ZrCl_2$/MAO catalysts system.[40] Isospecific polypropylene obtained using chiral C_2-symmetry group 4 metallocenes includes a small number (about 1%) of isolated regioirregular structural units resulting from 2,1- and 1,3-insertion of the monomer, as shown in Scheme 2.3.

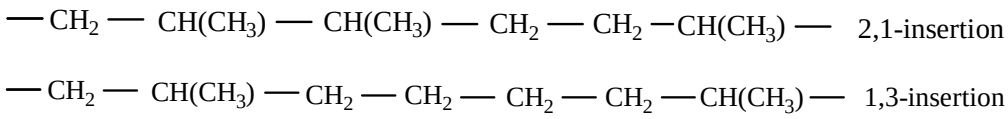

Scheme 2.3: 2,1- and 1,3-insertions in propylene polymerization.

Regioirregular insertions are revealed by the presence of $(CH_2)_2$ and $(CH_2)_4$ sequences in the polymer chain, respectively. The content of the two regioirregularities and their relative proportions depends on the π-ligands, polymerization temperature and monomer concentration.[117] In general, regioirregularities are mainly of the 2,1-type when the activity of the catalyst is very high.[109,118]

2.6.4.3 Transfer reactions

The investigation of transfer reactions is very important because these reactions determine the control of molecular weights and end-group structures of resultant polyolefins. In propylene polymerization using a metallocene catalyst/MAO, where no external terminating agents (such as hydrogen) are involved, β-hydride transfer reactions (either after a primary or a secondary propylene insertion), β-methyl transfer reactions, chain transfer to the aluminium

Stellenbosch University http://scholar.sun.ac.za

(mainly to trimethyl aluminium ($AlMe_3$) contained in MAO), and chain transfer to monomer constitute the entire set of chain transfer reactions. In general, β-hydride transfer reactions are predominant in metallocene catalyst systems.[6,119]

2.6.5 Influence of hydrogen on propylene polymerization

Hydrogen molecules are used to regulate the molecular weight of polyolefins prepared in the presence of both heterogeneous and metallocene catalysts.[117,120,121] Hydrogen response in metallocene-catalyzed propylene polymerization seems to be wide-ranging and reflects the strong dependence of the performance of metallocene catalysts on both their π-ligand structures and on the polymerization conditions. Addition of molecular hydrogen leads to different levels of molecular weight depression, depending on the hydrogen level, the concentration of the monomer, the type of catalyst and the polymerization temperature.[6] Catalyst productivity in the presence of hydrogen has been found to increase to a certain level, where after it remains constant, or is slightly decreased upon a further increase of partial hydrogen pressure. The hydrogen level required to reach maximum productivity is dependent on the nature of the catalyst. Productivity enhancement is mainly due to an increase of the initial polymerization rate; catalyst decay with time is either unaffected or slightly retarded by the presence of hydrogen.[122]

2.7 Fractionation techniques

To fractionate polymers produced using different catalyst systems, a number of methods described in the literature have been used for semi-crytalline polymers, including solvent-extraction, consecutive extraction with different solvents, fractionation with solvent/non-solvent pairs, consecutive extraction with a solvent at different temperatures,[65,123-125] and, more recently, temperature rising elution fractionation (TREF)[126-129] and crystallization analysis fractionation (CRYSTAF).[58,130-132] Recent developments in the field include new techniques such as crystallization elution fractionation (CEF)[133] and solution crsytallization analysis by laser light scattering (SCALLS).[134-136]

2.7.1 TREF

Shirayama *et al.*[137] were the first to use the expression “temperature rising elution fractionation” (TREF) in order to describe the method used to fractionate low-density polyethylene according to the degree of short-chain branching. The method was first

Stellenbosch University http://scholar.sun.ac.za

described by Desreux and Spiegels[138] when they recognized the possibility of achieving crystallization separation by elution at different temperatures. It was clearly noted that the elution of amorphous polymers under rising temperature conditions will cause fractionation on the basis of molecular weight, and not crystallinity. Size exclusion chromatography (SEC) is known to be used for the purpose of fractionation on the basis of molecular weight.[139] Consequently, little interest has been shown for the fractionation of amorphous polymers using TREF technique. TREF is a technique used for analyzing semi-crystalline polymers by separation of the molecular species according to their crystallizabilities. After the introduction of TREF by Desreux and Spiegels[138] a need for a more practical and capable system became clear. This led to the development of a system in which a polymer is crystallized onto a support in packed columns.[140]

There are two types of experimental TREF apparatus: analytical and preparative TREF. Analytical TREF is commonly automated. It is connected with other analytical instruments such as IR and SEC, and the structure of polymer fractions can be determined on-line. Preparative TREF is used to obtain a large amount of polymer fractions and the polymer fractions can be characterized off-line by NMR and/or DSC. Preparative TREF is time-consuming, but it usually provides more information than analytical TREF, and is often used for polypropylene.[141] Preparative TREF is a powerful tool, because the temperature for fractionation can be freely selected within a certain range. Preparative TREF fractionates polymers on the basis of crystallizability, and the TREF data directly reflects the tacticity of polypropylene.[126-128,142] In this context, TREF has gained increasing popularity over the past years. TREF has been used to probe the qualitative tacticity distribution that occurs upon modification of the catalyst.[127,142,143]

2.7.1.1 Fractionation set-up

The experimental set-up used for separation by TREF consists of two steps, the first is a slow cooling (crystallization) step and the second is a dissolution (elution) step, as shown in Figure 2.12. During the first step the hot polymer solution is cooled at a slow rate (6 °C or less per hour), thus resulting in controlled crystallization. The benefit of the cooling step was first recognised by Bergstrom, Avela and Wild.[144,145] Quick precipitation or normal cooling was used in earlier studies. To achieve reproducible fractionation, based on crystallizability, the crystallization step must be controlled. Slow cooling of the polymer solution can either occur on a support or in solution. Glass beads, Chromosorb P, silica gel, stainless steel balls and washed sea sand can all be used as supports.[145,146] The most crystalline polymer crystallizes

Stellenbosch University http://scholar.sun.ac.za

out of solution first, directly onto the support, followed by slightly less crystalline polymer. This continues until the least crystalline polymer (highly branched) crystallizes, thus effectively forming the so-called onion layers around the support (Figure 2.12, crystallization step). In the second step dissolution of the polymer at successively higher temperatures takes place (Figure 2.12, elution step). The increase in temperature can either be step-wise or a continuous temperature gradient.

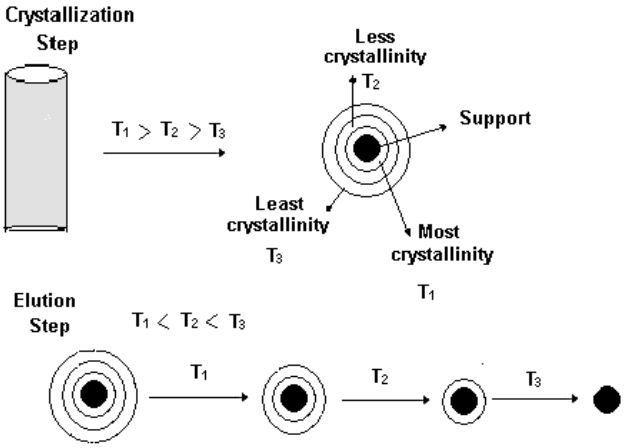

Figure 2.12: Schematic representation of the separation mechanism of TREF.

2.7.2 CRYSTAF

Crystallization analysis fractionation (CRYSTAF) is a relatively new technique for the analysis of the composition of polyolefin blends. After about only a decade since it was developed, CRYSTAF has become one of the most important characterization techniques in polyolefin characterization laboratories because it can be rapidly provides crucial information required for the understanding of polymerization mechanisms and structure–property relationships.[147,148] CRYSTAF fractionates blend components of different crystallizabilities by slow cooling of a polymer solution. During the crystallization step the concentration of the polymer solution is monitored as a function of temperature. Different from DSC, blends of polyolefins separated into the components and quantitative information can be obtained directly from the crystallization curves. Moreover, even very low quantities of one component in polyolefin blends can be quantified with good accuracy.

CRYSTAF was developed as an alternative to TREF. The two techniques are based on similar fractionation mechanisms and provide comparable results, but TREF operation is more time-

Stellenbosch University http://scholar.sun.ac.za

consuming because it involves two fractionation steps: crystallization and elution, while CRYSTAF requires only a single crystallization step.[149]

2.7.3 SCALLS

Solution crystallization by laser light scattering (SCALLS) is considered as one of the newest fractionation techniques for semi-crystalline polymers. It involves analysis of the turbidity of a polymer solution during cooling. In the past, turbidity measurements were focused on fractionating polyolefins based on molecular weight using either a solvent/non-solvent approach or a thermal gradient technique.[150] In 1966 Imhof studied a series of low-pressure ethylene–propylene copolymers and mixtures of ethylene homopolymers.[134] It was observed that the cloud point decreases with decreasing density and that turbidity could resolve blends of ethylene homopolymers. White light from a mercury lamp was used as a light source and the decrease in transmission of the light in the forward direction was measured by a light-scattering photometer.

Shan *et al*.[135] published an article describing how the short-chain branching distribution (SCBD) of polyethylene can be determined by a turbidimetric method. The technique involves the observation of the scattering of diode mercury laser lamp light after it passes through a polymer solution. The temperature of the polymer solution is controlled via a heating block which is subjected to a temperature ramp. As turbidity increases, the amount of laser light that can pass through the solution decreases, while the amount of scattering increases. An increase in turbidity occurs when the hot polymer solution is cooled and polymer starts to crystallize out of solution. The reverse of this process leads to the turbidity decreasing with an increase in temperature.

Compared to apparatus used for other analytical techniques such as CRYTAF and TREF, the SCALLS apparatus is simple to operate and is inexpensive (when compared to the cost of operation and maintenance of other fractionation instruments). Given the flexibility of the instrument, experiments can be designed to help further the understanding of the fractionation and crystallization of polymers. The simple equipment set-up and operation of SCALLS allows for the flexibility to perform crystallization experiments in different solvents. This is a distinct advantage over other techniques such as CRYSTAF and TREF, which mostly require use of TCB for its high temperature use and dissolution ability of polyolefins.[135]

Recently, van Reenen *et al*.[136] developed a similar apparatus which they used to examine several different polyolefins. They showed that SCALLS was able to differentiate between polymers of different chemical and morphological composition. Preliminary results indicated

Stellenbosch University http://scholar.sun.ac.za

that the experimental parameters played a big role in that set-up, which makes it difficult to compare chemically dissimilar polymers, but with chemically similar polymers, it is possible to compare materials. An apparent dependence of molecular weight during the solution crystallization of metallocene polypropylene samples was illustrated. Both cooling (crystallization from solution) and heating (melting and dissolution) experiments were successfully demonstrated, and it was shown that both cooling and heating rates, as well as polymer concentration, affected the molecular weight.

2.8 Polymer blends

Polyolefin blends have been studied comprehensively, with a view to improving the properties and processability of the polymers involved. The advantages of blends include, for example, improvements in impact strength, optical properties, low-temperature impact strength, rheological properties and overall mechanical behaviour. Blending is a natural manner to widen the range of properties of polymers. This is well illustrated by the history of polymer blends. In 1846 when only natural rubber (NR) and gutta percha (GP), were available, these were blended.[151] Once nitrocellulose (NC) was invented, its blend with NR was patented in 1865, three years before the commercialization of NC. In the 1960s, the major reason for blending was modification of a specific resin for a particular type of behaviour in most cases, improvement of impact strength. A while after that, blending was used for economic reasons; expensive engineering resins were diluted with commodity ones. During the 1980s, the processability of high temperature specialty resins was improved by blending. Presently, blending to prepare material with specific properties for envisaged applications.[151] The application of polymer blends has increased significantly and is expected to continue to grow. Of the total consumption of engineering polymers, more than 20 % is presently thought to be composed of blends, with important and various applications in the automotive, electrical and electronic industries, in computer and business equipment housings, in medical components, etc. Annually, about 4900 patents related to polymer blends are registered world wide.[151]

The properties and the morphology of the polyolefin blends have been systematically discussed in a series of papers published by Greco *et al.*[152-154] and D'Orazio *et al.*[155,156] The mechanical and thermal properties of PP/HDPE blends were first studied by Greco *et al.*[152] The addition of ethylene–propylene copolymers to polypropylene was reported by D'Orazio *et al.*[155] The authors specifically studied the morphology and mechanical properties of ternary PP/EPDM/HDPE blends on molded samples and extruded rods. In addition, blends of

Stellenbosch University http://scholar.sun.ac.za

isotactic and syndiotactic polypropylenes were studied.[157-161] Mulhaupt and coworkers[158] studied the behaviour of syndiotactic and isotactic polypropylene blends. In their work, the blends were made by solubilization of both polymers, mixing and precipitation. Results showed that, although phase separation can not be observed by microscopy, the crystallization of isotactic and syndiotactic polypropylene always occurs separately. The annealing treatment makes the phase separation, which confirms that blends of isotactic and syndiotactic polypropylene are completely phase separated. The morphology of the blends is widely influenced by crystallization kinetics. Mulhaupt and coworkers[157] also studied the influence of stereoregularity on miscibility of polypropylenes and concluded that atactic polypropylene is miscible with isotactic polypropylene but immiscible with syndiotactic polypropylene. On the other hand, Silvestri and Sgarzi[160] found that high molecular weight atactic polypropylene is partially miscible with syndiotactic polypropylene and immiscible with isotactic polypropylene, but the degree of tacticity of the components and the composition of blend can also affect miscibility, as does the molecular weight of the atactic polypropylene.

2.9 Mechanical properties

Polypropylene is a versatile material, whose stiffness, elasticity and transparency can be tailored by modifying the molecular architecture. Although today polymers are widely used in many structural products, given their low costs and ease of processing, the end use in engineering applications is often controlled by their macroscopic mechanical performance.

Among the advantages of semi-crystalline polymers, compared to amorphous ones, is that their maximum use temperature is set by the melting temperature rather than the glass transition temperature. A disadvantage is that the impact toughness of most of the polymers is low. A typical technique to increase impact toughness is rubber modification. The disadvantage, however, of adding rubber to a polymer system is, however, normally a further decrease in stiffness.

Over the past decade, much knowledge has been gathered on the relationship between molecular structure and mechanical behaviour of amorphous polymers. Although some of these concepts are also appropriate to semicrystalline polymers, the presence of a two phase, crystalline-amorphous structure yields more complex relationships, in which not only molecular constitution is important, but also microstructural aspects, e.g., the degree of crystallinity, crystal size, spherulite size and crystal orientation. These crystal micro-structures depend on molecular constitution, the presence of nucleating agents and, most strongly,

Stellenbosch University http://scholar.sun.ac.za

processing conditions, i.e. the thermal-mechanical history experienced by the polymer in the process.[162]. Molecular structure and mechanical properties of semicrystalline polymers have been extensively studied, but the focus was mostly on polyethylene and ethylene based copolymers.[163,164] In order to achieve as large as possible a variation in crystallinity and lamellar thickness, characteristics such as number of branches, molecular weight and type of comonomer were varied. The type of crystallization procedures were changed, ranging from solution to melt crystallization, and annealing processes at different concentrations, cooling rates and temperatures.

2.9.1 MH

Determination of microhardness (MH) involves the static penetration of a material with an indenter using a known force. The microhardness of a material is determined by dividing the load used by the residual deformation area on the surface of the material. It is basically a measure of the irreversible deformation processes characterising the material. There are two main zones of deformation in the material below the indenter: the plastic deformation zone and the larger elastic zone.[165]

Currently, the MH technique, being an almost non-destructive, sensitive and relatively simple method, enjoys extensive application. In addition to some methodological contributions to the technique, the MH method has been successfully used to gain a deeper understanding of the microhardness–structure correlation of polymers. A very attractive feature of this technique is that MH can be used for the micromechanical characterization of some components, phases or morphological entities that are otherwise not accessible for direct determination of their hardness and modulus.[166] These possibilities are very useful for the quantification of phase properties, for example, in semicrystalline polymorphic materials such as polypropylene, besides the most common α-modification of isotactic polypropylene, an amount of hexagonal β-modification often forms during polymer processing.

The amount of β-modification affects the mechanical properties; the material becomes tougher.[167] However, the β-phase is unstable upon stretching, which produces a transition to α-isotactic polypropylene.[168] With the α-phase, mechanical properties are changed, and knowledge of the phase properties and their interactions has an important practical meaning. This requires a measurement technique that enables the determination of phase and bulk properties on one specimen. The MH technique achieves this by controlling the indentation load or the indentation depth. MH is sensitive to morphological changes, as has been reported in a number of publications.[169-173] Some examples of polypropylene materials are given. One

Stellenbosch University http://scholar.sun.ac.za

can detect the glass transition temperature[169] and quantify the hardness and modulus of the α- and β-spherulites.[170] Some other works deal with the correlation between hardness and mechanical properties. Chua and Henderson[171] reported that creep modulus and MH have the same time dependence after different ageing times. MH increases linearly with the degree of crystallinity, and the elastic modulus is correlated to the MH by means of a power law.[172] Amitay-Sadovsky and Wagner[173] described the hardness and the modulus of transcrystalline polypropylene.

In the case of polymer blends, MH measurement is a useful tool for the assessment of the degree of interpenetrating of the blend components.[174] It has been shown that for blends of low- and high-density polyethylene[175] and for blends of poly(ethylene terephthalate) and poly(ethylene naphthalate), MH is an additive function of the MH values of the individual components of the blend. However, in blends of polyethylene/polypropylene and poly(butylene terephthalate)/polycarbonate a deviation from the additivity law was detected,[176,177] due to the changes in crystallinity as well as to the thickness of the crystals of the blend components. The negative deviation from the hardness additivity law for polyethylene/polypropylene gel blends has been explained by a crystallinity depression and by an increase in the surface free energy with composition.[174]

2.9.2 DMA

Dynamic mechanical analysis (DMA) is a well-established technique to demonstrate the relationship between crystallinity and elasticity. The technique can be defined as the application of an oscillated force to a sample and analysis of the materials response to the force. DMA can be used for the evaluation of storage modulus (E′), loss modulus (E″) and mechanical damping factor (tan δ).[178]

DMA methods have been widely used for investigating the structures and viscoelastic behaviour of polymeric materials for determining their considerable stiffness and damping characteristics for various applications. The dynamic properties of polymeric materials are of substantial practical significance for several reasons, particularly if they are determined over wide ranges of frequency and temperature. DMA over a wide range of temperatures and frequencies permits the determination of the viscoelastic behaviour of molten polymers and provides important insights into the relationship between structure, morphology and proportional properties of polymeric matrices and composites materials. The stress–strain response curves demonstrate the mechanical nature of the material.[179] Several studies on fiber-reinforced polypropylene composites based on structure–property relationships by

Stellenbosch University http://scholar.sun.ac.za

means of DMA are reported in the literature.[180-183]

Since fibre-reinforced thermoplastic materials experience various types of dynamic stress during service, studies of the viscoelastic properties of these materials are of great importance.[182-184] A significant amount of work has been reported on the viscoelastic properties of particulate and fibre-filled composites.[180,181,185] The dynamical mechanical properties of unidirectional composites are dependent on the fibre orientation.[186,187] Hence the performance of structural material can be measured by dynamic mechanical thermal analysis in the direction of fibre alignment at different volume fractions of fibres.[188] Carwalho and Bretas[189] investigated the relationship between interphase morphology and viscoelastic properties of thermoplastic carbon fibre composites. George *et al*.[190] studied the thermal properties of pineapple fibre low density polyethylene composites, with particular reference to the effect of fibre/matrix interface bonding. Kubat *et al*.[185] reported on the characterisation of interfacial interactions in high density polyethylene filled with glass spheres using DMA. Stricker *et al*.,[191] in their study on DMA, observed an unexpected thermal transition of glass bead-filled syndiotactic polypropylene at 54 °C. The signal intensity increased with increasing glass bead volume fraction and was not observed for a pure syndiotactic polypropylene.

In this study, mechanical analysis of the fractionated and blended materials as well as the polymers synthesized will be carried out via MH and DMA techniques. This will enable the investigation of the effect of molecular weight and tacticity on the mechanical properties of the fractionated and blended materials.

2.10 References

1. V. Busico, R. Cipullo, *Prog. Polym. Sci*. **2001**, 26, 443.
2. J. Huang, G. L. Rempel, *Prog. Polym. Sci*. **1995**, 20, 459.
3. K. Soga, T. Shiono, *Prog. Polym. Sci*. **1997**, 22, 1503.
4. E. P. Moore, Jr. *Polypropylene Handbook*, Hanser Publishers. Munich, **1996**, pp. 11-73.
5. H. Brintzinger, D. Fischer, R. Mülhaupt, B. Rieger. R. Waymouth, *Angew. Chem. Int. Ed.* **1995**, 34, 1143.
6. L. Resconi, L. Cavallo, A. Fait, F. Piemontesi, *Chem. Rev*. **2000**, 100, 1253.
7. J. Karger-Kocsis. *Polypropylene Structure, Blends and Composites*. 1st ed. Vol. 1. London: Chapman & Hall, **1995**, pp. 3-50.
8. P. Corradini, G. Natta, *Nuovo Cimento Soc*. **1960**, 1, 40.

Stellenbosch University http://scholar.sun.ac.za

9. F. van der Burgt. *Crystallization of isotactic polypropylene*. MSc. Thesis, Eindhoven University of Technology, **2002**.
10. S. Brückner, S. V. Meille, V. Petraccone, B. Pirozzi, *Prog. Polym. Sci*. **1991**, 16, 361.
11. F. C. Tsai, J. H. Chen, Y. H. Nien, P. H. Yeh, *Polymer* **2005**, 46, 5680.
12. G. Natta, *J. Polym. Sci*. **1959**, 34, 531.
13. G. Natta, P. Corradini, *Nuovo Cimento Supp*. **1960**, 15, 40.
14. C. De Rosa, F. Auriemma, T. Circelli, R. M. Waymouth, *Macromolecules* **2002**, 35, 3622.
15. G. Guerra, V. Petraccone, P. Corradina, C. DeRosa, R. Napolitano, B. Pirozzi, G. Giunchi, *J. Polym. Sci. Part B: Polym. Phys*. **1984**, 22, 1029.
16. C. De Rosa, G. Guerra, R. Napolitano, V. Pretaccone, B. Pirozzi, *Eur. Polym. J*. **1984**, 20, 937.
17. C. De Rosa, G. Guerra, R. Napolitano, V. Pretaccone, B. Pirozzi, *J. Therm. Anal*. **1985**, 30, 1331.
18. R. G. Alamo, G. M. Kim, L. Mandelkern, A. Lehtinen, R. Paukkeri, *Polymer* **1999**, 40, 3922.
19. B. Lotz, J. C. Wittmann, *Polymer* **1996**, 37, 4979.
20. H. Awaya, *Polymer* **1988**, 26, 591.
21. F. Auriemma, O. R. de Ballesteros, C. De Rosa, P. Corradini, *Macromolecules* **2000**, 33, 8764.
22. F. J. Padden, J. D. Keith, *J. Appl. Phys*. **1959**, 30, 1479.
23. S. Vleeshouwers, *Polymer* **1997**, 38, 3213.
24. D. Trifonova, J. Varga, G. J. Vancso, *Poylm. Bull*. **1998**, 41, 341.
25. E. Perez, D. Zucchi, M. C. Sacchi, F. Forlini, A. Bello, *Polymer* **1999**, 40, 675.
26. D. R. Ferro, S. V. Meille, S. Brückner, A. J. Lovinger, F. J. Padden, *Macromolecules* **1994**, 27, 2615.
27. D. C. Martin, W. Xu, E. M. Arrunda, *Polymer* **2005**, 46, 455.
28. W. Stocker, M. Schumacher, S. Graff, A. Thierry, J. C. Wittmann, B. Lotz, *Macromolecules* **1998**, 31, 807.
29. J. R. Isasi, L. Mandelkern, M. J. Galante, R. G. Alamo, *J. Polym. Sci., Part B: Polym. Phys*. **1999**, 57, 323.
30. W. Stocker, S. N. Magonov, H. J. Cantow, J. C. Wittmann, B. Lotz, *Macromolecules* **1993**, 26, 5915.
31. K. Mezghani, P. J. Phillips, *Polymer* **1997**, 38, 5725.
32. R. A. Campbell, P. J. Philips, *Polymer* **1993**, 34, 4809.
33. K. Mezghani, P. J. Philips, *Polymer* **1998**, 39, 3735.
34. B. Lotz, S. Graff, C. Straupé, J. C. Wittmann, *Polymer* **1991**, 32, 2903.
35. A. J. Lovinger, *J. Polym. Sci., Part B: Polym. Phys*. **1983**, 21, 97.
36. J. Suhm, *J. Mater. Chem*. **1998**, 8, 553.
37. R. Thomann, C. Wang, J. Kressler, R. Mulhaupt, *Macromolecules* **1996**, 29, 8425.
38. G. Natta, I. Pasquon, P. Corradini, M. Peraldo, M. Pegoraro, A. Zambelli, *Rend. Acad. Naz. Lincei*. **1960**, 28, 539.
39. G. Natta, I. Pasquon, A. Zambelli, *J. Am. Chem. Soc*. **1962**, 84, 1488.
40. J. A. Ewen, R. L. Johns, A. Razavi, J. D. Ferrara, *J. Am. Chem. Soc*. **1988**, 110, 6255.
41. J. Rodriguez-Arnold, Z. Bu, S. Z. Cheng, *J. Macromol. Sci., Rev. Macromol. Chem. Phys*. **1995**, C35, 117.
42. J. Schardl, L. Sun, S. Kimura, R. Sugimoto, *J. Plast. Film. Sheeting* **1996**, 12, 157.
43. G. Natta, P. Corradini, P. Ganis, *Makromol. Chem*. **1960**, 39, 238.
44. G. Natta, P. Corradini, P. Ganis, *J. Polym. Sci*. **1962**, 58, 1191.

Stellenbosch University http://scholar.sun.ac.za

45. G. Natta, M. Peraldo, G. Allegra, *Makromol. Chem*. **1964**, 75, 215.
46. P. Corradini, G. Natta, P. Ganis, P. Temussi, *J. Polym. Sci., Part C*. **1967**, 16, 2477.
47. B. Pirozzi, R. Napolitano, *Eur. Polym. J*. **1992**, 28, 703.
48. P. Corradini, R. Napolitano, V. Petraccone, B. Pirozzi, A. Tuzi, *Macromolecules* **1982**, 15, 1207.
49. R. Napolitano, B. Pirozzi, *Polymer* **1997**, 38, 4847.
50. B. Lotz, A. J. Lovinger, R. E. Cais, *Macromolecules* **1988**, 21, 2375.
51. Y. Chatani, H. Maruyama, K. Noguchi, T. Asanuma, T. Shiomura, *J. Polym. Sci., Part C*. **1990**, 28, 393.
52. Y. Chatani, H. Maruyama T. Asanuma, T. Shiomura, *J. Polym. Sci., Part B: Polym. Phys*. **1991**, 29, 1649.
53. C. De Rosa, F. Auriemma, P. Corradini, *Macromolecules* **1996**, 29, 7452.
54. C. De Rosa, F. Auriemma, *Prog. Polym. Sci*. **2006**, 31, 45.
55. C. De Rosa, M. C. Gargiulo, F. Auriemma, O. Ruiz de Ballesteros, A. Razavi, *Macromolecules* **2002**, 35, 9083.
56. R. Paukkeri, A. Lehtinen, *Polymer* **1993**, 34, 4075.
57. D. R. Burfield, P. S. Loi, Y. Doi, J. Mejzik, *J. Appl. Polym. Sci*. **1990**, 41, 1095.
58. L. Wild, T. R. Ryle, D. C. Knobeloch, I. R. Peat, *J. Polym. Sci., Polym. Phys. Ed*. **1982**, 20, 441.
59. E. Martuscelli, M. Pracella, L. Crispino, *Polymer* **1983**, 24, 693.
60. E. Martuscelli, M. Avella, A. L. Segre, E. Rossi, G. Di Drusco, P. Galli, T. Simonazzi, *Polymer* **1985**, 26, 259.
61. J. J. Janimak, S. Z. D. Cheng, *J. Polym. Eng*. **1991**, 10, 21.
62. S. Z. D. Cheng, J. J. Janimak, A. Zhang, E. T. Hsieh, *Polymer* **1991**, 32, 648.
63. J. J. Janimak, S. Z. D. Cheng, P. A. Giusti, E. T. Hsieh, *Macromolecules* **1991**, 24, 2253.
64. J. J. Janimak, S. Z. D. Cheng, A. Zhang, E. T. Hsieh, *Polymer* **1992**, 33, 728.
65. A. Lehtinen, R. Paukkeri, *Macromol. Chem. Phys*. **1994**, 195, 1539.
66. J. Xu, L. Feng, *Eur. Polym. J*. **1999**, 35, 1289.
67. J. Arranz-Andrés, B. Peña, R. Benavente, E. Perez, M. L. Cerrada, *Eur. Polym. J*. **2007**, 43, 2357.
68. J. Boor. *Ziegler-Natta Catalysts and Polymerizations*. Academic Press, New York, **1979**, pp. 1.
69. G. Natta, *Angew. Chem*. **1956**, 68, 393.
70. G. Natta, *Angew. Chem*. **1964**, 76, 553.
71. L. L. Böhm, *Angew. Chem. Int. Ed*. **2003**, 42, 5010.
72. G. Natta, G. Crespi, *J. Polym. Sci*. **1962**, 61, 83.
73. M. P. Stevens. *Polymer Chemistry: An Introduction*. 3rd ed. Oxford University: Oxford, **1999**.
74. A. Correa, F. Piemontesi, G. Morini, L. Cavallo, *Macromolecules* **2007**, 40, 9181.
75. E. Albizzati, U. Giannini, G. Morini, M. Galimberti, L. Barino, R. Scordamaglia, *Macromol. Symp*. **1995**, 89, 73.
76. C. Barbe, G. Cecchin, L. Noristi, *Adv. Polym. Sci*. **1987**, 81, 1.
77. L. Cavallo, S. Del Piero, J. Ducere, R. Fedele, A. Melchior, G. Morini, F. Piemontesi, M Tolazzi, *J. Phys. Chem. C* **2007**, 111, 4412.
78. J. V. Seppala, M. Harkonen, L. Luciani, *Makromol. Chem*. **1989**, 190, 2535.
79. J. C. Chadwick, A. Miedema, O. Sudmeijer, *Macromol. Chem. Phys*. **1994**, 195, 167.
80. J. C. Chadwick, G. M. van Kessel, O. Sudmeijer, *Macromol. Chem. Phys*. **1995**, 196, 1431.

Stellenbosch University http://scholar.sun.ac.za

81. J. C. Chadwick, G. Morini, G. Balbontin, I. Mingozzi, E. Albizzati, O. Sudmeijer, *Macromol. Chem. Phys*. **1997**, 198, 1181.
82. J. C. Chadwick, G. Morini, G. Balbontin, I. Camurati, J. R. Heere, I. Mingozzi, F. Testoni, *Macromol. Chem. Phys*. **2001**, 202, 1995.
83. P. C. Barbe, L. Noristi, G. Baruzzi, *Makromol. Chem*. **1992**, 193, 229.
84. G. Morini, E. Albizzati, G. Balbontin, I. Mingozzi, M. C. Sacchi, F. Forlini, I. Tritto, *Macromolecules* **1996**, 29, 5770.
85. J. Xu, L. Feng, S. Yang, Y. Yang, X. Kong, *Macromolecules* **1997**, 30, 7655.
86. B. Liu, T. Nitta, H. Nakatani, M. Terano, *Macromol. Chem. Phys*. **2003**, 204, 395.
87. H. Matsuoka, B. Liu, H. Nakatani, M. Terano, *Macromol. Rapid Commun*. **2001**, 22, 326.
88. H. Sinn, W. Kaminsky, *Adv. Oganomet. Chem*. **1980**, 18, 99.
89. A. Andersen, H. G. Cordes, J. Herwing, K. Kaminsky, A. Merck, R. Mottweiler, J. Pein, H. Sinn, H. J. Vollmer, *Angew. Chem. Int. Ed*. **1976**, 15, 630.
90. G. Wilkinson, M. Rosenblum, M. C. Whiting, R. B. Woodward, *J. Am. Chem. Soc*. **1952**, 74, 2125.
91. G. Martínez, P. Royo, M. E. G. Mosquera, *J. Organomet. Chem*. **2004**, 689, 4395.
92. W. Kaminsky, *Pure Appl. Chem*. **1998**, 70, 1229.
93. G. G. Hlatky, *Chem. Rev*. **2000**, 100, 1347.
94. G. G. Hlatky, *Coord. Chem. Rev*. **1999**, 181, 243.
95. G. Natta, P. Pino, G. Mazzanti, U. Giannini, *J. Am. Chem. Soc*. **1957**, 79, 2975.
96. D. S. Breslow, N. R. Newburg, *J. Am. Chem. Soc*. **1957**, 79, 5072.
97. K. H. Reichert, K. R. Meyer, *Macromol. Chem*. **1973**, 169, 163.
98. H. Sinn, W. Kaminsky, H. J. Vollmer, R. Woldt, *Angew. Chem., Int. Ed*. **1980**, 19, 390.
99. F. R. P. Wild, M. Wasiucionek, G. Huttner, H. H. Brintzinger, *J. Organomet. Chem*. **1985**, 288, 63.
100. W. Kaminsky, M. Arndt, *Adv. Polym. Sci*. **1997**, 127, 143.
101. Z. Bartczak, V. Chiono, M. Pracella, *Polymer* **2004**, 45, 7549.
102. K. Nishii, T. Ikeda, M. Akita, , T. Shiono, *J. Mol. Catal*. **2005**, 231, 241.
103. W. Kaminsky, *Catal. Today* **2000**, 62, 23.
104. M. Bochmann, *J. Organomet. Chem*. **2004**, 689, 3982.
105. N. J. Long, *Metallocenes*, Blackwell Science Ltd. **1998**.
106. F. Auriemma, C. De Rosa, T. Boscato, P. Corradini, *Macromolecules* **2001**, 34, 4815.
107. R. Schmidt, H. G. Alt, *J. Organomet. Chem*. **2001**, 621, 304.
108. D. T. Mallin, M. D. Rausch, J. C. W. Chien, B. Rieger, X. Mu, *Macromolecules* **1990**, 23, 3559.
109. W. Spaleck, F. Küber, B. Bachmann, M. Antberg, V. Dolle, J. Rohrmann, A. Winter, E. F. Paulus, *Organometallics* **1994**, 13, 954.
110. S. Lin, R. M. Waymouth, *Acc. Chem. Res*. **2002**, 35, 765.
111. X. Yang, C. L. Stern, T. J. Marks, *Organometallics* **1991**, 10, 840.
112. A. Zambelli, A. Grassi, P. Loungo, *Macromolecules* **1989**, 22, 2186.
113. A. Zambelli, P. Locatelli, M. C. Sacchi, I. Tritto, *Macromolecules* **1982**, 15, 831.
114. M. C. Sacchi, I. Tritto, P. Locatelli, *Prog. Polym. Sci*. **1991**, 16, 331.
115. J. A. Ewen, *J. Am. Chem. Soc*. **1984**, 106, 6355.
116. A. Zambelli, P. Ammendola, A. Grassi, P. Loungo, A. Proto, *Macromolecules* **1986**, 19, 2703.
117. V. Busico, R. Cipullo, J. C. Chadwick, J. F. Modder, O. Sudwiejer, *Macromolecules* **1994**, 27, 7538.

Stellenbosch University http://scholar.sun.ac.za

118. U. Stehling, J. Diebold, R. Kirsten, W. Roll, H. H. Brintzinger, S. Jungling, R. Mulhaupt, F. Langhauser, *Organometallics* **1994**, 13, 964.
119. G. Fan, J. Y. Dong, *J. Mol. Catal*. **2005**, 236, 246.
120. P. Pino, P. Cioni, J. Wei, *J. Am. Chem. Soc*. **1987**, 109, 6189.
121. A. Carvill, I. Tritto, P. Locatelli, M. C. Sacchi, *Macromolecules* **1997**, 30, 7056.
122. E. P. Moore, Jr. *Polypropylene Handbook*, Hanser Publishers. Munich, **1996**, pp. 77.
123. R. Paukkeri, E. Iiskola, A. Lehtinen, H. Salminen, *Polymer* **1994**, 35, 2636.
124. R. Paukkeri, A. Lehtinen, *Polymer* **1994**, 35, 1673.
125. R. Paukkeri, T. Väänänen, A. Lehtinen, *Polymer* **1993**, 34, 2488.
126. J. Xu, Y. Yang, L. Feng, X. Kong, S. Yang, *J. Appl. Polym. Sci*. **1996**, 62, 727.
127. X. Kong, Y. Yang, J. Xu, L. Feng, S. Yang, *Eur. Polym. J*. **1998**, 34, 431.
128. J. B. P. Soares, A. E. Hamielec, *Polymer* **1995**, 36, 1639.
129. P. Viville, D. Daoust, A.M. Jonas, B. Nysten, R. Legras, M. Dupire, J. Michel, G. Debras, *Polymer* **2001**, 42, 1953.
130. B. Monrabal, *J. Appl. Polym. Sci*. **1994**, 52, 491.
131. H. Pasch, R. BrüIl, U. Wahner, B. Monrabal, *Macromol. Mater. Eng*. **2000**, 279, 46.
132. J. R. BrülI, H. Pasch, H. G. Raubenheimer, R. D. Sanderson, A. J. van. Reenen, U. M. Wahner, *Macromol. Chem. Phys*. **2001**, 202, 1281.
133. B. Monrabal, J. Sancho-Tello, N. Mayo, L. Romero, *Macromol. Symp*. **2007**, 257, 71.
134. L. G. Imhof, *J. Appl. Polym. Sci*. **1966**, 10, 1137.
135. C. P. Shan, W. A. de Groot, L. G. Hazlitt, D. Gillespie, *Polymer* **2005**, 46, 11755.
136. A. J. van Reenen, E. G. Rohwer, P. Walters, M. Lutz, M. Brand, *J. Appl. Polym. Sci*. **2008**, 109, 3238.
137. K. Shirayama, T. Okada, S. Kita, *J. Polym. Sci. A-2* **1965**, 3, 907.
138. V. Desreux, M. C. Spiegels, *Bull. Soc. Chim. Belg*. **1950**, 59, 476.
139. J. C. Moore, J. *Appl. Polym. Sci. A* **1964**, 2, 835.
140. N. S. Schneider, *J. Polym. Sci. C* **1965**, 8, 179.
141. J. Xu, L. Feng, *Eur. Polym. J*. **2000**, 36, 867.
142. M. Kioka, H. Makio, A. Mizuno, N. Kashiwa, *Polymer* **1994**, 35, 580.
143. J. B. P. Soares, A. E. Hamielec, *Polymer* **1996**, 37, 4607.
144. C. Bergstrom, E. Avela, *J. Appl. Polym. Sci*. **1979**, 23, 163.
145. L. Wild, *Adv. Polym. Sci*. **1990**, 98, 1.
146. G. Glockner, *J. Appl. Polym. Sci.: Appl. Polym. Symp*. **1990**, 45, 1.
147. J. Tomba, M. Carella, J. Pastor, *J. Polym. Sci., Part B: Polym. Phys*. **2005**, 43, 3083.
148. S. Anantawaraskul, J. B. P. Soares, P. M. Wood-Adams, *Macromol. Symp*. **2004**, 206, 57.
149. L. J. D. Britto, J. B. P. Soares, A. Penlidis, B. Monrabal, *J. Polym. Sci., Part B: Polym. Phys*. **1999**, 37. 539.
150. L. W. Gamble, W. T. Wipke, T. Lane, *J. Appl. Polym. Sci*. **1965**, 9, 1503.
151. L. A. Utracki (Ed). *Polymer Blends Handbook*. Vol. 1. Kluwer Academic Publishers: Dordrech/ Boston/London. **2003**, pp. 1-122.
152. R. Greco, C. Mucciariello, G. Ragosta, E. Martuscelli, *J. Mat. Sci*. **1980**, 15, 845.
153. R. Greco, C. Mancarella, E. Martuscelli, G. Ragosta, J. Yin, *Polymer* **1987**, 28, 1922.
154. R. Greco, C. Mancarella, E. Martuscelli, G. Ragosta, J. Yin, *Polymer* **1987**, 28, 1929.

Stellenbosch University http://scholar.sun.ac.za

155. L. D'Orazio, R. Greco, C. Mancarella, E. Martuscelli, G. Ragosta, C. Sylvestre, *Polym. Eng. Sci*. **1982**, 22, 536.
156. L. D'Orazio, R. Greco, E. Martuscelli, G. Ragosta, *Polym. Eng. Sci*. **1983**, 23, 489.
157. R. Thomann, J. Kressler, B. Rudolf, R. Mulhaupt, *Polymer* **1996**, 37, 2635.
158. R. Thomann, J. Kressler, S. Setz, C. Wang, R. Mulhaupt, *Polymer* **1996**, 37, 2627.
159. R. Brüll, V. Grumel, H. Pasch, H. G. Raubenheimer, R. Sanderson, U. M. Wahner, *Macromol. Symp*. **2002**, 178, 81.
160. R. Silvestri, P. Sgarzi, *Polymer* **1998**, 39, 5871.
161. G. Singh, S. Kaur, A. V. Kothari, D. G. Naik, P. B. Vyas, V. K. Gupta, *J. Appl. Polym. Sci*. **2009**, 113, 3181.
162. H. E. H. Meijer, L. E. Govaert, *Prog. Polym. Sci*. **2005**, 30, 915.
163. M. Takayanagi, K. Imada, T. Kajiyama, *J. Polym. Sci., Part C* **1966**, 15, 263.
164. J. C. Halpin, J. L. Kardos, *J. Appl. Phys*. **1972**, 43, 2235.
165. F. J. Balta-Calleja, *Adv. Polym. Sci*. **1985**, 66, 117.
166. S. Seidler, T. Koch, *J. Macromol. Sci., Phys*. **2002**, B41, 851.
167. M. Raab, J. Kotek, W. Grellmann, *J. Appl. Polym. Sci*. **1998**, 69, 2255.
168. M. Krumova, J. Karger-Kocsis, F. J. Balta-Calleja, S. Fakirov, *J. Mater. Sci*. **1999**, 34, 2371.
169. B. Martin, J. M. Perena, J. M. Pastor, J. A. de Saja, *J. Mater. Sci. Lett*. **1986**, 5, 1027.
170. T. Labour, L. Ferry, C. Gauthier, P. Hajji, G. Vigier, *J. Appl. Polym. Sci*. **1999**, 74, 195.
171. S. M. Chua, P. J. Henderson, *J. Mater. Sci. Lett*. **1991**, 10, 1379.
172. V. Lorenzo, J. M. Perena, F. G. Fatou, *J. Mater. Sci. Lett*. **1989**, 8, 1455.
173. E. Amitay-Sadovsky, H. D. Wagner, *J. Polym. Sci., Part B: Polym. Phys*. **1999**, 37, 523.
174. F. J. Balta-Calleja, C. Santa Cruz, C. Sawatari, T. Asano, *Macromolecules* **1990**, 23, 5352.
175. J. Martinez-Salazar, F. J. Balta-Calleja, *J. Mater. Sci. Lett*. **1985**, 4, 324.
176. F. J. Balta-Calleja, L. Giri, Z. Roslaniec, T. Ezquerra, *J. Macromol. Sci., Phys*. **1997**, B36, 335.
177. F. Ania, J. Martinez-Salazar, F. J. Balta-Calleja, *J. Mater. Sci*. **1989**, 24, 2934.
178. K. Jayanarayanan, S. Thomas, K. Joseph, *Composites: Part A* **2008**, 39, 164.
179. M. A. Lopez-Manchado, M. Arroyo, *Polymer* **2000**, 41, 7761.
180. R. Schledjewski, J. Karger-Kocsis, *J. Thermoplast. Compos. Mater*. **1994**, 7, 270.
181. J. I. Kroschwitz (Ed). *Encyclopedia of Polymer Science and Engineering*. 2nd ed. Vol. 5. New York: Wiley, **1989**, p. 300.
182. J. M. Felix, P. Gatenholm. *J. Appl. Polym. Sci*. **1993**, 50, 699.
183. A. Amash, P. Zugenmaier, *J. Appl. Polym. Sci*. **1997**, 63, 1143.
184. J. George, K. Joseph, S. S. Bhagavan, S. Thomas, *Mater. Lett*. **1993**, 18, 163.
185. J. Kubat, M. Rigdahl, N. I. Welander, *J. Appl. Polym. Sci*. **1990**, 39, 1527.
186. K. Joseph, S. Thomas, C. Pavithran, *J. Reinf. Plast. Compos*. **1993**, 12, 139.
187. K. Joseph, S. Thomas, C. Pavithran, *Mater. Lett*. **1992**, 15, 224.
188. P.V. Joseph, G. Mathew, K. Joseph, G. Groeninckx, S. Thomas, *Composites: Part A* **2003**, 34, 275.
189. W. S. Carwalho, R. E Bretas, *Eur. Polym. J*. **1990**, 26, 817.
190. J. George, S. S. Bhagavan, S. Thomas, *J. Therm. Anal*. **1996**, 47, 1121.
191. F. Stricker, R. D. Maier, M. Bruch, R. Thomann, R. Mulhaupt, *Polymer* **1999**, 40, 2077.

Stellenbosch University http://scholar.sun.ac.za

CHAPTER 3

Fractionation and crystallization of isotactic polypropylenes prepared using a heterogeneous transition metal catalyst

3.1 Introduction

A series of polypropylenes was prepared by slurry polymerization using a $MgCl_2$-supported transition metal catalyst. Two different external donors (EDs) were used: diphenyl dimethoxysilane (DPDMS) and methylphenyl dimethoxysilane (MPDMS). The molecular weight of the polypropylenes was controlled using molecular hydrogen. In order to establish a correlation between the molecular weight and the crystallization of polypropylene polymers fractionation of the materials according to their crystallizability was performed by means of TREF. This affords the opportunity for blending materials of differing molecular weights but similar symmetry.

3.2 Experimental

3.2.1 Materials

Propylene was obtained from Sigma-Aldrich and used without any purification. High purity argon and hydrogen were obtained from Afrox (South Africa). Toluene (Sigma-Aldrich) was dried by refluxing over sodium/benzophenone and then distilling under an inert gas atmosphere. Triethylaluminium (TEA) was obtained from Sigma-Aldrich. A commercial Ziegler-Natta catalyst with 2.78 wt % Ti content was purchased from Star Chemicals & Catalysts Co. (China). The EDs, DPDMS and MPDMS were obtained from Fluka and used as received.

3.2.2 Polymerization procedure

All polymerization reactions were carried out under an inert gas atmosphere. The polymerization reactions were carried out in a 350-ml stainless steel Parr autoclave with a gas inlet and pressure gauge. Typically the reactor was charged with the catalyst (43 mg, Ti content 2.78 wt%), TEA (2 mmol, Al/Ti mole ratio 80) and ED (0.091 ml in the case of DPDMS and 0.072 ml in the case of MPDMS, Al/Si mole ratio 5) in toluene (25 ml). The catalyst solution was stirred for 5 min and then the propylene was added. The reactor was

Stellenbosch University http://scholar.sun.ac.za

pressurized with hydrogen and the contents stirred for 1 h at room temperature. The reaction was then quenched by the addition of 100 ml 10% HCl/MeOH. The resulting polymer was filtered off, washed several times with methanol, and subsequently dried under vacuum at 80 °C for 15 h, to yield about 3–5 g of polypropylene as a white powder.

3.2.3 TREF technique

A preparative TREF apparatus built in-house[1] was used to fractionate polymers during this study. The TREF technique is based on two separate steps, namely the crystallization step and the elution step.

3.2.3.1 The crystallization step

The crystallization setup of the TREF technique is illustrated in Figure 3.1. The polypropylene (3 g) and Irganox 1010 stabilizer (2 wt %) were first dissolved in 300 ml xylene at 130 °C in a stirred glass reactor. The reactor containing the dissolved polymer and stabilizer was then quickly transferred to a large oil bath which had been preheated by a computerized temperature controller to the same temperature. Another three polymer samples were dissolved in the same way and also placed in the large oil bath as explained. In this way four different batches of polymer could be cooled simultaneously. The inert support (washed sand, white quartz 50–70 mesh) was also preheated to 130 °C in order to prevent premature crystallization. The hot sand was then added to the reactor in sufficient amounts to prevent polymer from crystallizing in solution and not on the support. The entire oil bath was then cooled at a rate of 1 °C/h from 130 °C to room temperature (20 °C).

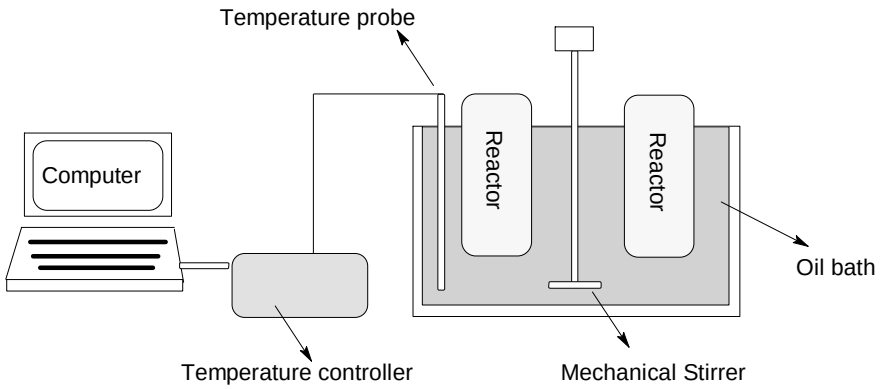

Figure 3.1: The setup used for the TREF crystallization step.

Stellenbosch University http://scholar.sun.ac.za

3.2.3.2 The elution step

The elution process followed the crystallization step. The elution step involves the transfer of the polymer and support to a stainless steel column, length 15 cm and internal diameter 7.5 cm, as illustrated in Figure 3.2.

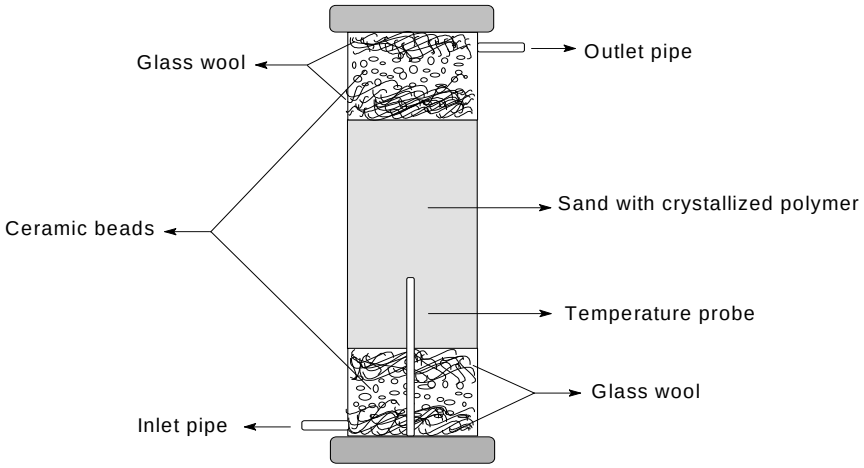

Figure 3.2: Illustration of the column packing for the TREF elution step.

The layers of glass wool and ceramic beads at the top and bottom of the column were used to prevent preferential solvent channeling by breaking up the solvent flow. The column was equipped with a temperature probe that measured the temperature in the centre of the packed column. The column was then placed inside a temperature controlled oven and connected to a xylene inlet and outlet. In this way the exact fractionation temperature for each eluted fraction could be monitored. A pump controlled the flow of solvent through the column at a constant rate.

The outlet pipe from the column was covered with a heating tape set to 130 °C in order to prevent deposition of the fractions onto the cold pipe during the collection of the fractions. The temperature of the oven was kept at the specific elution temperature until the temperature inside the column and the GC oven reached the desired elution temperature before the elution took place. Fractions were taken at various temperatures, depending on the number of fractions that were required. The xylene was removed from each fraction under reduced vacuum on a rotary evaporator. Fractions were then further isolated in a vacuum oven at 50 °C in order to remove any excess xylene.

Stellenbosch University http://scholar.sun.ac.za

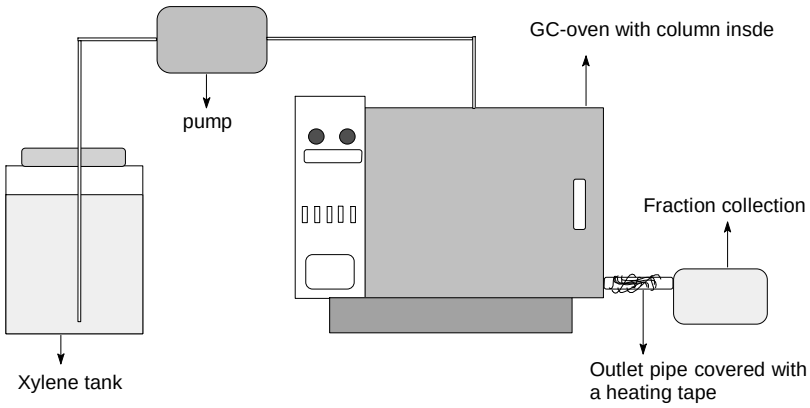

Figure 3.3: The TREF elution set-up.

3.2.4 Characterization

3.2.4.1 ^{13}C NMR

^{13}C NMR spectra were recorded at 120 °C on a 600 Varian Unity Inova NMR spectrometer equipped with an Oxford magnet (14.09 T), operating at 600 MHz, using a 5 mm inverse detection PFG probe. The pulse angle was 90°, the relaxation delay time was 15 sec, and the acquisition time was 1.8 sec. Resolution and accuracy were improved by zero-filling the data once before performing the Fourier transformation. Baseline correction was also applied in order to further enhance the accuracy and repeatability of the integrals measured for selected peaks in the spectra. Samples (60–80 mg) for ^{13}C NMR analyses were dissolved at 110 °C in a 9:1 mixture of 1,2,4,-trichlorobenzene (TCB) and benzene-d_6 (Bz_6).

In order to obtain useful spectra, samples need to be homogenous and without any defects or voids. This becomes even more crucial when running NMR spectra on higher resolution NMR spectrometers (600 MHz), since any inhomogeneity in the sample results in the validity and even the quality of data acquisition being suspect. In the present study, various solvents and different conditions with the available facilities and were used in order to optimize the quality of the spectra under existing condition. Weighed polymer samples were placed at the bottom of an NMR tube, and 0.5–0.8 ml deuterated solvent was added gradually, to allow the polymer to swell and dissolve. Samples were then heated to the desired temperature (120 °C) for two hours in an oil bath before recording the spectra.

Stellenbosch University http://scholar.sun.ac.za

3.2.4.2 HT-GPC

The number average molecular weight ($\overline{M_n}$), weight average molecular weight ($\overline{M_w}$) and molecular weight distribution (MWD) were determined by using high-temperature gel permeation chromatography (HT-GPC). Samples were analyzed with a PL-GPC 220. A flow rate of 1.0 ml/min was used. Columns packed with a polystyrene/divinylbenzene copolymer (PL gel MIXED-B [9003-53-6]) from Polymer Laboratories were used. A 50 mm guard column was also used. The length and diameter of these columns were 1200 mm and 7.5 mm, respectively. The particle size was 10 µm. The analyses were carried out in TCB, stabilized with 0.0125% 2,6-di-tert-butyl-4-methylphenol (BHT), as solvent, at 140 °C. The calibration was done with monodisperse polystyrene standards (EasiCal from Polymer Laboratories). The detector used was a differential refractive index detector.

3.2.4.3 DSC

The melting points and the degree of crystallinity were determined on a TA Instruments Q100 DSC. It was first calibrated by measuring the melting temperature of indium metal according to a standard procedure. All measurements were conducted under a nitrogen atmosphere, and at a purge gas flow rate of 50 ml/min. Three cycles were performed for each sample. First the samples were heated in crimped aluminium pans from -30 °C to 220 °C at a rate of 10 °C/min. Samples were then cooled from 220 °C to -30 °C. The peak crystallization temperature, T_c (DSC), was determined from the cooling cycle. Finally, the samples were heated for a second time at rate of 10 °C/min to 220 °C. This was done to determine the peak melting temperature, T_m, from the peak maximum of the second heating cycle.

3.2.4.4 WAXD

Wide-angle X-ray diffraction (WAXD) analysis was performed at iThemba LABS (South Africa) on a Bruker AXS D8 Advance diffractometer at room temperature with filtered CuKα radiation. All samples were scanned at 2θ angles, ranging from 6° to 50°, with a sampling width of 0.02°, where 2θ is the diffraction angle.

3.2.4.5 FT-IR

Fourier-transform infrared spectroscopy (FT-IR) was used to determine the crystallinity and tacticity of polypropylene polymers. Infrared spectra of the polypropylene samples were recorded on a Perkin Elmer FT-IR spectrometer (model Paragon 1000 PC). This instrument is

Stellenbosch University http://scholar.sun.ac.za

a single-beam Fourier-transform IR spectrometer with a FS-DTGS-Detector, 32 bit processor and IRDM software (resolution better than 1 cm^{-1}). All samples were recorded from 350 to 4 700 cm^{-1} by using a photo-acoustic detector (PAS).

3.3 Results and discussion

3.3.1 Characterization of the non fractionated polypropylenes

As mentioned in Section 3.2.2, a series of polypropylenes was prepared by slurry polymerization using a $MgCl_2$-supported transition metal catalyst. The reaction conditions were kept constant for all the polymerization reactions. The characteristics of these polypropylenes prepared in the absence and presence of the two different EDs, DPDMS and MPDMS, and in the presence of different amounts of hydrogen, are summarized in Table 3.1.

Table 3.1: Results of propylene polymerizations carried out with DPDMS, MPDMS and various concentrations of hydrogen[a]

Runs	ED	H_2 (wt %)	Activity (kg PP/(g Ti.h))	M_w[d]	M_w/M_n	*mmmm* %[e]	T_m (°C)	T_c (°C)	ΔH_m[f] (J/g)	X_c (%)
Z13	None	0.0	2.5	388 428	11.4	55.0	158.8	116.2	62.7	30.0
Z14	None	0.2	2.8	215 397	5.9	86.0	157.5	119.8	90.5	43.0
Z15	None	0.6	3.1	137 965	5.6	87.0	156.4	118.7	83.9	40.0
Z16	None	1.4	3.2	97 587	9.3	88.0	157.2	121.3	88.3	42.0
Z17	None	2.0	1.9	65 498	8.2	93.0	156.5	120.8	100.5	48.0
Z6	DPDMS[b]	0.0	1.6	1 105 416	6.6	87.0	160.6	114.0	77.8	37.0
Z5	DPDMS	0.2	4.7	312 580	4.1	96.0	161.9	118.4	108.9	52.0
Z4	DPDMS	0.6	4.1	252 956	5.4	94.0	160.6	116.5	103.9	50.0
Z3	DPDMS	1.4	1.4	184 759	6.1	93.0	161.2	124.2	104.5	50.0
Z2	DPDMS	2.0	0.4	135 115	4.8	92.0	159.3	121.9	102.0	49.0
Z7	MPDM[c]	0.0	2.9	1 047 184	4.6	86.0	158.5	114.1	89.5	43.0
Z8	MPDM	0.2	3.3	228 960	6.4	94.0	162.0	124.4	103.9	50.0
Z9	MPDM	0.6	3.6	164 327	5.4	97.0	161.1	122.4	118.6	57.0
Z10	MPDM	1.4	2.7	147 528	6.0	96.0	160.4	121.6	110.0	53.0
Z12	MPDM	2.0	2.0	96 137	9.4	90.0	159.2	121.2	114.4	55.0

[a] propylene polymerization was carried out in toluene at room temperature for 1 h using different concentrations of hydrogen.
[b] diphenyl dimethoxysilane (Al/Ti molar ratio 80).
[c] methylphenyl dimethoxysilane (Al/Ti molar ratios 80).
[d] determined by GPC.
[e] determined by ^{13}C NMR.
[f] determined by DSC.

Stellenbosch University http://scholar.sun.ac.za

3.3.1.1 Activity

The effect of the hydrogen concentration on the catalyst activity is shown in Figure 3.4. As expected, the presence of hydrogen caused an increase in polymerization activity in the presence of both EDs. Polymerization activity in the presence of DPDMS as ED increased up to 3-fold in the presence of 0.2 wt % of hydrogen, from 1.6 to 4.7 kg PP/(g Ti.h), while it increased up to 1.5-fold in the presence of 0.6 wt % of hydrogen in the case of MPDM. The most common explanation for this activating effect is the regeneration of an active species from the "dormant sites" formed after a regio-irregular olefin insertion (2,1-insertion).[2-4] A slight decrease in the catalyst activity is caused by further increasing the hydrogen content. This decrease could be as a result of the retarded level of propylene insertion into the Ti-C bond of the growing chain due to the high hydrogen level, depending on the nature of the catalyst.

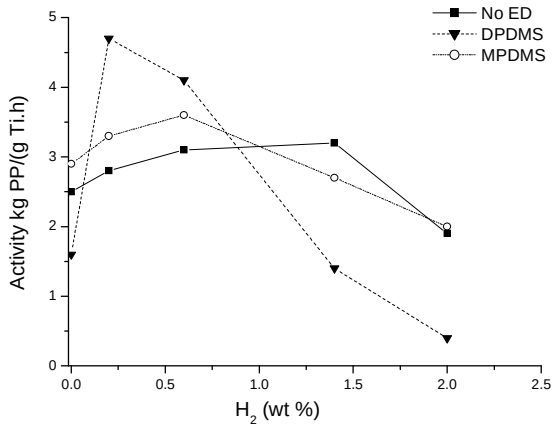

Figure 3.4: Activity (kg PP/(g Ti.h)) of propylene polymerization as a function of the added hydrogen concentrations.

In the absence of EDs, only a slight increase in catalyst activity with increasing hydrogen concentration is seen (Figure 3.4). Several authors have reported similar results,[5-8] and Chadwick *et al.*[9] remarked that the magnitude of the hydrogen activation effect observed with the $TiCl_4$/phthalate ester/$MgCl_2$ catalyst was affected by the type of alkoxysilane used as the ED in the polymerization.

Stellenbosch University http://scholar.sun.ac.za

3.3.1.2 Microstructure

The results in Table 3.1 illustrate that the stereoregularity of the isotactic polypropylene samples, as indicated by the *mmmm* pentad content, is dependent on the type of the ED present in the catalyst system. The microstructure of the isotactic polypropylene samples was analyzed by solution ^{13}C NMR. Various researchers have reported different results for different systems.[10-14] From Table 3.1 and Figure 3.5 it is clear that the effect of hydrogen is twofold: we see a noticeable increase in tacticity in all cases when hydrogen is used versus those cases where hydrogen is not used. Furthermore, isotactic stereoregularity of the polymers produced in the presence of the EDs indicates a high proportion of isotactoid sequences. It is likely that the EDs block the aspecific sites of the catalyst, leading to an increase in tacticity.

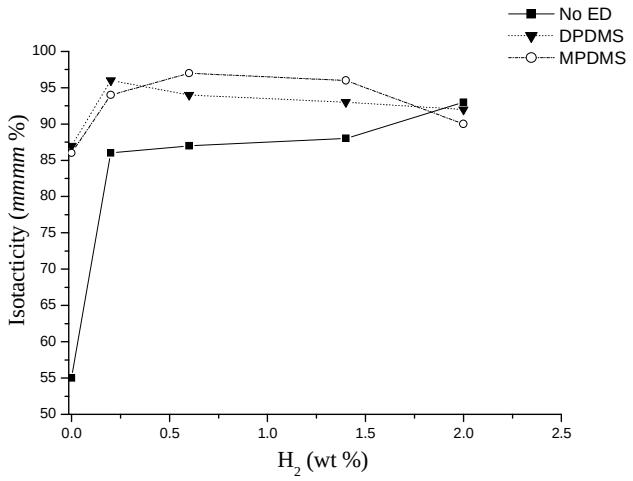

Figure 3.5: Dependence of the isotacticity of polypropylenes, on hydrogen concentration, prepared in the presence and absence of EDs.

The results in Table 3.1 and Figure 3.5 are in agreement with the results obtained by Harkonen *et. al.*[15] They proved that the high stereospecificity obtained using silanes that have one or more bulky hydrocarbyl groups is due to the silane stabilizing "fluctuating" isospecific sites; the bulky hydrocarbyl groups protect the silane from removal from the catalyst surface via complexation with aluminium alkyl. It is clear that some aspecific active sites were converted into isospecific active sites by the addition of the EDs. Based on the results presented above, it can be postulated that the active sites of the $MgCl_2$-supported Ziegler-Natta catalyst can be classified into three types: (i) isospecific titanium species, which are not affected by their local environment and produce polypropylene of high isotacticity, (ii)

Stellenbosch University http://scholar.sun.ac.za

aspecific titanium species, which produce atactic polypropylene, and (iii) sterically hindered aspecific titanium species, which preferably produce a polymer of moderate and high isotacticity. The EDs sterically affect a coordination vacancy of each aspecific titanium species and, consequently, transfers it into an isospecific active site of high isospecificity.

3.3.1.3 Molecular weight and molecular weight distribution

Figure 3.6 shows the relationship between the amount of molecular hydrogen added and the molecular weights of polypropylene samples. It is noted that a large decrease in molecular weight is obtained upon the addition of a small amount of hydrogen to the polypropylenes prepared using both types of ED, but significantly more hydrogen must be added in order to decrease the molecular weight further, and this becomes increasingly difficult as the hydrogen concentration increases. The limited ability of hydrogen to control the molecular weight of polypropylene at high hydrogen concentrations has been discussed in detail by Kissin *et al.*[16,17] The presence of EDs during the propylene polymerization (see Table 3.1) had a noticeable effect on the molecular weight. The use of DPDMS resulted in somewhat higher molecular weights than MPDMS, showing that the bulkier groups on DPDMS have a stronger stabilizing effect on the stereospecific centers, as evident from the resulting higher increase in the molecular weight.[18] It is possible that the presence of the bulkier substituents on the DPDMS could be more effective in preventing 2,1-misinsertion, which often leads to chain termination in the presence of hydrogen. In addition, the activity of the isospecific sites of the catalyst in the presence of DPDMS is generally much higher than that of the aspecific sites, leading to higher molecular weights.

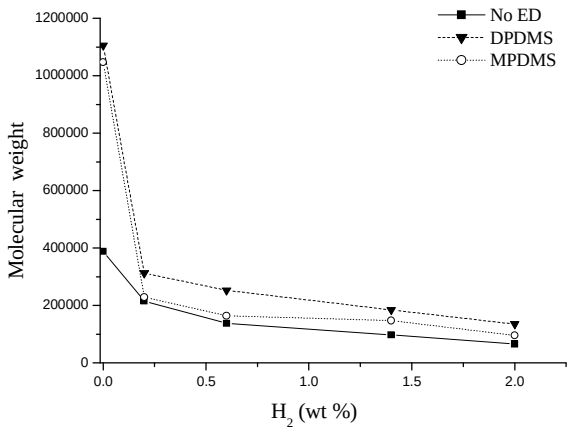

Figure 3.6: Dependence of the molecular weight of polypropylenes, on hydrogen concentration, prepared in the presence and absence of EDs.

Stellenbosch University http://scholar.sun.ac.za

The molecular structure of the ED also affects the polypropylene molecular weight distribution in the presence of hydrogen concentrations, as can be seen in Figure 3.7. Relatively narrow molecular weight distribution and high hydrogen response is obtained with catalyst system in the presence of DPDMS as ED. Chadwick *et al.*[19] obtained samilar results with diether-containing systems. In contrast, a relatively broad molecular weight distribution was obtained with the catalyst system $MgC1_2$/$TiCI_4$/ethyl benzoate-$A1Et_3$-aromatic ester.[20] It is suggested that this system also gives a significant proportion of high molecular weight, stereoregular polymer, and the hydrogen response is relatively low. Moreover, this system contains a significant proportion of species for which high selectivity is not dependent on the presence of an ED in the immediate vicinity of the active site.

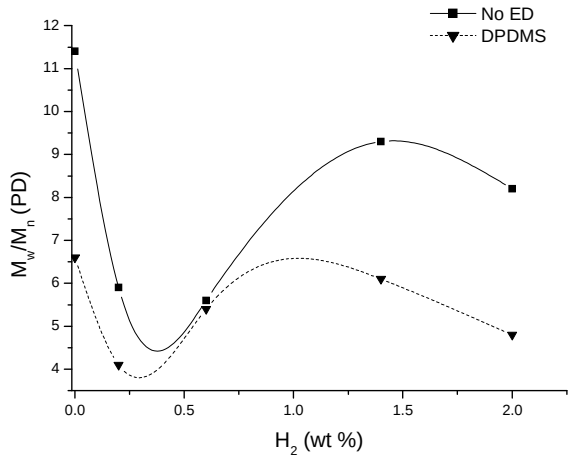

Figure 3.7: Dependence of the molecular weight distribution of polypropylenes, on hydrogen concentrations, prepared in the presence and absence of EDs.

3.3.1.4 Crystallinity and melting behaviour

DSC is the most popular method to use to study the thermal properties of semi-crystalline polymers. Detailed structural information can be obtained by careful interpretation of DSC thermograms generated under different conditions (cooling and heating at various rates, multiple cooling and heating conditions, etc.). Table 3.1 tabulates the results of the DSC analyses of the polypropylenes, with and without hydrogen, prepared in the presence of the two types of EDs. The degree of crystallinity was calculated by recording the ratio of the measured heat of fusion to that of a standard of known crystallinity, as shown in the equation below. The crystallinity of polypropylene samples can be determined from heating scans, using the following equation:

Stellenbosch University http://scholar.sun.ac.za

$$X_c\,\% = \frac{\Delta H_f}{\Delta H_f^o} \times 100$$

where ΔH_f is the specific heat of fusion of the samples and ΔH_f^o is the heat of fusion of the hypothetically 100% crystalline polypropylene (ΔH_f^o = 209 J/g).[21] The crystallinity of the samples with varying hydrogen content varies considerably as the hydrogen content is increased. Figure 3.8 illustrates the general increase in crystallinity of the samples with increasing hydrogen content. The lower molecular weight of the samples appears to be the main driving force behind the increase in crystallinity, as can be seen in Figure 3.9, although a possible slight increase in average tacticity of the samples can not be discounted. This would also assist in improving the degree of crystallinity as shown in Figure 3.10. It is also noted that increasing the hydrogen content from 0.5 to 2.0 wt % does not result in a major change in the crystallinity.

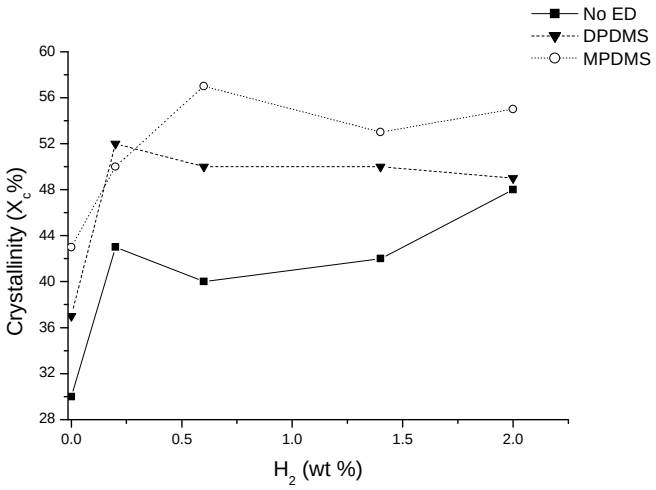

Figure 3.8: Effect of hydrogen concentrations on the crystallinity of the polypropylenes in the presence and absence of EDs.

Stellenbosch University http://scholar.sun.ac.za

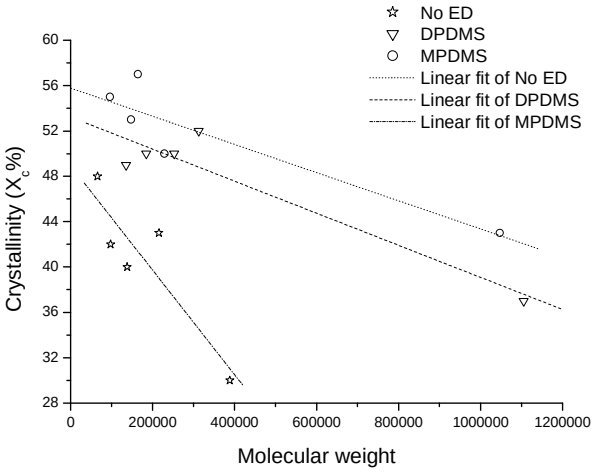

Figure 3.9: Effect of molecular weight on the crystallinity of the polypropylenes in the presence and absence of EDs.

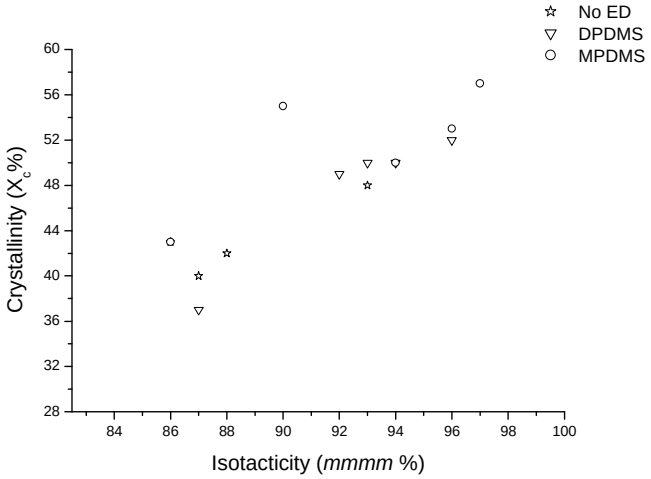

Figure 3.10: Effect of isotacticity on the crystallinity of the polypropylenes in the presence and absence of EDs.

Stellenbosch University http://scholar.sun.ac.za

3.3.1.5 Crystalline structure

There are three crystalline forms of isotactic polypropylene: monoclinic (α form), hexagonal (β form) and triclinic (γ form).[22] Among these three crystal structures, the α form is the most common and exists extensively in normal melt crystallized or solution crystallized samples. WAXD was used to determine the crystal modification with respect to tacticity and molecular weight difference in the polypropylenes that have similar thermal histories. Figure 3.11 shows typical WAXD patterns of the α form, in which three strong equatorial peak of the (110), (040) and (130) planes appear at $2\theta = 13.83°$, 16.90° and 18.34°, respectively.[23] Only the α crystal form existed in all polypropylene polymers prepared in the absence (Figure 3.11 A) and the presence of EDs (Figure 3.11 A and B). The main difference between the samples is the intensity of the main peaks, which is an indication of the extent of the crystallinity of each polypropylene sample. According to Morrow and Newman[24] this can be regarded as the morphology of highly isotactic polypropylenes, with few stereo-defects.

Stellenbosch University http://scholar.sun.ac.za

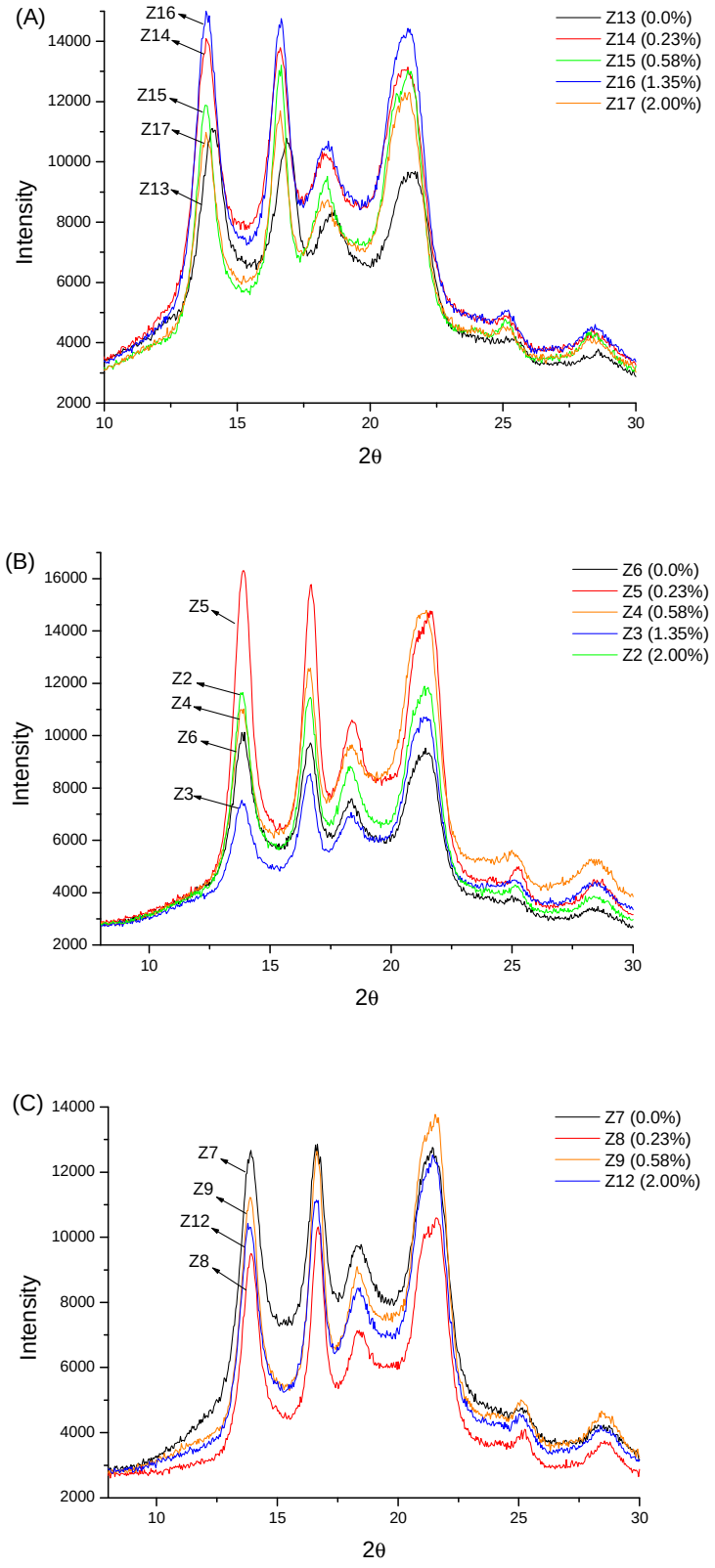

Figure 3.11: Typical X-ray diffraction patterns of polypropylenes produced: (A) in the absence of ED, (B) in the presence of DPDMS as ED and (C) in the presence of MPDMS as ED.

Stellenbosch University http://scholar.sun.ac.za

3.3.2 Fractionation and characterization of the polypropylenes

3.3.2.1 Polypropylenes prepared with no ED

The polypropylene samples for TREF fractionation were chosen in order to establish a correlation between the molecular weight and the crystallization of the polypropylene polymers. Fractionation of the polypropylene samples according to crystallizability was performed by means of TREF. TREF analyses of three different isotactic polypropylenes prepared without any EDs (Z13, Z15 and Z16) were carried out to determine the differences in their characteristics. First the original polymers were fractionated into eight different fractions, eluting at 25, 60, 80, 90, 100, 110, 120 and 140 °C. In this way the weight of the fractions, except the 140 °C fraction, was kept relatively large (> 100 mg) in order to ensure that sufficient material of each fraction was available for full analysis.

The TREF fractionation data are summarized in Table 3.2 and the TREF curves obtained are illustrated in Figure 3.12. It is clear that the 25 °C fraction amount of sample Z13 (27.1 wt %), which was produced in the absence of hydrogen, is larger than the fractions obtained at the same elution temperature (T_e) of samples Z15 and Z16 (11.4 and 11.3 wt %, respectively). This means that sample Z13 contains more atactic material than samples Z15 and Z16. The size of the fractions increased from the 60 °C fraction to the largest fraction eluting at 110°C (excluding fractions eluted at 90 °C) for all samples. Thereafter, smaller fraction sizes were obtained for the other elution temperatures.

A more accurate interpretation would, however, be to investigate the differential weight fraction to temperature ($W_i\%/\Delta T$) and accumulative weight fraction ($\Sigma W_i\%$) values, rather than the individual fraction sizes. The reason for this is that when interpreting only the individual fraction sizes, the temperature range for the specific fractions is not taken into account. We can therefore, conclude that the 110 °C fraction produced the highest mass of polymer fraction when the temperature range for the various fractions is taken into consideration. According to the graph of the $W_i\%/\Delta T$ over the fractionation temperature in Figure 3.12 (A) we find an increase in $W_i\%/\Delta T$ for the first four fractions collected after the 25 °C fraction and then a decrease for the last two fractions. The mass of the fractions eluted at 140 °C was very low and not nearly sufficient for complete analysis. Furthermore, it is observed that the peak value of elution temperature for all three samples is nearly the same (T_e = 110 °C), as shown in Figure 3.12 (A), but that the distributions are different, which results in a wider peak for sample Z13. This probably indicates that more than one type of active site exists in the heterogeneous catalysts. This result is somewhat different to that

Stellenbosch University http://scholar.sun.ac.za

reported by Morini and his co-workers.[25] They found that using ED all fractions eluted before 110 °C.

Table **3.2: TREF fractionation data for the fractions of samples Z13, Z15 and Z16**

Te (°C)	Sample Z13				Sample Z15				Sample Z16			
	Wt (mg)	W_i%	ΣW_i%	W_i%/ΔT	Wt (mg)	W_i%	ΣW_i%	W_i%/ΔT	Wt (mg)	W_i%	ΣW_i%	W_i%/ΔT
25	802	27.1	27.1	-	334	11.4	11.4	-	329	11.3	11.3	-
60	309	10.4	37.5	0.3	180	6.2	17.6	0.2	168	5.8	17.1	0.2
80	287	9.7	47.2	0.5	188	6.4	24.0	0.3	167	5.7	22.8	0.3
90	174	5.8	53.0	0.6	123	4.2	28.2	0.4	125	4.3	27.1	0.4
100	313	10.6	63.6	1.1	327	11.2	39.4	1.1	297	10.2	37.3	1.0
110	784	26.4	90.0	2.6	1 300	44.4	83.8	4.5	1 591	54.6	91.9	5.5
120	261	8.8	98.8	0.9	447	15.3	99.1	1.5	220	7.6	99.5	0.8
140	35	1.2	100.0	0.1	25	0.9	100.0	0.1	15	0.5	100.0	0.1

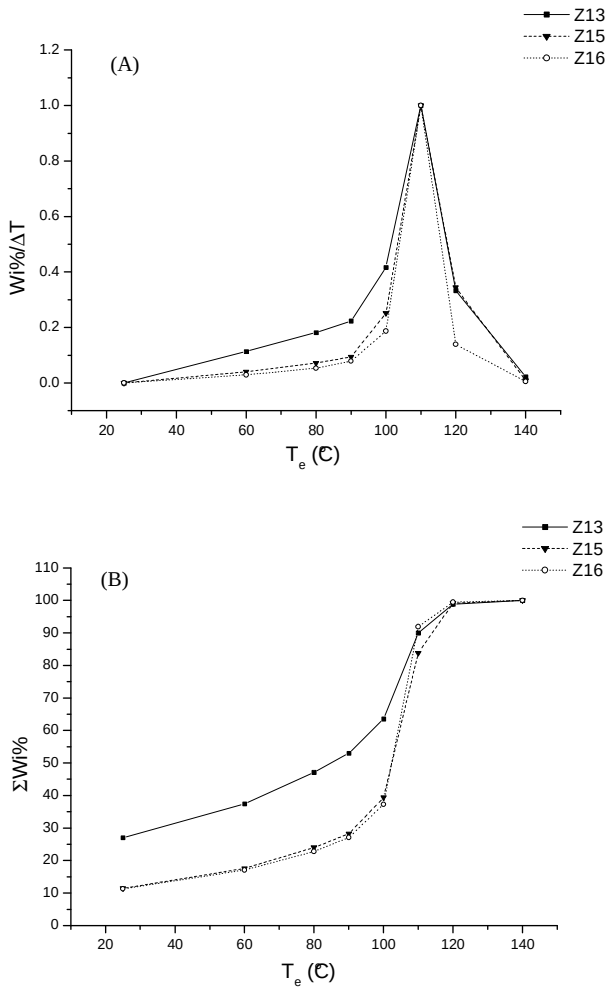

Figure 3.12: TREF curves of samples Z13, Z15 and Z16: (A) Wi%/ΔT and (B) ΣWi%.

Stellenbosch University http://scholar.sun.ac.za

Figure 3.12 (B) demonstrates the accumulative weight fraction percentage ($\Sigma W_i\%$) versus the fractionation temperatures of the three polymers Z13, Z15 and Z16. We find the most significant increase in the curves of Figure 3.12 (A) for the fractions collected between 100 and 120 ℃. For this range there is a definite increase in the sum of the weight fraction percentage. On the other hand, it is clear that the curve obtained for the sample Z13 in Figure 3.12 (B) is slightly different to the curves obtained for the other two samples Z15 and Z16. This is due to the broad distribution of the molecular species in sample Z13.

The weight fraction as a function of elution temperature is shown in Figure 3.13. The superimposed graphs provide a clear comparison of the samples. It is evident that the three samples have different weight fraction distributions. Other researchers have reported that for polypropylenes the TREF histograms qualitatively reflect the distribution of isotacticity, with isotacticity increasing almost linearly with the elution temperature.[26-29]

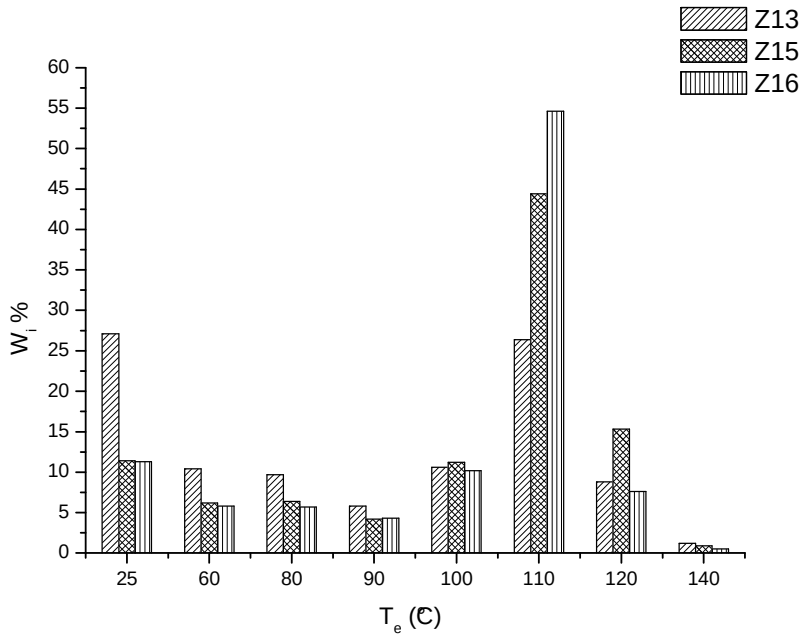

Figure 3.13: Distribution of weight percentage of Z13, Z15 and Z16 fractions vs. elution temperature (°C).

Stellenbosch University http://scholar.sun.ac.za

3.3.2.1.1 Microstructure

The microstructure of the fractions was investigated using ^{13}C NMR, to examine the stereo-regularity of the fractions. There was unfortunately insufficient material available to characterize all the fractions by ^{13}C NMR and so representative fractions were taken for analysis, including the room temperature soluble fraction and selected major fractions from the main elution peak.

The ^{13}C NMR data for the fractions are summarized in Table 3.3. The isotacticity of the fractions increases with the elution temperature up to the 110 °C fraction as one would expect, confirming that the TREF of polypropylenes is mainly conducted on the basis of tacticity. Of course, some dependence of fractionation on molecular weight is unavoidable, since there is some coincidence between tacticity and molecular weight of polypropylene.[26] This result is in agreement with the results reported by Viville *et al*.[28]

Table 3.3: GPC, ^{13}C NMR and DSC results of fractionation data of Z13, Z15 and Z16 samples

Runs	Fraction (T_e °C)	M_w	M_w/M_n	*mmmm*%	T_m (°C)	T_c (°C)	ΔH_m (J/g)	X_c (%)
Z13	25	25 677	8.8	35.0	-	-	-	-
	60	107 909	6.6	54.0	105.8	64.8	46.4	22.2
	80	125 876	5.6	67.0	124.0	88.7	70.8	33.9
	90	130 801	4.0	68.0	137.2-146.0	103.3	96.7	46.3
	100	143 773	4.0	82.0	147.4-156.2	107.5	83.9	40.2
	110	373 864	5.0	92.0	156.4	113.6	102.4	49.0
	120	264 098	4.2	91.0	156.6	112.0	117.3	56.1
	140	212 659	3.9	-	152.8	107.0	60.1	28.8
Z15	25	21 315	8.1	33.0	-	-	-	-
	60	30 149	5.2	59.0	112.4	78.0	49.7	23.8
	80	49 718	4.2	72.0	129.6	97.7	94.7	45.3
	90	115 139	4.1	76.0	141.0-149.3	108.4	98.4	47.1
	100	114 819	3.8	91.0	149.3-158.1	112.3	112.7	53.9
	110	130 212	4.3	95.0	158.3	115.9	122.2	58.5
	120	122 118	3.9	94.0	158.9	115.9	142.1	68.0
	140	83 325	3.8	-	152.7	103.9	57.1	27.3
Z16	25	5 339	9.1	39.0	-	-	-	-
	60	12 343	6.2	63.0	114.8	85.2	67.7	32.4
	80	10 951	5.1	78.0	133.5	103.9	79.6	38.1
	90	21 468	4.5	89.0	144.6-151.4	112.1	120.9	57.9
	100	60 324	4.0	92.0	151.2-158.8	115.0	120.0	57.4
	110	79 819	3.8	97.0	159.0	116.4	132.5	63.4
	120	83 150	4.3	95.0	159.3	118.6	124.0	59.4
	140	65 919	3.7	-	155.9	108.8	59.8	28.6

Stellenbosch University http://scholar.sun.ac.za

An interesting outcome of this analysis is that the isotacticity of the Z15 and Z16 fractions is systematically slightly greater than that of Z13 fractions, at a given elution temperature. This is illustrated in Figure 3.14, which shows the evolution of *mmmm* % pentads for fractions of Z13, Z15 and Z16 as a function of elution temperature. This is due to the higher isotacticities of the original polymer samples of Z15 and Z16 over Z13 (87%, 88% and 55%, respectively, as shown in Table 3.1). These results indicate that, conversely to what is sometimes implicitly assumed, TREF does not essentially fractionate polyolefins as a function of chain tacticity. In fact, it separates chains according to their ability to pack in a crystal having a thickness determined by the temperature during crystallization. Therefore, only one regular sequence of sufficient length is required to get a chain in a given TREF fraction.[30] Depending on whether the rest of the chain consists of regular sequences of similar or shorter lengths, the average tacticity of the fraction will be larger or smaller.

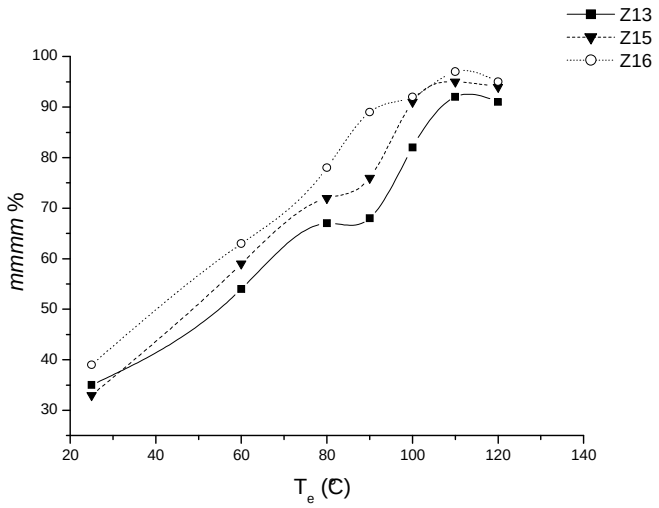

Figure 3.14: Meso pentad percentages (*mmmm* %) of Z13, Z15 and Z16 fractions vs. TREF elution temperature.

3.3.2.1.2 Molecular weight and molecular weight distribution

The above results appear to indicate that tacticity alone does not determine the crystallizability of polypropylene from solution, and that other factors may be involved. Crystallization may start due to immobilization of a given chain of sufficient regularity and length, and subsequent crystallization may then occur by chains that are chemically dissimilar.

Stellenbosch University http://scholar.sun.ac.za

Figure 3.15 shows the weight average molecular weight of the TREF fractions of Z13, Z15 and Z16 with respect to the TREF elution temperature. Table 3.3 and Figure 3.15 show that there is a rather sharp increase in molecular weight for the samples eluting above 80 °C, demonstrating that those chains that crystallize out of solution at high temperatures are of a much higher molecular weight than those that crystallize out at low temperatures. What is noted, however, is that while the increase in molecular weight of the polypropylene sample's fractions increases drastically from the 80 °C fraction to the 110 °C fraction, the polypropylene sample's fractions' molecular weights increase over a broader range of temperatures, from the 25 °C fraction to the 80 °C fraction, which shows that there is a relationship between molecular weight and tacticity to some extent. It can also be seen that the lower isotacticity fractions (i.e. these fractionated at lower temperatures) exhibited a lower molecular weight. This indicates that those active sites that allow stereoerrors also allow regioerrors (2,1-insertions, leading to dormant sites) and facile chain transfer.

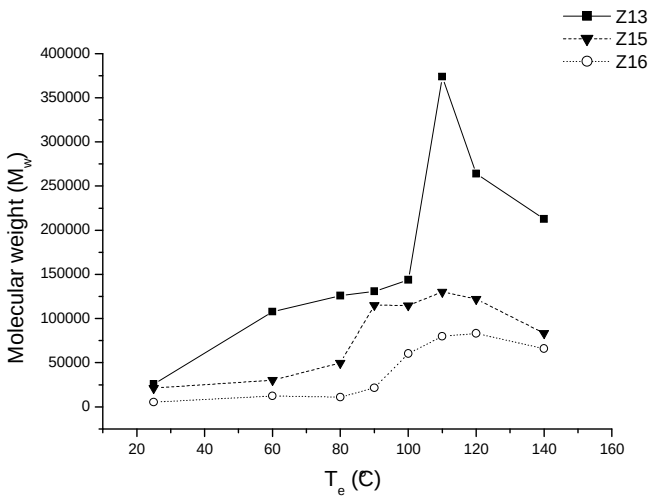

Figure 3.15: Evolution of molecular weight of TREF fractions of Z13, Z15 and Z16 vs. TREF elution temperature.

Closer observation of Figure 3.15, reveals that there are significant differences between Z13, Z15 and Z16. The curve representative of Z16 is shifted to a higher elution temperature compared to that of Z13 and Z15. For a given elution temperature (given crystallizability), molecular weight is systematically lower for Z16 than for Z13 and Z15. This means that shorter chains of Z16 have thus the same crystallizability than longer chains of Z13 and Z15. This behaviour reflects the effect of the difference in the reaction conditions used to produce

Stellenbosch University http://scholar.sun.ac.za

these different polypropylene polymers, and which leads to different distributions of tacticity as a function of the molecular weight. In other words, Z13, Z15 and Z16 do not have the same intermolecular heterogeneity. From all the data obtained thus for from ^{13}C NMR and HT-GPC characterization of the TREF fractions, we can say that the tacticity and the molecular weight of the polypropylene fractions possibly play a major significant role in the fractionation mechanism of TREF. This is in agreement with the results reported by other authors.[1,28, 31,32]

The polydispersity (PD) of the fractions (Figure 3.16) decreases as the fractionation temperature increases, however, the polydispersity of each fraction (except the first one) is considerably lower than that of the non-fractionated material (Tables 3.1 and 3.3). This decrease is a further indication of the influence of the catalyst. Polypropylenes produced with conventional heterogeneous Ziegler-Natta catalysts are characterized by broad molecular weight distributions, ranging from 4 to 12, as a result of the existence of several types of sites on these catalysts. Several authors report that these distributions can be sufficiently described as superpositions of a series of narrower distributions, one for each type of catalytic site, with each site type producing a Flory's most probable chain-length distribution of about 2.[28]

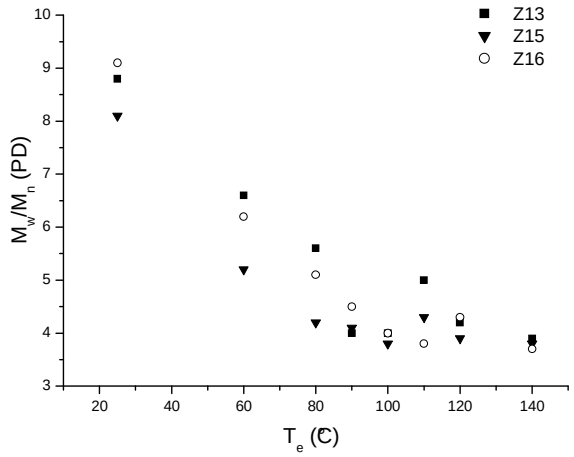

Figure 3.16: Polydispersity data for the TREF fractions of samples Z13, Z15 and Z16.

Interestingly, it appears that the active sites producing the material with the ability to crystallize out of solution at higher temperatures are more uniform and therefore produce a more uniform distribution of molecular species.

Stellenbosch University http://scholar.sun.ac.za

3.3.2.1.3 Crystallinity and melting behaviour

Figure 3.17 presents a waterfall plot of the DSC melting endotherms for the fractions of sample Z13. The data for samples Z15 and Z16 show similar trends. Figure 3.18 presents the evolution of melting temperatures for Z13, Z15 and Z16 fractions as a function of elution temperature. As can be seen from the DSC endotherms in Figures 3.17 and 3.18, as well as the data in Table 3.3, there is a characteristic increase in the melting temperature of the fractions with an increase in elution temperature. This trend is only observed up to a certain point however (120 °C fraction in this case), thereafter there is a decrease in the peak melting temperature for the highest temperature fractions. This clearly demonstrates that lamellar thicknesses, corresponding to the fractions crystallized under given conditions, increase as a function of elution temperature (or molecular weight) for all polymers, which is a clear indication of the inter-molecular heterogeneity. However, slight differences between melting temperatures of Z13, Z15 and Z16 fractions can be seen. Z16 fractions are characterized by higher melting temperatures than the Z13 and Z15 fractions. These Z16 fractions are therefore characterized, on average, by longer crystallizable sequences than equivalent fractions of other samples. These results are in good agreement with the tacticity data obtained by ^{13}C NMR.

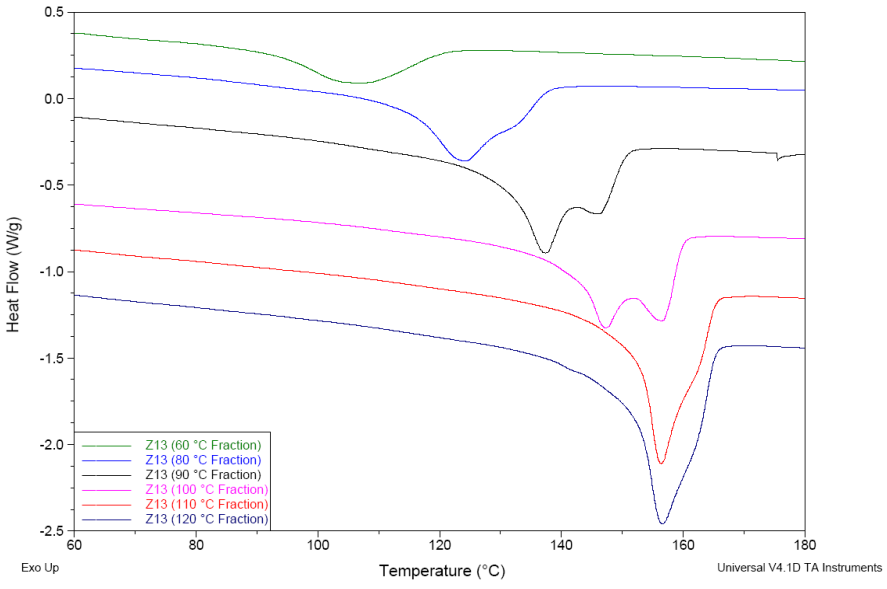

Figure 3.17: Waterfall plot of the DSC melting endotherms for the fractions of sample Z13.

Stellenbosch University http://scholar.sun.ac.za

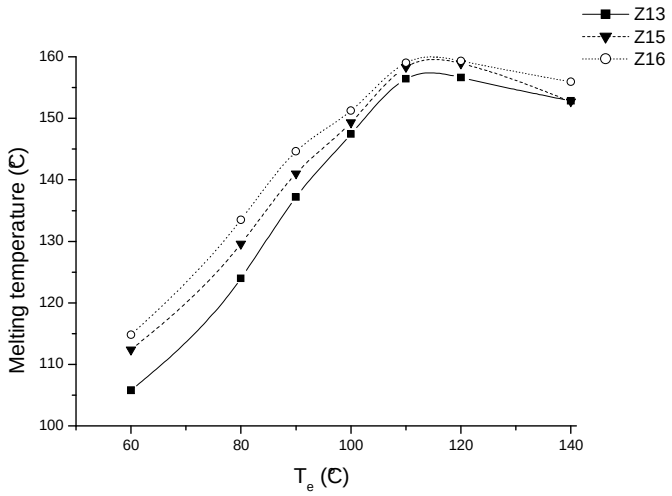

Figure 3.18: Evolution of melting temperatures (T_m) of TREF fractions of Z13, Z15 and Z16 samples versus TREF elution temperature.

On the other hand, the double melting peaks observed in the DSC endotherms must also be considered. There has been much discussion surrounding the cause of the multiple melting endotherms.[33-36] Multiple melting endotherms could be the result of different polymorphic forms, melting and recrystallization, segregation by tacticity or molecular weight, the melting of different regions in the crystalline structure such as radial and transverse lamellae, or even orientation effects. In this study, the most likely explanation for the double melting peaks is the melting of daughter and mother lamellae, or melting of the so-called disordered α_1 and the more perfect α_2 modifications.

If we now consider crystallization temperature, the differences between the equivalent fractions of the three different samples Z13, Z15 and Z16 are generally maintained, as can be seen in Figure 3.19, indicating that crystallization temperature is mostly dependent on isotacticity. On the other hand, a slight decrease in crystallization temperature is observed for the last TREF fractions of each sample. This is most likely caused by the restricted mobility and lower tacticities of the long chains in these fractions.

According to Burfield *et al.*[37] crystallinity (ΔH_m) is a better measure of isotacticity than melting temperature. As shown in Table 3.3 and Figure 3.20, the degree of crystallinity of the fractions does not increase as linearly in the series as does the melting temperature value. This means that the fractions have been separated, not only according to average isotacticity, but also according to lamellar thickness or the lengths of the crystallizable sequences in the chains.

Stellenbosch University http://scholar.sun.ac.za

The degree of crystallinity of the fractions increases with fractionation temperature over the temperature range of the fractions, with the exception of the 100 °C fractions of samples Z13 and Z16, which show a slight decrease (Figure 3.20). Figure 3.20 shows that there is a significant decrease in the crystallinity for the 140 °C fractions of all samples. This could only be due to the decrease in the isotacticity of these fractions. It is believed that the higher crystallinity is due to the higher tacticity of the sample (as shown in Figure 3.21), allowing an improvement in the crystallization of the chains, even the chains with higher molecular weights. It is obvious that a balance must be struck in order to achieve the maximum degree of crystallization.

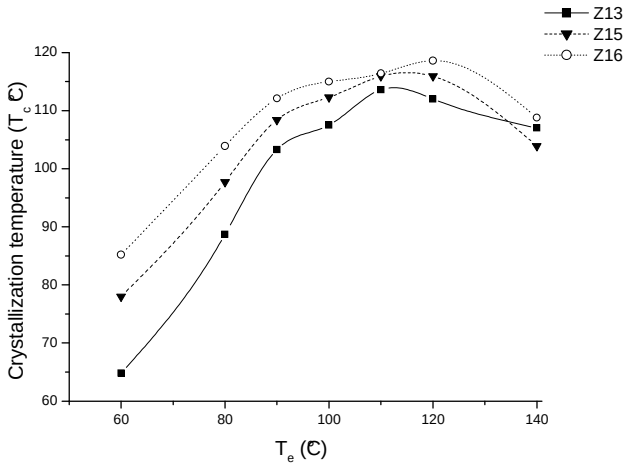

Figure 3.19: Evolution of crystallization temperature (T_c) of Z13, Z15 and Z16 TREF fractions versus TREF elution temperature.

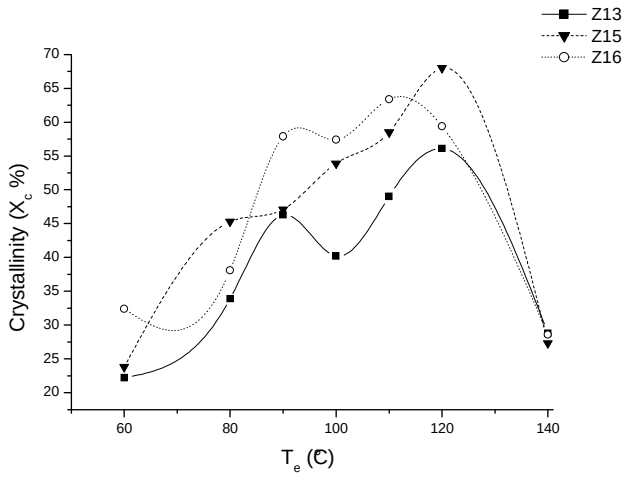

Figure 3.20: Degree of crystallinity of the TREF fractions of samples Z13, Z15 and Z16 versus TREF elution temperature.

Stellenbosch University http://scholar.sun.ac.za

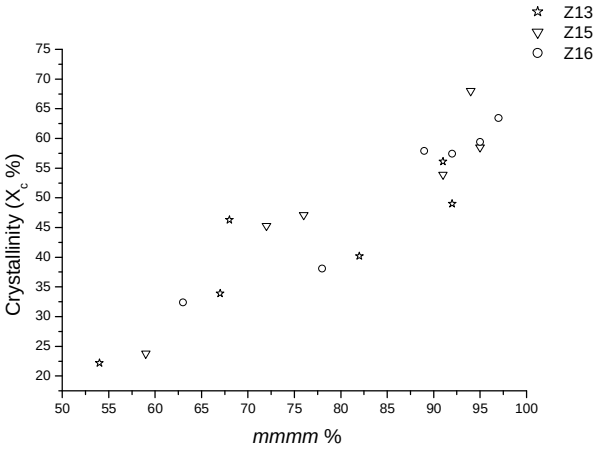

Figure 3.21: Effect of isotacticity on the crystallinity degree of the TREF fractions of samples Z13, Z15 and Z16.

Infrared spectroscopy (IR) is commonly used to study the conformational order of polymers. For isotactic polypropylene, the majority of the absorption bands appearing in the frequency region below 1470 cm^{-1} belong to the regularity bands, and they are linked with intramolecular vibration coupling in an individual chain.[38,39] The existence of these regularity bands reflects the existence of helical sequences. FT-IR analyses were performed for all TREF fractions.

The spectra of the TREF fractions of sample Z15 are shown in Figure 3.22 (the FT-IR data for TREF fractions of samples Z13 and Z16 show similar trends). The absorption bands in the structure range from 1350 to 1460 cm^{-1}, and are characteristic of propylenic structures. The ratio of the absorbances at 998 and 970 cm^{-1} characterizes the crystalline form of polypropylene and the ratio of the band at 1168 cm^{-1} and the shoulder at 1155 cm^{-1} is influenced by the tacticity of the polypropylene.[40,41] It can be seen from the Figure 3.22 that the absorbance ratio $R(A_{998}/A_{970})$ of TREF fractions increases with increasing elution temperature, which illustrates that crystallinity increases with increasing elution temperature. These results are in agreement with the results obtained using the DSC technique. Furthermore, the absorbance ratio $R(A_{1168}/A_{1155})$ of TREF fractions also increases with increasing elution temperature, which means increasing isotacticity of the TREF fractions. These results are also in agreement with the results obtained using ^{13}C NMR.

Stellenbosch University http://scholar.sun.ac.za

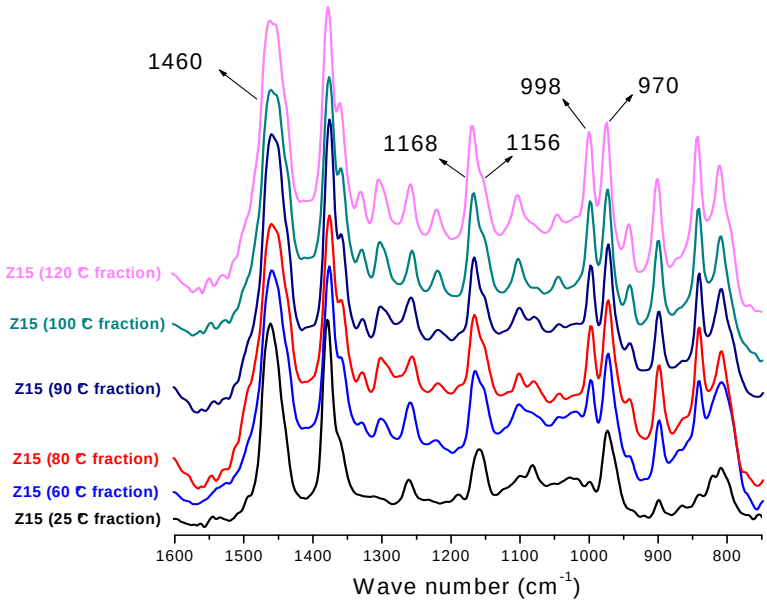

Figure 3.22: FTIR spectra of the TREF fractions of sample Z15.

3.3.2.1.4 Crystal phase analysis

Figure 3.23 illustrates the WAXD results for selected TREF fractions of sample Z15 which had been analyzed in exactly the same way as the original samples, as described in Section 3.3.1.5. Figure 3.23 shows that only the α crystal form existed in all TREF fractions of sample Z15. The main difference between the TREF fractions is the intensity of the peaks, which is an indication of the crystallinity content of each fraction.

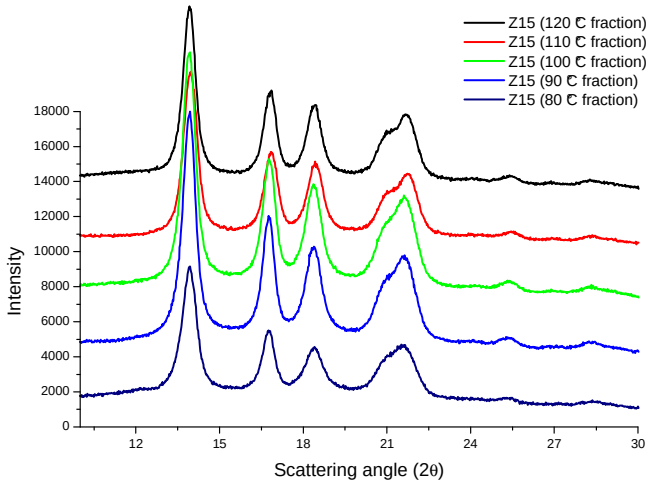

Figure 3.23: Typical X-ray diffraction patterns of the different TREF fractions of the Z15 sample.

Stellenbosch University http://scholar.sun.ac.za

3.3.2.2 Polypropylenes prepared with MPDMS as external donor

TREF analyses of the three isotactic polypropylenes Z8, Z9 and Z10, prepared in the presence of MPDMS as ED, were carried out to determine the differences in their characteristics. Table 3.4 tabulates the TREF fractionation data of polypropylene samples Z8, Z9 and Z10 and Figure 3.24 shows the TREF curves obtained. The addition of EDs to $MgCl_2$-supported Ziegler-Natta catalysts reduces the weight percentage of the fractions that eluted at lower temperature and increase the weight percentage of fractions that eluted at higher temperature, compared to those polymers made with no EDs. External and internal electron donors could also have different influences on some fractions.[42] It is clear from Table 3.4 that the 25 °C fraction amounts of samples Z8, Z9 and Z10 (5.7, 6.8 and 7.5 wt %, respectively), which were produced in the presence of MPDMS as ED, are significantly smaller than those obtained at the same elution temperature of samples Z13, Z15 and Z16 (27.1, 11.4 and 11.3 wt %, respectively), which were produced in the absence of any EDs. This shows that the addition of an ED decreases the amount of atactic, non-crystalline material, as expected.[26]

Table 3.4: TREF fractionation data for the TREF fractions of samples Z8, Z9 and Z10

Te (°C)	Sample Z8				Sample Z9				Sample Z10			
	Wt (mg)	W_i%	ΣW_i%	W_i%/ΔT	Wt (mg)	W_i%	ΣW_i%	W_i%/ΔT	Wt (mg)	W_i%	ΣW_i%	W_i%/ΔT
25	170	5.7	5.7	-	200	6.8	6.8	-	223	7.5	7.5	-
60	56	1.9	7.6	0.1	65	2.2	9.0	0.1	65	2.2	9.7	0.1
80	82	2.7	10.3	0.2	88	3.0	12.0	0.2	93	3.1	12.8	0.2
100	283	9.5	19.8	0.5	298	10.1	22.1	0.5	311	10.5	23.3	0.5
110	1 041	34.8	54.6	3.5	1 127	38.0	60.1	3.8	1 044	35.2	58.5	3.5
120	1 189	39.7	94.3	4.0	1 095	37.0	97.1	3.7	1 095	36.9	95.4	3.7
140	169	5.7	100.0	0.3	90	2.9	100.0	0.2	136	4.6	100.0	0.2

According to the graph of the W_i%/ΔT over the fractionation temperature range in Figure 3.24 (A) there is an increase in W_i%/ΔT for the first four fractions collected after the 25 °C fraction and then a decrease for the last fraction. The graphs in Figure 3.24 (A) have similar distributions but differ only slightly in the shape. This indicates that comparable types of active sites exist in the catalyst in the presence of MPDMS, even when different amounts of hydrogen are used. Figure 3.24 (B) illustrates the cumulative weight fraction percentage versus the fractionation temperatures of the three polymers Z8, Z9 and Z10. The curves are very similar, they differ only slightly in the range.

Stellenbosch University http://scholar.sun.ac.za

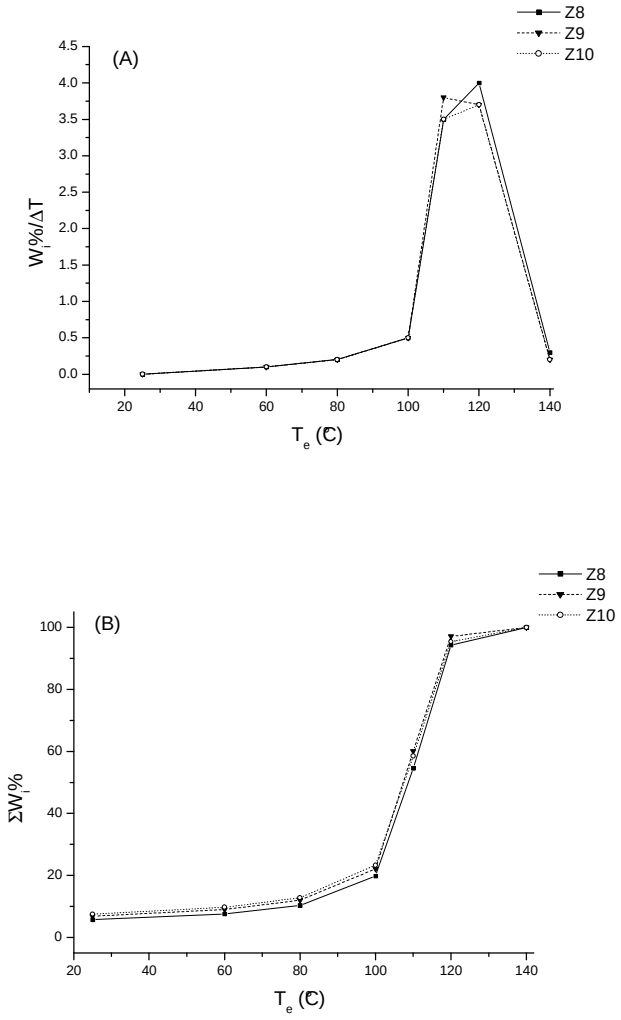

Figure 3.24: TREF curves of samples Z8, Z9 and Z10: (A) Wi%/ΔT and (B) ΣWi %.

The weight fraction as a function of elution temperature is shown in Figure 3.25. The bar graphs provide a clear and easy way to compare the samples. The graphs show that the three samples have slightly different weight fraction distributions. More than 70 wt % of the original material for all samples eluted in the two fractions at 110 and 120 °C. These results are in agreement with the results reported by Morini *et al.*[25] They found that most of the fractions of samples produced with supported heterogeneous catalysts in the presence of different types of EDs eluted at 112 °C. This means that highly isospecific active sites are only formed after the addition of EDs.[32]

Stellenbosch University http://scholar.sun.ac.za

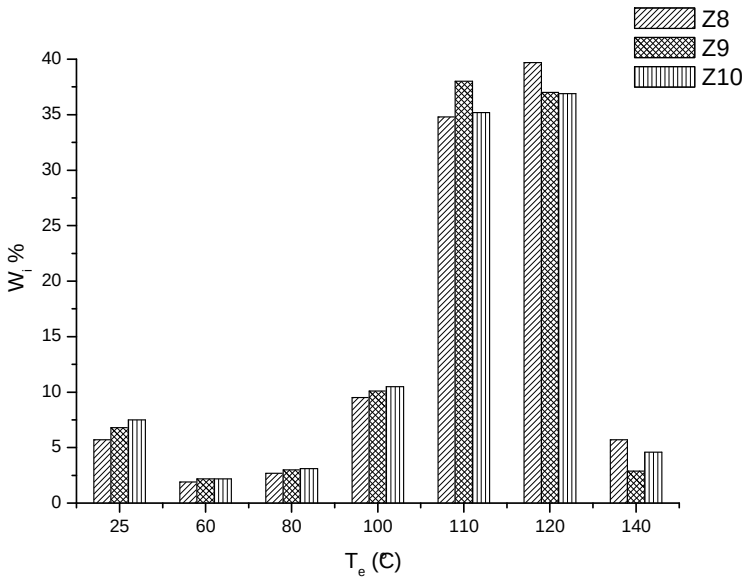

Figure 3.25: Distribution of weight percentage of Z8, Z9 and Z10 fractions vs. elution temperature (°C).

3.3.2.2.1 Microstructure

The ^{13}C NMR data of the TREF fractions of Z8, Z9 and Z10 samples are summarized in Table 3.5. The meso pentad percentages (*mmmm* %) of the Z8, Z9 and Z10 fractions vs. TREF elution temperature are shown in Figure 3.26. Table 3.5 and Figure 3.26 show that isotacticity of the fractions increases with the elution temperature, as expected.[43,44] The overall isotacticity of the TREF fractions was increased by the addition of EDs to $MgCl_2$-supported Ziegler-Natta catalysts. This is clearly seen when we compare the results of the TREF fractions eluted from polypropylene samples produced without any EDs (Table 3.3 and Figure 3.14) to the TREF fractions that eluted in the presence of electron donors (Table 3.5 and Figure 3.26). These results indicate that EDs can convert aspecific active sites into different isospecific active sites and the conversion is related to the structure of internal electron donors. The electron donors reduce the weight percentage of the fractions eluted at lower temperature and increase the weight percentage of fractions having high isotacticity.[42] Xu *et al.*[26] illustrated that all polypropylene samples produced with different catalysts eluted in the same temperature range and that electron donors only changed the distributions of polypropylene in this range.

Stellenbosch University http://scholar.sun.ac.za

Table 3.5: GPC, ^{13}C NMR and DSC results of fractionation data of Z8, Z9 and Z10 samples

Runs	Fraction (T_e °C)	M_w	M_w/M_n	*mmmm* %	T_m (°C)	T_c (°C)	ΔH_m (J/g)	X_c (%)
Z8	25	16 474	14.3	45.0	-	-	-	-
	60	15 970	5.6	59.0	116.7	84.4	24.4	11.7
	80	18 986	3.9	63.0	131.6	100.3	53.9	25.8
	100	28 270	2.4	84.0	148.9-158.7	111.5	83.7	40.1
	110	126 452	3.2	94.0	157.3	115.8	103.3	49.4
	120	178 423	3.5	96.0	158.6	116.3	106.9	51.2
	140	80 155	2.5	99.0	156.8	114.3	83.6	40.0
Z9	25	7 194	8.7	48.0	-	-	-	-
	60	11 467	4.2	64.0	117.2	87.0	37.5	18.0
	80	14 126	3.3	80.0	134.3	102.8	55.1	26.4
	100	25 918	2.4	93.0	149.5-158.3	113.0	87.1	41.7
	110	110 387	3.4	98.0	158.7	118.4	110.7	53.0
	120	173 434	3.2	98.0	159.5	117.8	102.3	49.0
	140	82 736	2.6	99.0	155.3	113.6	76.9	36.8
Z10	25	5 187	7.2	51.0	-	-	-	-
	60	16 180	6.9	61.0	119.1	91.4	34.9	16.7
	80	9 204	3.0	72.0	135.1	102.5	67.9	32.5
	100	21 739	2.5	85.0	149.2-158.5	111.3	87.6	41.9
	110	92 596	3.5	93.0	157.9	117.2	110.1	52.7
	120	114 747	3.2	94.0	159.9	119.2	101.2	48.4
	140	71 010	2.5	94.0	155.5	113.1	70.2	33.6

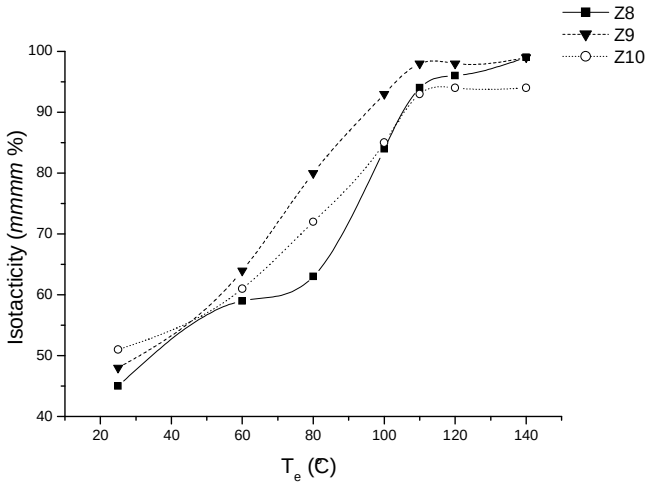

Figure 3.26: Meso pentad percentages (*mmmm* %) of Z8, Z9 and Z10 fractions vs. TREF elution temperature.

The isotacticity of the first four fractions of Z9 and Z10 samples are slightly greater than the Z8 fractions, as shown in Figure 3.26 and Table 3.5. This is due to the higher isotacticities of

Stellenbosch University http://scholar.sun.ac.za

the original polymer samples of Z9 and Z10 compared to Z8 (97%, 96% and 94%, respectively). See Table 3.1

3.3.2.2.2 Molecular weight and molecular weight distribution

Figure 3.27 shows the weight average molecular weight of TREF fractions of the Z8, Z9 and Z10 samples with respect to the TREF elution temperature. Table 3.5 and Figure 3.27 show that there is a quite sharp increase in molecular weight of the samples eluting above 100 °C.

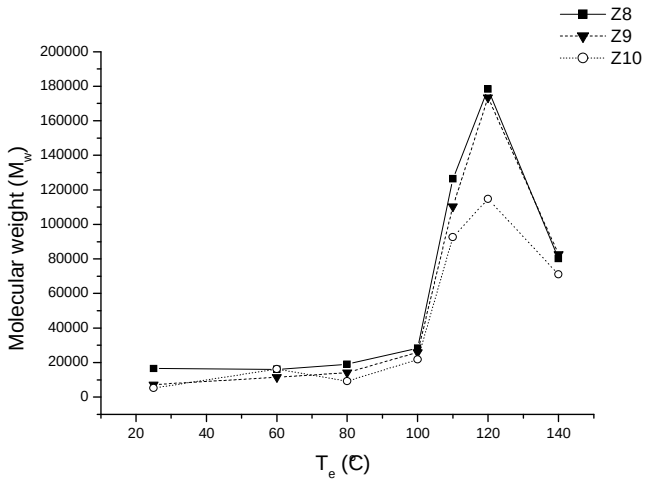

Figure 3.27: Evolution of molecular weight of TREF fractions of Z8, Z9 and Z10 vs. TREF elution temperature.

Figure 3.27 also shows that there is a significant difference between the curves of Z8, Z9 and Z10. The curve representative of Z10 is shifted to a higher elution temperature compared to the curves of Z8 and Z9. For a given elution temperature (fraction 120 °C), the molecular weight of the Z10 fraction is notably lower than the molecular weights of the Z8 and Z9 fractions. This means that shorter chains of Z10 have the same crystallizability as longer chains of Z8 and Z9. An explanation for this is that the Z8, Z9 and Z10 samples do not have the same inter-molecular heterogeneity.

Figure 3.28 shows the PD values of each fraction of the Z8, Z9 and Z10 samples. The PD of the fractions tends to decrease as the elution temperature increases; however, the PD of each fraction (except the first one) is considerably lower than that of the non-fractionated material (Tables 3.1 and 3.3).

Stellenbosch University http://scholar.sun.ac.za

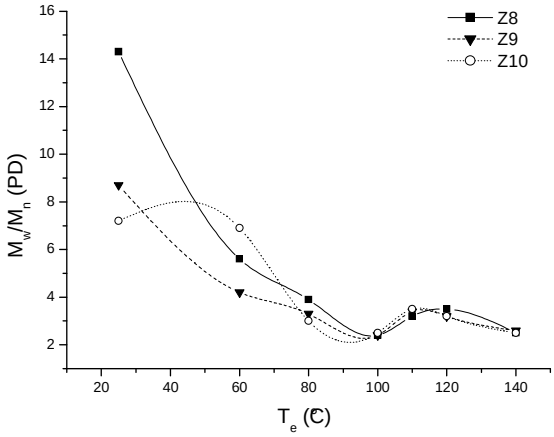

Figure 3.28: Polydispersity data for the TREF fractions of samples Z8, Z9 and Z10.

3.3.2.2.3 Crystallinity and melting behaviour

Figure 3.29 presents a waterfall plot of the DSC melting endotherms for the fractions of sample Z9. The data for samples Z8 and Z9 show similar trends. Figure 3.30 presents the evolution of melting temperatures for Z8, Z9 and Z10 fractions as a function of elution temperature. As can be seen from the DSC endotherms in Figures 3.29 and 3.30, as well as the data in Table 3.5, there is a characteristic increase in the melting temperature of the fractions with an increase in elution temperature (except the last fraction). This clearly demonstrates that lamellar thicknesses, resultant of the fractions crystallized under given conditions, increase as a function of elution temperature (or molecular weight) for all polymers, which is a clear indication of the inter-molecular heterogeneity. However, slight differences between melting temperature of polymer fractions can be seen. The Z10 fractions are characterized by slightly higher melting temperatures than the Z8 and Z9 fractions.

Upon comparing the melting temperatures of the Z13, Z15 and Z16 fractions, obtained in the absence of any EDs (Table 3.3, and Figures 3.17 and 3.18), to the melting temperatures of the Z8, Z9 and Z10 fractions, obtained in the presence of MPDMS (Table 3.5, and Figures 3.29 and 3.30), we notice that in the absence of MPDMS, the melting temperatures of the fractions are generally slightly lower. Besides, the addition of MPDMS leads not only to the disappearance of the low melting temperature peak, but also to the appearance of a high melting temperature shoulder peak. Clearly the low stereospecific sites were converted into high stereospecific by the addition of MPDMS as ED.

Stellenbosch University http://scholar.sun.ac.za

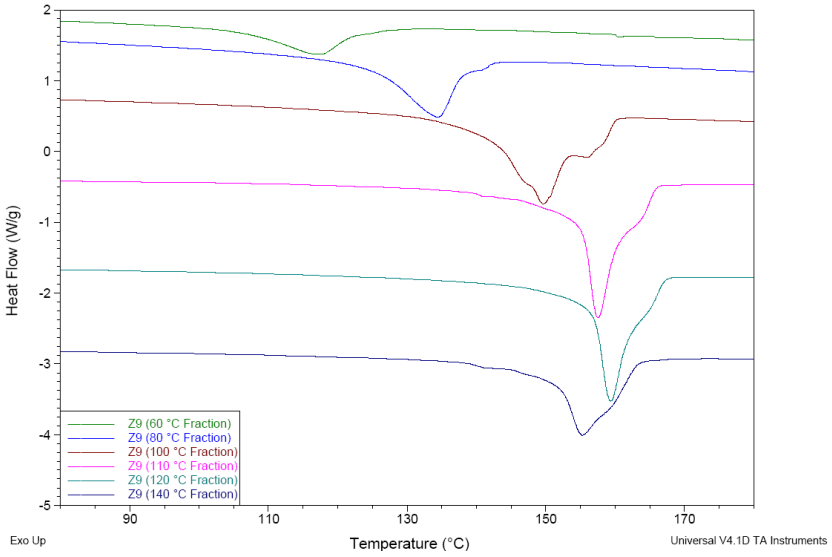

Figure 3.29: Waterfall plot of the DSC melting endotherms for the TREF fractions of sample Z9.

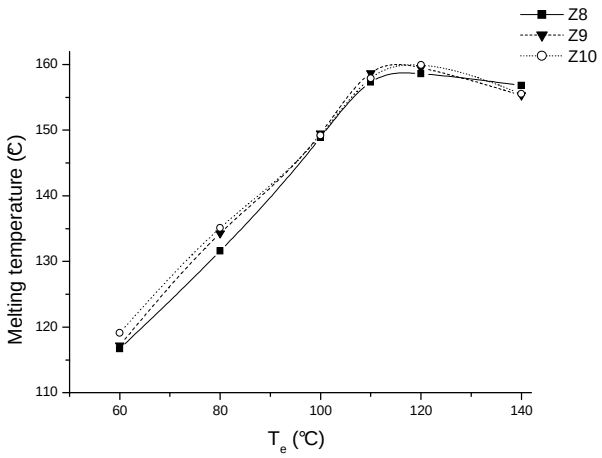

Figure 3.30: Evolution of melting temperatures (T_m) of TREF fractions of Z8, Z9 and Z10 samples versus TREF elution temperature.

The crystallization temperatures of different TREF fractions of the three different samples Z8, Z9 and Z10 increase with increasing elution temperature, as can be seen in Figure 3.31. This indicates that the crystallization temperature is dependent on isotacticity. A slight decrease in crystallization temperature is observed for the last TREF fractions of each sample. This is

Stellenbosch University http://scholar.sun.ac.za

most likely caused by the restricted mobility and lower tacticities of the chains in these fractions.

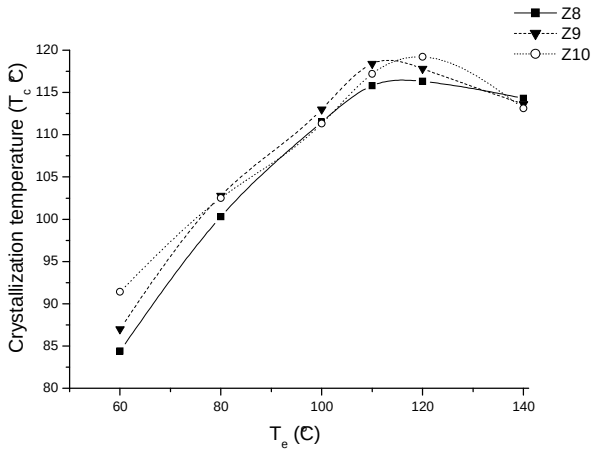

Figure 3.31: Evolution of crystallization temperature (T_c) of Z8, Z9 and Z10 TREF fractions versus TREF elution temperature.

The degree of crystallinity of the fractions of samples Z8, Z9 and Z10 also increases with increasing fractionation temperature over the temperature range, as can be seen in Figure 3.32. However, there is a remarkable decrease in the crystallinity of the last fractions of all samples. The reason for this could only be due to the dramatic decrease in the molecular weight of these fractions, as can be seen in Table 3.5.

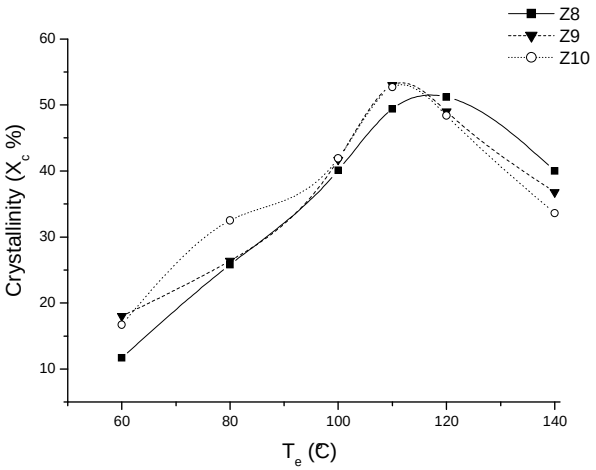

Figure 3.32: Degree of crystallinity of the TREF fractions of samples Z8, Z9 and Z10 versus TREF elution temperature.

Stellenbosch University http://scholar.sun.ac.za

When considering the effect of both molecular weight and isotacticity on the crystallinity of TREF fractions of samples Z8, Z9 and Z10 (see Figures 3.33 and 3.34, respectively) it is noticeable that there is a sharp increase in the crystallinity with increasing the molecular weight in the low molecular weight fractions, which would appear to be the main driving force behind the improvement in crystallinity. This may be because most of the stereoerrors occur in the initial stages of chain growth (note the increased amount of stereoerrors in the first fractions that have lower molecular weights), thus most of the stereoerrors are located at the chain ends, which are usually excluded from the crystalline areas.

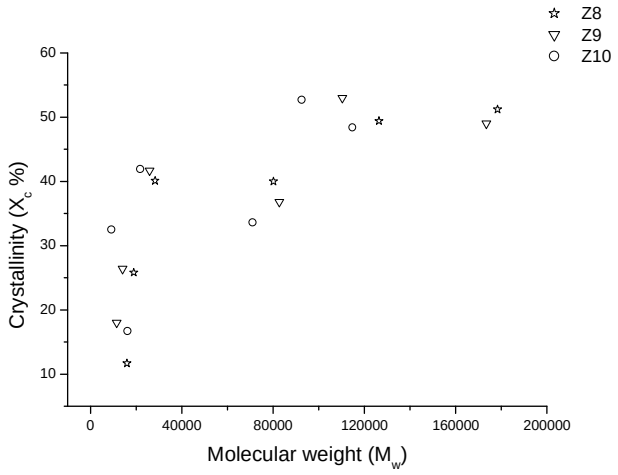

Figure 3.33: Effect of molecular weight on the degree of crystallinity of the TREF fractions of samples Z8, Z9 and Z10.

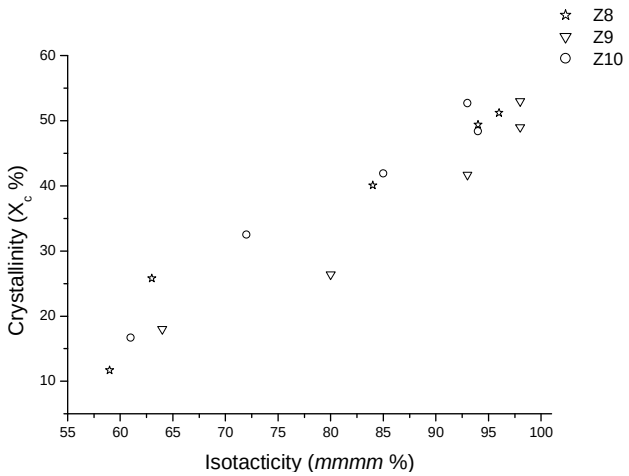

Figure 3.34: Effect of isotacticity on the degree of crystallinity of the TREF fractions of samples Z8, Z9 and Z10.

Stellenbosch University http://scholar.sun.ac.za

It is also noticeable that there is generally a linear increase over a wide range of crystallinity with increasing tacticity, as can be seen in Figure 3.34. This also indicates that the fractionation process is dependent on the tacticities and molecular weights of the polymers. It is obvious here that a balance must be struck in order to achieve the maximum degree of crystallization.

3.3.2.2.4 Crystal phase analysis

Figure 3.35 shows the WAXD results for selected TREF fractious of sample Z10 which was produced in the presence of MPDMS. This sample was analyzed in exactly the same way as the samples described in Sections 3.3.1.5 and 3.3.2.1.4. The figure shows that only the α crystal form is present in all TREF fractions of sample Z10.

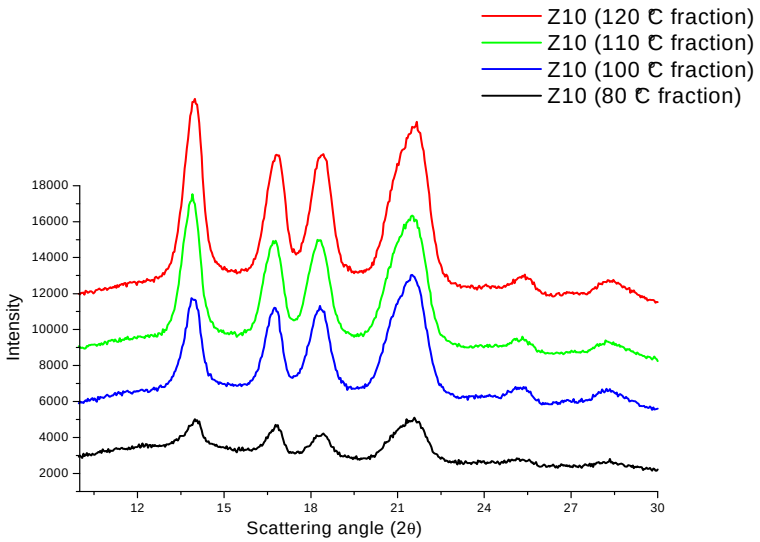

Figure 3.35: Typical X-ray diffraction pattern of different TREF fractions of the Z10 sample.

3.3.2.3 Polypropylenes prepared with DPDMS as external donor

TREF analyses of two different isotactic polypropylenes Z4 and Z5, produced in the presence of DPDMS as an ED, were carried out to determine the differences in their characteristics. Table 3.6 tabulates the TREF fractionation data of polypropylene samples Z4 and Z5. The TREF curves obtained of these polymers are illustrated in Figure 3.36. As discussed in Section 3.3.2.2, the addition of electron donors (DPDMS in this case) to $MgCl_2$-supported Ziegler-Natta catalysts reduces the weight percentage of the fractions that elute at lower

Stellenbosch University http://scholar.sun.ac.za

temperature and increase the weight percentage of fractions that elute at higher temperature. This confirms that the addition of an ED results in a significant decrease in the amount of room temperature fractions.[26]

Table 3.6: TREF fractionation data for the TREF fractions of samples Z4 and Z5

T_e (°C)	Sample Z5				Sample Z4			
	Wt (mg)	W_i%	ΣW_i%	W_i%/ΔT	Wt (mg)	W_i%	ΣW_i%	W_i%/ΔT
25	168	5.6	5.6	-	232	7.7	7.7	-
60	54	1.8	7.4	0.1	52	1.7	9.4	0.1
80	75	2.5	9.9	0.1	58	1.9	11.3	0.1
100	233	7.7	17.6	0.4	251	8.3	19.6	0.4
120	2 053	68.4	86.0	3.4	2 103	70.0	89.6	3.5
140	424	14.0	100.0	0.7	356	11.4	100.0	0.6

According to the curves of the W_i%/ΔT over the fractionation temperature in Figure 3.36 (A) it is obvious that there is an increase in W_i%/ΔT for the first four fractions collected after the 25 °C fraction and then a decrease for the last fractions of both samples Z4 and Z5. Furthermore, the two curves in Figure 3.36 (A) have similar distributions and shapes. This means that comparable types of active sites exist in the heterogonous catalysts in reactions carried out in the presence of DPDMS and with different amounts of hydrogen. Similar results were obtained in the case of MPDMS. Figure 3.36 (B) illustrates the accumulative weight fraction percentage versus the fractionation temperatures of the Z4 and Z5 samples. The curves are very similar.

Figure 3.37 shows the TREF distribution profiles for polymers Z4 and Z5. Subtle yet clear differences are visible, particularly with respect to the soluble fractions, and the 120 °C and 140 °C fractions. This was in line with what was expected, as these polymers are different with respect to tacticity, molecular weight and molecular weight distribution.

Stellenbosch University http://scholar.sun.ac.za

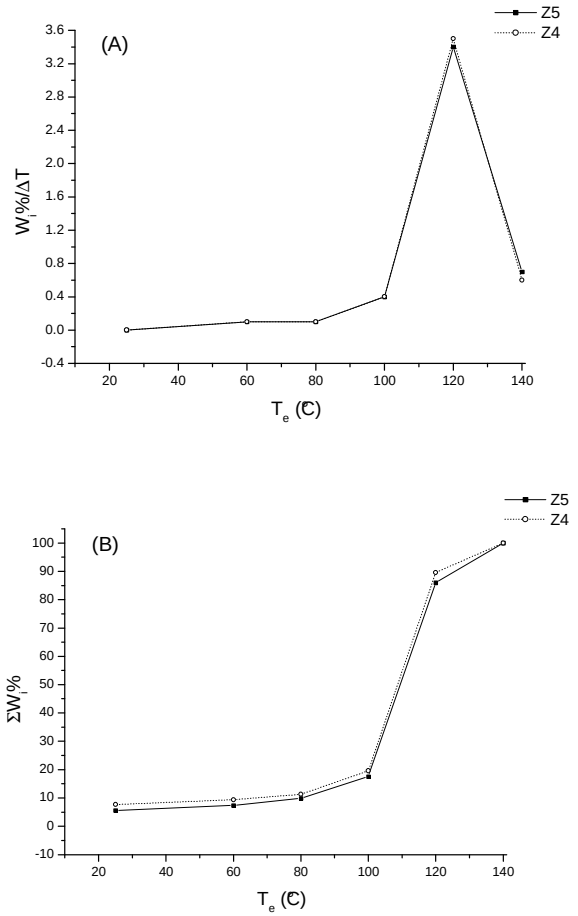

Figure 3.36: TREF curves of samples Z8, Z9 and Z10: (A) Wi%/ΔT and (B) ΣWi %.

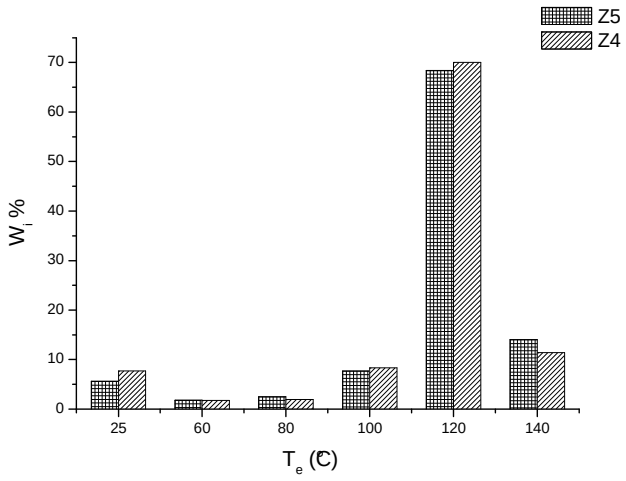

Figure 3.37: Distribution of weight percentage of Z4 and Z5 fractions vs. elution temperature (°C).

Stellenbosch University http://scholar.sun.ac.za

3.3.2.3.1 Microstructure

The ^{13}C NMR data for the TREF fractions of the Z4 and Z5 samples are summarized in Table 3.7. The isotacticity (*mmmm* %) of the Z4 and Z5 fractions vs. TREF elution temperature is shown in Figure 3.38. Other researchers have clearly demonstrated that for polypropylene the TREF profiles qualitatively reflect the distribution of isotacticity, with isotacticity increasing almost linearly with the elution temperature.[43,44] Table 3.7 and Figure 3.38 show that both Z4 and Z5 samples are composed of fractions with very different tacticities, ranging from rather atactic (elution temperature 25 °C) to highly isotactic (elution temperature 140 °C).

Table 3.7: GPC, ^{13}C NMR and DSC results of fractionation data of Z4 and Z5 samples

Runs	Fraction (T_e °C)	M_w	M_w/M_n	*mmmm* %	T_m (°C)	T_c (°C)	ΔH_m (J/g)	X_c (%)
Z5	25	9 993	33.4	48.0	-	-	-	-
	60	18 156	4.3	57.0	112.0	78.0	21.0	10.0
	80	11 696	5.9	63.0	129.0	96.0	39.3	19.0
	100	34 454	2.7	89.0	150.0-161.0	112.0	95.6	46.0
	120	207 823	2.9	96.0	161.0	118.0	103.2	49.0
	140	155 483	2.8	99.0	158.0	116.0	88.1	42.0
Z4	25	8 396	25.7	48.0	-	-	-	-
	60	16 375	10.4	59.0	114.0	84.0	24.2	12.0
	80	14 655	7.3	64.0	132.0	102.0	49.6	24.0
	100	25 109	2.6	93.0	148.0-157.0	111.0	91.2	44.0
	120	195 693	4.3	98.0	160.0	116.0	119.7	57.0
	140	142 342	3.6	99.0	158.0	114.0	102.1	49.0

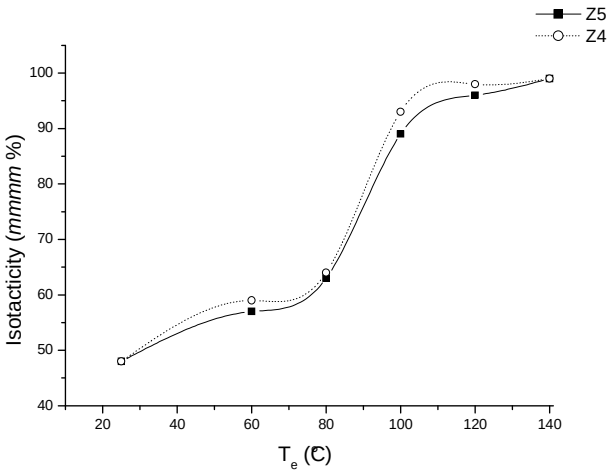

Figure 3.38: Isotacticity (*mmmm* %) of Z4 and Z5 fractions vs. TREF elution temperature.

Stellenbosch University http://scholar.sun.ac.za

An interesting outcome of this analysis is that the isotacticity of the Z4 fractions are systematically slightly greater than those of the Z5 fractions, at a given elution temperature. This is in spite of the tacticity of the Z5 parent polymer being higher than that of the Z4 parent polymer (Table 3.1).

3.3.2.3.2 Molecular weight and molecular weight distribution

Table 3.7 and Figure 3.39 show that the molecular weight of the fractions increases with the elution temperature. This indicates that, there exists a coincidence between molecular weight and tacticity to some extent, the molecular weights of the lower isotacticity fractions (i.e. fractionated at lower temperatures) also exhibited a lower molecular weight. This is in agreement with results reported by other authors.[1,28,31,32]

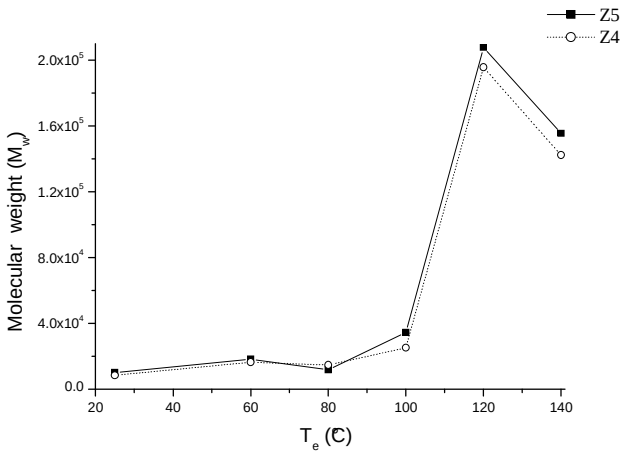

Figure 3.39: Evolution of molecular weight of TREF fractions of Z4 and Z5 samples vs. TREF elution temperature.

The PD of the TREF fractions of samples Z4 and Z5, on the other hand, tends to decrease as the elution temperature increases, as shown in Figure 3.40. The values are all relatively low (except the 25 °C fraction, which has high PD), as one would expect from TREF fractions where only small quantities of a polymer are isolated.

Stellenbosch University http://scholar.sun.ac.za

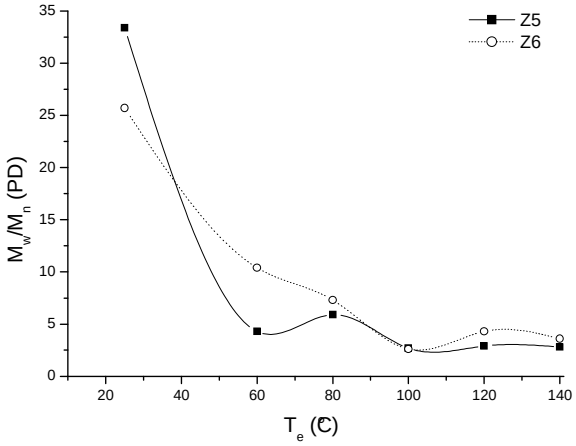

Figure 3.40: PD values of the TREF fractions of samples Z4 and Z5.

3.3.2.3.3 Crystallinity and melting behaviour

As discussed in Section 3.3.2.2.3, the melting temperature, crystallization temperature and degree of crystallinity of the TREF fractions of samples Z4 and Z5, according to DSC data, increase with increasing elution temperature, as shown in Figures 3.41, 3.42 and 3.43, respectively. This indicates that lamellar thicknesses, resultant of the fractions crystallized under given conditions, increase as a function of elution temperature for both polymers, which is a clear indication of the inter-molecular heterogeneity.

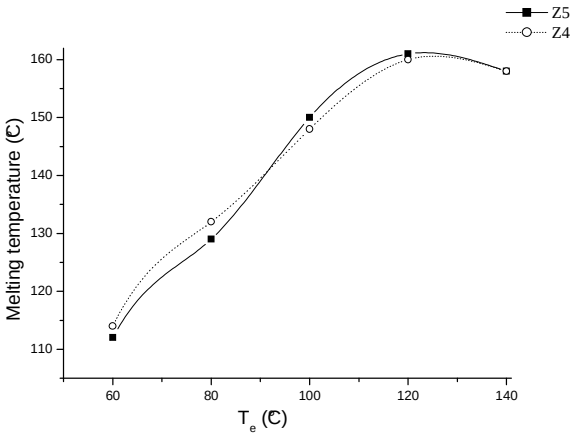

Figure 3.41: Evolution of melting temperatures (T_m) of TREF fractions of Z4 and Z5 samples versus TREF elution temperature.

Stellenbosch University http://scholar.sun.ac.za

However, slight differences in the melting and crystallization temperatures, and degree of crystallinities, of the TREF fractions, between the Z4 and Z5 can be seen. This is due to the characteristic differences between the Z4 and Z5 parent polymers (Table 3.1).

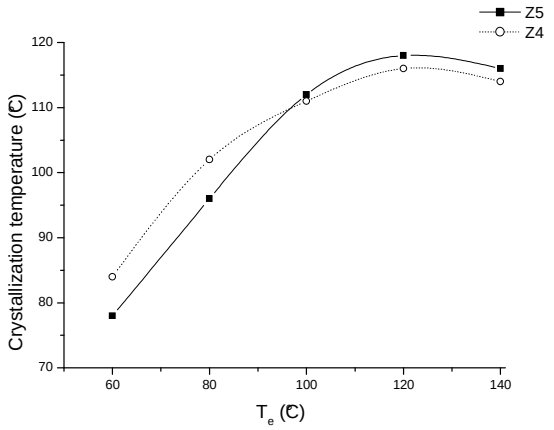

Figure 3.42: Evolution of crystallization temperature (T_c) of Z4 and Z5 TREF fractions versus TREF elution temperature.

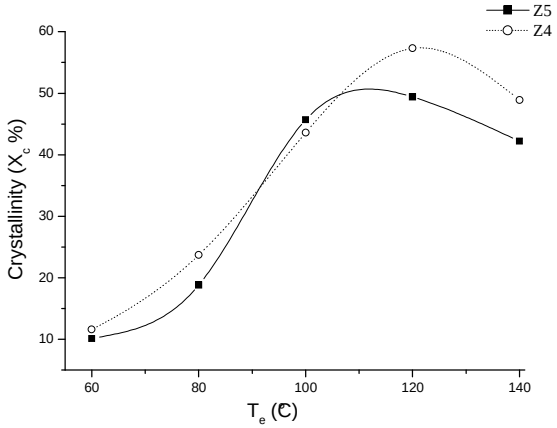

Figure 3.43: Degree of crystallinity of the TREF fractions of samples Z4 and Z5 versus TREF elution temperature.

As mentioned in the case of using MPDMS in Section 3.3.2.2.3. It is clear that there is a sharp increase in the crystallinity with increasing molecular weight in low molecular weight fractions (Figure 3.44). It appears that molecular weight is the main factor that influencing the crystallinity in these fractions.

Stellenbosch University http://scholar.sun.ac.za

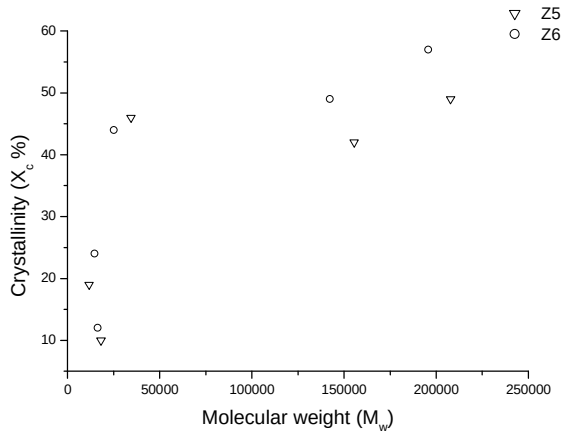

Figure 3.44: Effect of molecular weight on the crystallinity degree of the TREF fractions of samples Z4 and Z5.

A linear increase over a wide range of crystallinity with increasing tacticity is observed (Figure 3.45). This is a clear indication that the fractionation process is dependent on the tacticities and molecular weights of the polymers. It is obvious here that a balance must be struck in order to achieve the maximum degree of crystallization.

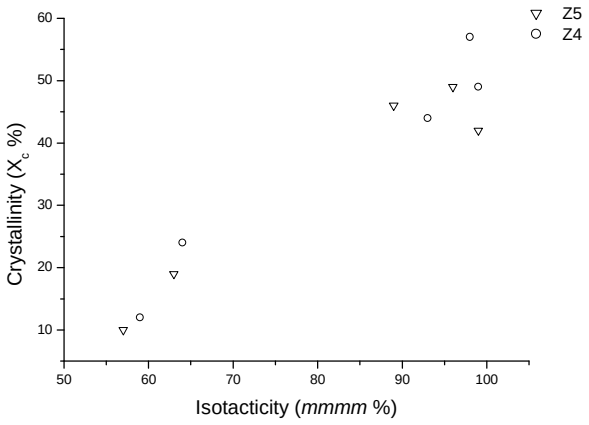

Figure 3.45: Effect of isotacticity on the crystallinity degree of the TREF fractions of samples Z4 and Z5.

3.3.2.3.4 Crystal phase analysis

For all the crystalline TREF fractions of sample Z4, WAXD analyses revealed only the presence of the α crystalline form, as illustrated in Figure 3.46. These results are similar to those results reported in Section 3.3.2.2.4.

Stellenbosch University http://scholar.sun.ac.za

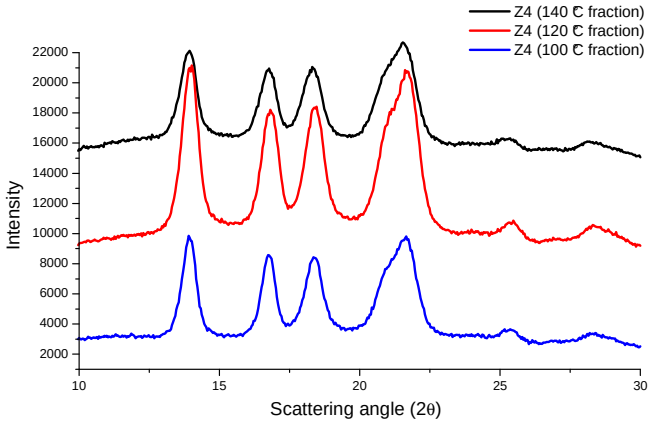

Figure 3.46: Typical X-ray diffraction pattern of different TREF fractions of the Z4 sample.

3.4 Conclusions

Using a Ziegler-Natta catalyst system under various conditions, it was possible to produce polymer samples that varied widely in terms of tacticity and molecular weight. Preparative TREF was used to obtain polymer fractions of well-defined structure in terms of molecular weight, molecular weight distributions and tacticity. It is obvious that the polymerization conditions play a major role in the production of materials with distinct differences in their composition. There are a number of different ways to control the composition of the polymers produced using these catalysts, and therefore the microstructure and the properties can be tailored via the polymerization conditions to obtain polymers with certain characteristics. The conditions can essentially be tailored to adapt a certain application for which the material is required.

Firstly, regarding the use of molecular hydrogen as a terminating agent to control the molecular weights of the produced polymers, a decrease in molecular weight with increasing hydrogen concentration was observed. It was noted that the addition of even a small amount of hydrogen can cause a significant drop in the molecular weight of the chains. A sharp increase in the degree of crystallinity of the chains was also noticed upon increasing the amount of hydrogen. This was due to the lower molecular weight, which makes the motion of chain molecules easier, allowing the reorganization of the chains in order for the polymers to crystallize more perfectly. It is also possible that the tacticity of the chains was improved slightly as the amount of hydrogen was increased due to increased chain transfer to hydrogen after 2,1-insertions, therefore forming chain ends rather than incorporating defects into the chains. This improves the overall chain stereoregularity.

Stellenbosch University http://scholar.sun.ac.za

The effect of the type of ED was also investigated. The presence of EDs in $MgC1_2$-supported catalyst systems for polypropylene polymerizations play an essential role in determining not only the isotacticity but also the polymer yield, molecular weight and molecular weight distribution. These factors are interrelated and, to a large extent, are dependent on the regioselectivity and stereoselectivity of the active species, which can change during chain growth depending on the nature of donor coordination in the environment of the active species. The catalyst with MPDMS as an ED is a bit more active than in the case where DPDMS was used, in the absence of hydrogen. This is most probably due to the decreased steric bulk of the methyl group of MPDMS compared to the phenyl group of DPDMS. This has the effect that the active sites protected by the ED are less hindered than those with DPDMS in the vicinity. The stereospecificity of the sites shows various results dependence on the amount of hydrogen that used in the propylene polymerization reaction, which shows that the two EDs have different responses to the molecular hydrogen. This can also be seen in the case of the molecular weight, which decreases when MPDMS is used. In general, the isotactic stereoregularity of the polymers produced in the presence of the two EDs indicates a high proportion of isotactoid sequences. It is likely that the EDs are easily displaced from the catalyst surface, giving a relatively labile coordination. This will possibly lead to the formation of highly isospecific active sites on the catalyst surface. On other hand, the crystallinty of the polymers produced using MPDMS is slightly higher than those produced using DPDMS. Differences in the type of ED and the amount of molecular hydrogen used clearly result in differences in the microstructure of the produced polymers.

TREF can be used to fractionate polypropylene polymers into any number of fractions desired, depending on the minimum mass of the fractions needed for the necessary analyses. TREF gave a good recovery percentage of above 99 wt %. TREF fractionation of the samples showed that the samples produced without any ED eluted mainly in the 100 and 110 °C fractions, while the samples produced using DPDMS and MPDMS eluted mainly in the 110 and 120 °C fractions. Furthermore, the weight fraction results showed that polymers produced using the two EDs, have significantly lower weight percentage fractions for the room temperature fraction than those produced without any ED. It appeared that DPDMS had more influence on the active sites, producing chains that eluted in the lower temperature fractions than in the case of the MPDMS, i.e. DPDMS is better at changing the active sites to those of increased stereospecificity than MPDMS is. The molecular weight of the fractions increased significantly for all samples after the 100 °C fraction, irrespective of ED type. This is a clear indication that the molecular weight plays a significant role in the fractionation mechanism of

Stellenbosch University http://scholar.sun.ac.za

TREF. There are fractions present with negligible differences in *mmmm* pentad content that elute in consecutive fractions.

In the case of the PD of the TREF fractions, it was clear that the lower temperature fractions have a broader distribution of molecular weight chains than the higher temperature fractions. Overall, the PD of the TREF fractions tends to decrease as the elution temperature increases. The values are all relatively low (the exception being the 25 °C fraction, which has a high PD), as one would expect from TREF fractions where only small quantities of a polymer are isolated. The isotacticity of the fractions also increases with the elution temperature. The overall isotacticity of the TREF fractions can be increased by the addition of electron donors to $MgCl_2$-supported Ziegler-Natta catalysts. This is quite clear if we compare the results of the TREF fractions eluted from polypropylene samples produced without any electron donors (Table 3.3 and Figure 3.14) to the TREF fractions that eluted in the presence of two different external electron donors (Tables 3.5, 3.7 and Figures 3.26, 3.38). These results indicate that electron donors can convert aspecific active sites into different isospecific active sites, and that the conversion is related to the structure of internal electron donors.

In general, the thermal properties in terms of T_c, T_m and degree of crstallinity of the TREF fractions improved with fractionation temperature, up to the 120 °C fractions, for all fractions produced in the presence and absence of EDs, after which there was a slight decrease in the properties due to the co-crystallization of material trapped during the TREF crystallization process.

Only the α crystal form existed in all TREF fractions of different samples. The main difference in the α crystal peaks of the various TREF fractions was the strong diffraction of these peaks, which depends on the crystallinity content of each fraction.

3.5 References

1. G. W. Harding, A. J. van Reenen, *Macromol. Chem. Phys*. **2006**, 207, 1680.
2. H. Mori, M. Endo, M. Terano, *J. Mol. Catal. A: Chem*. **1999**, 145, 211.
3. I. Kouzai, T. Wada, T. Taniike, M. Terano, *Macromol. Symp*. **2007**, 260, 179.
4. V. Busico, R. Cipullo, G. Talarico, A. L. Segre, J. C. Chadwick, *Macromolecules* **1997**, 30, 4786.
5. G. Guastalla, U. Giannini, *Macromol. Rapid Commun.* **1983**, 4, 519.
6. K. Soga, T. Shiono, *Polym. Bull*. **1982**, 8, 261.
7. E. Albizzati, M. Galimberti, U. Giannini, G. Morini, *Macromol. Symp.* **1991**, 49, 223.
8. G. D. Bukatov, V. S. Goncharov, V. A. Zakharov, *Macromol. Chem. Phys.* **1995**, 196, 1751.
9. J. C. Chadwick, G. M. Kessel, O. Sudmeijer, *Macromol. Chem. Phys*. **1995**, 196, 1431.

Stellenbosch University http://scholar.sun.ac.za

10. J. Stephan, M. Rolf, S. Udo, B. Hans, F. David, L. Franz, *J. Polym. Sci., Part A: Polym. Chem*. **1995**, 33, 1305.
11. J. A. Ewen, *J. Am. Chem. Soc*. **1984**, 106, 6355.
12. S. Lin, M. Waymouth, *Macromolecules* **1999**, 32, 8283.
13. A. Carvill, I. Tritto, P. Locatelli, C. Sacchi, *Macromolecules* **1997**, 30, 7056.
14. G. Moscardi, F. Piemontesi, L. Resconi, *Organometallics* **1999**, 18, 5264.
15. M. Harkonen, J. V. Seppala, R. Chujo, Y. Kogure, *Polymer* **1995**, 36, 1499.
16. V. Y. Kissin, L. A. Rishina, E. I. Vizen, *J. Polym. Sci., Part A: Polym. Chem*. **2002**, 40, 1899.
17. V. Y. Kissin, L. A. Rishina, *J. Polym. Sci., Part A: Polym. Chem*. **2002**, 40, 1353.
18. C. M. Forte, F. M. Countinho, *Eur. Polym. J*. **1996**, 32, 605.
19. J. C. Chadwick, G. Morini, E. Albizzati, G. Balbontin, I. Mingozzi, A. Cristofori, *Macromol. Chem. Phys*. **1996**, 197,2501.
20. J. C. Chadwick, *Macromol. Symp*. **2001**, 173, 21.
21. P. Deukkil, I. Kim, H. Yang, S. Soo, B. Kim, H. Chang, *J. Appl. Polym. Sci*. **2005**, 95, 231.
22. D. R. Morrow, *J. Macromol. Sci., Phys. B*. **1969**, 3, 53.
23. P. Supaphol, *J. Appl. Polym. Sci*. **2001**, 82, 1083.
24. D. R. Morrow, B. A. Newman, *J. Appl. Phys*. **1968**, 39, 4944.
25. G. Morini, E. Albizatti, G. Balbontin, I. Mingozzi, M. C. Sacehi, F. Forlini, I. Tritto, *Macromolecules*, **1996**, 29, 5770.
26. J. T. Xu, L. X. Feng, S. L. Yang, Y. Q. Yang, X. M. Kong, *Eur. Polym. J*. **1998**, 34, 431.
27. M. Kioka, *Polymer* **1994**, 35, 580.
28. P. Viville, D. Daoust, A. M. Jonas, B. Nysten, R. Legras, M. Dupire, J. Michel, G. Debrasb, *Polymer* **2001**, 42, 1953.
29. J. B. Soares, A. E. Hamielec, *Polymer* **1996**, 37, 4607.
30. P. Lodefier, A. M. Jonas, R. Legras, *Macromolecules* **1999**, 32, 7135.
31. E. P. Moore, Jr. *Polypropylene Handbook*, Hanser Publishers. Munich, **1996**.
32. J. Xu, L. Feng, *Eur. Polym. J*. **2000**, 36, 867.
33. T. W. Huang, R. G. Alamo, L. Mandelkern, *Macromolecules* **1999**, 32, 6374.
34. R. G. Alamo, G. M. Brown, L. Mandelkern, A. Lehtinen, R. Paukkeri, *Polymer* **1999**, 40, 3933.
35. R. Paukkeri, A. Lehtinen, *Polymer* **1993**, 34, 4083.
36. Z. Bartczak, V. Chiono, M. Pracella, *Polymer* **2004**, 45, 7549.
37. D. R. Burfield, P. S. T. Loi, Y. Doi, J. Mejzik, *J. Appl. Polym. Sci*. **1990**, 41, 1095.
38. G. Zerbi, F. Ciampelli, V. Zamboni, *J. Polym. Sci. C* **1963**, 7, 141.
39. L. Chen, X. Zhu, D. Yan, *Polym. Prepr*. **2003**, 44, 1187.
40. J. P. Luongo, *J. Polym. Sci*. **1960**, 42, 302.
41. U. Mierau, D. Voigt, F. Bohme, E. Brauer, *J. Appl. Polym. Sci*. **1997**, 63, 283.
42. J. T. Xu, L. X. Feng, S. L. Yang, *Chem. J. Chin. Univ*. **1997**, 18, 1734.
43. J. T. Xu, Y. Q. Yang, L. X. Feng, X. M. Kong, S. L. Yang, *J. Appl. Polym. Sci*. **1996**, 62, 727.
44. M. Kakugo, T. Miyatake, Y. Natio, K. Mizunumn, *Macromolecules* **1988**, 21, 314.

Stellenbosch University http://scholar.sun.ac.za

CHAPTER 4

Fractionation and crystallization of isotactic polypropylenes prepared using homogenous metallocene catalysts

4.1 Introduction

Metallocene catalyst systems have been around for just as long as the Ziegler-Natta systems.[1] Metallocenes are special members of a class of organometallic compounds. They are activated with methylaluminoxane (MAO) to form single-site catalyst systems that are effective for α-olefin polymerization. These catalysts produce polymers with uniform and controlled properties. Chiral metallocene catalysts possessing C_2-symmetry have been widely studied in order to optimize, and to better understand, their ability to catalyze the stereoregular polymerization of propylene.[2,3] Ansa C_2-symmetric metallocene catalysts are highly isoselective in propylene polymerization and have high activity. This allows for their use in most industrial applications for the production of polypropylene homopolymers and polypropylene copolymers. Control of the molecular weight of polymers produced by C_2-metallocene catalysts can be easily achieved by introducing hydrogen to the polymerization system or by increasing the reaction temperature. Unlike conventional Ziegler-Natta catalysts, metallocenes require only small amounts of hydrogen to significantly reduce the molecular weight of polymer produced.[4]

This chapter reports on propylene polymerization and analysis of the microstructure, molecular weight, molecular weight distribution and thermal properties of these polymers produced using *rac*-ethylene-bis(indenyl) zirconium dichloride, $Et(Ind)_2ZrCl_2$ (EI), and *rac*-ethylene-bis(4,5,6,7-tetrahydro-1-indenyl) zirconium dichloride, $Et(H4Ind)_2ZrCl_2$ (EI(4H)) (Figure 4.1 A and B) as metallocene catalysts in the absence and presence of molecular hydrogen as transfer agent. In order to establish a correlation between the molecular weight and the crystallization of these polymers, fractionation of the materials according to their crystallizability was performed by means of TREF. This affords the opportunity for blending materials of differing molecular weight but similar symmetry. In addition, a full fractionation and characterization of a commercial syndiotactic polypropylene was carried out in order to obtain different fractions with different tacticities and molecular weights.

Stellenbosch University http://scholar.sun.ac.za

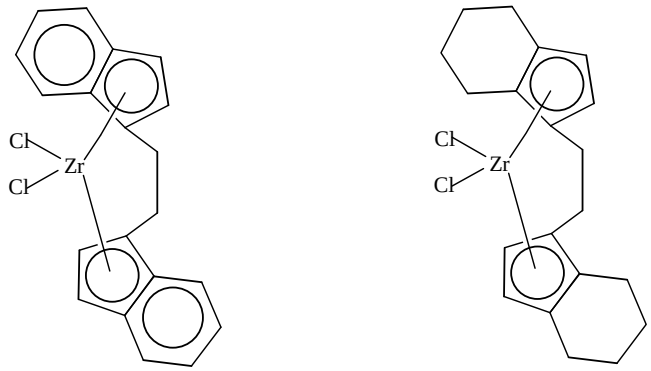

A **B**

Figure 4.1: (A) *rac*-Et(Ind)$_2$ZrCl$_2$ (EI) and (B) *rac*-Et(H4Ind)$_2$ZrCl$_2$ (EI(4H)).

4.2 Experimental

4.2.1 Material

Propylene was obtained from Sigma-Aldrich and used as received. High purity argon and hydrogen were obtained from Afrox (South Africa). Toluene (Sigma-Aldrich) was dried by refluxing over sodium/benzophenone and then distilling under an inert gas atmosphere. MAO was purchased from Sigma-Aldrich (10 wt % solution in toluene) and used as received. The catalysts used in this chapter, EI and EI(4H), were obtained from Sigma-Aldrich and used as received. Metallocene catalysts comprising group 4 metallocene complexes and MAO are air and moisture sensitive, and thus experiments must be performed under an inert atmosphere and in dry solvents. Syndiotactic polypropylene was obtained from Sigma-Aldrich and used as received for the fractionation.

4.2.2 Polymerization

All reactions were carried out under an inert gas atmosphere using standard Schlenk techniques. The polymerization reactions were carried out in a 350-ml stainless steel Parr autoclave with an inlet and a pressure gauge. Typically, the reactor was charged with MAO (10 wt % solution in toluene), catalyst (0.55 µmol in 5 ml toluene) and toluene (30 ml). The catalyst solution was stirred for 5 minutes and then the monomer was added. The reactor was pressurized with hydrogen and the content stirred for 1 hour at room temperature. The following polymerization conditions were used for all reactions:

Stellenbosch University http://scholar.sun.ac.za

- the catalyst/MAO ratio was kept at 1:2000,
- 4–5 g propylene was used,
- all reactions were carried out at room temperature, and
- different amounts of hydrogen were used as terminating agent to control the molecular weight.

After 1 hour the reaction was quenched with 10% HCl/MeOH. The resulting polymer was filtered off, washed several times with methanol and then dried under vacuum at 80 °C for 15 hours to yield about 2–4 g of polypropylene as a white powder.

4.2.3 TREF procedure

The general TREF procedure is described in Chapter 3 (Section 3.2.3).

4.2.4 Characterization techniques

The ^{13}C NMR, HT-GPC, DSC, WAXD and FT-IR data of samples were obtained according to procedures described in Chapter 3 (Section 3.2.4).

4.3 Results and discussion

4.3.1 Characterization of the non-fractionated polypropylenes

The characteristics of the polypropylenes prepared using EI and EI(4H) metallocene catalysts in the absence and presence of different amounts of molecular hydrogen are summarized in Table 4.1. The samples prepared using EI catalyst were coded as EIP15-1 in Table 4.1, while the samples prepared using EI(4H) were coded as D9-3. The catalysts activities, microstructures, molecular weights, molecular weight distributions, melting points and percentage of crystallinity observed in polypropylenes prepared in the absence and presence of hydrogen, with full explanations, will be the subjects of the following sections.

Stellenbosch University http://scholar.sun.ac.za

Table 4.1: Results of propylene polymerizations carried out with EI and EI(4H) catalyst systems using various concentrations of hydrogen[a,b]

Run	H_2 (wt %)[c]	Activity[d]	M_w[e]	M_w/M_n	*mmmm* %[f]	T_m (°C)	T_c (°C)	ΔH_m[g] (J/g)	X_c[h] (%)
EIP15	0.0	1 073	44 202	2.2	94.0	138.2	108.0	94.3	45.1
EIP14	0.3	1 879	19 232	1.9	93.8	137.6	108.2	107.4	51.4
EIP13	0.7	1 990	9 901	2.0	89.0	132.2	102.7	95.5	45.7
EIP12	1.0	2 528	10 922	2.0	89.5	137.5	108.9	106.7	51.1
EIP11	1.3	2 737	9 959	1.9	90.1	137.5	110.0	102.6	49.1
EIP10	1.7	2 041	10 240	2.0	90.0	138.1	109.9	108.3	51.8
EIP2	2.0	2 344	3 738	2.2	88.7	135.7	106.8	103.5	49.5
EIP1	2.3	2 062	4 512	2.0	84.3	135.2	106.2	103.6	49.5
D9	0.0	1 785	24 809	2.0	88.0	138.0	107.7	87.4	41.8
D8	0.3	2 171	7 188	2.0	85.8	137.2	104.4	96.9	46.4
D7	0.7	2 191	5 262	1.9	85.1	135.0	102.8	101.4	48.5
D6	1.0	2 235	4 369	1.9	81.9	135.6	105.8	102.4	49.0
D5	1.3	2 287	3 290	1.8	79.0	132.0	99.8	79.4	38.0
D4	1.7	2 151	2 825	1.8	77.7	132.1	102.4	94.9	45.4
D3	2.0	2 424	2 244	1.7	70.3	127.3	95.8	81.7	39.1

[a] Al/Zr ratio 1:2000
[b] room temperature (25 °C)
[c] (g H_2/g propylene) × 100
[d] (kg PP/(mol Zr.h))
[e] determined by GPC
[f] determined by ^{13}C NMR
[g] determined by DSC
[h] ΔH_m = 209 J/g of PP 100% crystallinity[5]

4.3.1.1 Activity

Table 4.1 and Figure 4.2 show that, as expected, the presence of hydrogen caused an increase in polymerization activity for EI and EI(4H) catalysts. The most common explanation of this activating effect is the regeneration of an active species from the "dormant sites" formed after a regio-irregular olefin insertion (2,1-insertion).[6-8] The chain transfer from a Zr-2,1-unit to hydrogen is about twice as fast as 1,2-insertion of propylene into this unit. Moreover, polymerization activity for EI increased (up to 2.5-fold in presence of 1.3 wt % hydrogen), from 1 073 to 2 737 kg PP/(mol Zr.h), while in the case of EI(4H) the polymerization activity increased only up to 1.5-fold in presence of 2.0 wt % hydrogen (from 1 785 to 2 424 kg PP/mol Zr.h). The increased activity of the EI catalyst compared with the EI(4H) catalyst was expected, but the greater effect of hydrogen on the activity for the former catalyst can not be explained. What is noticeable is that the increased activity with increasing hydrogen content is maintained to higher levels of hydrogen for the EI(4H) catalyst than for the EI catalyst.

Stellenbosch University http://scholar.sun.ac.za

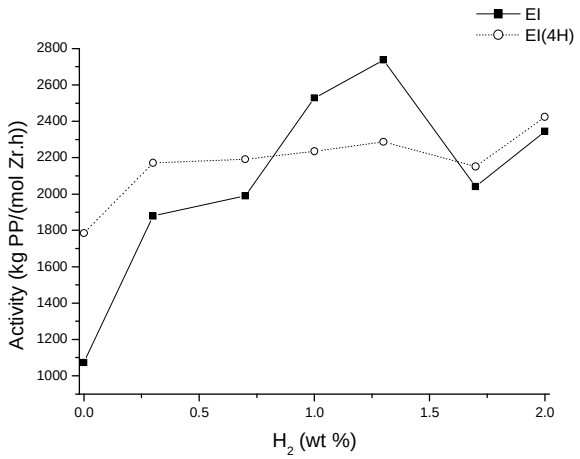

Figure 4.2: Catalyst activities of EI and EI(4H) in the presence different amounts of hydrogen.

4.3.1.2 Microstructure

The microstructures of the isotactic polypropylene samples were analyzed by solution ^{13}C NMR. The isotacticity (measured as *mmmm* %) is affected by hydrogen. Conflicting results have been reported for different systems. Tsutsui *et al.*[9] reported a slight decrease in stereoregularity, from 91.7 to 89.0 % *mm* triads, for the *rac*-$C_2H_4(1\text{-Ind})_2ZrCl_2$/MAO catalyst system. A stronger negative effect was found for bis(2-arylindenyl)Zr/MAO catalysts by Lin and Waymouth.[10] No effect of hydrogen on isotacticity has been found in liquid propylene at 50 °C with the *rac*-$Me_2C(3\text{-t-Bu-1-Ind})_2\text{-}ZrCl_2$/MAO catalyst system.[11] Carville *et al.*[12] also reported that low hydrogen levels do not influence tacticity.

In the present study, under similar polymerization conditions, the isotacticity of polypropylenes produced by both catalysts is decreased, as can be seen in Figure 4.3. Table 4.1 and Figure 4.3 also show that there is a difference in tacticities of the polypropylene polymer prepared using the two different catalyst systems. The tacticity ([*mmmm*]) of the polymers produced using the EI(4H) catalyst system decreased significantly (from 88.0 % in the absence of hydrogen to 70.3 % in the presence of 2.0 wt % hydrogen), while in the case of the EI catalyst system the decrease was somewhat less (from 94.0 % in the absence of hydrogen to 84.3 % with 2.3 wt % hydrogen). The decrease in the isotacticity of these polymers is due to the increase of stereo-irregular pentads, [*mmmr*], [*mmrr*] and [*mrrm*], which could be attributed to the decreasing stereoselectivity of the catalyst with an increasing the amount of hydrogen. The decrease in the isotacticity can also be attributed to the decreasing molecular weights of these polymers with increasing hydrogen, which leads to loss in the active site control over the chain propagation.

Stellenbosch University http://scholar.sun.ac.za

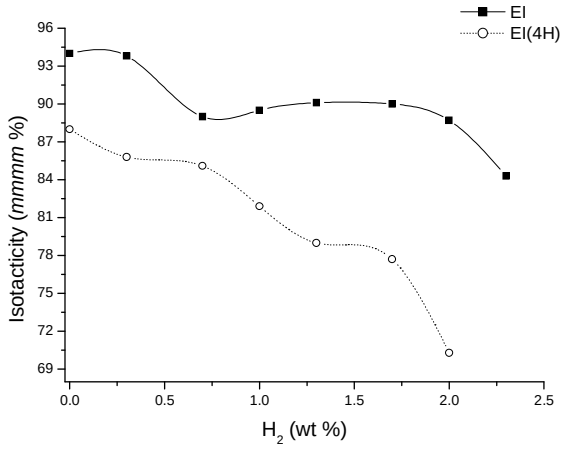

Figure 4.3: Dependence of the isotacticity of polypropylenes on the hydrogen content for EI and EI(4H) catalysts.

4.3.1.3 Molecular weight and molecular weight distribution

In general, and as can be seen from Table 4.1, the molecular weights of polypropylenes prepared with the EI(H4) catalyst are much lower than those prepared with the EI catalyst under our experimental conditions used. This suggests that EI(H4) has a stronger tendency to undergo chain transfer reactions (under such conditions) because of the electronic structure of its hydrogenated ligands.[13] On the other hand, Table 4.1 and Figure 4.4 show that, as expected, the presence of a small amount of hydrogen caused an remarkable reduction in polymer molecular weights in the cases of both catalysts ($\overline{M_w}$ = 44 202 g mol^{-1} in the absence of hydrogen to $\overline{M_w}$ = 19 232 g mol^{-1} in the presence of 0.3 wt % of hydrogen in the case of EI catalyst and from 24 809 g mol^{-1} to 7 188 g mol^{-1} in the case of EI(4H) catalyst). This decrease in the molecular weight can be explained as a result of an increase of chain termination by hydrogen. Of note here is that the EI(4H) catalyst seemed far more sensitive to low amounts of hydrogen than the EI catalyst. It can also be seen in Figure 4.4 that the molecular weight of polypropylenes produced in the presence of hydrogen decreases to a certain level and then remains constant, or slightly decreases, by further increasing the hydrogen amount, which is dependent on the nature of the catalyst.

Stellenbosch University http://scholar.sun.ac.za

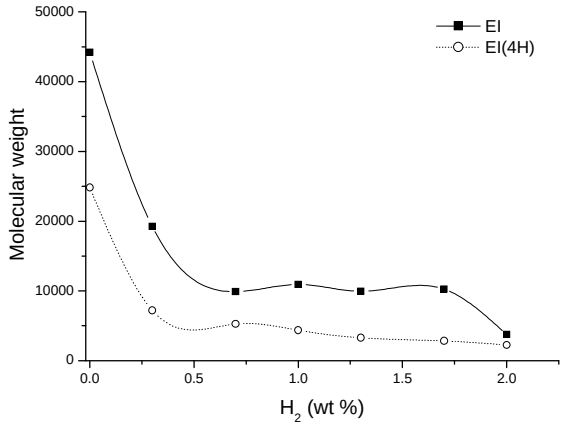

Figure 4.4: Dependence of molecular weight of polypropylenes produced using EI and EI(4H) catalysts on the hydrogen content.

Consistent with the literature values,[14,15] the polypropylenes produced with the EI(H4) catalyst system showed slightly narrower molecular weight distributions than those produced with the EI catalyst system (M_w/M_n = 1.7–2.0 and 1.9–2.2, respectively, as shown in Table 4.1). The fact that the molecular weight distribution of polypropylenes is narrower in the case of EI(4H), catalyst and corresponds to Schulz-Flory molecular weight distributions, strongly suggests that the catalytically active sites of EI(4H) are more uniform; i.e., only one type of active species exists in the reaction system for the polymerization reactions of EI(4H) catalyst.[13] Nevertheless, the molecular weight distributions of both catalysts are very characteristic of single-site catalysts, which produce polymers with uniform molecular weights.

4.3.1.4 Crystallinity and melting behaviour

Table 4.1 gives the results of the DSC analyses of the polypropylenes, with and without hydrogen, produced with the bridged EI and EI(4H) catalysts. The degree of crystallinity was calculated by recording the ratio of the measured heat of fusion to that of a standard of known crystallinity. The heat of fusion of a perfect polypropylene crystal, used in the determination of the crystallinity, was taken as 209 J/g.[5]

Figure 4.5 presents a waterfall plot of the DSC melting endotherms for the polypropylenes produced using EI(4H) metallocene catalyst (the data for polypropylenes produced using EI catalyst show a slightly uneven trend). The melting temperature (T_m) of the obtained polymer produced when using EI catalyst in the absence of hydrogen (138.2 °C) is slightly higher than

Stellenbosch University http://scholar.sun.ac.za

those obtained using different amounts of hydrogen (135.2 °C in the presence of 2.3 wt % of hydrogen), while the melting temperature of the polymer produced using EI(4H) catalyst in the absence of hydrogen (138.0 °C) is significantly higher than those produced using different amount of hydrogen (127.3 °C in the presence of 2.0 wt % hydrogen) . This decrease in the melting points could be due to the amount of misinsertions and the low molecular weight of polypropylenes ($\overline{M_w}$ = 4 512 and 2 244, respectively), which is usually caused by performing the polymerizations in the presence of 2.3 and 2.0 wt % hydrogen.

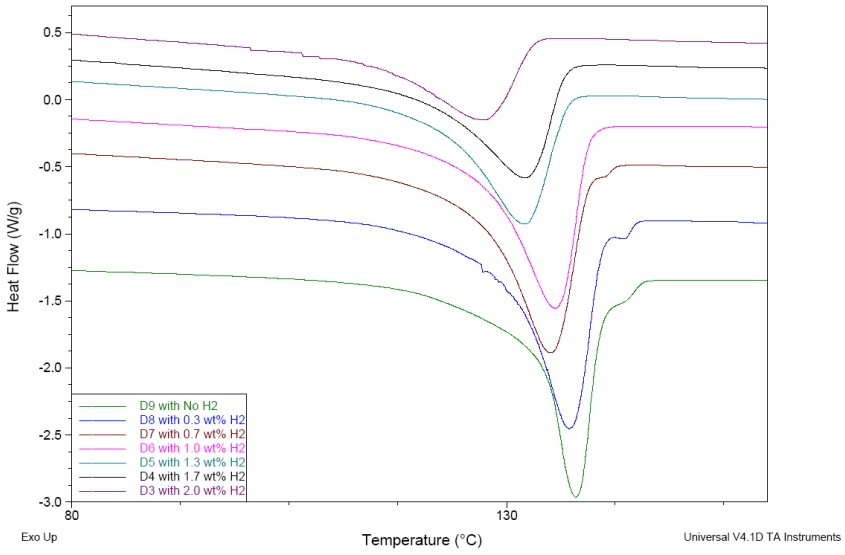

Figure 4.5: Waterfall plot of the DSC melting endotherms for polypropylenes produced using EI(4H) metallocene catalyst.

Generally, as the molecular weights decrease, so do the melting points. This can clearly be seen in Figure 4.6. On the other hand, Figure 4.7 shows the relationship between the melting temperature and the tacticity. It is noticeable that a linear decrease of T_m with decreasing tacticity is observed for polypropylene samples produced using both catalysts.

Stellenbosch University http://scholar.sun.ac.za

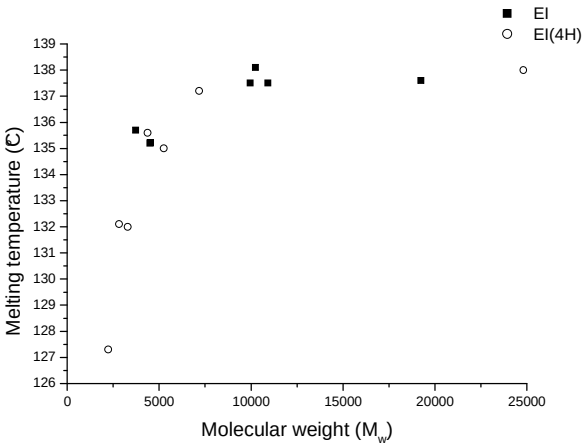

Figure 4.6: Molecular weights of polypropylenes produced with EI and EI(4H) catalyst versus melting temperatures.

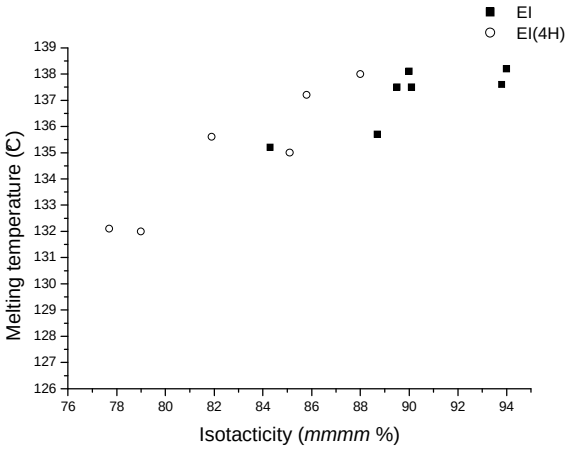

Figure 4.7: Isotacticities of polypropylenes produced with EI and EI(4H) catalyst versus melting temperatures.

4.3.1.5 Crystalline structure

The different crystalline phases of isotactic polypropylene could be identified from the X-ray diffraction data. The peaks at 2θ = 14.8°, 16.95° and 18.5° relate to the indices 110, 040 and 130, respectively, and are typical for the α-phase. The 117 peak at 2θ = 20.07° is related to the γ-phase.[16] Figure 4.8 shows typical WAXD patterns of the α form, in which three strong equatorial peaks of the (110), (040) and (130) phases appear at 2θ = 13.83°, 16.90° and 18.34°, respectively. Only the α crystal form is present in all polypropylene polymers

prepared in the absence and presence of small amounts of hydrogen, using EI catalyst (Figure 4.8 A) and EI(4H) catalyst (Figure 4.8 B). Moreover, the presence of the γ crystal form in the polypropylene samples prepared by both metallocene catalysts in the presence of high amounts of hydrogen (EIP1 and D3 with 2.3 and 2.0 wt % hydrogen, respectively) at 2θ = 20.0 can clearly be seen in Figure 4.8 A and B. This result is in contrast with the results obtained using Ziegler-Natta catalyst in the previous chapter. It has been reported that isotactic polypropylene samples prepared with a commercial, heterogeneous Ziegler-Natta catalyst crystallize mainly in the α-phase.[17] This can be attributed to the uneven distribution of defects along the polymer chains.

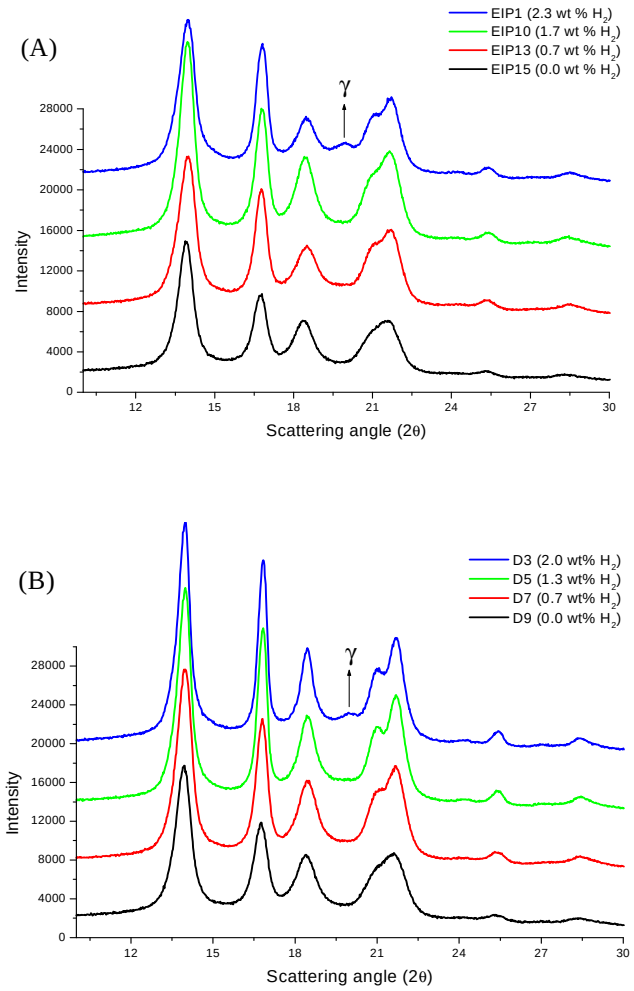

Figure 4.8: Typical X-ray diffraction pattern recorded for polypropylenes produced using (A) EI catalyst and (B) EI(4H) catalyst.

The distribution of tacticity in the Ziegler-Natta derived samples is not homogeneous over the molecular weight distribution and also not homogeneous within the chains itself. Ziegler-Natta samples have a blocky distribution of the stereo-defects. The defects are accumulated in a small portion of non-crystallizable chains or form small blocks of irregular sequences among long regular chains. This leads to long regular isotactic sequences, which favour the formation of the α-phase. It has also been reported that the formation of the γ-phase is favoured in the presence of stereo-defects and regio-defects (as in the case of EIP1 and D3 samples, which have slightly low tacticities: [*mmmm*] % = 84.3 and 70.3, respectively. See Table 4.1), and also by the presence of comonomer units, which shorten the regular isotactic sequences.[18]

4.3.2 Fractionation and characterization of polypropylenes

4.3.2.1 Polypropylenes produced using the EI catalyst

The polypropylene samples for TREF fractionation were chosen in order to establish a correlation between the molecular weight and the crystallization of the polypropylene polymers. Fractionation of the polypropylene samples according to crystallizability was performed by means of TREF. TREF analyses of three different isotactic polypropylenes prepared with EI metallocene catalysts EIP12, EIP13 and EIP14 were carried out to determine the differences in their characteristics. First, the original polymers were fractionated into seven different fractions, eluting at 25, 60, 80, 90, 100, 110 and 130 °C.

The TREF fractionation data are summarized in Table 4.2 and the TREF curves obtained are illustrated in Figure 4.9. Table 4.2 shows that for the samples EIP14, EIP13 and EIP12 more than 59 wt % of the material eluted at the elution temperatures 80 and 90 °C. When these results are compared with the results reported in the previous chapter for the polypropylenes produced with Ziegler-Natta catalysts, we find that as expected, the former isotactic polypropylenes elute at a lower temperature compared to the latter. This arises from the presence of regio-irregularities, and is in accordance with the fact that metallocene-based isotactic polypropylenes commonly have a lower melting temperature.[19]

The curves of the $W_i\%/\Delta T$ over the fractionation temperature in Figure 4.9 (A) shows that there is an increase in $W_i\%/\Delta T$ for the first three fractions collected after the 25 °C fraction, followed by a decrease for the last three fractions for all samples. Moreover, the curves in Figure 4.9 (A) have different distributions and slightly different shapes. This indicates that the

presence of different amounts of hydrogen can change the stereoselectivity of the active sites that exist in the metallocene catalysts. Figure 4.9 (B) illustrates the accumulative weight fraction percentage versus the fractionation temperatures of the three polymers EIP14, EIP13 and EIP12. The curves have slightly different shapes. This could be due to the different tacticities and molecular weights of the original samples (Table 4.1).

Table 4.2: TREF fractionation data for the fractions of samples EIP14, EIP13 and EIP12

T_e (°C)	Sample EIP14				Sample EIP13				Sample EIP12			
	Wt (mg)	Wi%	ΣWi%	Wi%/ΔT	Wt (mg)	Wi%	ΣWi%	Wi%/ΔT	Wt (mg)	Wi%	ΣWi%	Wi%/ΔT
25	180	6.0	6.0	-	261	8.7	8.7	-	325	10.8	10.8	-
60	323	10.8	16.8	0.3	466	15.5	24.2	0.4	277	9.2	20.0	0.3
80	721	24.0	40.8	1.2	1 285	42.8	67.0	2.1	875	29.2	49.2	1.5
90	1 061	35.4	76.2	3.5	695	23.2	90.2	2.3	900	30.0	79.2	3.0
100	460	15.3	91.5	1.5	165	5.5	95.7	0.6	469	15.6	94.8	1.6
110	137	4.4	95.9	0.5	85	2.8	98.5	0.3	116	3.9	98.7	0.4
130	125	4.1	100.0	0.2	45	1.5	100.0	0.1	39	1.3	100.0	0.1

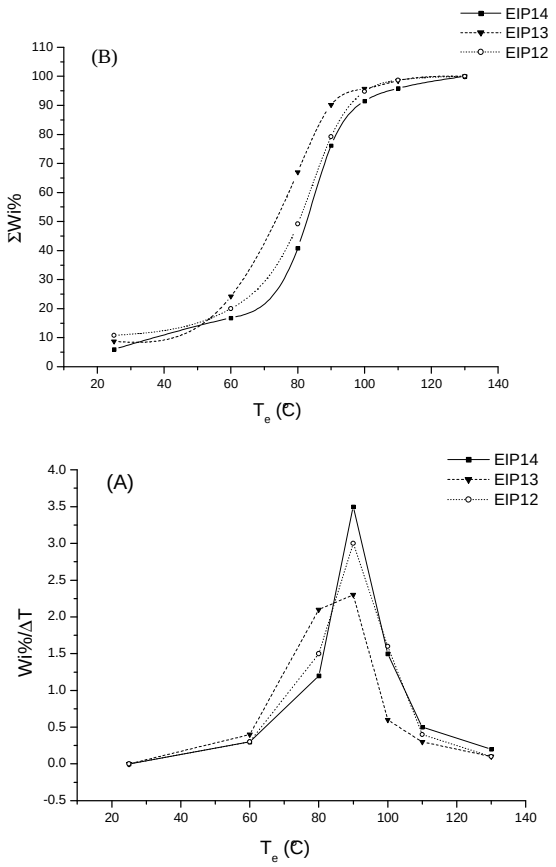

Figure 4.9: TREF curves of samples EIP14, EIP13 and EIP12: (A) Wi%/ΔT and (B) ΣWi %.

The weight fraction as a function of elution temperature for polymers EIP14, EIP13 and EIP12 is shown in Figure 4.10. The superimposed graphs provide a clear and easy way to compare the samples. Apparent differences are visible, particularly with respect to the 80, 90 and 100 °C fractions. This was in line with what was expected, as these polymers differ with respect to their tacticity, molecular weight and molecular weight distribution (Table 4.1).

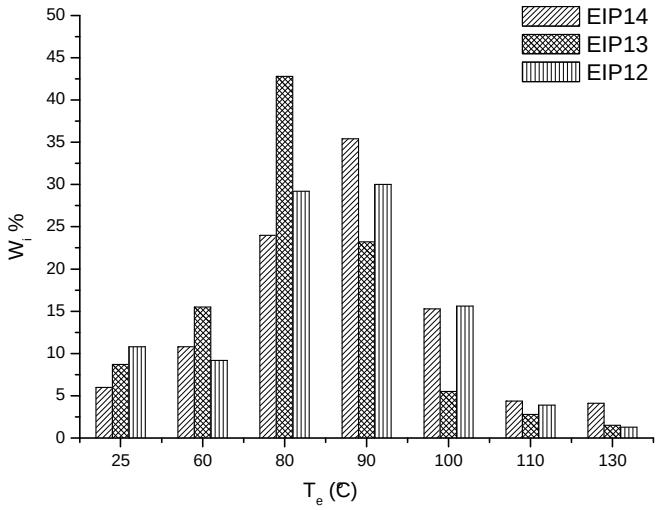

Figure 4.10: Distribution of weight percentage of EIP14, EIP13 and EIP12 fractions vs. elution temperature (°C).

4.3.2.1.1 Microstructure

The ^{13}C NMR data for the TREF fractions of EIP14, EIP13 and EIP12 samples are summarized in Table 4.3. The isotacticity (*mmmm* %) of EIP14, EIP13 and EIP12 fractions versus TREF elution temperature is shown in Figure 4.11. The TREF results obtained for isotactic polypropylenes produced with the metallocene catalysts showed different trends to polypropylenes with Ziegler-Natta catalysts.[19,20] Mizuno *et al.* [20] found that the TREF of isotactic polypropylene prepared with $(Ind)_2HfCl_2$ catalyst was performed according to molecular weight over the whole elution temperature range. All the fractions had the same tacticity and melting temperatures, but different molecular weights. Xu and Feng[19] found that the TREF of isotactic polypropylenes prepared with silica-supported metallocene catalyst showed that the first seven fractions had a difference in tacticity, but the last seven fractions had similar isotacticity and differ only in molecular weight. Molecular weight becomes the

main factor that controls the fractionation.

Table 4.3: GPC, ^{13}C NMR and DSC results of fractionation data of samples EIP14, EIP13 and EIP12

Runs	Fraction (T_e °C)	M_w	M_w/M_n	*mmmm* %	T_m (°C)	T_c (°C)	ΔH_m (J/g)	X_c (%)
EIP14	25	4 348	3.4	63.0	-	-	-	-
	60	6 931	2.6	79.0	122.4	89.1	53.0	25.4
	80	15 906	1.7	85.0	133.1	101.7	72.2	34.6
	90	22 178	1.6	87.0	137.7	104.0	82.8	39.6
	100	21 351	1.5	88.0	137.6	105.9	65.5	31.3
	110	18 089	2.7	84.0	139.0	106.1	50.4	24.1
	130	12 904	1.2	-	131.0	93.4	45.6	21.8
EIP13	25	2 382	2.4	65.0	-	-	-	-
	60	5 645	1.6	80.0	118.8	88.3	69.6	33.3
	80	10 566	1.6	85.0	131.8	100.5	85.7	41.0
	90	12 491	1.7	88.0	135.6	103.6	92.3	44.2
	100	12 995	1.5	91.0	137.6	104.7	87.0	41.6
	110	12 932	1.3	86.0	133.5	95.4	60.8	29.1
	130	9 404	1.3	-	131.7	86.4	52.6	25.2
EIP12	25	1 625	2.5	62.0	-	-	-	-
	60	4 452	1.5	80.0	121.1	90.3	52.7	25.2
	80	9 318	1.6	88.0	133.3	101.7	86.9	41.6
	90	12 828	1.7	89.0	138.3	105.2	92.9	44.4
	100	13 613	1.5	89.0	139.6	106.2	83.2	39.8
	110	14 075	1.8	88.0	140.1	106.6	79.9	38.2
	130	8 677	1.4	-	136.8	91.4	59.4	28.4

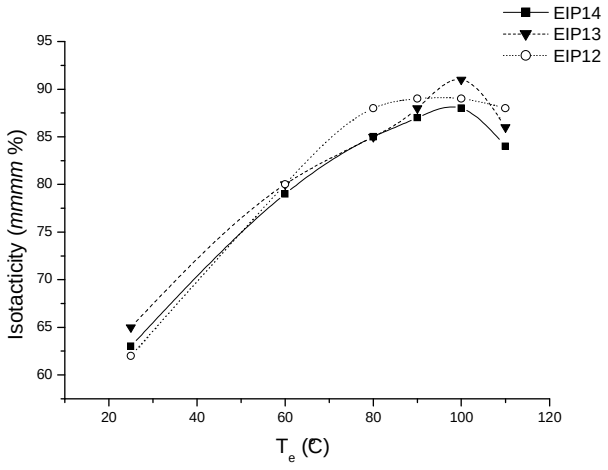

Figure 4.11: Isotacticity (*mmmm* %) of EIP14, EIP13 and EIP12 fractions vs. TREF elution temperature.

In this study, Table 4.3 and Figure 4.11 show that EIP14, EIP13 and EIP12 samples are composed of fractions with considerably different tacticities, ranging from rather atactic

(elution temperature 25 °C) to isotactic (elution temperature 100 °C). An interesting outcome of this analysis is that the isotacticity of EIP13 and EIP12 fractions are systematically slightly greater than those of EIP14 fractions, at a given elution temperature. This is in spite of the tacticity of the EIP14 parent polymer being higher than the tacticities of the EIP13 and EIP12 parent polymers (Table 4.1).

4.3.2.1.2 Molecular weight and molecular weight distribution

Upon examining the variation of molecular weight of the fractions with elution temperature, different tendencies are found. The weight average molecular weight increases steadily with increasing elution temperature up to the elution temperature 100 °C, as can be seen in Table 4.3 and Figure 4.12. This result could be interpreted to mean that these fractions were mainly separated according to molecular weight. By comparing these results to the results obtained in the case of Ziegler-Natta polypropylenes in Chapter 3, we notice that the extent of the increase in the molecular weights of Ziegler-Natta polypropylenes is much greater than that for metallocene-polypropylenes. It is likely that the higher stereospecific active sites produce polypropylenes of higher molecular weight, especially when supported Ziegler-Natta catalysts are used.

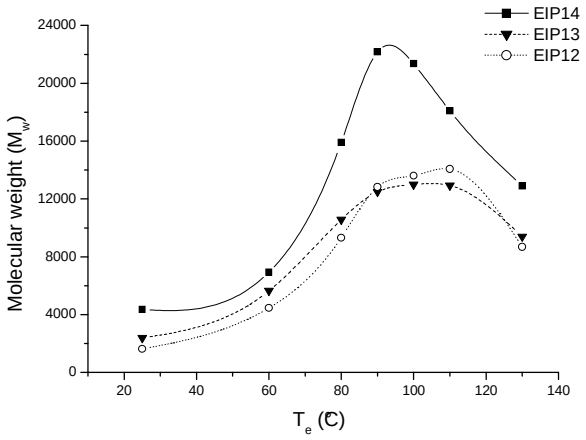

Figure 4.12: Evolution of molecular weight of TREF fractions of EIP14, EIP13 and EIP12 vs. TREF elution temperature.

Figure 4.12 also shows that there is a significant difference between the curves of the EIP14 sample and the other two samples EIP13 and EIP12. The curve representative of EIP14 is shifted to a lower elution temperature compared to that of EIP13 and EIP12. For a given elution temperature (fraction 90 °C), the molecular weight of the EIP14 fraction is particularly

higher than the molecular weights of the EIP13 and EIP12 fractions. This means that longer chains of EIP14 have thus the same crystallizability as the shorter chains of EIP13 and EIP12. An explanation for this is that EIP14, EIP13 and EIP12 samples do not have the same inter-molecular heterogeneity, which could be due to the effect of different amounts of hydrogen on the catalyst during the polymerization reactions.

Table 4.3 also shows that the PD of the samples fractions of EIP14, EIP13 and EIP12 generally tends to decrease as the elution temperature increases (except the fraction at 110 °C of the samples EIP14 and EIP12); however, the PD of each fraction (except the first one) is considerably lower than those of the non-fractionated material (Tables 4.1 and 4.3). On the other hand, we see that the TREF fractions in Chapter 3 (prepared using Ziegler-Natta catalyst) have a broader molecular weight distribution compared to those reported in this Chapter (prepared using metallocene catalysts). The broad molecular weight distributions indicate that fractionation is mainly due to tacticity differences. The controlling factor is, however, not the average isotacticity, but the lengths of the crystallizable isotactic sequences.[21]

4.3.2.1.3 Crystallinity and melting behaviour

Figure 4.13 presents a waterfall plot of the DSC melting endotherms for the TREF fractions of sample EIP12. The data for the TREF fractions of the samples EIP14 and EIP13 show similar trends. Figure 4.14 presents the evolution of melting temperatures for the TREF fractions of the samples EIP14, EIP13 and EIP12 as a function of elution temperature. The DSC endotherms in Figures 4.13 and 4.14, and the data in Table 4.3 show that there is a significant increase in the melting temperature of the fractions with an increase in elution temperature (except the last fraction of the EIP14 and EIP12 samples and the last two fractions of the EIP13 sample). This could be due to the increase in the isotacticities and the molecular weights of the fractions with increasing elution temperature. However, noticeable differences between melting temperature of polymer fractions can be seen. EIP12 fractions are characterized by slightly higher melting temperatures than EIP14 and EIP13 fractions, especially at the elution temperatures 100, 110 and 130 °C.

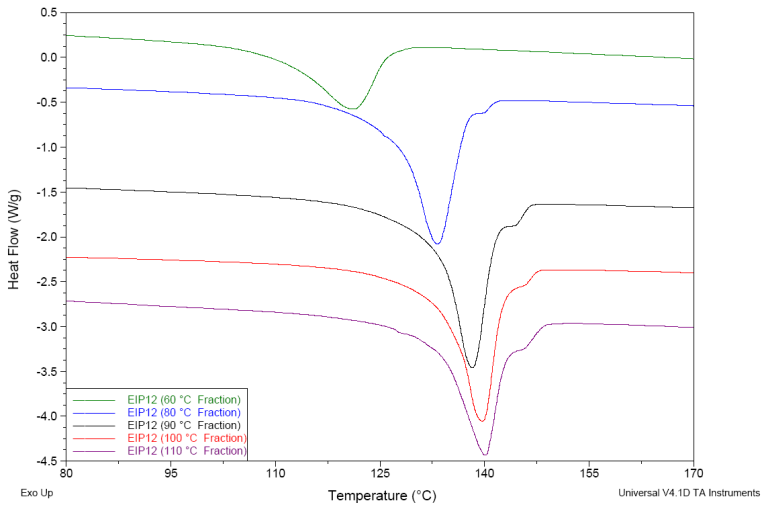

Figure 4.13: Waterfall plot of the DSC melting endotherms for the TREF fractions of sample EIP12.

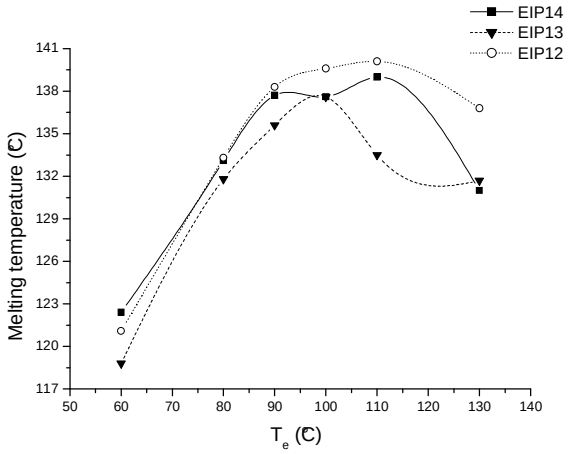

Figure 4.14: Evolution of melting temperatures (T_m) of the TREF fractions of samples EIP14, EIP13 and EIP12 versus TREF elution temperature.

The crystallization temperatures of the different TREF fractions of the three different samples EIP14, EIP13 and EIP12 showed similar behavior to the melting temperatures. Temperatures increased with increasing elution temperature (Figure 4.15), demonstrating that crystallization temperature is mostly dependent on isotacticity. On the other hand, there was a considerable decrease in crystallization temperature for the last TREF fractions of samples EIP14 and EIP12 and for the last two fractions of sample EIP13. This is most likely caused by the restricted mobility, and lower tacticities and molecular weights of these fractions.

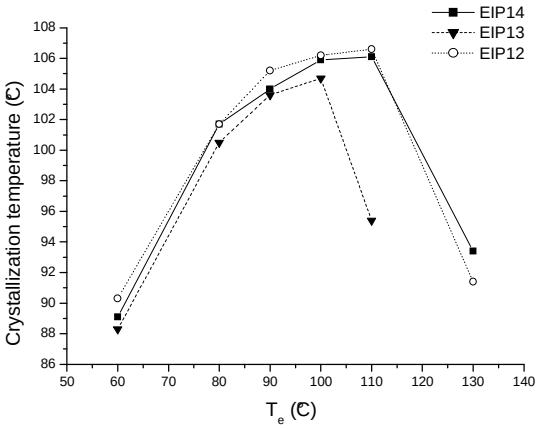

Figure 4.15: Evolution of crystallization temperature (T_c) of EIP14, EIP13 and EIP12 TREF fractions versus TREF elution temperature.

The degree of crystallinity of the first three fractions of samples EIP14, EIP13 and EIP12 increases with fractionation temperature, as can be seen in Figure 4.16. However, there is a remarkable decrease in the crystallinity of the last three fractions of all samples as can be seen in Figure 4.16. The reason for this could only be the decreased molecular weights and tacticities of these fractions.

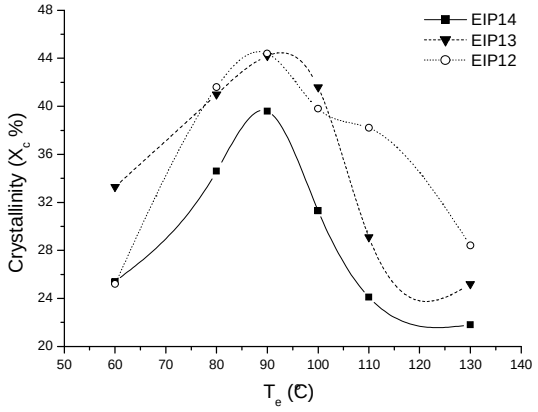

Figure 4.16: Degree of crystallinity of the TREF fractions of samples EIP14, EIP13 and EIP12 versus TREF elution temperature.

On the other hand, EIP13 and EIP12 TREF fractions are described by a systematically higher crystallinity than EIP14 TREF fractions, as shown in Figure 4.16, owing to the higher tacticity percentage of EIP13 and EIP12 fractions (Table 4.3). Figure 4.16 also shows that the crystallinities of the fractions do not increase as linearly in the series as do the melting

temperature values in Figure 4.14. This means that the fractions have been fractionated, not according to average isotacticity, but according to lamellar thickness or the lengths of the crystallizable sequences in the chains.[21]

4.3.2.1.4 Crystal phase analysis

Figure 4.17 shows the WAXD results for selected TREF fractions of sample EIP13. It shows that only the α crystal form exists in all TREF fractions of sample EIP13. These results were similar to the results observed for the polymer fractions produced by Ziegler-Natta catalysts (Chapter 3, Sections 3.3.2.1.4, 3.3.2.2.4 and 3.3.2.3.4).

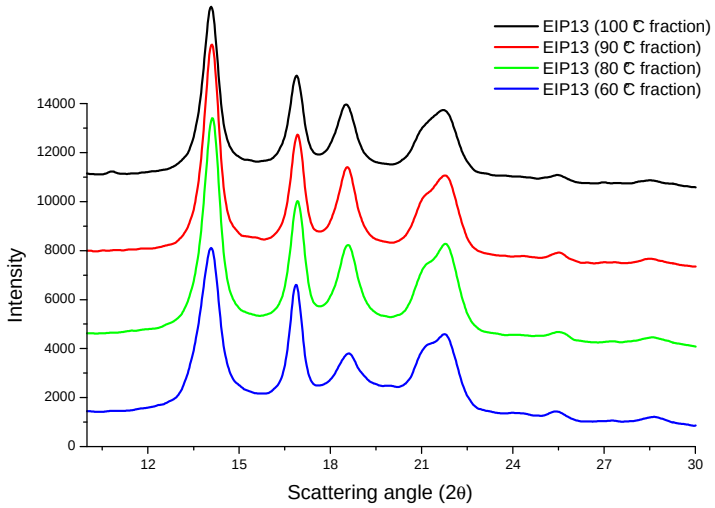

Figure 4.17: Typical X-ray diffraction pattern of different TREF fractions of the EIP13 sample.

4.3.2.2 Polypropylenes produced using the EI(4H) catalyst

TREF analyses of three different isotactic polypropylenes D9, D8 and D7 produced using EI(4H) metallocene catalyst were carried out to determine the differences in their characteristics. Table 4.4 tabulates the TREF fractionation data of polypropylene samples D9, D8 and D7. Their TREF curves are shown in Figure 4.18.

Table 4.4: TREF fractionation data of the TREF fractions of samples D9, D8 and D7

T_e (°C)	Sample D9				Sample D8				Sample D7			
	Wt (mg)	Wi%	ΣWi%	Wi%/ΔT	Wt (mg)	Wi%	ΣWi%	Wi%/ΔT	Wt (mg)	Wi%	ΣWi%	Wi%/ΔT
25	184	6.1	6.1	-	520	16.8	16.8	-	650	21.7	21.7	-
60	226	7.5	13.6	0.4	448	14.5	31.3	0.4	560	18.7	40.4	0.5
80	788	26.3	39.9	1.3	952	30.8	62.1	1.5	1 160	38.6	79.0	1.9
90	1 300	43.3	83.2	4.3	676	21.9	84.0	2.2	370	12.3	91.3	1.2
100	337	11.2	94.4	1.1	373	12.1	96.1	1.2	123	4.1	95.4	0.4
110	85	2.7	97.1	0.3	61	2.0	98.1	0.2	73	2.4	97.8	0.2
130	89	2.9	100.0	0.2	60	1.9	100.0	0.1	65	2.2	100.0	0.1

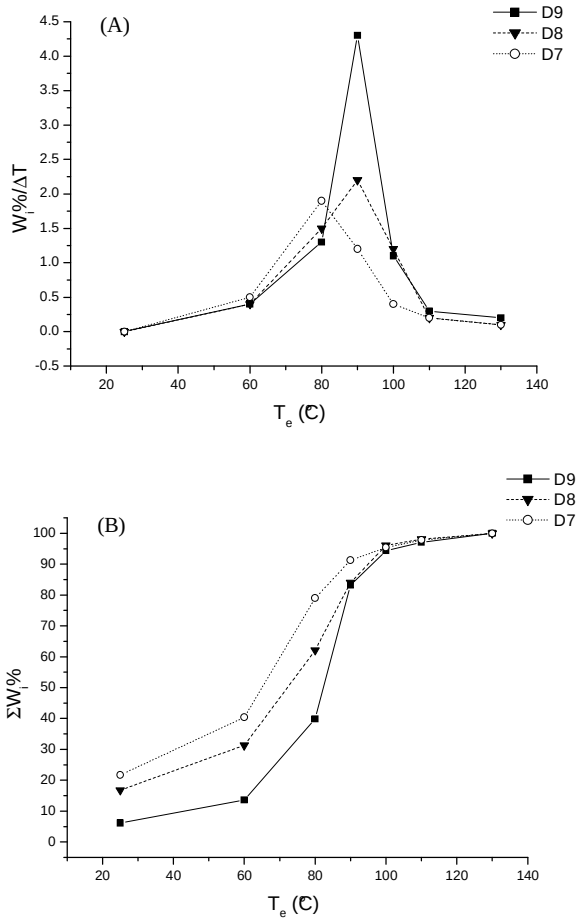

Figure 4.18: TREF curves of samples D9, D8 and D7: (A) Wi%/ΔT and (B) ΣWi %.

When we compare the TREF results of polypropylene fractions produced using EI catalyst (Table 4.2) and the TREF results of polypropylene fractions produced using EI(4H) catalyst (Table 4.4) we see that the weight percentage of the EI polypropylene fractions eluting at lower temperature is less than that eluting at the same elution temperature of the

polypropylene fractions produced by EI(4H), and vice versa. For instance, Table 4.2 and Table 4.4 show that the 25 °C fraction amounts of samples EIP14 and EIP13 produced using EI catalyst in the presence of 0.3 and 0.7 wt % hydrogen are 6.0 and 8.7 wt %, respectively, which are significantly less than those obtained at the same elution temperature of samples D8 and D7 (16.8 and 21.7 wt %, respectively), which produced by EI(4H) catalyst in the presence of same amounts of hydrogen (0.3 and 0.7 wt % of hydrogen, respectively). This shows that the EI catalyst is able to decrease the amount of room temperature fractions significantly. The reason for this could be the higher stereoselectivity of the EI catalyst than the EI(4H) catalyst.

Furthermore, from the curves of the $W_i\%/\Delta T$ versus the fractionation temperature in Figure 4.18 (A) shows that there is an increase in $W_i\%/\Delta T$ for the first three fractions collected after the 25 °C fraction, and then a decrease for the last three fractions. The curves in Figure 4.18 (A) have different distributions and shapes. On the other hands, Figure 4.18 (B) illustrates the accumulative weight fraction percentage versus the fractionation temperatures of the three polymers D9, D8 and D7. It is clear that the curves are considerably different, which is due to the difference in the characteristics of the original polymers.

The weight fraction as a function of elution temperature is shown in Figure 4.19. The superimposed graphs provide a clear and easy way to compare the samples. It is clear from the graph that the three samples have different weight fraction distributions. It is also observed that more than 50 wt % of the original material for all samples eluted at the 80 and 90 °C fractions.

4.3.2.2.1 Microstructure

The ^{13}C NMR data of the TREF fractions of samples D9, D8 and D7 are summarized in Table 4.5 and the isotacticity (*mmmm* %) of the D9, D8 and D7 fractions vs. TREF elution temperature is shown in Figure 4.20. Table 4.5 and Figure 4.20 show that the isotacticity of the fractions increases with the elution temperature. Similar results were obtained by other researchers.[22,23]

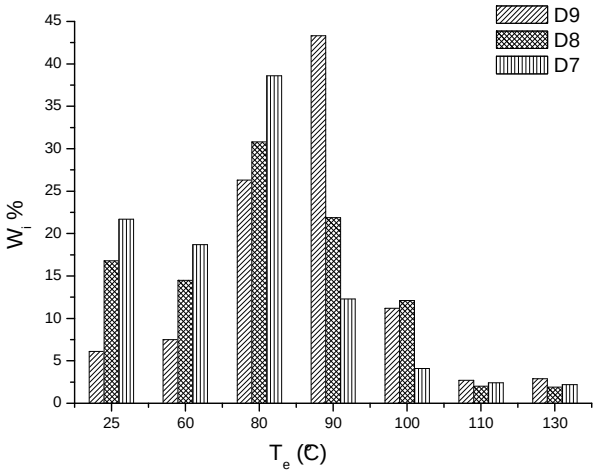

Figure 4.19: Distribution of weight percentage of D9, D8 and D7 fractions vs. elution temperature (°C).

Table 4.5: GPC, ^{13}C NMR and DSC results of fractionation data of samples Z8, Z9 and Z10

Runs	Fraction (T_e °C)	M_w	M_w/M_n	*mmmm* %	T_m (°C)	T_c (°C)	ΔH_m (J/g)	X_c (%)
D9	25	1 557	1.6	57.0	-	-	-	-
	60	7 438	1.6	81.0	121.1	91.6	53.6	25.7
	80	20 634	1.8	83.0	131.7	100.5	76.7	36.7
	90	28 875	1.6	87.0	137.4	104.6	79.9	38.2
	100	26 801	1.6	89.0	136.5	104.8	73.6	35.2
	110	28 481	1.6	86.0	136.4	98.1	68.8	32.9
	130	22 195	1.5	-	132.2	95.8	60.3	28.9
D8	25	1 420	1.4	56.0	-	-	-	-
	60	3 463	1.4	78.0	122.9	91.8	78.6	37.6
	80	7 042	1.5	84.0	135.7	104.1	85.0	40.7
	90	9 664	1.6	89.0	140.0	107.3	89.9	43.0
	100	9 777	1.6	91.0	141.0	109.2	95.8	45.8
	110	10 645	1.3	87.0	139.5	101.8	86.4	41.3
	130	6 930	1.2	-	133.7	98.5	81.9	39.2
D7	25	1 303	1.4	56.0	-	-	-	-
	60	3 240	1.3	77.0	125.1	96.3	77.4	37.0
	80	6 261	1.5	82.0	137.2	104.9	79.1	37.9
	90	8 478	1.5	87.0	141.4	108.9	90.5	43.3
	100	8 307	1.4	90.0	142.2	109.0	92.6	44.3
	110	7 736	1.3	85.0	140.1	102.5	84.7	40.5
	130	5 901	1.2	-	135.6	98.7	82.2	39.3

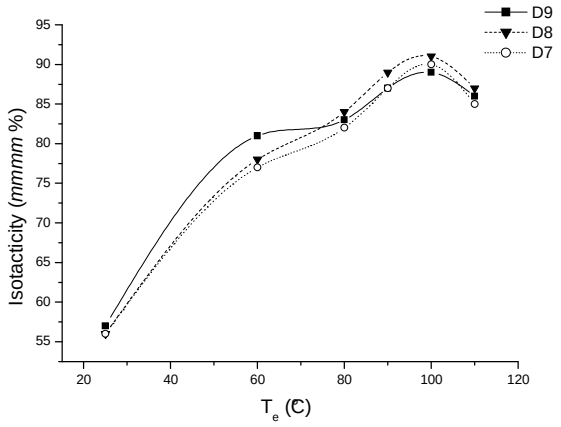

Figure 4.20: Isotacticity (*mmmm* %) of D9, D8 and D7 fractions vs. TREF elution temperature.

Moreover, Table 4.5 and Figure 4.20 show that samples D9, D8 and D7 comprise fractions with significantly different tacticities, ranging from rather atactic (eluted fraction at 25 °C) to isotactic (eluted fraction at 100 °C). An interesting outcome of this analysis is that the isotacticity of TREF fractions of the samples produced using the EI catalyst (Section 4.3.2.1.1) are systematically similar to those produced using the EI(4H) catalyst (Table 4.5 and Figure 4.20).

4.3.2.2.2 Molecular weight and molecular weight distribution

Figure 4.21 shows the weight average molecular weight of TREF fractions of samples D9, D8 and D7 with respect to the TREF elution temperature. Table 4.5 and Figure 4.21 show that the weight average molecular weight increases gradually with increasing elution temperature up to the elution temperature 110 °C and then decreases in the last fraction for all samples. Figure 4.21 shows a similar trend to that of Figure 4.12 (for samples prepared using EI catalyst); there is a clear difference in the curves between those for D9 sample and those for the other two samples D8 and D7. The curve representative of sample D9 is shifted to a lower elution temperature compared to those of samples D8 and D7. Table 4.5 shows that the PD of the TREF fractions of samples D9, D8 and D7 is generally in the range 1.2–1.8, which is slightly lower than that of the TREF fractions of the samples produced using EI catalyst (EIP14, EIP13 and EIP12 in Table 4.3) which is in the range 1.3–3.4.

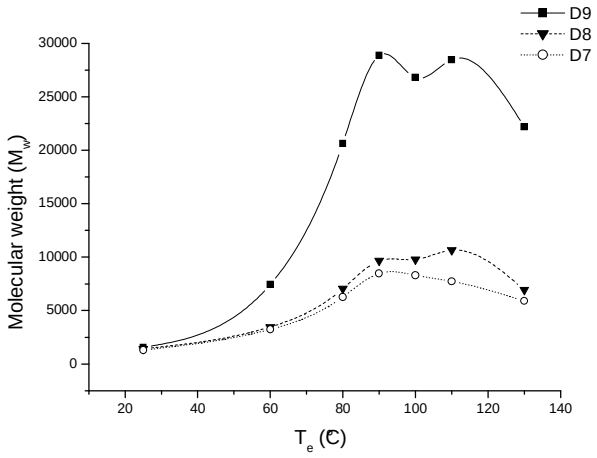

Figure 4.21: Evolution of molecular weight of TREF fractions of D9, D8 and D7 samples vs. TREF elution temperature.

4.3.2.2.3 Crystallinity and melting behaviour

Figure 4.22 shows the evolution of melting temperatures of D9, D8 and D7 fractions as a function of elution temperature. As can be seen from Figure 4.22 and as well as the data in Table 4.5 there is a characteristic increase in the melting temperature of the fractions with an increase in elution temperature (except the last two fractions of samples D8 and D7 and the last three fractions of sample D9). However, apparent differences between the melting temperature of polymers fractions are observed. TREF fractions of sample D7 are characterized, to some extent, by higher melting temperatures than D8 and D9 TREF fractions. The crystallization temperatures of the different TREF fractions of the three different samples D9, D8 and D7 are clearly increase with increasing elution temperature (except for the last two fractions of all samples), as can be seen in Figure 4.23. On other hand, the degree of crystallinity of TREF fractions of samples D8 and D7 increases with elution temperature for the first four fractions and then starts to decrease for the last two fractions, while it only increases for the first three TREF fractions of sample D9 and then starts to decrease. This is clearly seen in Figure 4.24. The reason for the decreasing crystallinity of the last fractions is the significant decrease in the molecular weight and tacticity of these fractions, as evident in Table 4.5.

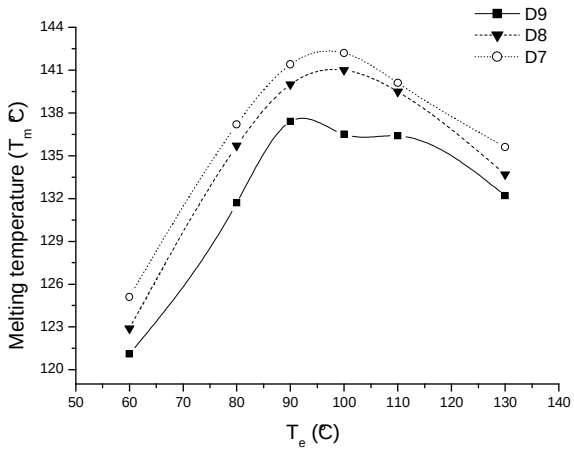

Figure 4.22: Evolution of melting temperature (T_m) of TREF fractions of samples D9, D8 and D7 versus TREF elution temperature.

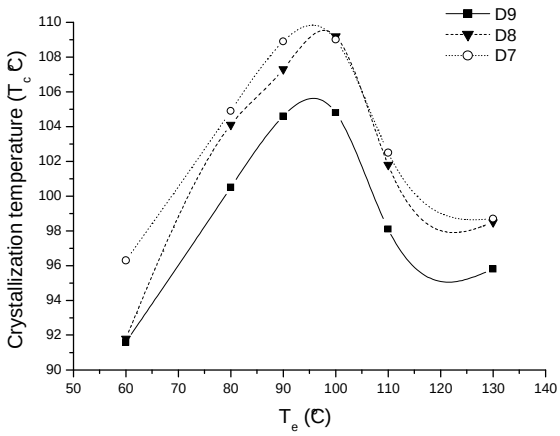

Figure 4.23: Evolution of crystallization temperature (T_c) of TREF fractions of samples D9, D8 and D7 versus TREF elution temperature.

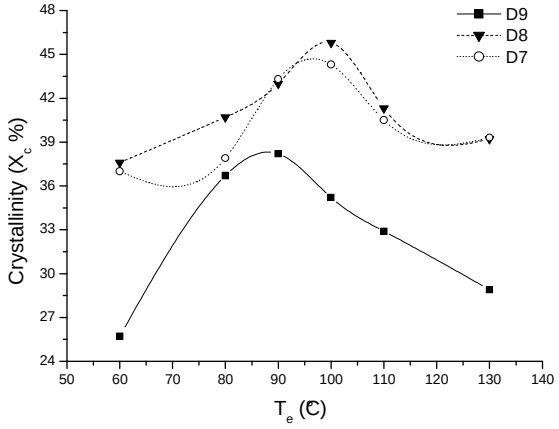

Figure 4.24: Degree of crystallinity of TREF fractions of samples D9, D8 and D7 versus TREF elution temperature.

4.3.2.2.4 Crystal phase analysis

Figure 4.25 shows typical WAXD patterns of the α form of selected TREF fractions of sample D9, in which three strong equatorial peak of (110), (040) and (130) appear at 2θ = 14.10°, 16.90° and 18.58°.

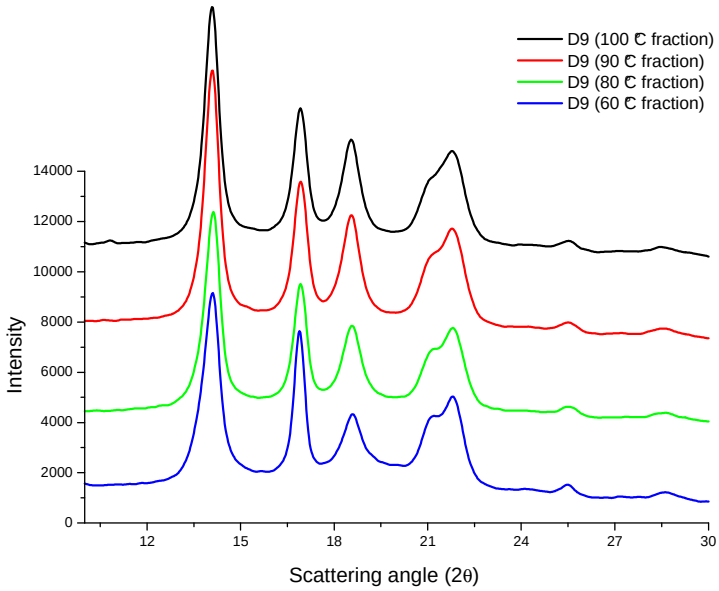

Figure 4.25: Typical X-ray diffraction pattern of various TREF fractions of sample D9.

4.3.2.3 Commercial syndiotactic polypropylene

The data of the commercial syndiotactic polypropylene sample SPP1 are tabulated in Table 4.6. The DSC show multiple melting peaks. this was proposed to be a result of partial melting, recrystallization of the less stable crystallites, remelting of the recrystallized crystallites, and normal melting of the primary crystallites formed under the crystallization conditions.[16] Table 4.6 also shows that the crystallinity degree of the SPP1 sample is much lower than that of samples of isotactic polypropylenes (Table 4.1). This is attributed to the slow and complex crystallization behaviour of syndiotactic polypropylene.[24-26]

Table 4.6: Data of the commercial syndiotactic polypropylene sample SPP1

Run	M_w	M_w/M_n	*rrrr* %	T_m (°C)	T_c (°C)	ΔH_m (J/g)	X_c (%)
SPP1	174 000	2.3	93.0	114.6-127.2	66.3	39.0	18.7

TREF analysis of the syndiotactic polypropylene sample SPP1 was carried out to yield fractions with different tacticities and molecular weights. Fractionation data and syndiotacticity, molecular weight and melting temperature of the fractions are tabulated in Table 4.7. Figure 4.26 shows the TREF curves of the SPP1 sample. The $W_i\%/\Delta T$ vs. T_e curve approximates the differential of cumulative weight curves. The $W_i\%/\Delta T$ vs. T_e curve is relatively wide, but has only one peak.

Table 4.7: Fractionation and related data of SPP1

Te (°C)	Wt (mg)	$W_i\%$	$\Sigma W_i\%$	$W_i\%/\Delta T$	M_w	M_w/M_n	*rrrr* %	T_m (°C)	T_c (°C)	ΔH_m (J/g)	X_c %
25	382	12.7	17.7	-	51 022	2.5	45.0	-	-	-	-
60	1 028	34.3	47.0	1.0	141 689	2.4	75.0	107.4-120.2	67.2	38.6	18.5
70	833	27.8	74.8	2.8	148 593	2.2	79.0	117.3-128.2	77.7	43.8	21.0
80	486	16.2	91.0	1.6	159 815	2.4	80.0	114.7-126.1	73.8	45.0	21.5
90	168	5.6	96.6	0.6	195 399	2.4	81.0	116.4-127.0	75.7	40.4	19.3
100	51	1.7	98.3	0.2	156 439	2.7	-	115.0-124.0-146.7	82.5-96.1	33.1	15.8
120	53	1.7	100.0	0.1	126 224	2.2	-	145.7-155.0	106.5	25.1	12.0

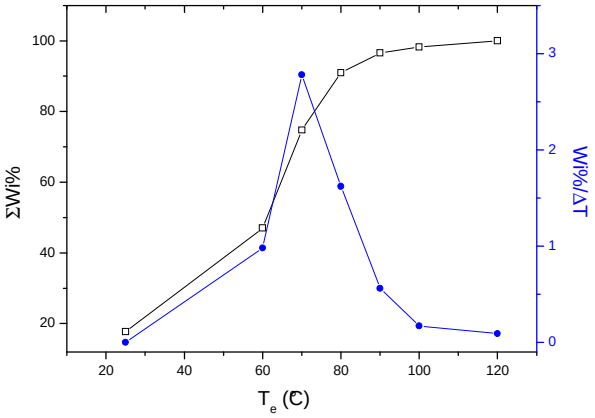

Figure 4.26: TREF curves of the commercial syndiotactic polypropylene sample SPP1.

^{13}C NMR data show that the syndiotacticity (*rrrr* %) of the TREF fractions increased gradually with elution temperature, as can be seen in Table 4.7 and Figure 4.27. The variation in the syndiotacticity of the fractions in the range 70–90 °C was small.

The melting temperatures of the fractions revealed similar tendency, but the difference in melting temperature is more obvious than the difference in syndiotacticity (see Figure 4.28). This indicates that the syndiotacticity of SPP1 is the main factor influencing fractionation of the fractions below 70 °C and then the molecular weight starts to play a role in the fractionation of fractions above 70 °C.

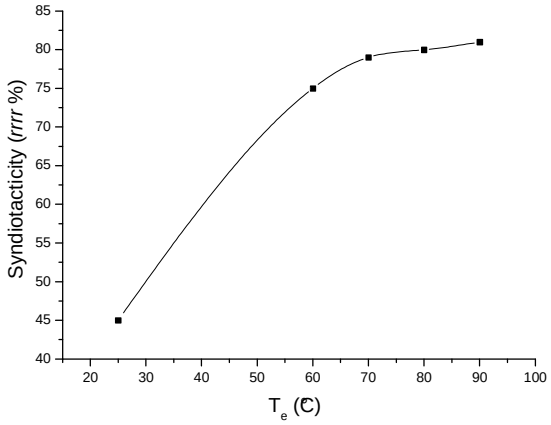

Figure 4.27: Syndiotacticity (*rrrr* %) of SPP1 fractions vs. TREF elution temperature.

The variation in the molecular weight of fractions with elution temperature is less regular. In the initial stage it also increases with elution temperature and reaches a maximum for the fraction eluted at 90 °C, but it begins to decrease in the later fractions.

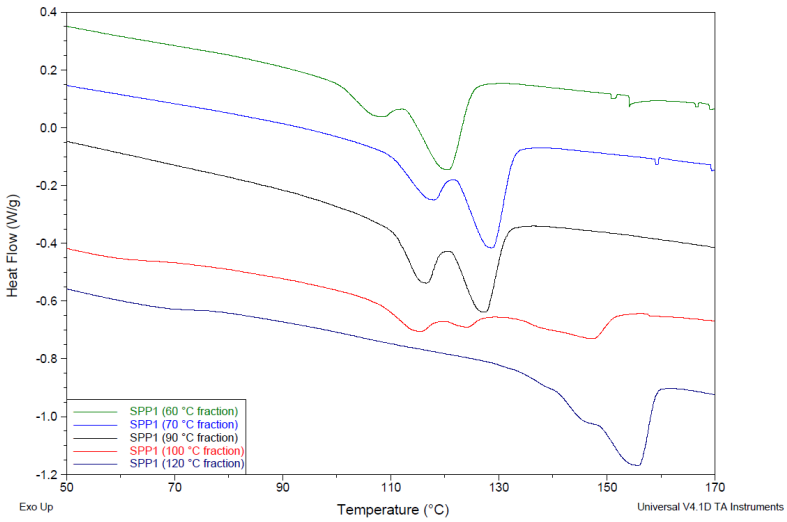

Figure 4.28: Waterfall plot of the DSC melting endotherms for the TREF fractions of SPP1.

In contrast to the FT-IR spectra of isotactic polypropylene, the majority of the absorption bands of syndiotactic polypropylene FT-IR spectra appear in the frequency region below 1150 cm^{-1}, these absorption bands belong to the regularity bands. The FT-IR spectra of the TREF fractions of sample SPP1 are shown in Figure 4.29. This figure provides a detailed description of the helical (Form I) and the trans-planar (Form III) conformations of syndiotactic polypropylene fractions, which can be clearly identified. Moreover, Figure 4.29 depicts that the bands that present at 810, 867, 904, 935, 977 and 1005 cm^{-1} are due to the Form I structure, while the bands that appear at 840, 963 and 1129 cm^{-1} are due to the Form III structure. According to the literature,[27] Form I is characterized by chains in s(2/1)2 helical conformation packed in different orthorhombic crystalline lattices (as shown in Chapter 2, Figure 2.7 A) and Form III presents polymer chains in the trans-planar conformation with t*cm* symmetry (as shown in Chapter 2, Figure 2.7 C).

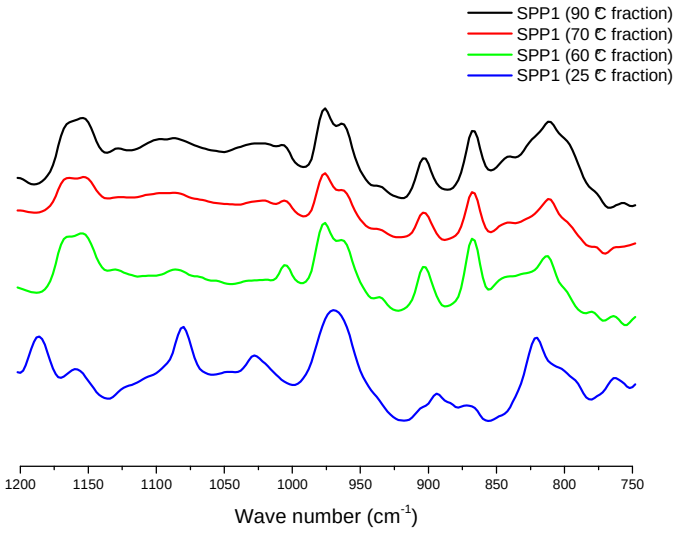

Figure 4.29: FTIR spectra of the TREF fractions of sample SPP1.

Typical WAXD diffraction patterns of selected TREF fractions of sample SPP1 are shown Figure 4.30. According to literature,[28] the presence of reflections at 2θ = 12.3°, 16.3°, 20.9° and 24.7° corresponding to the observations of (200), (010), (111) and (400) reflection planes, respectively, and the absence of a reflection plane (211) at 2θ = 18.8° (in the case of 60, 70 and 80 °C fractions), as can be seen in Figure 4.30, indicate that these fractions are crystallized in the disordered Form I structure. Figure 4.30 also shows the appearance of reflection plane (211) at 2θ = 18.8° of the fraction 90 °C. This provides evidence of the presence of the ordered Form I structure in this fraction. The existence of Form I is mainly controlled by the amounts of defects present in the packing of the chains,[27-29] which is revealed by either the weakness or the absence of the (211) reflection at 2θ = 18.8° in crystallized samples.

The greater the amount of defects present the higher the deviation is from the fully antichiral packing.[28] A small amount of the isochiral helical Form II of fraction 90 °C, as indicated by the presence of the 110 reflection at 2θ = 17.0° of Form II, as a shoulder of the 010 reflection at 2θ = 16.3°.[30]

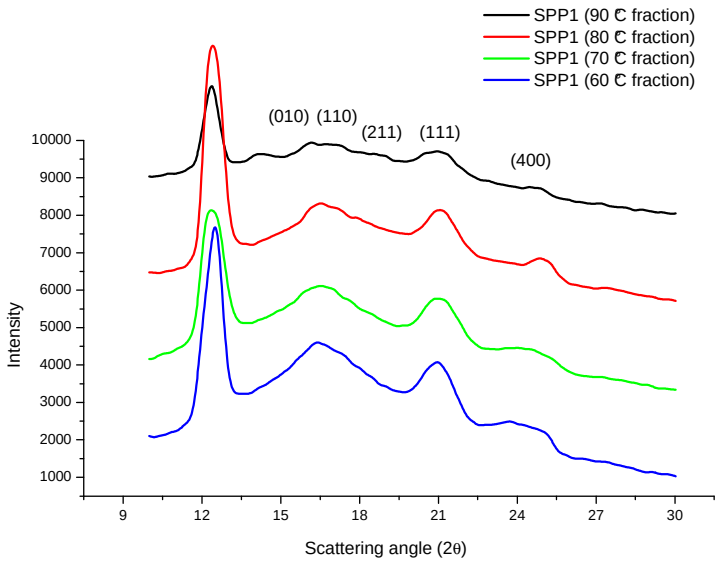

Figure 4.30: Typical X-ray diffraction pattern of different TREF fractions of the SPP1 sample.

4.4 Conclusions

As in the case of Ziegler-Natta catalyst system, metallocene catalyst systems make it possible to produce polymer samples with a wide variation in tacticity and molecular weight under different reaction conditions. By using preparative TREF, it is possible to obtain polymer fractions of well defined structure in terms of molecular weight and molecular weight distributions, as well as tacticity.

The addition of molecular hydrogen to propylene polymerizations catalyzed using the EI and EI(4H) catalyst systems resulted in an increase in catalytic activity and a reduction in polymer molecular weight. The isotacticity of the polypropylenes was also slightly reduced. A major increase in the degree of crystallinity was also noticed upon increasing the amount of hydrogen. This is most likely due to the lower molecular weight, which makes the motion of chain molecules easier, allowing the reorganization of the chains in order to crystallize more perfectly. It is also possible that the tacticity of the chains could have improved slightly as the amount of hydrogen was increased due to increased chain transfer to hydrogen after 2,1-insertions, therefore forming chain ends rather than incorporating defects into the chains. This would improve the overall chain stereoregularity.

TREF fractionation of the samples produced by both types of metallocene catalysts, EI and EI(4H), shown that the samples eluted mainly in the 80 ℃ and 90 ℃ fractions. However, the weight percentage of the room temperature fractions of polymers produced using the EI

catalyst is significantly lower than the room temperature fractions produced using EI(4H) catalyst.

In general, the molecular weight and the isotacticity of the TREF fractions all increased significantly with increasing elution temperature for all samples produced using EI and EI(4H) metallocene catalysts.

In case of the PD of the TREF fractions, it is clear that the room temperature fractions of polymers produced using the EI catalyst system have a slightly broader distribution of molecular weight chains than the higher temperature fractions. The PD is in the same range (1.2−1.6) as that of the polymer fractions produced using the EI(4H) catalyst system.

The thermal properties, in terms of T_c, T_m and degree of crstallinity, of the TREF fractions were increased with fractionation temperature up to the 100 ℃ fractions for all fractions produced using EI and EI(4H) metallocene catalyst systems.

It is interesting that only the α crystal form existed in all TREF fractions of different samples. The main difference between the α peaks of TREF fractions of the different samples, is the strong diffraction of these peaks, which depends on the crystallinity content of each fraction.

For the syndiotactic polypropylene sample SPP1, the molecular weight, syndiotacticity, melting temperature and degree of crystallinity of the TREF fractions all increased to some extent with increasing elution temperature, which is similar to the isotactic polypropylene samples. The only distinguish difference of syndiotactic TREF fractions on the isotactic TREF fractions is the multi-melting peaks that are observed in all TREF fractions.

4.5 References

1. F. Auriemma, C. De Rosa, T. Boscato, P. Corradini, *Macromolecules* **2001**, 34, 4815.
2. V. Busico, R. Cipullo, L. Caporaso, G. Angelini, A. L. Segre, *J. Mol. Catal*. **1998**, 128, 53.
3. K. Soga, T. Shiono, *Prog. Polym. Sci*. **1997**, 22, 1503.
4. S. Lin, R. Kravchenko, R. M. Waymouth, *J. Mol. Catal*. **2000**, 158, 423.
5. P. Deukkil, I. Kim, H. Yang, S. Soo, B. Kim, H. Chang, *J. Appl. Polym. Sci*. **2005**, 95, 231.
6. T. Hayashi, Y. Inoue, R. Chujo, T. Asakura, *Macromolecules* **1988**, 4, 519.
7. V. Busico, R. Cipullo, J. C. Chadwick, J. F Modder, O. Sudwiejer, *Macromolecules* **1994**, 27, 7538.
8. A. Carvill, I. Tritto, P. Locatelli, M. C. Sacchi, *Macromolecules* **1997**, 30, 7056.
9. T. Tsutsui, N. Kashiwa, A. Mizuno, *Macromol. Rapid Commun*. **1990**, 11, 565.
10. S. Lin, M. Waymouth, *Macromolecules* **1999**, 32, 8283.
11. G. Moscardi, F. Piemontesi, L. Resconi, *Organometallics* **1999**, 18, 5264.
12. A. Carvill, I. Tritto, P. Locatelli, M. C. Sacchi, *Macromolecules* **1997**, 30, 7056.

13. J. Huang, G. L. Rempel, *Ind. Eng. Chem. Res*. **1997**, 36, 1151.
14. W. Kaminsky, R. Steiger, *Polyhedron* **1988**, 7, 2375.
15. T. Tsutsui, A. Mizuno, N. Kashiwa, *Macromol. Chem. Phys*. **1989**, 190, 1177.
16. P. Supaphol, *J. Appl. Polym. Sci*. **2001**, 82, 1083.
17. R. G .Alamo, M. H. Kim, M. J. Galante, J. R. Isasi, L. Mandelkern, *Macromolecules* **1999**, 32, 4050.
18. I. L. Hosier, R. G. Alamo, J. S. Lin, *Polymer* **2004**, 45, 3441.
19. J. Xu, L. Feng, *Eur. Polym. J*. **2000**, 36, 867.
20. A. Mizuno, T. Abiru, M. Motowoka, M. Kioka, M. Onda, *J. Appl. Polym. Sci: Appl. Polym. Symp.* **1993**, 52, 159.
21. V. Virkkunen, P. Laari, P. Pitkanen, F. Sundholm, *Polymer* **2004**, 45, 3091.
22. J. T. Xu, Y. Q. Yang, L. X. Feng, X. M. Kong, S. L. Yang, *J. Appl. Polym. Sci*. **1996**, 62, 727.
23. M. Kakugo, T. Miyatake, Y. Natio, K. Mizunumn, *Macromolecules* **1988**, 21, 314.
24. D. Choi, J. L. White, *Int. Polym. Proc*. **2000**, 15, 398.
25. D. Choi, J. L. White, *Polym. Eng. Sci*. **2001**, 41, 1743.
26. D. Choi, J. L. White, *Polym. Eng. Sci*. **2002**, 42, 8.
27. C. De Rosa, F. Auriemma, P. Corradini, *Macromolecules* **1996**, 29, 7452.
28. C. De Rosa, F. Auriemma, V. Vinti, *Macromolecules* **1997**, 30, 4137.
29. C. De Rosa, F. Auriemma, V. Vinti, M. Galimberti, *Macromolecules* **1998**, 31, 6206.
30. C. De Rosa, F. Auriemma, V. Vinti, *Macromolecules* **1998**, 31, 7430.

CHAPTER 5

Use of DSC and SCALLS for studying the bulk and solution crystallization of different polypropylenes

5.1 Introduction

Both the crystallization behaviour and crystalline form of polypropylene polymer are strongly affected by the configuration (tacticity) and conformational structure of the chain. Isotactic and syndiotactic polypropylene can crystallize. The degree of crystallinity is commonly in the range 40−70% and depends on the level of the tacticity of the polymer. Atactic polypropylene is considered as uncrystallizable, since the chain structure lacks regularity.[1]

The effects of molecular weight,[2-5] molecular weight distribution[6] and tacticity[7-9,5] on the crystallization have been investigated by a several researchers. Results indicate that the linear growth rate of crystals markedly decreases with increasing molecular weight,[3] but the overall crystallization rate increases because an increasing number of intramolecular folded chain nuclei could result in a higher nucleation density.[4] For samples with similar molecular weights and different tacticities the linear crystal growth rate might increase by three orders of magnitude when the isotacticiy (*mmmm* %) of isotactic polypropylene increases from 78.7 to 98.8%.[8,10]

Several methods are described in the literature to fractionate semi-crystalline polymers: solvent extraction, consecutive extraction with different solvents, fractionation with solvent/non-solvent pairs, consecutive extraction with a solvent at different temperatures[11-14] and, most recently, TREF[15-19] and crystallization analysis fractionation (CRYSTAF).[20-22] Developments in the field include new techniques such as crystallization elution fractionation (CEF)[23] and solution crystallization analysis by laser light scattering (SCALLS).[24-27] SCALLS is considered as one of the newest fractionation techniques for semi-crystalline polymers. It involves analysis of the turbidity of a polymer solution.

Long ago, turbidity measurements were used for fractionating polyolefins based on molecular weight, using either a solvent/non-solvent approach or thermal gradient technique.[28] In 1966 Imhof studied a series of low-pressure ethylene-propylene copolymers and mixtures of ethylene homopolymers.[24] Recently, Shan *et al.*[25] published an article describing how the

short chain branching distribution (SCBD) of polyethylene can be determined by a turbidimetric method. The technique involves the observation of the scattering of laser lamp after it passes through a polymer solution. The temperature of the polymer solution is controlled via a heating block that is subjected to a temperature ramp. As turbidity increases, the amount of laser light that can pass through the solution decreases and the amount of scattering increases. An increase in turbidity occurs when the hot polymer solution is cooled and the polymer starts to crystallize out of solution. The reverse of this process leads to the turbidity decreasing with an increase in temperature.

Recently, van Reenen *et al.*[26,27] developed a similar instrument which they used to investigate several different polyolefins. Both cooling (crystallization from solution) and heating (melting and dissolution) experiments were successfully carried out, and it was shown that both the cooling and heating rates, as well as polymer concentration, affect the crystallization process.

This chapter describes the use of the DSC technique was used to study the bulk crystallization of different polypropylenes and the use of the SCALLS technique to differentiate between different isotactic and syndiotactic polypropylenes with similar chemical structure but different tacticity and molecular weight.

5.2 Experimental

5.2.1 Materials

Different isotactic polypropylenes were prepared in our laboratory using both heterogeneous transition-metal and homogenous metallocene catalysts with differing molecular weights and tacticities (Table 5.5, Section 5.3.2.1). The polymerization reaction procedures are described in the Sections 3.2.2 and 4.2.2. A commercial syndiotactic polypropylene (SPP1) was obtained from Sigma-Aldrich.

5.2.2 SCALLS

The SCALLS setup used to measure the turbidity of polymer solutions was based on the design described by Shan *et al.*[25] A similar instrument was developed and built in our laboratory. A full description of the experimental setup used for the SCALLS technique is given in a recent paper.[26] The development of the SCALLS instrument included the addition of two photodiode detectors to the instrument, at 90° and 270° angles of the incident light.

The in-line photodiode detector is denoted as the 180° detector. This detector measures laser light intensity and will record a decrease in intensity as crystallization occurs. The 90° and 270° detectors measure scattered light intensity. In a further development a neutral density filter was placed between the sample cell and the 180° detector. The general layout is shown in Figures 5.1 and 5.2.

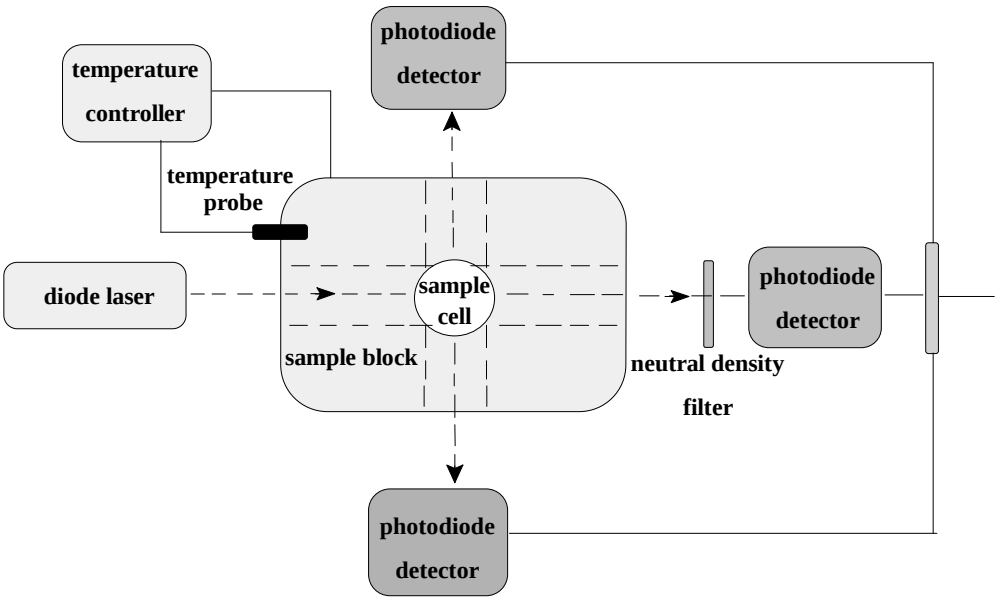

Figure 5.1: Schematic diagram of SCALLS.

For SCALLS experiments, polypropylene samples were dissolved in TCB at 130 °C, in concentrations of between 0.5 and 1 mg/ml. The samples were then placed into the SCALLS aluminium heating/cooling block in a quartz sample holder (inside diameter 21 mm, length 100 mm) and then cooled in a controlled fashion from 100 °C to room temperature at a rate of between 0.5 and 1.5 °C/min. Throughout the experiment, the samples were stirred to maintain a uniform temperature in the solution and to prevent the formed crystals from aggregating. Heating experiments involved heating the stirred polymer precipitate obtained from the cooling experiment at rate of 1.5 °C/min. The setup allows for different sampling rates, allowing up to 3600 data points to be captured in a typical cooling or heating experiment. Generally a sampling rate was selected that yielded about 1500 data points per experiment.

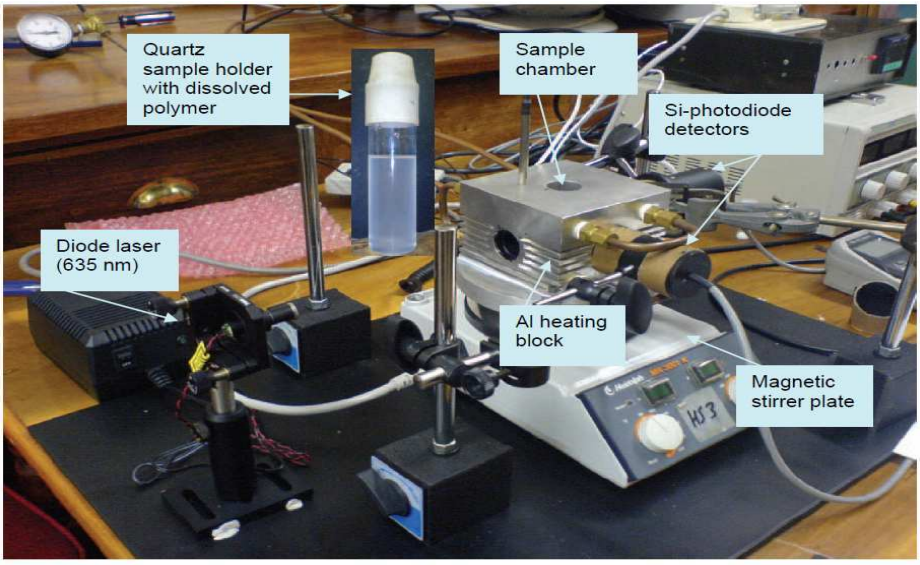

Figure 5.2: Setup used for SCALLS analysis.

5.2.3 CRYSTAF

Crystallization analysis fractionation was carried out using a CRYSTAF apparatus Model 200 (Polymer Char S.A.). The crystallization was carried out in stirred, stainless steel reactors (volume of 60 ml). Typically, approximately 15 mg of sample was dissolved in 30 ml TCB. The temperature was decreased at a rate of 0.1 °C/min from 100 to 30 °C. Fractions were taken automatically and the polymer concentration of the solution was determined by an IR detector, using 3.5 mm as the chosen wavelength.

5.2.4 TREF

The general TREF procedure is described in Chapter 3 (Section 3.2.3).

5.2.5 Characterization techniques

The ^{13}C NMR, HT-GPC and DSC data of samples were obtained according to procedures described in Chapter 3 (Section 3.2.4).

5.3 Results and discussion

5.3.1 Use of DSC for studying the bulk crystallization of different polypropylene blends

Blending of two or more different polymers is often used to develop new polymeric materials. Blending allows the combination of desirable properties of different polymers, affording new materials. The properties of polymer blends are a strong function of the blend morphology. This morphology and the associated phase behaviour strongly depend on the cocrystallization between the components of the blend. Blending also allows us to determine the effect of the molecular weight and tacticity on the crystallinity of the new materials. The manner in which materials crystallize affects the morphology, which has a significant effect on the properties of the material.

5.3.1.1 Ziegler-Natta polypropylene blends

5.3.1.1.1 Blends of polypropylenes with similar tacticities and different molecular weights

The fact that it was possible to synthesize a series of different polypropylene homopolymers, and then fractionate these materials by preprative TREF meant that we could now select fractions isolated by these techniques and then blend them. Table 5.1 presents data for the individual fractions as well as data for the blended fractions. The fractions and blends (50: 50 wt %) given in Table 5.1 were selected based on their differences in the molecular weights and similarities in their tacticities.

Table 5.1: GPC, NMR and DSC results of different TREF fraction blend polymers with the same tacticities but different molecular weights, produced using heterogeneous catalysts

Fractions	M_w	M_w/M_n	*mmmm* %	T_m (°C)	T_c (°C)	ΔH_m (J/g)	X_c (%)
Z4 (120)	195 693	4.3	98.0	160.0	116.0	119.7	57.0
Z4 (140)	142 342	3.6	99.0	158.0	114.0	102.1	49.0
Z4 (120)/ Z4 (140) blend	-	-	-	160.2	115.4	91.5	44.0
Z9 (100)	25 918	2.4	93.0	149.5-158.3	113.0	87.1	41.7
Z10 (110)	92 596	3.5	93.0	157.9	117.2	110.1	52.7
Z9 (100)/ Z10 (110) blend	-	-	-	155.8	115.5	96.1	46

DSC scans of selected TREF fraction blends are presented in Figure 5.3 (A, B). Both the blends showed only one melting peak, even though the fraction Z9 (100) has two melting

peaks, which indicates that cocrystallization of the blends occurred. Although single melting peaks of blends are usually associated with a high extent of cocrystallization, two broad overlapping distributions of thicknesses of separate crystals, one from each component, could also lead to single broad endotherms.[29] Initial results here indicate that molecular weight appears to play some role in the crystallization of these blends in the bulk. When reasonably high molecular weight samples Z4 (120) and Z4 (140) with similar tacticities are blended (Figure 5.3 (A)), the resultant blend melts at a similar (albeit slightly higher) temperature than the higher molecular weight fraction. With lower or intermediate molecular weight fractions Z9 (100) and Z10 (110) in Figure 5.3 (B), it shows a similar pattern, although the melting temperature is lower than that of the higher molecular weight material.

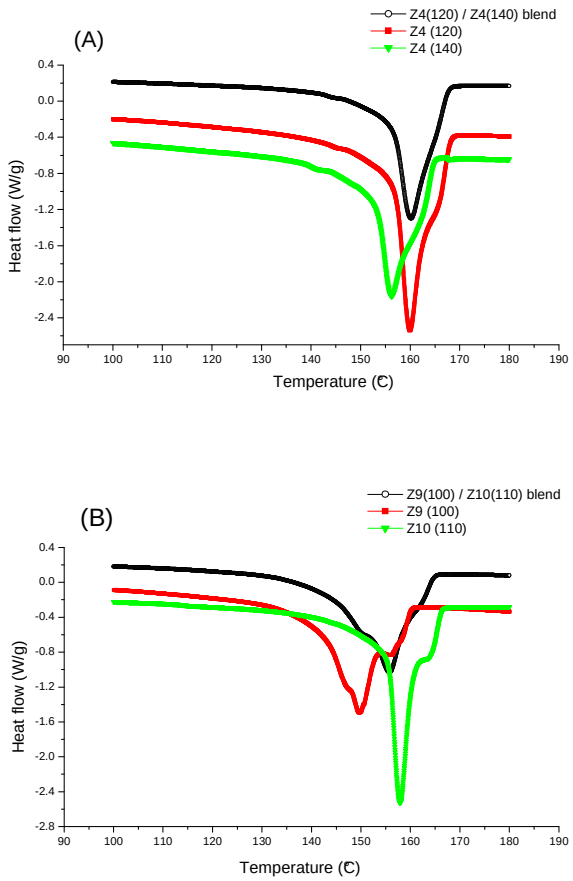

Figure 5.3: DSC thermograms of selected TREF fraction blends: (A) and (B) polymers with same tacticities but different molecular weights produced using heterogeneous catalysts.

5.3.1.1.2 Blends of polypropylenes with similar molecular weights and different tacticities

Table 5.2 shows data for individual fractions as well as data for blended fractions. The fractions and blends given in Table 5.2 were selected based on their differences in the tacticities and similarities in the molecular weights.

Figure 5.4 (A, B) presents DSC scans of selected TREF fraction blends based on their differences in the tacticities and similarities in the molecular weights. In the case of two low molecular weight fractions with different tactcities (Z8 (80) and Z9 (80)), it is quite clear that the melting temperature of the blend is influenced by the material with the highest tacticity. It is interesting to note that the crystallinity percentage of the blend is higher than that of either of the individual fractions.

Table 5.2: GPC, NMR and DSC results of different TREF fraction blends with the same molecular weights but different tacticities, produced using heterogeneous catalysts

Fractions	M_w	M_w/M_n	*mmmm* %	T_m (°C)	T_c (°C)	ΔH_m (J/g)	X_c (%)
Z8 (80)	18 986	3.9	63.0	131.6	100.3	53.9	25.8
Z9 (80)	14 126	3.3	80.0	134.3	102.8	55.1	26.4
Z8 (80)/ Z9 (80) blend	-	-	-	132.9	101.5	58.8	28.2
Z8 (100)	28 270	2.4	84.0	148.9-158.7	111.5	83.7	40.1
Z9 (100)	25 918	2.4	93.0	149.5-158.3	113.0	87.1	41.7
Z8 (100)/ Z9 (100) blend	-	-	-	148.5-158.7	111.7	76.0	36.4

In contrast, it is obvious that the melting temperature of the blend of higher or intermediate molecular weights (Z8 (100) and Z9 (100)), is influenced more by the material with the lowest tacticity. The appearance of double peaks in the samples in Figure 4.5 (B) could be due to recrystallization processes. Recrystallization can usually be excluded by employing the DSC method with a wide range of heating rates, as shown in Figure 5.5. The results in Figure 5.5 show that the recrystallization occurs to a considerable degree only at heating rates lower than 10 °C/min. For greater heating rates (higher than 10 °C/min) recrystallization on scanning does not have time to occur and determination of the effective ΔH_m and T_m of the samples becomes possible.

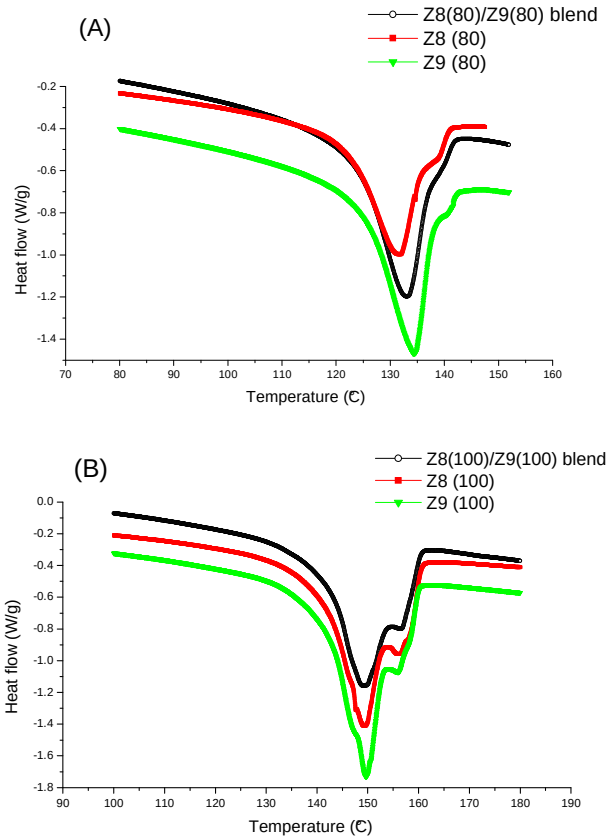

Figure 5.4: DSC thermograms of selected TREF fraction blends: (A) and (B) polymers with the same molecular weights but different tacticities produced using heterogeneous catalysts.

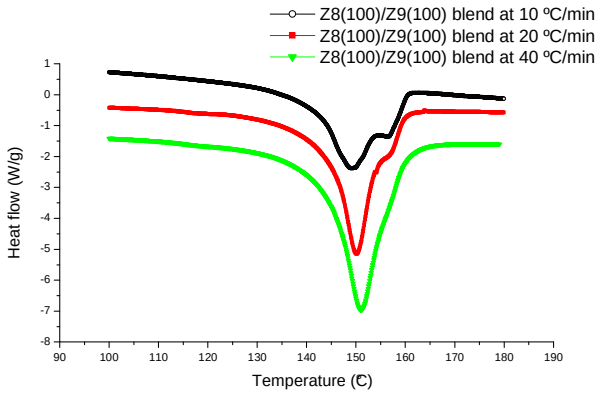

Figure 5.5: DSC thermograms of the Z8 (100)/Z9 (100) blend at different heating rates.

Although these are only preliminary results, indications are that there are two variables that influence cocrystallization in the bulk: molecular weight and tacticity. It is, however, not as clear-cut as to what effect the magnitude of the molecular weight (differences in molecular weight of individual components) and a variation in tacticity might have.

Figure 5.6 shows the modulated DSC (MDSC) reversible (rev), nonreversible (nonrev) and total heat flow traces of the Z8(100)/Z9(100) blend. MDSC, in which a small sinusoidal oscillation (modulation) is superimposed on the conventional linear heating programme, is a useful thermal analysis technique to separate the total heat flow (such as that acquired from conventional DSC) into the heat capacity related (reversible) component and heat flow and kinetic (nonreversible) components.[30] The reversble heat flow is calculated by multiplication of the heat capacity with the negative heating rate. The kinetic component or nonreversible heat flow is the arithmetic difference between the total heat flow and the reversble heat flow. Thus, exothermic signals are detected only in the nonreversible data, but endothermic melting behaviour can contribute to both reversible and nonreversible signals.[31] Hence MDSC can separate exotherms (including crystallization and recrystallization) from glass transitions, reversible melting, or other heat capacity related events. As can be seen in Figure 5.6, in the nonreversible heat flow curve, there is an exothermic peak followed by an endothermic peak. Since the nonreversible component is kinetic in nature and can be attributed to nonreversible melting and crystallization on heating, the existence of the processes of recrystallization and melting on heating was confirmed. The reversible heat flow curve also shows that double reverse melting peaks exist. The endothermic peak in the nonreversible heat flow curve corresponds to the highest endothermic peak in the reversible peak, i.e. they represent the nonreversible and reversible components of the melting of recrystallized materials, respectively. Thus, the remaining reversible melting peak indicates the melting peak of the original crystals in the blend. This means that the different polypropylene polymers show a miscible blends and the appearance of double melting peaks is due to the recrystallization processes.

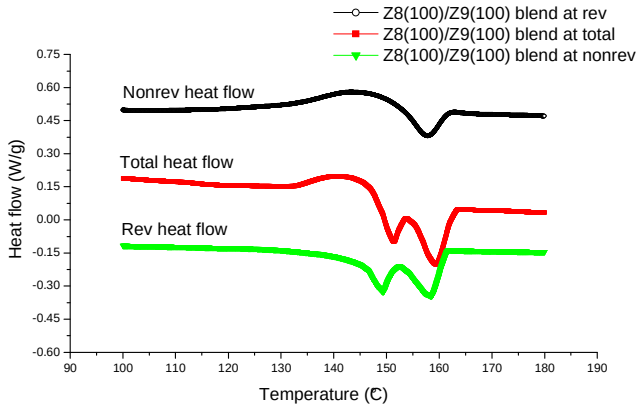

Figure 5.6: MDSC heat flow curves of the Z8 (100)/Z9 (100) blend.

5.3.1.2 Metallocene polypropylene blends

5.3.1.2.1 Blends of polypropylenes with similar tacticities and different molecular weights

Table 5.3 and Figure 5.7 show some DSC results of the TREF fraction blends that were selected according to their difference in the molecular weight and similarity in tacticity. As in the case of the polypropylene TREF fractions produced using heterogeneous catalysts, all the blends indicated in Table 5.3 and Figure 5.7 showed only one melting peak, which indicates that cocrystallization occured. Cocrystallization of the blends occurred due to their similarities in molecular structures, crystalline lattice structures and crytallization rates.

Table 5.3: GPC, NMR and DSC results of polypropylene TREF fraction blends with the same tacticities but different molecular weights, produced using metallocene catalysts

Fractions	M_w	M_w/M_n	*mmmm* %	T_m (°C)	T_c (°C)	ΔH_m (J/g)	X_c (%)
EIP14 (90)	22 178	1.6	87.0	137.7	104.0	82.8	39.6
D7 (90)	8 478	1.5	87.0	141.4	108.9	90.5	43.3
EIP14 (90)/ D7 (90) blend	-	-	-	139.9	107.0	88.9	42.6
EIP13 (100)	12 995	1.5	91.0	137.6	104.7	87.0	41.6
D8 (100)	9 777	1.6	91.0	141.0	109.2	95.8	45.8
EIP13 (100)/ D8 (100) blend	-	-	-	140.7	108.1	98.5	47.1

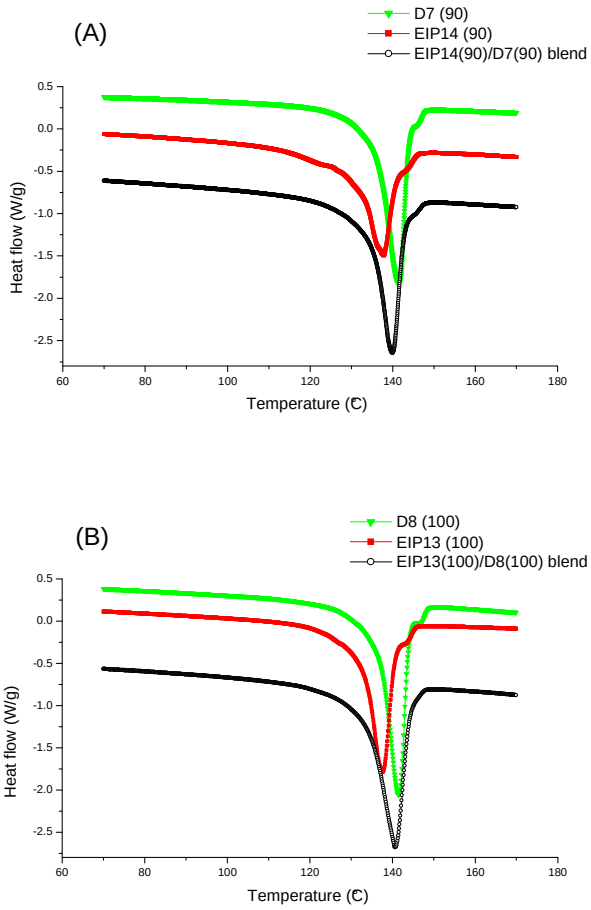

Figure 5.7: DSC thermograms of selected TREF fraction blends: (A) and (B) polymers with same tacticities but different molecular weights produced by homogeneous metallocene catalysts.

5.3.1.2.2 Blends of polypropylenes with similar molecular weights and different tacticities

Table 5.4 tabulates DSC results and Figure 5.8 (A, B) shows DSC scans of selected TREF fraction blends with different tacticities and similar molecular weights. It is evident that the melting temperatures of the two blends of the low and intermediate molecular weight fractions with different tacticities (EIP14 (100)/D9 (80) blend and EIP13 (80)/D8 (100) blend respectively) are influenced by the material with the highest tacticity. This differs slightly to the results that obtained of the TREF blends of the polypropylene produced using heterogeneous catalysts (see Section 5.3.1.1.2). Moreover, the crystallinity percentage of the two blends is higher than that of either of the individual fractions. This provides further evidence that cocrystallization in the bulk of the blends had occurred.

Table 5.4: GPC, NMR and DSC results of polypropylene TREF fraction blends with the same molecular weights but different tacticities

Fractions	M_w	M_w/M_n	*mmmm* %	T_m (°C)	T_c (°C)	ΔH_m (J/g)	X_c (%)
EIP14 (100)	21 351	1.5	88.0	137.6	105.9	65.5	31.3
D9 (80)	20 634	1.8	83.0	131.7	100.5	76.7	36.7
EIP14 (100)/ D9 (80) blend	-	-	-	137.8	104.1	78.8	37.7
EIP13 (80)	10 566	1.6	85.0	131.8	100.5	85.7	41.0
D8 (100)	9 777	1.6	91.0	141.0	109.2	95.8	45.8
EIP13 (80)/ D8 (100) blend	-	-	-	138.2	106.6	106.7	51.1

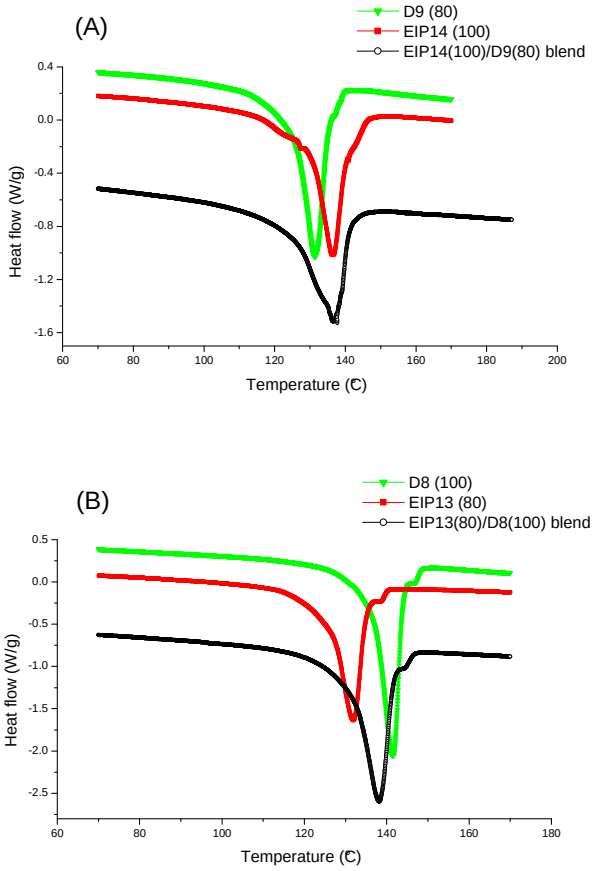

Figure 5.8: DSC thermograms of selected TREF fraction blends: (A) and (B) polymers with the same molecular weights but different tacticities produced using homogeneous metallocene catalysts.

5.3.2 Use of the SCALLS for studying the solution crystallization of different polypropylenes

SCALLS involves the observation of the intensity of light after it passes through a polymer solution. An increase in scattering occurs when the hot polymer solution is cooled and the polymer starts to crystallize out of solution. This decreases in the intensity of light is measured. The reverse of this process leads to a decrease in the scattering with an increase in temperature. According to this concept, it is possible to follow the solution crystallization of different polypropylenes under controlled cooling. In addition, SCALLS is capable of differentiating between different isotactic and syndiotactic polypropylenes with similar chemical structure but different tacticity and molecular weight. SCALLS provides good crystallization information, similar to that provided by CRYSTAF and TREF. SCALLS can also be used as a quantitative tool for the measurement of weight fractions during dissolution.

5.3.2.1 SCALLS cooling and heating experiments

During SCALLS cooling, light is scattered as soon as the polymer starts to crystallize. In the case of CRYSTAF, samples are removed by filtration from the precipitating polymer solution during cooling, and the turbidity is measured. This procedure limits the number of samples that can be taken in given experiment (typically about 40-45 points). During a SCALLS experiment the crystallization process can be continuously monitored and numerous data points obtained. This may lead to higher resolution. Data are then analyzed with Origin® software. In order to get a peak, and be able to analyze the peak maximum and peak width, the first derivative of the voltage data was calculated. Data were smoothed as the derivative was calculated.

The different polymers that were used for analyses and their molecular characteristics are tabulated in Table 5.5. Figures 5.9 (A) and (B) show SCALLS cooling and heating profiles of isotactic polypropylene sample Z15, prepared using a heterogeneous Ziegler-Natta catalyst. Figures 5.10 (A) and (B) show the same profiles of sample Z2, a polymer with higher tacticity and a similar molecular weight. In these experiments the concentration of the polymer solution was 0.5 g/ml, and the SCALLS cooling and heating rates were 1 °C/min and 1.5 °C/min, respectively. It is quite clear that the peak crystallization temperatures of the two samples are different (66.9 °C versus 69.1 °C), and that the cooling peak of Z2 is narrower than that of Z15. The heating profiles are also different. The Z2 sample shows a more distinct maximum, and a higher peak “solution melting” temperature than Z15 (106.3 °C versus 103.2 °C), as expected.

Table 5.5: Characterization data of the polypropylenes used in this study

Samples	M_w	M_w/M_n	*mmmm* %	T_m (°C)	T_c (°C)	ΔH_m (J/g)	X_c (%)
Z17	65 498	8.2	93.0	156.5	120.8	100.5	48.0
Z12	96 137	9.4	90.0	159.2	121.2	114.4	55.0
Z16	97 587	9.3	88.0	157.1	121.3	88.3	42.0
Z2	135 115	4.8	92.0	159.3	121.9	102.0	49.0
Z15	137 965	5.6	87.0	156.4	118.7	83.9	40.0
Z3	184 759	6.1	93.0	161.2	124.2	104.5	50.0
Z8	228 960	6.4	94.0	162.0	124.4	103.9	50.0
Z4	238 155	6.3	94.0	160.6	116.5	103.9	50.0
EIP 14	19 232	1.9	93.8	137.6	108.2	107.4	51.4
D9	24 809	2.0	88.0	138.0	107.7	87.4	41.8
SPP1	174 000	2.3	93.0[a]	111.9-126.5	66.1	33.3	15.9

[a] syndiotacticity (*rrrr* %)

In the case of sample Z2, there are three melting peaks, which could be due to the different sizes of crystals formed during the crystallization process. The differences in melting and crystallization temperatures are very similar to those determined by DSC (Table 5.5).

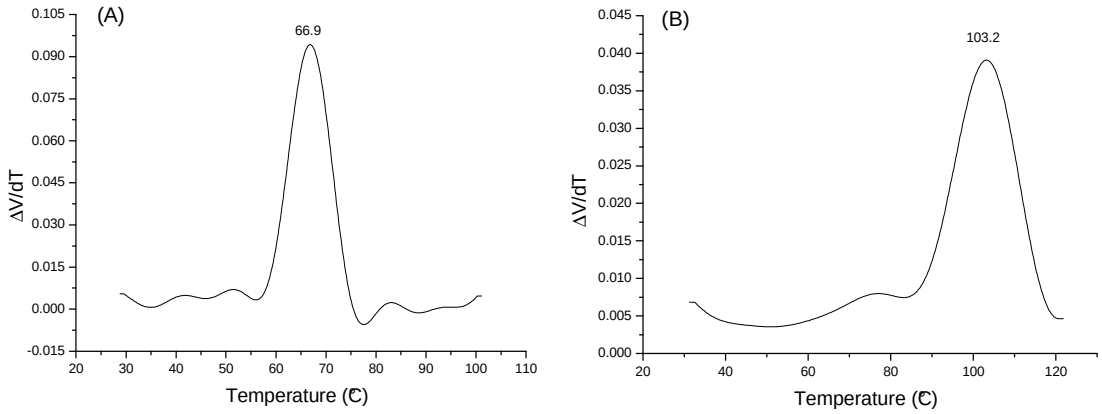

Figure 5.9: SCALLS profiles of cooling (A) and heating (B) of sample Z15 (concentration 0.5 mg/ml, cooling at 1 °C/min and heating at 1.5 °C/min).

Figure 5.11 shows the SCALLS cooling profile (A) and SCALLS heating profile (B) (recorded using the same conditions as in earlier experiments) of an isotactic polypropylene polymer D9 prepared using a homogenous metallocene catalyst. The crystallization peak of sample D9 in Figure 5.11 (A) is different to that of the two other samples Z15 and Z2 (53.2

°C versus 66.9 and 69.1 °C), and the crystallization peak of D9 is narrower than that of Z15 and Z2. The SCALLS heating profile of sample D9 in Figure 5.11 (B) is also different to that of Z15 and Z2 (85.1 versus 106.3 and 103.2 °C). These experiments clearly demonstrate that SCALLS differentiates well between the crystallization and melting behaviour of different isotactic polypropylenes.

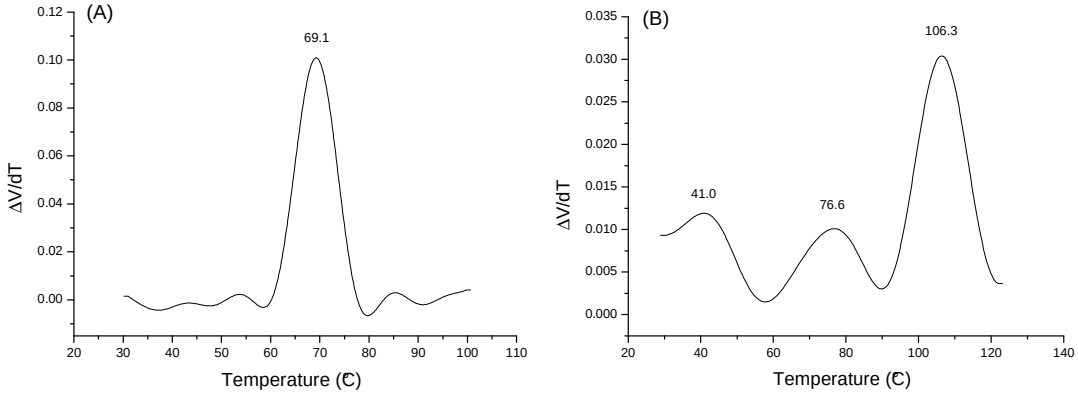

Figure 5.10: SCALLS profiles of cooling (A) and heating (B) of sample Z2 (concentration 0.5 mg/ml, cooling at 1 °C/min and heating at 1.5 °C/min).

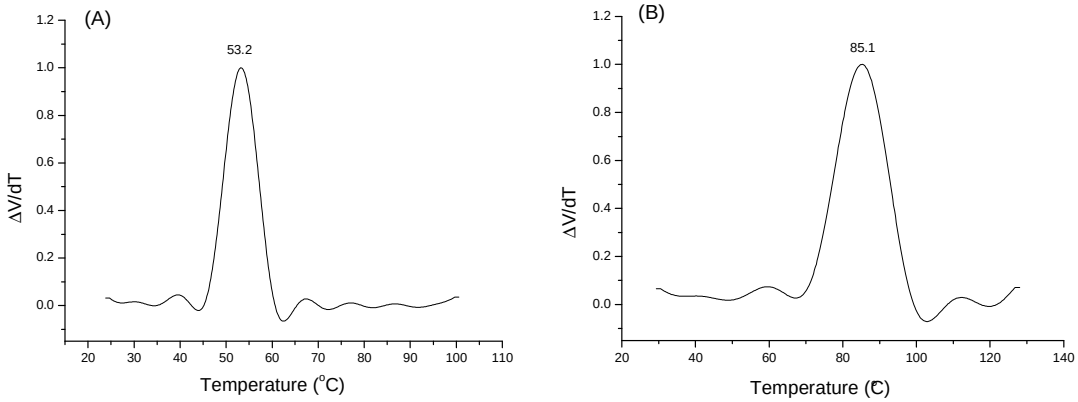

Figure 5.11: The SCALLS profiles of cooling (A) and heating (B) of sample D9. concentration 0.5 mg/ml, cooling at 1 °C/min and heating at 1.5 °C/min.

5.3.2.2 Analysis of solution blending of different polypropylene polymers

The ability of SCALLS to measure the effect of solution blending of two different polymers was evaluated. Results are now described.

5.3.2.2.1 Blends with similar molecular weights and different tacticities

The results of the SCALLS analysis of (50/50 wt %) blends of Z2/Z15 and Z12/Z16 are presented in Figures 5.12 and Figures 5.13, respectively,

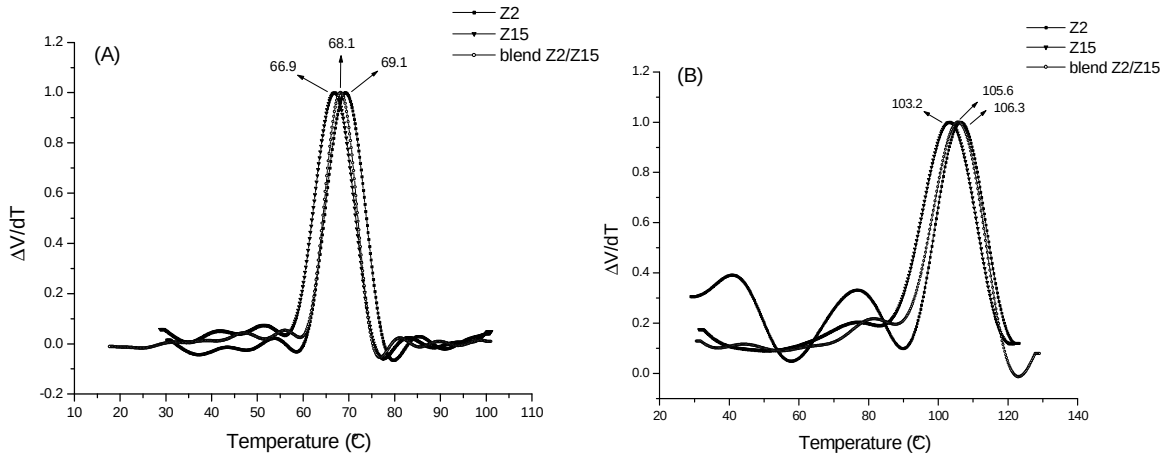

Figure 5.12: SCALLS profiles of cooling (A) and heating (B) of a blend (50/50 wt %) of Z2 and Z15.

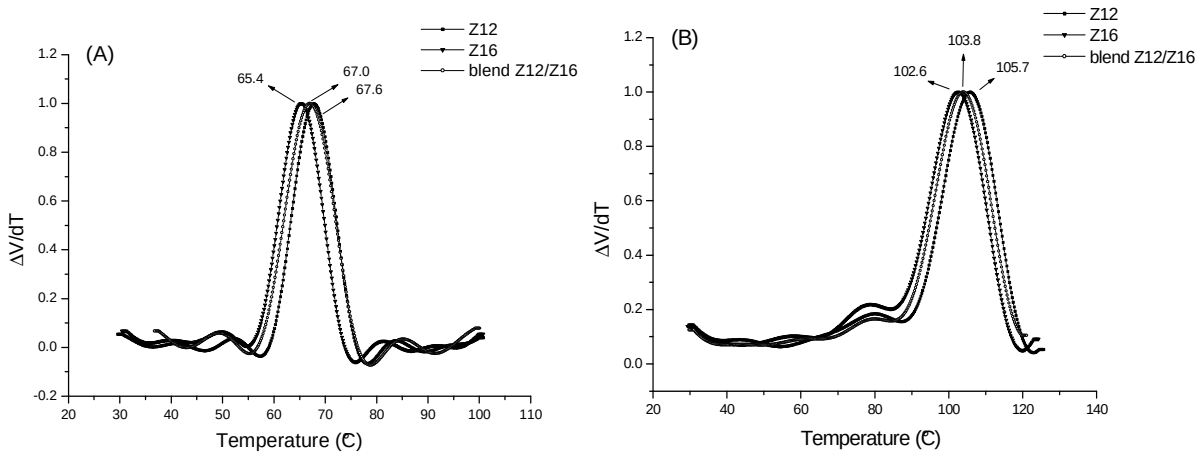

Figure 5.13: SCALLS profiles of cooling (A) and heating (B) of a blend (50/50 wt %) of Z12 and Z16.

Figures 5.12 (A) and 5.13 (A) clearly show that during cooling a single crystallization peak is observed for both blends, with the peak value between that of the two respective pure polymers, as is the case for the heating scans (Figures 5.12 (B) and 5.13 (B)). These results are in agreement with literature.[7-9] The tacticity effect appears during the solution crystallization of the polymers. These results indicate that the blends are miscible and that cocrystallization occurred, which confirms that cocrystallization of the blends occurred due to the similarities in molecular structures, crystalline lattice structures and crytallization rates of the pure polymers.

5.3.2.2.2 Blends with similar tacticities and different molecular weights

Using samples Z3 and Z17, two materials with similar tacticities, but with different molecular weights were blended. Details of the crystallization profiles of the blends are shown in Figures 5.14 (A) and (B). The molecular weight effect appeared to be present during the solution crystallization of the polymers. This was significant, as molecular weight effects are generally ignored during fractionation crystallization experiments.

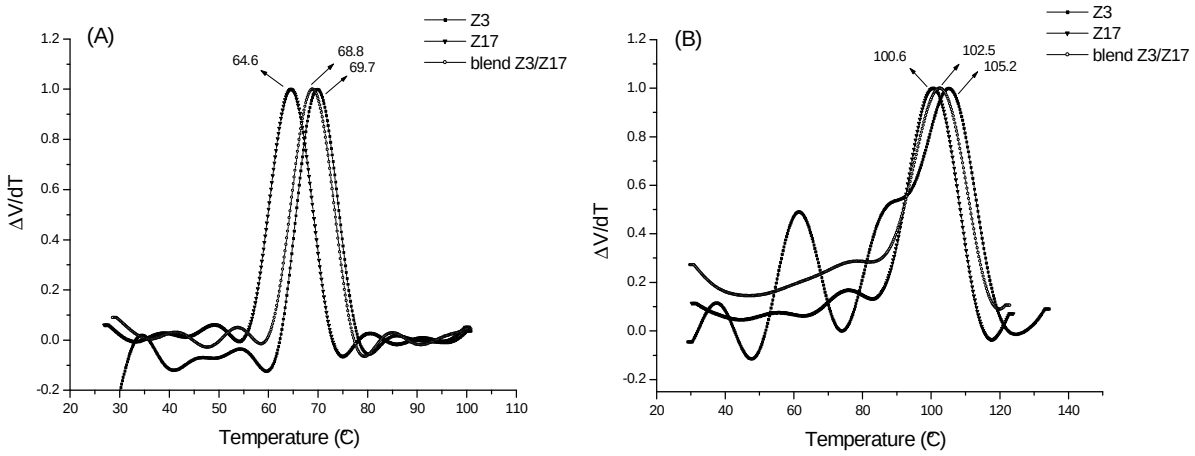

Figure 5.14: SCALLS profiles of cooling (A) and heating (B) of a blend (50/50 wt %) of Z3 and Z17.

Moreover, once again the blend showed only a single peak in both the SCALLS cooling and heating profiles in Figures 5.14 (A) and (B), respectively, which indicates that the blend is miscible and cocrystallization had occurred. Results here indicate that the crystallization peak of the blend during the cooling cycle is influenced more by the higher molecular weight material.

5.3.2.2.3 Blends of isotactic and syndiotactic polypropylene polymers

The crystallization of syndiotactic polypropylene is greatly influenced by the conditions under which it is crystallized. Even highly syndiotactic polypropylene generally has relatively low crystallinity since the syndiotactic run lengths in its molecular structure are relatively short. As a result of the relatively low crystallinity, syndiotactic polypropylene has a low density and it behaves rheologically differently from isotactic polypropylene. The crystallization rate, crystallization temperature, and melting point are all affected by the microtacticity of the resins. Since syndiotactic polypropylene has a lower crystallization rate than isotactic polypropylene, syndiotactic polypropylene requires a longer crystallization time. For these reasons, 25/75 wt % blends compositions of isotactic and syndiotactic polypropylene were analyzed in this study. Here the SCALLS cooling rate was reduced to 0.5 °C/min but the SCALLS heating rate was the same as used in the previous experiments (1.5 °C/min).

The molecular weights and tacticities of selected polymers were tabulated in Table 5.5. The SCALLS cooling and heating profiles of the Z4/SPP1 and Z3/SPP1 blends are shown in Figures 5.15 and 5.16, respectively. Figures 5.15 (A) and 5.16 (A) show that isotactic polypropylenes Z4 and Z3 have crystallization peaks at 76.1 and 69.8 °C, while syndiotactic polypropylene SPP1 has a crystallization peak at 46.5 °C. As expected, the blends exhibited two crystallization peak temperatures.

In the blends, the crystallization temperatures of both materials Z4 and Z3 were slightly changed compared to the ones had been crystallized separately, in the peak temperatures (76.5 °C versus 71.1 °C for Z4 and 69.8 °C versus 76.1 for Z3 sample), peak shape and peak areas. This suggests that although the materials were not miscible, but there was some interaction between the phases. The obtained results are in agreement with those of Mülhaupt and coworkes.[32] They studied the behaviour of syndiotactic and isotactic polypropylene blends. In their work, the blends were made by solubilization of both polymers, mixing and precipitation. Their work also shows that phase separation can not be observed by microscopy, but the crystallization of isotactic and syndiotactic polypropylene always occurs separately. However, in the SCALLS heating cycles the dissolution peaks for isotactic and syndiotactic polypropylene blends (Figure 5.15 (B) and 5.16 (B)) are also separated. Therefore SCALLS is certainly a useful method to obtain qualitative information about blend compositions.

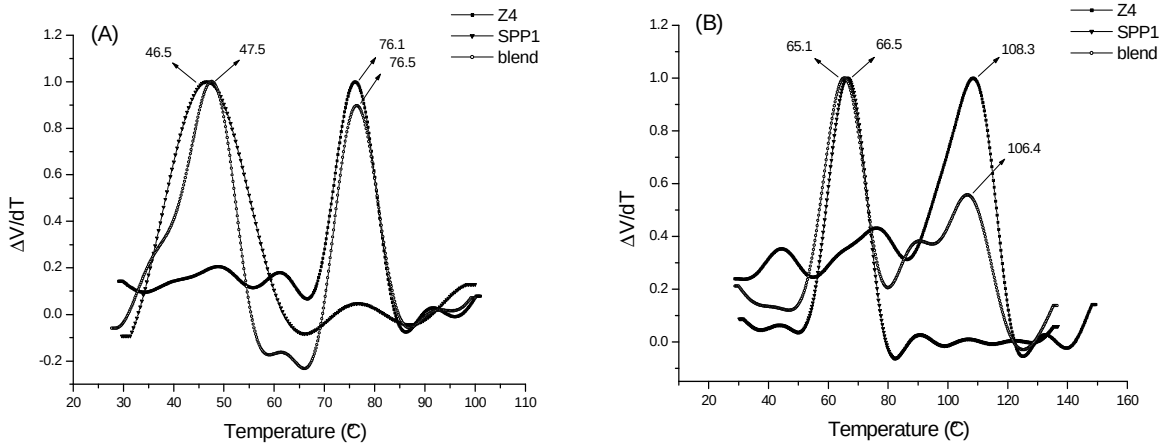

Figure 5.15: SCALLS profiles of cooling (A) and heating (B) of a blend (25/75 wt %) of Z4 and SPP1 (concentration 0.5 mg/ml, cooling at 0.5 °C/min and heating at 1.5 °C/min).

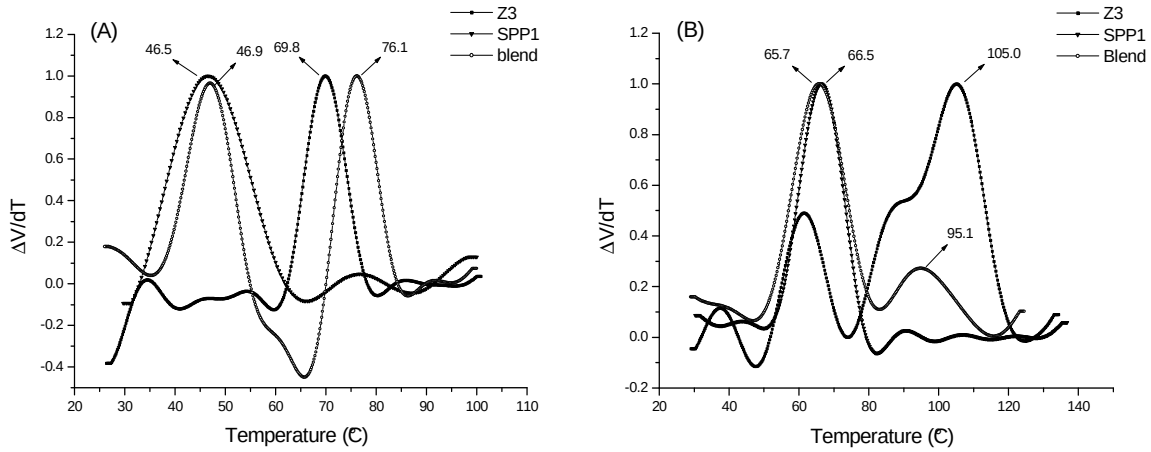

Figure 5.16: SCALLS profiles of cooling (A) and heating (B) of a blend (25/75 wt %) of Z3 and SPP1 (concentration 0.5 mg/ml, cooling at 0.5 °C/min and heating at 1.5 °C/min).

5.3.2.3 Use of the SCALLS heating cycle to determine weight fraction distributions of different polypropylenes

Two different isotactic polypropylenes Z15 and Z8 (Table 5.5) with different molecular weights and tacticities were chosen in order to investigate the weight fraction distribution

using SCALLS method. Figure 5.17 shows the results of SCALLS heating curves for the isotactic polypropylene samples Z15 and Z8. The SCALLS heating data tabulated in Table 5.6 were calculated according to the percentage area of each temperature to the total areas of all the other peaks. It can be seen that the weight fractions of the two polymers were different. The major amount of material of sample Z15 was obtained at fraction temperatures 100 and 110 °C, in the case of sample Z8 it was at 90 and 110 °C. Furthermore, the weight fraction distributions of both samples are considerably different (see Figure 5.15). SCALLS can thus be used as an analytical technique to differentiate between different polypropylenes with different molecular composition.

Table 5.6: SCALLS heating weight fractions data of the isotactic polypropylene samples Z15 and Z8

Z15			Z8		
Fraction (T, °C)	Wi %	ΣWi %	Fraction (T, °C)	Wi %	ΣWi %
35	2.0	2.0	35	5.0	5.0
50	1.6	3.6	50	2.2	7.2
70	1.5	5.1	70	6.7	13.9
90	5.4	10.5	90	16.9	30.8
100	29.9	40.4	100	9.1	39.9
110	48.6	88.0	110	43.7	83.6
120	12.0	100.0	120	16.4	100.0

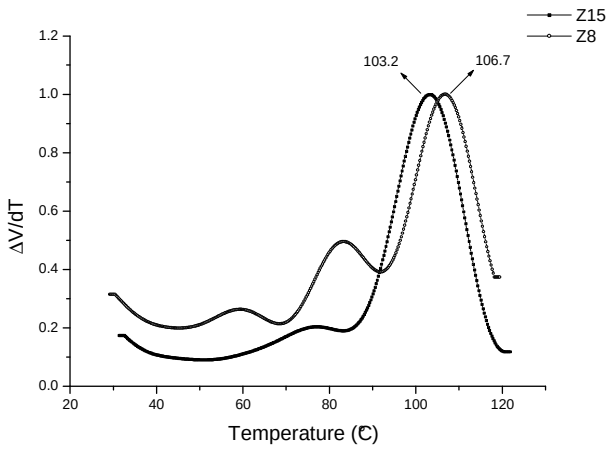

Figure 5.17: SCALLS heating profiles of samples Z15 and Z8.

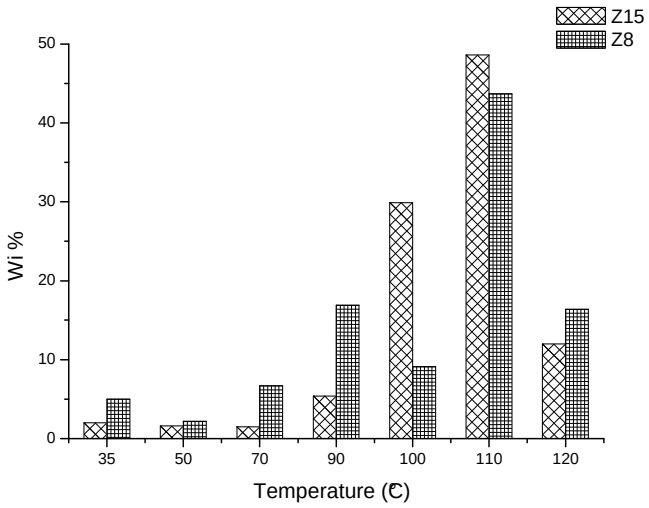

Figure 5.18: Distribution of weight percentage of Z15 and Z8 fractions vs. temperature (°C).

5.3.2.4 Comparison of estimation of weight fractions from SCALLS, TREF and CRYSTAF

Figures 5.19 (A) and (B) show a comparison of the results of SCALLS cooling and heating to CRYSTAF and TREF for the isotactic polypropylene sample Z4. The analyses were carried out at a cooling rate of 1 °C/min and a heating rate of 1.5 °C/min. Remarkably, the results from SCALLS cooling and CRYSTAF are comparable in terms of peak shapes and peak areas and are about 7 °C apart in terms of the peak temperatures (76.1 versus 82.9 °C). This difference in the temperature could be due to the difference between the cooling rates of SCALLS and CRYSTAF. The quick cooling probably results in smaller crystals that are more uniform in size, while the slow cooling may allow for larger, and a wider range of, crystal sizes, which might account for the variation in the peak temperatures and peak shapes. Moreover, the results of SCALLS heating and TREF are also comparable, seen in Figure 5.19 (B). However, they do differ in peak temperatures and (slightly) in shapes.

Figures 5.20 (A) and (B) show further comparison results between SCALLS cooling and heating to CRYSTAF and TREF for the isotactic polypropylene sample produced using the metallocene catalyst EIP14. Once again, the SCALLS profiles (cooling and heating) show a comparable response to the crystalline regions as in CRYSTAF and TREF. Actually, SCALLS showed a higher resolution and a narrower response to the isotactic polypropylenes than CRYSTAF and TREF. This is represented by the small peaks that were observed between 35 and 90 °C in the SCALLS profiles.

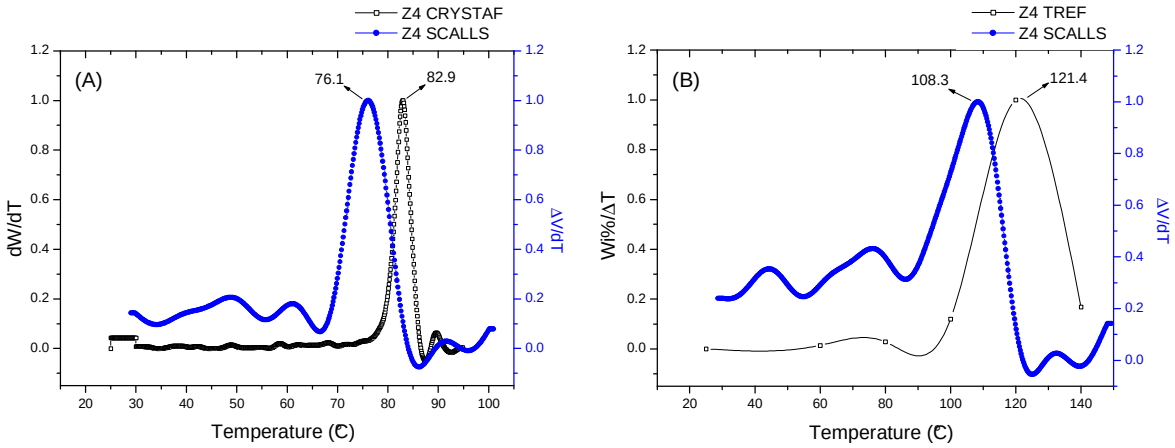

Figure 5.19: Comparison of SCALLS cooling (A) and heating (B) to CRYSTAF and TREF results of sample Z4.

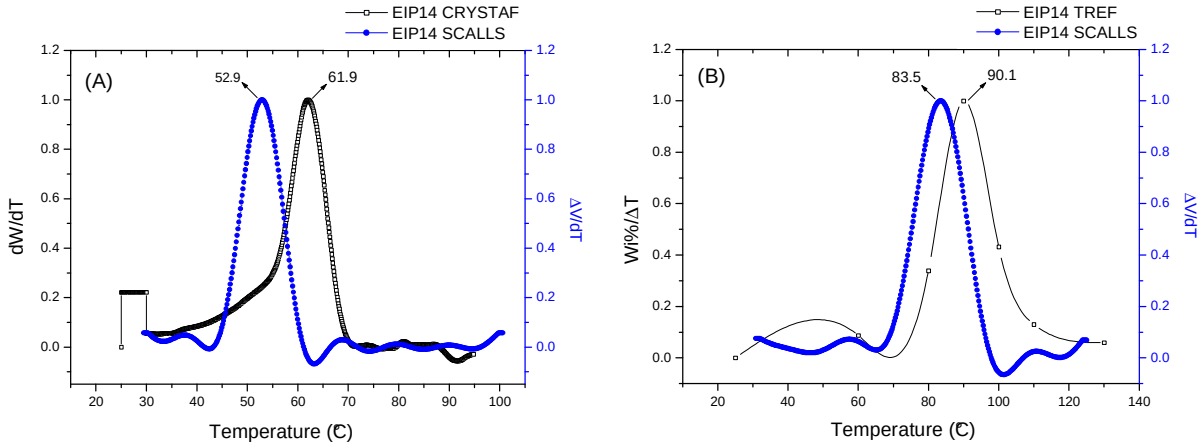

Figure 5.20: Comparison of SCALLS cooling (A) and heating (B) to CRYSTAF and TREF results of sample EIP 14.

In the case of syndiotactic polypropylene (SPP1), and as mentioned earlier (Section 5.3.2.2.3) the SCALLS cooling rate was reduced to 0.5 °C/min due to the slow crystallization rate of this polymer, while the heating rate kept the same as in the case of isotactic polypropylenes (1.5 °C/min). The comparison results of SCALLS cooling and heating to CRYSTAF and TREF results for the SPP1 are shown in Figures 5.21 (A) and (B). Basically, the results from SCALLS heating and TREF (Figure 5.21 (B)) are comparable in terms of the peak shapes, but there are slight differences in peak widths and peak areas, and the peak temperatures are about

4.5 °C apart (66.4 versus 70.9 °C) for this polymer. This could be due to the cooling rates differences and to the temperature calibration of each instrument. In addition, more details can be obtained using SCALLS heating curve at the area ranges 30–50 °C and 80–120 °C. This is possibly due to the different crystal sizes that formed during the cooling step. On the other hand, the crystallization peak of SPP1 was not completely obtained from CRYTAF, as can be seen in Figure 5.21 (A). This is due to the low crystallization temperature of SPP1. Conversely, as shown in Figure 5.21 (A), SCALLS was able to capture the crystallization peak of the same sample at 46.5 °C. However, the crystallization temperatures of SCALLS cooling and CRYSTAF are different. These different temperatures generally result from the different crystallization conditions imposed by the different cooling and heating histories. Different cooling and heating histories would certainly influence the size and number of the resulting crystallites and subsequently affect the measured turbidity.

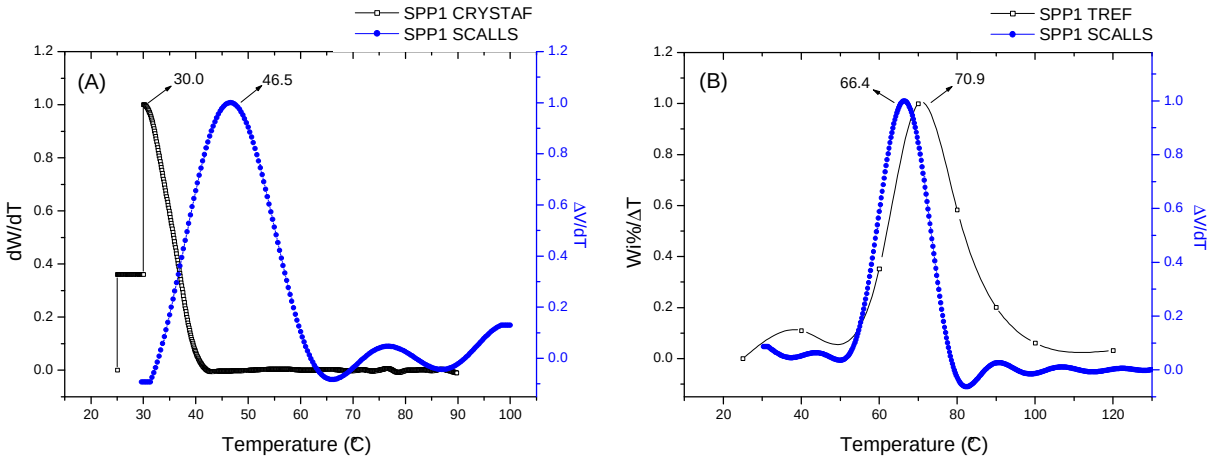

Figure 5.21: Comparison of SCALLS cooling (A) and heating (B) to CRYSTAF and TREF results for the syndiotactic polypropylene sample SPP1.

To investigate the quantitative measurement of the SCALLS technique, three different polypropylenes (Z4, Z16 and SPP1 Table 5.5) with different molecular weights were studied. Table 5.7 compares the weight fractions of the isotactic polypropylene sample Z4 as measured by SCALLS heating and TREF. The SCALLS heating data were calculated according to the percentage area of each peak temperature to the total area of all the other peaks.

Figure 5.19 (B) shows that the TREF peak elution temperature is about 13 °C higher than the equivalent SCALLS heating peak temperature (121.4 versus 108.3 °C, respectively). As a result, if we compare the weight percentage of each SCALLS peak temperature after adding the difference in the temperature to TREF, we see that the calculated areas (weight percentages) for each peak are practically identical to the actual weight fractions obtained from TREF. For example, if we take the peak temperature of SCALLS heating at 108 °C, which equates to a TREF elution temperature of about 121 °C (with the added difference of 13 °C), and compare it to the 120 °C fraction eluted during TREF, the total material crystallized out at this temperature using both techniques is 94.7 and 89.8 wt % respectively. This experiment demonstrates that SCALLS can be used as a quantitative tool for the measurement of weight fractions during dissolution.

Table 5.7: Comparison of the SCALLS heating and TREF weight fraction results of the isotactic polypropylene sample Z4

TREF data			SCALLS heating data		
Fraction (T, °C)	Wi %	ΣWi %	Peak temperature (°C)	Wi %	ΣWi %
25	7.7	7.7	45	4.9	4.9
60	1.7	9.4	75	9.6	14.5
80	2.0	11.4	108	80.2	94.7
100	8.3	19.7	130	2.3	97.0
120	70.1	89.8	> 130	3.0	100.0
140	11.9	100.0	-	-	-

Table 5.8 shows a comparison of data for the weight fractions of the isotactic polypropylene sample Z16 as measured by SCALLS heating and from TREF. The SCALLS heating data were calculated in the same manner as mentioned above.

Table 5.8: Comparison of the SCALLS heating and TREF weight fraction results of the isotactic polypropylene sample Z16

TREF data			SCALLS heating data		
Fraction (T, °C)	Wi %	ΣWi %	Peak temperature (°C)	Wi %	ΣWi %
25	11.3	11.3	32	1.8	1.8
60	5.8	17.1	57	1.2	3.0
80	5.7	22.8	77	3.3	6.3
90	4.3	27.1	102	92.4	98.7
100	10.2	37.3	125	1.3	100.0
110	54.6	91.9	-	-	-
120	7.6	99.5	-	-	-
140	0.5	100.0	-	-	-

Figure 5.22 shows that the TREF peak elution temperature is about 8.4 °C higher than the equivalent SCALLS heating peak temperature. This is attributed to the difference in the heating rates of the two techniques. Once again, if we compare the results of the weight fractions of the SCALLS heating process and TREF, we find that they are equivalent techniques.

A further example is described. If we take the peak temperature of SCALLS heating at 102 °C, which equates to a TREF elution temperature of about 110.4 °C (with the added difference of 8.4 °C), and compare it to the 110 °C fraction eluted during TREF, the total material crystallized out at this temperature for both techniques is 91.9 and 98.7 wt %, respectively. The reason for differences in the weight fraction estimations during heating may be as described below.

During crystallization, the polymer chains precipitate out of solution once their crystallization temperature is reached. The amount that precipitates is independent of the crystal structure formed. During dissolution or elution, the amount of crystallized polymer that melts or dissolves at a given temperature depends on the crystallite size. If a wide range of crystallite sizes is formed during the crystallization step then a broader temperature range will be observed during dissolution.

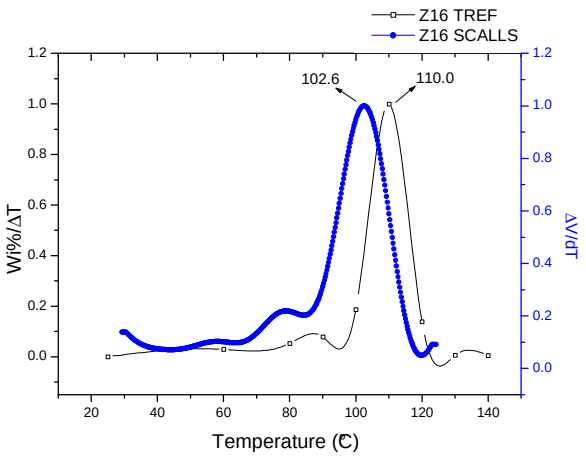

Figure 5.22: Comparison of SCALLS heating to TREF results of sample Z16.

Table 5.9 compares the weight percentage results from SCALLS heating and TREF for the syndiotactic polypropylene sample SPP1. The results from SCALLS heating and TREF are comparable, as in the case of the isotactic polypropylene samples Z4 and Z16. Throughout all of the observed results, it is surprising that the weight fractions of the individual polymers

measured from SCALLS are quantitative. The turbidimetric response to the crystallized polymer depends on the number and size of crystals present.

Table 5.9: Comparison of the SCALLS heating and TREF weight fraction results of the syndiotactic polypropylene SPP1

TREF data			SCALLS heating data		
Fraction (T, °C)	Wi %	ΣWi %	Peak temperature (°C)	Wi %	ΣWi %
25	12.7	17.7	33	1.8	1.8
60	34.3	47.0	44	2.1	3.9
70	27.8	74.8	67	86.9	90.8
80	16.2	91.0	90	3.8	94.6
90	5.6	96.6	107	3.1	97.7
100	1.7	98.3	122	2.3	100.0
120	1.7	100.0	-	-	-

5.4 Conclusions

DSC results of the bulk crystallization of all the various polypropylene blends showed only one melting peak, which indicates that that cocrystallization of the blends occurred. Although single melting peaks of blends are usually associated with a high extent of cocrystallization, two broad overlapping distributions of thicknesses of separate crystals, one from each component, could also lead to single broad endotherms. This leads us to believe that the crystallization behaviour of the polymer blends in the bulk is strongly affected by the configuration (tacticity) and molecular weight of the polypropylene polymers.

Turbidity analysis of the polypropylene polymers obtained using SCALLS provides good crystallization information that is similar to CRYSTAF and TREF. In a SCALLS experiment, the turbidity of a polymer solution is measured while changing its temperature at a controlled rate. The resulting turbidity profile represents the precipitation or dissolution of the crystallized polymer at a given temperature.

In this study, it was possible to differentiate between polypropylenes with similar chemical structure but different tacticity and molecular weight. SCALLS data showed that the blends of different isotactic polypropylene polymers were miscible and cocrystallization occurred, whereas the blends of syndiotactic polypropylene and different isotactic polypropylenes were not miscible and some interaction between phases occurred. In addition, SCALLS can be used as a quantitative tool for the measurement of weight fractions during dissolution.

According to results obtained in this study and previous literature,[22,23] we can conclude that a SCALLS apparatus is simple to operate and is inexpensive, compared to the cost of operation

and maintenance of other fractionation instruments. Given the flexibility of the instrument, experiments can be designed to help further the understanding of the fractionation and crystallization of polymers. Moreover, the simple equipment set-up and operation of the SCALLS allows for the flexibility to perform crystallization experiments in different solvents. This is a distinct advantage over other techniques such as CRYSTAF and TREF that generally require the use of TCB for its high temperature use and ability to dissolve of polyolefins.

5.5 References

1. E. P. Moore, Jr. *Polypropylene Handbook*, Hanser Publishers. Munich, **1996**, pp. 11-73.
2. J. D. Hoffman, R. L. Miller, *Macromolecules* **1988**, 21, 3038.
3. S. Z. Cheng, J. J. Janimak, A. Zhang, *Macromolecules* **1990**, 23, 298.
4. B. D. Carvalho, R. E. Bretas, *J. Appl. Polym. Sci*. **1998**, 68, 1159.
5. J. Andres, B. Pena, R. Benavente, E. Perez, M. Cerrada, *Eur. Polym. J*. **2007**, 43, 2357.
6. P. J. Phillips, N. Vatansever, *Macromolecules* **1987**, 20, 2138.
7. S. Z. Cheng, J. J. Janimak, A. Zhang, *Polymer* **1991**, 32, 648.
8. J. J. Janimak, S. Z. Cheng, P. A. Giust, E. T. Hsieh, *Macromolecules* **1991**, 24, 2253.
9. J. J. Janimak, S. Z. Cheng, A. Zhang, *Polymer* **1992**, 33, 728.
10. L. Hongbin, Q. Jinliang, X. Yibin, Y. Yuliang, *J. Appl. Polym. Sci*. **2002**, 85, 333.
11. R. Paukkeri, E. Iiskola, A. Lehtinen, H. Salminen, *Polymer* **1994**, 35, 2636.
12. R. Paukkeri, A. Lehtinen, *Polymer* **1994**, 35, 1673.
13. A. Lehtinen, R. Paukkeri, *Macromol. Chem. Phys*. **1994**, 195, 1539.
14. R. Paukkeri, T. Väänänen, A. Lehtinen, *Polymer* **1993**, 34, 2488.
15. J. Xu, Y. Yang, L. Feng, X. Kong, S. Yang, *J. Appl. Polym. Sci*. **1996**, 62, 727.
16. X. Kong, Y. Yang, J. Xu, L. Feng, S. Yang, *Eur. Polym. J*. **1998**, 34, 431.
17. J. B. P. Soares, A. E. Hamielec, *Polymer* **1995**, 36, 1639.
18. P. Viville, D. Daoust, A. M. Jonas, B. Nysten, R. Legras, M. Dupire, J. Michel, G. Debras, *Polymer* **2001**, 42, 1953.
19. I. Amer, A. van. Reenen, *Macromol. Symp*. **2009**, 282, 33.
20. B. Monrabal, *J. Appl. Polym. Sci*. **1994**, 52, 491.
21. H. Pasch, R. BrüIl, U. Wahner, B. Monrabal, *Macromol. Mater. Eng*. **2000**, 279, 46.
22. J. R. BrülI, H. Pasch, H. G. Raubenheimer, R. D. Sanderson, A. J. van. Reenen, U. M. Wahner, *Macromol. Chem. Phys*. **2001**, 202, 1281.
23. B. Monrabal, J. Sancho-Tello, N. Mayo, L. Romero, *Macromol. Symp*. **2007**, 257, 71.
24. L. G. Imhof, *J. Appl. Polym. Sci*. **1966**, 10, 1137.
25. C. P. Shan, W. A. de Groot, L. G. Hazlitt, D. Gillespie, *Polymer* **2005**, 46, 11755.
26. A. J. van Reenen, E. G. Rohwer, P. Walters, M. Lutz, M. Brand, *J. Appl. Polym. Sci*. **2008**, 109, 3238.
27. A. van Reenen, M. Brand, E. Rohwer, P. Walters, *Macromol. Symp*. **2009**, 282, 25.
28. L. W. Gamble, W. T. Wipke, T. Lane, *J. Appl. Polym. Sci*. **1965**, 9, 1503.
29. M. H. Kim, G. R. Alamo, J. S. Lin, *Polym. Eng. Sci*. **1999**, 39, 2117.

30. X. Wang, J. Zhou, L. Li, *Eur. Polym. J.* **2007**, 43, 3163.
31. B. B. Sauer, W. G. Kampert, E. Neal Blanchard, S. A. Threefoot, B. S. Hsiao, *Polymer* **2000**, 41, 1099.
32. R. Thomann, J. Kressler, S. Setz, C. Wang, R. Mülhaupt, *Polymer* **1996**, 37, 2726.

CHAPTER 6

Morphological and mechanical properties of polypropylene and polypropylene blends

6.1 Introduction

Polypropylene is one of the commodity polymers used in the largest quantity today. Its good mechanical properties and relatively low price result in the continuous growth of its production and the expansion of its market. Its continuously increasing application accelerates research in all related fields, including the preparation of isotactic polypropylene based composites and blends.

The mechanical and physical properties of polypropylene are influenced by a number of factors. The mechanical properties of the majority of polypropylene homopolymers, are apart from processing conditions, influenced by their rheological and crystallization behaviour. The degree of crystallinity is probably considered as the most influential property that can affect the physical and mechanical properties of a polypropylene sample.[1-3] An increase in crystallinity is often related to an increase in properties such as the stiffness or modulus of a sample, while other factors such as the impact strength generally decrease with increasing crystallinity. Molecular weight also plays a significant role in determining the degree of crystallinity and crystallization rate, and also the mechanical and physical properties.[4] The molecular weight has also been shown to influence the glass transition temperature (T_g) of polymers, with higher molecular weight samples having a higher T_g.[5] This in turn influences the mobility of chains at room temperature, and since polypropylene has a T_g range in the region of 0 °C, variations in the T_g temperature range can have an effect on the ability of the material to displace energy at low temperatures. The tacticity of polypropylene samples also influences the mechanical and physical properties. Generally polymers of higher tacticity have improved crystallinity and form stiffer materials.[6]

Polymer blends have received much attention for many decades. Their morphology, crystallinity, microstructure, melting and crystallization behaviour are strongly dependent on the blend components.[7-14] The preparation of polymer blends is an important way to modify the target properties of individual polymers according to the requirements of the applications. Isotactic polypropylene based blends have been widely studied.[15-18] Blends of isotactic

polypropylene and syndiotactic polypropylene have been widely studied, due to the fact that syndiotactic polypropylene exhibits good mechanical and optical properties, which depends on the syndiotactic degree and the average molecular weight. These characteristics can be used to improve the commercial isotactic polypropylene produced using conventional Ziegler-Natta catalysts. These blends can compete with PET and PVC for packaging applications.[19] Moreover, the blends show that phase separation can not be observed by microscopy; although the crystallization of isotactic and syndiotactic polypropylene always occurs separately. The morphology of the blends is widely influenced by the crystallization kinetics.[19]

6.2 Experimental

6.2.1 Sample preparation for mechanical tests

Test specimens were injection moulded into standard disks for morphological and mechanical tests with a HAAKE MiniJet II injection moulder. The injection moulding temperature was 190 °C and the injection pressure was 200 bar. The dimensions of the standard disks are 20.0 mm in diameter and 1.5 mm in thickness.

6.2.2 Preparation of etching reagent

Permanganic etching of polyolefins was used to prepare samples for the study of the morphology. This technique has been used by several groups for polyolefins.[20-23] Potassium permanganate (1 g) was dissolved in 100 ml of a concentrated solution of 33 vol % phosphoric acid and 67 vol % sulphuric acid. The solution was prepared by adding potassium permanganate very slowly to the beaker containing both acids, with rapid agitation. After adding all the potassium permanganate, the beaker was closed and the content stirred until all the potassium permanganate was dissolved (a dark green purple solution formed). All polypropylene samples were etched at room temperature.

6.2.3 Procedure of the etching process

Specimens from each polymer, with approximate dimensions of length 10 mm, width 5 mm and thickness 1.5 mm, were cut from the disks prepared as described in Section 6.2.1. Each sample was immersed in about 10 ml of the etching reagent in a beaker for a period of 60 minutes. This permananic acid solution preferentially etches the amorphous part of the

polymer in the spherulites, in such a way that the lamellae then appear clearly. Subsequently, the specimens were carefully washed with hydrogen peroxide, distilled water and acetone, in order to avoid any artefacts caused by pollution effects. samples were finally dried in a vacuum oven at 45 °C for 5 hours.

6.2.4 Determination of morphology

6.2.4.1 Optical microscopy

A Zeiss Axiolab optical microscope (magnification x 50–100 μm) with a high resolution camera CCD-IRIS (Sony) was used to examine the etched disks, to investigate the crystal structure.

6.2.4.2 Scanning electron microscopy

Scanning electron microscopy (SEM) analysis of etched disks was performed using a Leo® 1430VP scanning electron microscope operated at 15 kV of acceleration voltage at room temperature. All the surfaces to be studied were coated with gold under vacuum in order to eliminate any undesirable charge effects during the SEM observations.

6.2.5 Determination of mechanical properties

6.2.5.1 Dynamic mechanical analysis

Samples for compressive dynamic mechanical analysis (DMA) were analyzed using a Perkin Elmer DMA 7e calibrated according to standard procedures. The samples were first melted at 180 °C for 8 minutes and then melt pressed at that temperature at 5 MPa pressure. The samples were analyzed using a 5 °C/min heating ramp with an applied force oscillating at a frequency of 1 Hz. The static force was kept constant at 110% of the dynamic force. The temperature range analyzed was between -40 °C and 230 °C.

6.2.5.2 Microhardness

Microhardness (MH) measurements were conducted on a UHL microhardness tester equipped with a Vickers indenter. Measurements were obtained using an indentation speed of 25 μm/s and a dwell time of 15 s. Samples were analyzed at indentation loads of 10 gf. Ten measurements were recorded for each sample analyzed.

6.3 Results and discussion

6.3.1 Morphological properties

OM and SEM were used to study the effect of the molecular weight and tacticity on the crystal structure of the polypropylene polymers and also to observe the crystalline structures of different polypropylene blends. Table 6.1 summarizes the selection of polypropylene polymers and fractions used in the morphological study.

Table 6.1: Characterization data of the polypropylenes used in the morphological study

Samples	M_w	M_w/M_n	*mmmm* %	T_m (°C)	T_c (°C)	ΔH_m (J/g)	X_c (%)
Z4	252 956	5.4	94.0	160.6	116.5	103.9	50.0
Z5	312 580	4.1	96.0	161.9	118.4	108.9	52.0
Z14	215 397	5.9	86.0	157.5	119.8	90.5	43.0
Z4(120)	195 693	4.3	98.0	160.0	116.0	119.7	57.0
Z5(120)	207 823	2.9	96.0	161.0	118.0	103.2	49.0
Z9 (110)	110 387	3.4	98.0	158.7	118.4	110.7	53.0
Z5(120)/ Z4(120) blend	-	-	-	160.2	115.4	91.5	44.0
SPP1	174 000	2.3	93.0[a]	111.9-126.5	66.1	33.3	15.9

[a] syndiotacticity (*rrrr* %)

6.3.1.1 Optical microscopy analysis

First, the effect that the molecular weight has on the crystal structure of different polypropylene samples was studied. Figures 6.1 A, B and C show OM micrographs of polypropylene fractions Z5 (120), Z4 (120) and Z9 (110) respectively, which differ in their molecular weight (see Table 6.1). They exhibit a typical α-modification spherulite structure of isotactic polypropylenes crystallized from the melt. These figures show that all the isotactic polypropylene fractions have well-defined and large α-spherulitic morphology. The spherulites grew, impinged on each other, and formed particular polygonal spherulites with clear boundaries. Indications are that, since all the observed spherulites grew at the same rate and their observed size is uniform, the nuclei are formed immediately after cooling to the crystallization temperature and their number remains constant thereafter. The only effect of the molecular weight that can be noticed in Figure 6.1 is the slightly morphological differences in the sign of birefringence, magnitude of the birefringence and spherulite texture.

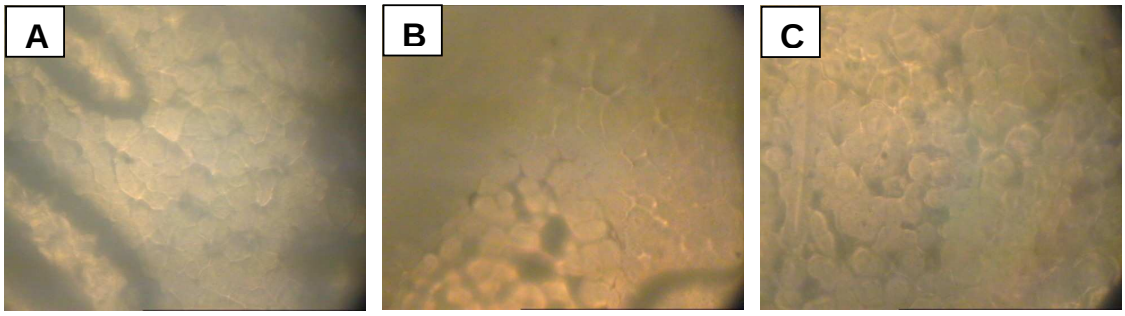

Figure 6.1: Optical micrographs of isotactic polypropylene fractions: A) Z5 (120), B) Z4 (120) and C) Z9 (110) (magnification: 5 x 10^2).

Second, the effect of tacticity on the crystal structure of different isotactic polypropylenes was studied. Figures 6.2 A, B and C show OM micrographs of polypropylenes Z5, Z4 and Z14, which differ in their tacticities (Table 6.1). The figures show that, under similar crystallization conditions, the dimensions of the crystal structures of these different isotactic polypropylene samples decrease in size with tacticity. This effect can be explained by the restriction of movement of polymer chains caused by chain defects in low tacticity polymers during the crystallization process, resulting in slower crystallization and hence the formation of smaller spherulites. Similar results were obtained by a other of researchers.[24-26]

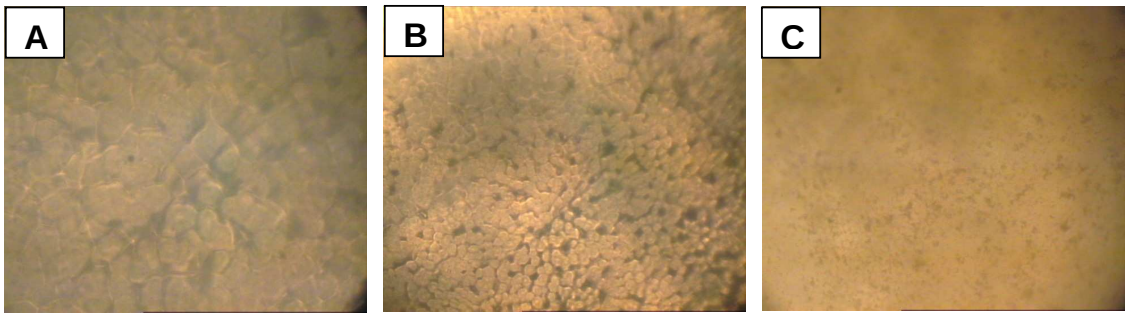

Figure 6.2: Optical micrographs of isotactic polypropylene polymers: A) Z5, B) Z4 and C) Z14 (magnification: 5 x 10^2).

The OM micrographs of isotactic polypropylene blends of two different isotactic polypropylene fractions Z5 (120) and Z4 (120), shown in Figures 6.3, show that the blend of the two fractions (Figure 6.3 C) has the same type of α-modification spherulite structure of isotactic polypropylenes. The only slight differences are the size of the crystals and the manifestation of birefringence. These results indicate that the two isotactic polypropylene fractions are miscible.

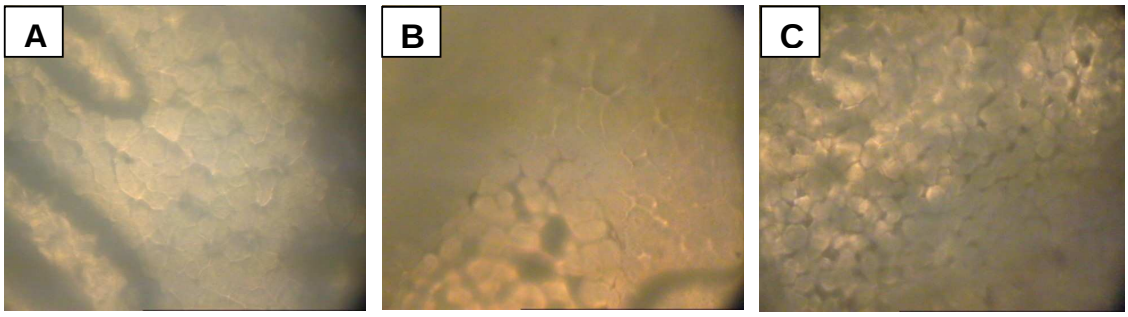

Figure 6.3: Optical micrographs of isotactic polypropylene fractions and their blend: A) Z5 (120), B) Z4 (120) and C) Z5(120)/Z4(120) blend (magnification: 5 x 10^2).

Figures 6.4 A, B and C show the OM micrograph of isotactic polypropylene (Z5), syndiotactic polypropylene (SPP1) and isotactic/syndiotactic polypropylene blend (Z5/SPP1) respectively. In general, syndiotactic polypropylene usually appears as needle-like entities (Figure 6.4 B), whereas for isotactic polypropylene, spherulites are usually observed.

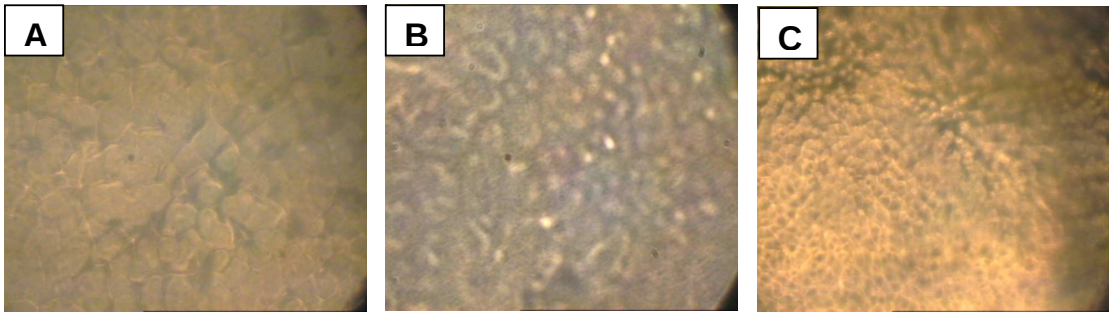

Figure 6.4: Optical micrographs of : A) isotactic polypropylene Z5, B) SPP1 and C) Z5/SPP1 (magnification: 5 x 10^2).

The presence of syndiotactic polypropylene appears to influence the growth and size of isotactic polypropylene spherulites, resulting in grainy crystal structure. As it is shown in Figure 6.4 C, for the blend, isotactic polypropylene spherulites are almost unable to be seen, indicating a decrease in the crystal size. The small and imperfect crystallites formed in the Z5/SPP1 blend are beneficial to promote the elasticity of isotactic/syndiotactic polypropylene blends. Similar results were reported in a number of articles.[19, 27-29]

6.3.1.2 Scanning electron microscopy analysis

SEM is a particularly well-suited instrument, especially since specific etchants have been developed which are capable of revealing the spherulite substructure. The structure of bulk samples of polypropylene can be investigated by simple SEM examination, at much higher magnification and with better resolution than when using the optical microscope.

Figures 6.5 A, B and C show SEM micrographs of the typical crystallization morphologies of the isotactic polypropylenes fractions Z5 (120), Z4 (120) and Z9 (110), respectively, which differ in their molecular weights. All these isotactic polypropylenes revealed well-defined and large spherulitic morphology, comprising a mixture of α1 (disordered) and α2 (ordered) crystal form structures. The spherulites grew, impinged on each other, and formed particular polygonal spherulites with clear boundaries. Moreover, one can clearly see the individual lamellae and lamellar branching structure in the SEM micrographs in Figure 6.5. The samples consist of crosshatch-type lamellar branching structures, which is the typical characteristic of the α crystal form of isotactic polypropylenes.[30,31] In contrast to OM results, clear differences can be distinguished between the three different isotactic polypropylene samples shown in Figure 6.5.

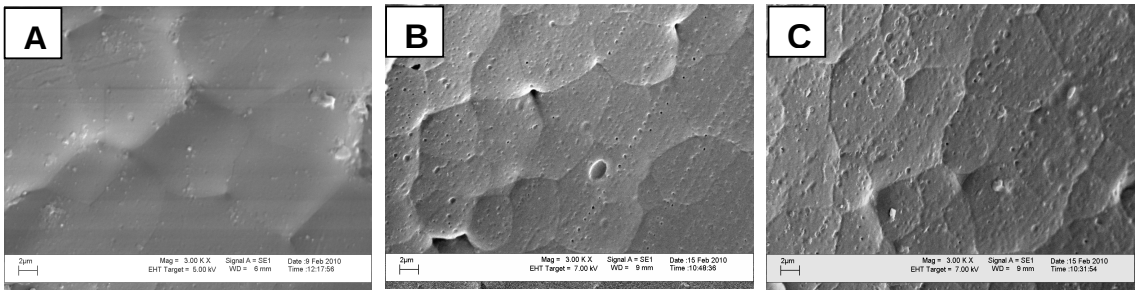

Figure 6.5: SEM micrographs of isotactic polypropylene fractions: A) Z5 (120), B) Z4 (120) and C) Z9 (110) (3000x magnification).

These exist in the variety of spherulite sizes and spherulite types classified by their appearance, including the sign and nature of birefringence and crystal lattice. The average diameter of Z5 (120) spherulites is about 5–15 μm (Figure 6.5 A). Smaller dominant α spherulites (about 5–10 μm) are observed for Z4 (120) and Z9 (110) (Figures B and C respectively).

Figures 6.6 A, B and C illustrate SEM micrographs of polypropylenes (Z5, Z4 and Z14) that differ in their tacticities (Table 6.1). Similar to those results obtained from OM above, SEM also showed in Figure 6.6 that the sizes of the spherulites were decreased drastically with decreasing tacticity. In addition, with decreasing tacticity, the spherulites showed less perfection and the sharp spherulite boundaries became more diffuse (Figure 6.6 C). The sample Z5 with 96.0% tacticity has the biggest spherulite sizes (15–25 μm) while samples Z4 and Z14 with 94.0 % and 86.0% tacticities have spherulite sizes about 5–15 and 1–3 μm respectively. SEM micrographs (Figures 6.6 A and B) also show that there are small dimples on the etched surface of samples Z5 and Z4 may grow to craters and holes. This is due to the extractions of the rubbery materials by the etchant solution.[21, 22, 32, 33]

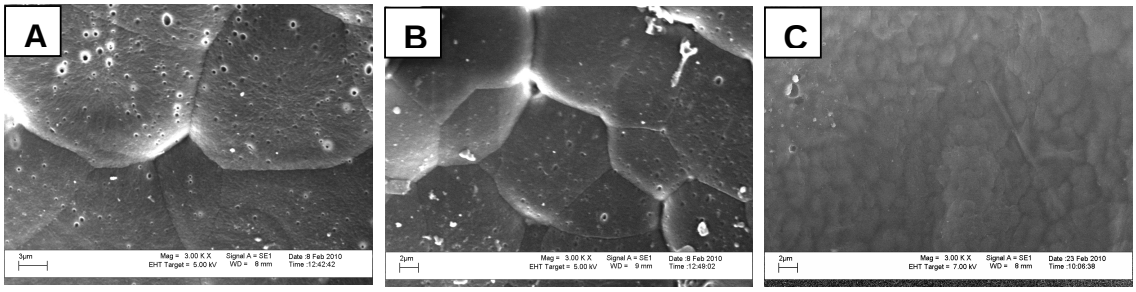

Figure 6.6: SEM micrographs of isotactic polypropylene polymers: A) Z5, B) Z4 and C) Z14 (3000x magnification).

Figure 6.7 C shows the SEM micrographs of isotactic polypropylene blend (Z5(120)/Z4(120)) of two different isotactic polypropylene fractions Z5 (120) and Z4 (120) (Figures 6.7 A and B). One can clearly see from Figures 6.7 A, B and C that the sign and nature of birefringence and crystal lattice of the α-spherulites of the blend are similar to those of the polypropylene fraction with higher molecular weight (Z5 (120) in Figure 6.7 A). In general, the blend has the same type of α-modification spherulite structure of isotactic polypropylenes which indicates that the two isotactic polypropylene fractions are miscible polymers.

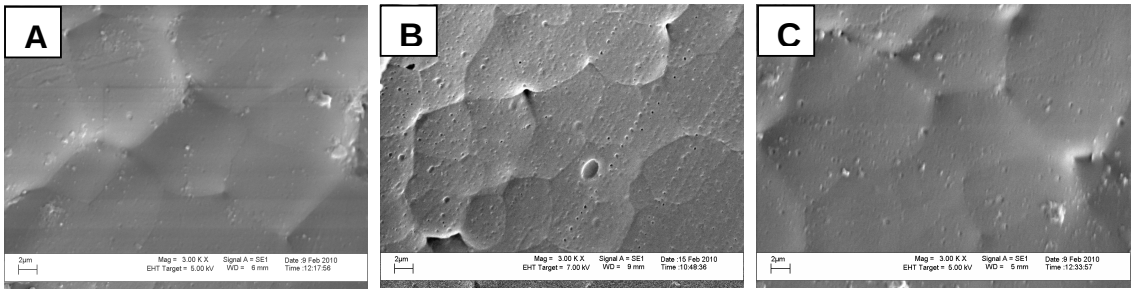

Figure 6.7: SEM micrographs of isotactic polypropylene fractions and their blend: A) Z5 (120), B) Z4 (120) and C) Z5(120)/Z4(120) blend (3000x magnification).

Figure 6.8 C shows the SEM micrograph of isotactic/syndiotactic polypropylene blend (Z5/SPP1) of isotactic polypropylene sample (Z5) (Figure 6.8 A) and syndiotactic polypropylene sample (SPP1) (Figure 6.8 C). As mentioned above in the OM results (Figure 6.4 C), the blend presents a grainy crystal structure. This indicates that the presence of syndiotactic polypropylene influences the growth and the size of isotactic polypropylene spherulites, which leads to less perfect spherulites.

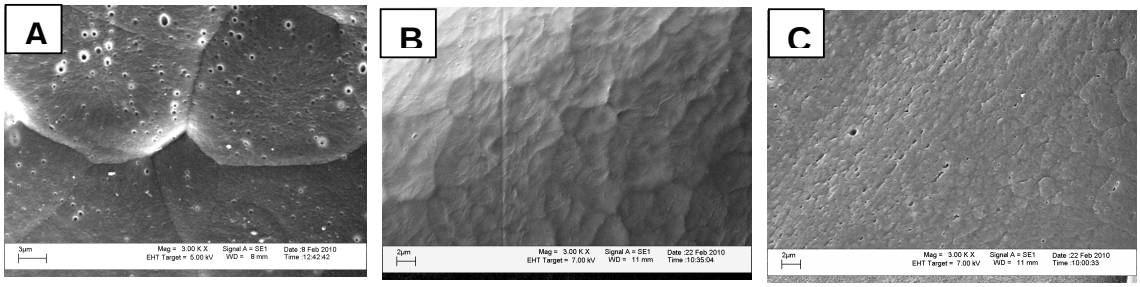

Figure 6.8: SEM micrographs of: A) Z5, B) SPP1 and C) Z5/SPP1 blend (3000x magnification).

6.3.2 Mechanical properties

In order to correlate the structure of the polypropylene homopolymers and polypropylene blends with the mechanical properties, the samples were analyzed using microhardness and DMA.

6.3.2.1 Microhardness

Microhardness (MH) is a significant mechanical magnitude in polymers. It indicates the resistance of a material to plastic deformation and, accordingly, provides an idea about local strain. MH involves a complex combination of properties (elastic modulus, yield strength, strain hardening, toughness). It is dependent upon structural parameters (molecular weight and degree of isotacticity) and thermal treatment.

According to literature,[34-37] all the parameters that lead to an increase of crystallinity and crystallite sizes (lamellar thickness) will also lead to higher MH values. Hence, the higher the isotacticity is the greater the MH values are found. The effect of the molecular weight and molecular weight distribution on the crystallinity of the polypropylene samples was investigated and results are illustrated in Figure 6.9.

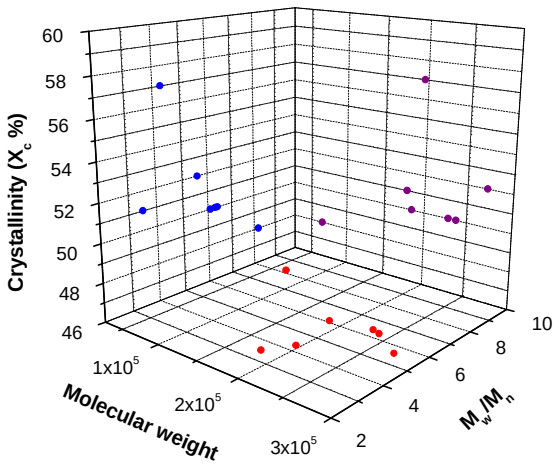

Figure 6.9: The effect of molecular weight and molecular weight distribution on the crystallinity of the isotactic polypropylene polymers.

The samples of low molecular weight generally have a broader molecular weight distribution, and vice versa. The molecular weight distribution has an effect on the crystallinity; the samples with a higher degree of crystallinity also have a lower molecular weight distribution, and samples with lower degree of crystallinity a have higher molecular weight distribution. On the other hand, there is a slight increase in the crystallinity of the samples with an increase in the molecular weight.

Figure 6.10 shows the combined effect of the molecular weight and isotacticity on the degree of crystallinity of the polypropylene samples. There is a remarkable increase in crystallinity as the isotacticity is increased, from about 93% to 98%. It is also notable that the samples with higher molecular weight have a higher isotacticity, as expected, since the more stereospecific sites have a higher propagation constant rate (K_p). This is in agreement with the results obtained by Sakurai *et al.*[38] with regards to the relationship between isotacticity and molecular weight. Moreover, Figures 6.9 and 6.10 show that the crystallinity of the samples was largely affected by the isotacticity, which clearly dominates over other effects such as molecular weight and molecular weight distributions. But molecular weight and molecular weight distributions do play a role when the isotacticity values are similar.

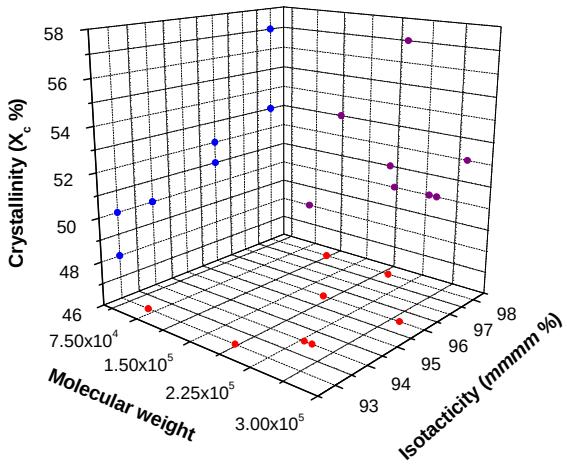

Figure 6.10: The combined effect of molecular weight and isotacticity on the crystallinity of the isotactic polypropylene polymers.

Looking at the combined effect of the molecular weight and crystallinity on the microhardness of the samples, as shown in Figure 6.11, generally one can see that there is a major increase in the MH with increasing molecular weight and crystallinity of the samples.

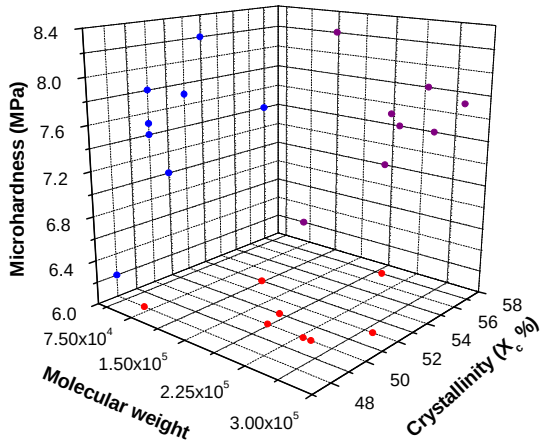

Figure 6.11: The combined effect of molecular weight and crystallinity on the microhardness of the isotactic polypropylene polymers.

Since that the most important factor affecting the crystallinity of these polypropylene polymers is the isotacticity content, the combined effect of the molecular weight and isotacticity on the MH of the samples is illustrated in Figure 6.12.

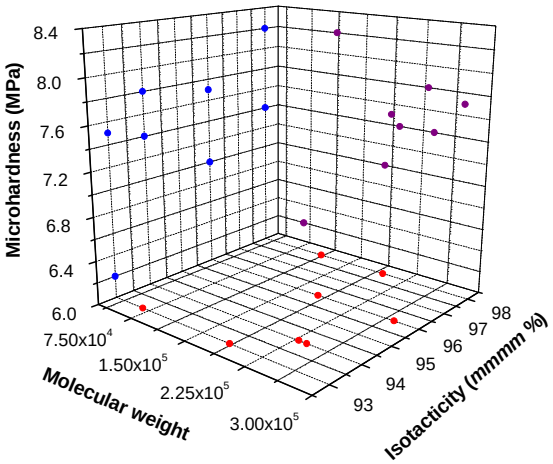

Figure 6.12: The combined effect of molecular weight and isotacticity on the microhardness of the isotactic polypropylene polymers.

It appears that there is a significant increase in the MH with increasing isotacticities of the samples. Hence, it can be said that the higher the isotacticity the greater the MH. This means

that the most important factors affecting the MH of these polypropylene homopolymers are those that lead to an increase of crystallinity. Accordingly, the main parameter effect the crystallinity can be considered as the isotacticity degree of the samples. It is reasonable that the higher isotacticity content allows easier recrystallization upon the application of an external force to the sample, thus improving the hardness of the sample upon indentation. The magnitude of the effect of the tacticity of the polypropylenes on the properties of the polymer has also been discussed by De Rosa *et al*.[39]

The results of the MH of different polypropylene blends (50/50 wt %) are shown in Table 6.2. According to Flores *et al.*,[37] MH of a polymer blend can be described in terms of an additive system of two independent components, as in the equation below.

$$MH_b = MH_1\,\phi + MH_2\,(1 - \phi)$$

where MH_b is the hardness of the blend and MH_1 and MH_2 are the hardness values of the single components and ϕ is the weight fraction of component 1. However, deviations from this equation may occur, depending on the variation in crystallinity of each phase in the blend. As can be seen in Table 6.2, the blends of the two different isotactic polypropylenes, Z3/Z17 and Z4/Z14 blends, have MH values between the values of the two homopolymers, which depend on the type and degree of the crystallinity of the blends.

Table 6.2: MH results of different polypropylene blends (50/50 wt %)

Sample	Hardness (HV 0.01)	*mmmm* %	M_w	M_w/M_n	X_c (%)
Z3	7.5	93.0	184 759	6.1	50.0
Z17	6.2	93.0	65 498	8.2	48.0
Z3/Z17 Blend	6.6	-	-	-	51.0
Z4	7.4	94.0	238 960	6.3	50.0
Z14	6.1	86.0	215 397	5.9	43.0
Z4/Z14 Blend	6.3	-	-	-	44.0
Z5	7.7	96.0	271 974	5.6	52.0
SPP1	4.2	93.0[a]	174 000	2.3	16.0
Z5/SPP1 Blend	4.8	-	-	-	36.2

[a] syndiotacticity (*rrrr* %)

It is also noteworthy that syndiotactic polypropylene sample (SPP1 in Table 6.2) has a low MH value, due to the low crystallinity degree and the different types of crystals. The presence of syndiotactic polypropylene in the Z5/SPP1 blend leads to a decrease the MH value of the

isotactic polypropylene sample Z5. This is due to a reduction in the growth and the size of isotactic polypropylene spherulites, which leads to less spherulite perfection, as shown in the OM and SEM results.

6.3.2.2 DMA

The DMA technique is often used to get an indication of the physical properties of samples. It is a very sensitive technique, and capable of detecting a number of different transitions and relaxations that take place in a material at a certain temperature. Semicrystalline polymers show several types of relaxation phenomena that can be detected by DMA. As a result of certain molecular motions, a storage modulus depression or a loss modulus peak appears on the mechanical relaxation curve. In the case of isotactic polypropylene, three different relaxation processes (γ, β and α) due to molecular motions can be observed from -50 °C to nearly the melting temperature.[40-43] However, only a few studies have focused on the influence of molecular weight and tacticity on the relaxation mechanisms of isotactic polypropylene.[4,35,44]

The α relaxation is associated with motion within the crystal phase of isotactic polypropylene. It has been reported that this relaxation is due to the diffusion of defects in the crystal.[45,46] However, links between crystalline and amorphous phases imply that the amorphous phase around crystallites also contributes to this process, and is induced by the migration of defects. The β relaxation has been known with the glass transition of the amorphous fraction of isotactic polypropylene, but it has been reported that interaction with the crystal phase is a variable to be considered. Eventually, the γ relaxation varies little with crystallinity. It has been attributed to local motions of methyl groups within the amorphous phase of isotactic polypropylene.[35,47]

6.3.2.2.1 Effect of molecular weight

Figure 6.13 shows the storage modulus of different isotactic polypropylene samples with different molecular weights, as a function in temperature. The storage modulus values practically increase with increasing molecular weight in the temperature range measured for the different samples. This is in agreement with the results obtained above from the microhardness test. Moreover, similar behaviour has been observed by other researchers.[4]

The reason for the increase in the storage modulus values with increasing molecular weight is due to the higher degree of crystallinity and the presence of a larger number of molecular weight entanglements per chain for the higher molecular weight polymers. Furthermore, an

increase in the lamellar thickness as the molecular weight increases also lead to higher storage modulus values.[4]

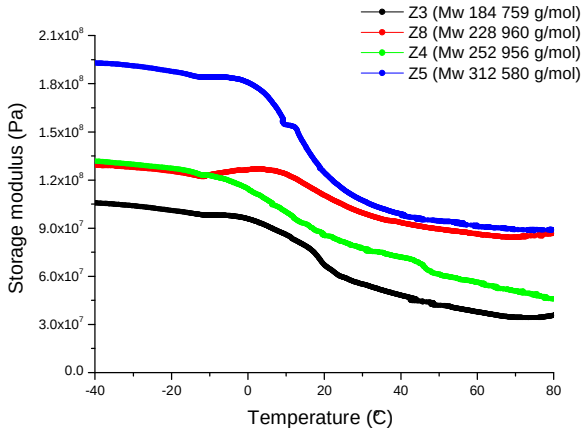

Figure 6.13: Storage modulus curves as a function of temperature for isotactic polypropylene samples with various molecular weights.

The detailed plot of tan δ of these isotactic polypropylene samples, as a function of the temperature, ranging from -40 to 80 °C is presented in Figure 6.14. Actually, the tan δ curves basically represent the ratio of the ability of the material to store and lose energy, which is sometimes referred to as the clamping ability of a material. It can also be taken as a measurement of the impact properties of the material. It is apparent from Figure 6.14 that β-transition, corresponding to the T_g of isotactic polypropylenes, which occurs over the temperature range 10–20 °C, is slightly shifted to a higher temperature as the molecular weight increases (from 16 °C for Z3 sample with M_w 184 759 g/mol to 20 °C for Z5 sample with M_w 312 580 g/mol). As that the samples with lower molecular weights are less crystalline and therefore contain more amorphous material. The explanation is that the chains have far greater mobility in the amorphous phase in the lower molecular weight samples compared to the samples with higher molecular weights. We do however also have to take into consideration the change in the molecular packing in the amorphous phase. Denser packing of the molecular chains leads to a reduction in the molecular motion.

The areas of the β-transitions of the samples, after subtraction of a linear baseline, are given in Figure 6.15. Figure 6.15 shows that the magnitude of the β-transition increases with increasing molecular weight. Similar results were obtained by Stern *et al.*,[4] who found that the higher molecular weight polymers are generally characterized by larger β-transition. In fact, a decrease in the mechanical transition of the β process is associated with a reduction in the mobility of the polymer chains in the amorphous phase.[4,46,48]

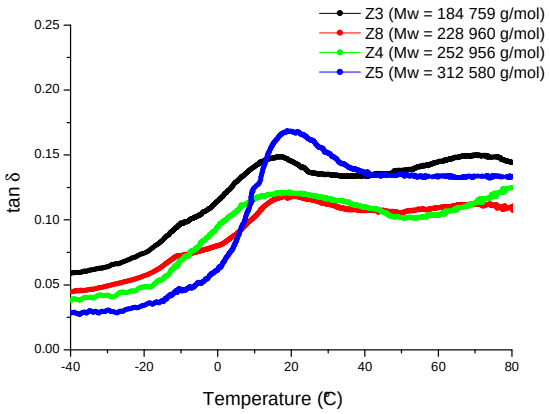

Figure 6.14: Tan δ curves as a function of temperature for isotactic polypropylene samples with various molecular weights.

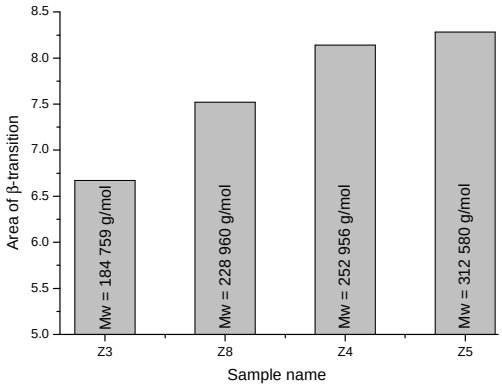

Figure 6.15: The magnitude of the area of the β-transition for isotactic polypropylene samples with various molecular weights.

6.3.2.2.2 Effect of isotacticity

Figure 6.16 shows the difference in the storage modulus curves as a function of temperature for isotactic polypropylene samples with various isotacticities. Compared to the results obtained from varying the molecular weight in Section 6.3.2.2.1, isotactity of isotactic polypropylene samples has further effect on the overall viscoelastic response as shown in Figure 6.16.

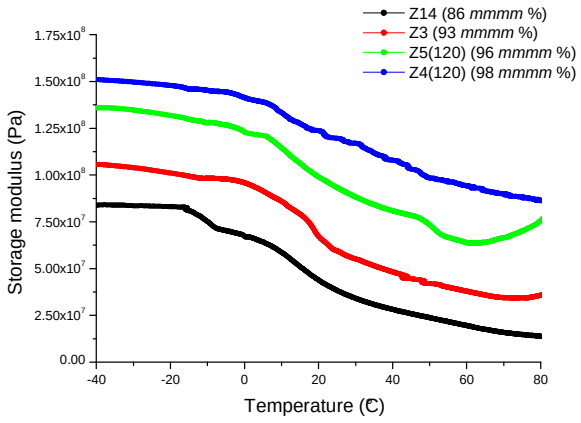

Figure 6.16: Storage modulus curves as a function of temperature for isotactic polypropylene samples with various isotacticities.

The storage modulus is greater in the higher isotactic polypropylene samples than in those with lower tacticity over the whole temperature range studied (1.51 x 10^8 Pa for Z4(120) with 98 *mmmm* % vs 0.84 x 10^8 Pa for Z14 with 86 *mmmm* %) as shown in Figure 6.16. Moreover, this effect is also observed in the location and intensity of the β-transition temperature, as shown in Figure 6.17. As the isotactic content increases, the location of the β-transition temperature is considerably shifted to higher temperatures but its intensity decreases significantly in the higher isotactic polypropylene fractions Z5(120) and Z4(120), as seen in Figure 6.18, which shows the areas of the β-transitions of the different samples.

All of these features can be associated with the higher degree of crystallinity that more regular chains can reach during their crystallization, i.e., as isotacticity is increased in the isotactic polypropylene macromolecules. Therefore, the lowest content of amorphous regions is in the Z4(120) sample, because its higher crystallinity (X_c = 57%, Table 6.1) leads to its higher storage modulus, a decrease in magnitude of the β-transition and the displacement of its

location to higher temperatures, due to the higher hindrance of motions within the crystalline phase.

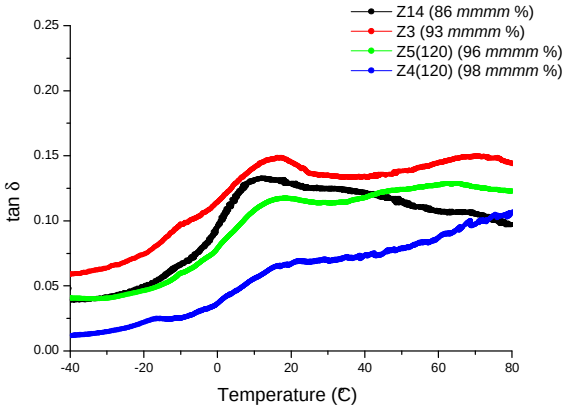

Figure 6.17: Tan δ curves as a function of temperature of isotactic polypropylene samples with various isotacticities.

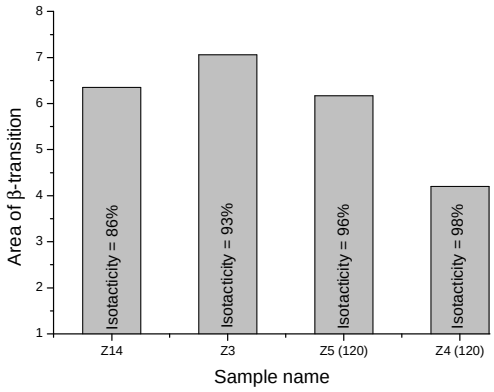

Figure 6.18: The magnitude of the area of the β-transition of isotactic polypropylene samples with various isotacticities.

6.3.2.2.3 DMA of blends

Figures 6.19 shows the storage modulus curves as a function of temperature for a 50/50 wt % blend of two different isotactic polypropylene samples. Figure 6.20 shows the storage modulus curves as a function of temperature for a 50/50 wt % blend of isotactic and syndiotactic polypropylene samples. Over the full temperature range of the experiment, the storage modulus curve of the blend of the two different isotactic polypropylenes is always

between the storage modulus curves of the two isotactic homopolymers, which indicates that the two isotactic polymers are miscible.

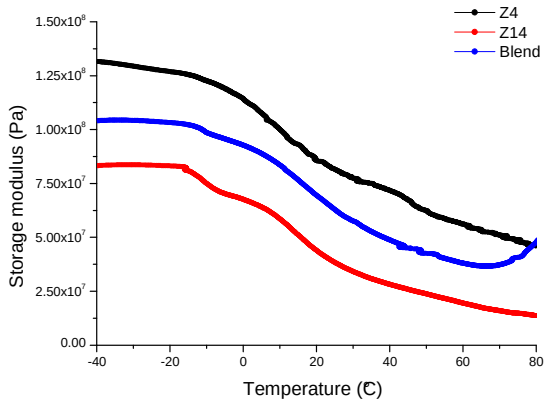

Figure 6.19: Storage modulus values as a function of temperature for a 50/50 wt% blend of two different isotactic polypropylene samples.

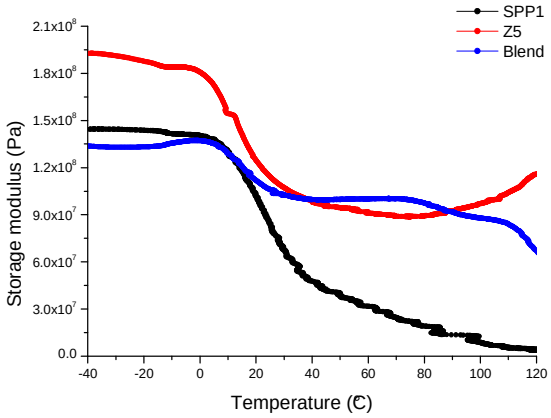

Figure 6.20: Storage modulus values as a function of temperature for a 50/50 wt% blend of isotactic and syndiotactic polypropylene samples.

On the other hand, the storage modulus curve of the isotactic/syndiotactic polypropylene blend in Figure 6.20 shows a different behaviour. Within the temperature range of -40 to 10 °C (below the T_g), the blend shows a lower storage modulus values than both polypropylene homopolymers. After that (above 10 °C) the storage modulus of the blend begins to have higher values than the storage modulus values of the syndiotactic polypropylene sample. This could be due to the partial miscibility of the isotactic and syndiotactic polymers at temperatures higher than their glass temperatures. Generally, and as shown above in the OM

and SEM results, the addition of syndiotactic polypropylene markedly destroys the isotactic polypropylene spherulites and creates defects in the isotactic polypropylene crystals, hence decreasing the crystallinity of the blends, and leading to the decrease of storage modulus values for the isotactic/syndiotactic polypropylene blends.

6.4 Conclusions

OM results showed that, all isotactic polypropylene samples had well-defined α-spherulitic morphology. Molecular weight had same effect on the morphology of the polymers, which was attributed to the morphological differences in the sign and magnitude of the birefringence, and spherulite texture of the polypropylene samples. OM results also showed that tacticity had a graeter effect on the morphological structure of the isotactic polypropylenes. The decrease in isotacticity leads to a clear decrease in the dimensions of the crystal structures for the different isotactic polypropylene samples. Furthermore, OM indicated that the blends of two different isotactic polypropylene samples are good miscible polymers, while the blends of isotactic/syndiotactic polypropylene samples are immiscible polymers.

SEM analysis showed that the various isotactic polypropylenes presented well-defined and large spherulitic morphology comprising mixture of α1 (disordered) and α2 (ordered) crystal form structures. Moreover, by using SEM analysis it was possible to visualize the individual lamellae and lamellar branching structure. Similar to the results obtained from OM analysis, SEM also showed that there is a clear effect of molecular weight and tacticity on the crystal structure of the various polypropylene samples. For instance, SEM images showed that the sizes of the spherulites were decreased drastically with decreasing tacticity. In addition, with decreasing tacticity the spherulites showed less perfection, and the sharp spherulite boundaries became more diffuse.

Results of the MH test showed that, all the parameters that lead to an increase in crystallinity and crystallite sizes (lamellar thickness) will provide higher MH values. The crystallinity of the samples was shown to be clearly related to the molecular weight and molecular weight distribution, as well as to the isotacticity of the samples. Higher molecular weights, narrower molecular weight distributions and higher isotacticities improved the crystallinity of the polypropylene samples. The molecular weight and crystallinity both had an effect on the MH. The harder samples generally comprised more crystalline material of a higher molecular weight. However, the property found to affect the MH the most was the isotacticity of the

samples. Samples with higher isotacticity had higher MH values. Results of the MH tests also showed that blends of two different isotactic polypropylenes presented MH values between the values of the respective two MH values of the homopolymer samples, which depended on the type and degree of the crystallinity of the blends. Moreover, MH tests showed syndiotactic polypropylene has a low MH value due to the low crystallinity degree and the different types of crystals. The presence of syndiotactic polypropylene in a blend with isotactic polypropylene leads to a decrease in the MH value of the isotactic polypropylene samples. This is due to the reduced growth and size of isotactic polypropylene spherulites, which leads to less spherulite perfection, as evident in OM and SEM results.

DMA analysis showed that the storage modulus and β-transition temperature values practically increased with increasing molecular weight and isotacticity over the temperature range measured for the different samples. This is in agreement with the results obtained from the MH tests. The reason for the increasing storage modulus values with increasing the molecular weight and isotacticity is the higher degree of crystallinity and the presence of a larger number of molecular weight entanglements per chain for the higher molecular weight polymers. Furthermore, an increase in the lamellar thickness as the molecular weight increases also leads to higher storage modulus values.

Reference

1. M. Lima, M. Vasconcellos, D. Samios, *J. Polym. Sci., Part B: Polym. Phys*. **2002**, 40, 896.
2. T. Asano, C. Balta, A. Flores, M. Tanigaki, M. Mina, C. Sawatari, *Polymer* **1999**, 40, 6475.
3. E. Bedia, S. Murakami, T. Kitade, S. Kohjiya, *Polymer* **2001**, 42, 7299.
4. C. Stern, A. Frick, G. Weickert, *J. Appl. Polym. Sci*. **2007**, 103, 519.
5. D. Samios, S. Tokumoto, E. Denardin, *Int. J. Plast*. **2006**, 22, 1924.
6. C. De Rosa, F. Auriemma, *J. Am. Chem. Soc*. **2006**, 128, 11024.
7. Z. Wang, R. Phillips, B. Hsiao, *J. Polym. Sci., Part B: Polym. Phys*. **2000**, 38, 2580.
8. R. Phillips, *J. Polym. Sci., Part B: Polym. Phys*. **2000**, 38, 1947.
9. Z. Wang, R. Phillips, B. Hsiao, *J. Polym. Sci., Part B: Polym. Phys*. **2001**, 39, 1876.
10. T. Foresta, S. Piccarolo, G. Goldbeck-Wood, *Polymer* **2001**, 42, 1167.
11. J. Torre, M. Cortazar, M. Gomez, G. Ellis, C. Marco, *J. Polym. Sci., Part B: Polym. Phys*. **2004**, 42, 1949.
12. R. Silvestri, P. Sgarzi, *Polymer* **1998**, 39, 5871.
13. R. Phillips, R. Jones, *Macromol. Chem. Phys*. **1999**, 200, 1912.
14. J. Li, R. Shanks, Y. Long, *J. Appl. Polym. Sci.* **2001**, 82, 628.
15. J. Chen, F. Tsai, Y. Nien, P. Yeh, *Polymer* **2005**, 46, 5680.
16. R. Maier, R. Thomann, J. Kressler, R. Mulhaupt, B. Rudolf, *J. Polym. Sci., Part B: Polym. Phys*. **1997**, 35, 1135.

17. M. Hill, R. Morgan, P. Barham, *Polymer* **1997**, 38, 3003.
18. R. Silvestri, P. Sgarzi, *Polymer* **1998**, 39, 5871.
19. R. Thomann, J. Kressler, S. Setz, C. Wang, R. Mülhaupt, *Polymer* **1996**, 37, 2627.
20. R. Olley, A. Hodge, D. Bassett, *J. Polym. Sci., Part B: Polym. Phys*. **1979**, 17, 627.
21. A. Freedman. D. Bassett, A. Vaughan, R. Olley, *Polymer* **1986**, 27, 1163.
22. R. Olley, *Sci. Prog*. **1986**, 70, 17.
23. M. Aboulfaraj, B. Ulrich, A. dahoun, C. Gsell, *Polymer* **1993**, 34, 4817.
24. B. Lotz, J. Wittmann, A. Lovinger, *Polymer* **1996**, 37, 4979.
25. D. Morrow, B. Newman, *J. Appl. Phys*. **1968**, 39, 4944.
26. F. van der Burgt, Crystallization of isotactic polypropylene: The influence of stereo-defects, Masters thesis, Technical University of Eindhoven, **2002**, p. 34.
27. R. Thomann, J. Kressler, B. Rudolf, R. Mulhaupt, *Polymer* **1996**, 37, 2635.
28. Z. Wang, R. Phillips, B. Hsiao, *J. Polym. Sci., Part B: Polym. Phys*. **2001**, 39, 1876.
29. X. Zhang, Y. Zhao, Z. Wang, C. Zheng, X. Dong, Z. Su, P. Sun, D. Wang, C. Han, D. Xu, *Polymer* **2005**, 46, 5956.
30. J. Park, K. Eom, O. Kwon, S. Woo, *Microsc. Microanal*. **2001**, 7, 276.
31. J. Wang, Q. Dou, *Colloid. Polym. Sci*. **2008**, 286, 699.
32. R. Olley. D. Bassett, *Polymer* **1982**, 23, 1707.
33. F. Rybnikar, *J. Appl. Polym. Sci*. **1985**, 30, 1949.
34. S. Seidler, T. Koch, *J. Macromol. Sci., Part B: Phys*. **2002**, B41, 851.
35. J. Andres, B. Pena, R. Benavente, E. Perez, M. Cerrada, *Eur. Polym. J*. **2007**, 43, 2357.
36. T. Koch, S. Seidler, E. Halwax, S. Bernstorff, *J. Mater. Sci*. **2007**, 42, 5318.
37. A. Flores J. Aurrekoetxea, R. Gensler, H. Kausch, F. Calleja, *Colloid. Polym. Sci*. **1998**, 276, 786.
38. I. Sakurai, Y. Nozue, T. Kasahara, K. Mizunuma, N. Yamaguchi, K. Tashiro, Y. Amemiya, *Polymer* **2005**, 46, 8846.
39. C. De Rosa, F. Auriemma, A. Di Capua, L. Resconi, S. Guidotti, I. Camuratie, I. Nifantev, I. Laishevtsev, *J. Amer. Chem. Soc*. **2004**, 126, 17040.
40. S. Mansel, E. Perez, R. Benavente, J. Perena, A. Bello, W. Roll, *Macromol. Chem. Phys*. **1999**, 200, 1292.
41. J. Sauer, R. Wall, N. Fuschillo, A. Woodward, *J. Appl. Phys*. **1958**, 29, 1385.
42. S. Turley, H. Keskkula, *J. Appl. Polym. Sci*. **1965**, 9, 2693.
43. R. Benavente, J. Perena, A. Bello, E. Perez, P. Locatelli, Z. Fan, *Polym. Bull*. **1996**, 36, 249.
44. H. Palza, J. Lopez-Majada, R. Quijada, R. Benavente, E. Perez, M. Cerrada, *Macromol. Chem. Phys*. **2005**, 206, 1221.
45. J. Skinner, P. Wolynes, *J. Chem. Phys*. **1980**, 73, 4022.
46. C. Jourdan, J. Cavaille, J. Perez, *J. Polym. Sci., Part: B Polym. Phys*. **1989**, 27, 2361.
47. O. Prieto, J. Perena, R. Benavente, E. Perez, M. Cerrada, *J. Polym. Sci., Part: B Polym. Phys*. **2003**, 41, 1878.
48. M. Pluta, Z. Bartczak, A. Galeski, *Polymer* **2000**, 41, 2271.

CHAPTER 7

Synopsis and conclusions

By using Ziegler-Natta and metallocene catalyst systems under different conditions it was possible to produce polymer samples of a wide variation in tacticity and molecular weight. Preparative TREF allowed us to produce polymer fractions of well defined structure in terms of molecular weight and molecular weight distributions, as well as tacticity. Furthermore, it is obvious that the polymerization conditions play a major role in the production of materials with distinct differences in their composition. There are a number of different ways to control the composition of the polymers produced by these different catalysts, and that therefore the microstructure of the properties can be tailored via the polymerization conditions to obtain polymers with certain characteristics. The conditions can essentially be tailored to adapt a certain application for which the material is required.

Firstly and with regarding to the use of molecular hydrogen as a terminating agent to control the molecular weights of the produced polymers, a decrease in molecular weight with increasing hydrogen amount was observed and it is noted that the addition of a small amount of hydrogen can cause a significant drop in the molecular weight of the chains. A sharp increase in the degree of crystallinity of the chains was also noticed upon increasing the amount of hydrogen, most likely due to the lower molecular weight which makes the motion of chain molecules easier allowing the reorganization of the chains in order to crystallize more perfectly. It is also possible that the tacticity of the chains could have improved slightly as the amount of hydrogen was increased in case of Ziegler-Natta polymers, while the isotacticity of the polypropylenes produced metallocene catalysts was slightly reduced.

The effect of the type of electron donor on Ziegler-Natta catalysts was also investigated. In general we can say that the presence of electron donors in $MgC1_2$-supported catalyst systems for polypropylene polymerizations play an essential role in determining not only isotacticity but also polymer yield, molecular weight and molecular weight distribution. These factors are interrelated and to a large extent are dependent on the regio- and stereoselectivity of the active species, which can change during chain growth depending on the nature of donor coordination in the environment of the active species. In general, the isotactic stereoregularity of the

polymers produced in the presence of the EDs (DPDMS and MPDMS) indicates a high proportion of isotactoid sequences. It is likely that the EDs are more easily displaced from the catalyst surface, giving a relatively labile coordination. This possibly will lead to the formation of high isospecific active sites on the catalyst surface. Moreover, it is noted that differences in the type of ED and amount of hydrogen clearly result in differences in the microstructure of the produced polymers.

TREF was efficiently used to fractionate polypropylene polymers into different amounts of fractions desired, depending on the minimum weight of the fractions needed for the necessary analyses. TREF gave a good recovery percentage of above 99 wt %. TREF fractionation of the polypropylene samples produced by Ziegler-Natta catalysts in the presence of EDs were eluted mainly at 110 ℃ and 120 ℃ fraction while the polypropylene samples produced using metallocene catalysts were eluted at mainly the 80 ℃ and 90 ℃ fractions. Furthermore, the weight fraction results showed that polymers produced using Ziegler-Natta catalysts have significantly lower weight percentage fractions for the room temperature fraction than those produced by metallocene catalysts. In general, the molecular weight and the isotacticity of the TREF fractions are all increased significantly with increasing the elution temperature for all samples produced using Ziegler-Natta and metallocene catalysts. This is a clear sign that the molecular weight plays a significant task in the fractionation mechanism of TREF. There are fractions present with negligible differences in *mmmm* pentad content which elute in consecutive fractions. In case of the polydispersity of the TREF fractions, it was clear that the lower temperature fractions have a broader distribution of molecular weight chains than the higher temperature fractions. Overall, the polydispersity of the TREF fractions of all fractions tends to decrease as the elution temperature increases. The values are all relatively low (exception being the 25 ℃ fraction which has high polydispersity) as one would expect from TREF fractions where small sections of a polymer are isolated. Generally, the thermal properties in terms of T_c, T_m and degree of crystallinity of the TREF fractions improved with fractionation temperature up to 120 ℃ and 100 ℃ fractions for all fractions produced using Ziegler-Natta and metallocene catalysts respectively, after which there was a slight decreases in the properties due to the co-crystallization of material trapped during the TREF crystallization process.

For syndiotactic polypropylene sample SPP1, molecular weight, syndiotacticity, melting temperature and degree of crystallinity of the TREF fractions are all increased to some extent with increasing the elution temperature which is similar to isotactic polypropylene samples.

The only distinguish difference of syndiotactic TREF fractions on the isotactic TREF fractions is the multi-melting peaks which are observed in all TREF fractions.

Furthermore, X-ray diffraction showed that only α crystal form existed in all TREF fractions of different samples. The main difference is being the strong diffraction of these peaks, which depends on the crystallinity content of each fraction.

The bulk crystallization of all different polypropylene blends was done by DSC. DSC showed only one melting peak of all isotactic polypropylene blends, which indicates that that cocrystallization of the blends occurred. Although single melting peaks of blends are usually associated with a high extent of cocrystallization, two broad overlapping distributions of thicknesses of separate crystals, one from each component, could also lead to single broad endotherms. This leads us to believe that the crystallization behavior of the polymer blends in the bulk is strongly affected by the configuration (tacticity) and molecular weight of the polypropylene polymers. On the other hand, turbidity analysis of different polypropylene polymers using solution crystallization analysis by laser light scattering can provide good crystallization information that is similar to CRYSTAF and TREF. In a SCALLS experiment, the turbidity of a polymer solution is mentored while changing its temperature at a controlled rate. The resulting turbidity profile represents the precipitation or dissolution of the crystallized polymer at a given temperature. In this study, it was possible to differentiate between polypropylenes with similar chemical structure but different tacticity and molecular weight. Furthermore, SCALLS showed that the blends of different isotactic polypropylene polymers are miscible and cocrystallization occurred, whereas, the blends of syndiotactic polypropylene and different isotactic polypropylenes were not miscible and some interaction between phases occurred. In addition, SCALLS can be used as a quantitative tool for the measurement of weight fractions during dissolution.

With regards to OM and SEM results, all different isotactic polypropylenes revealed well-defined and large spherulitic morphology of a mixed of α1 (disordered) and α2 (ordered) crystal form structures. Moreover, by using SEM analysis it was able to observe and visualize the individual lamellae and lamellar branching structure. OM and SEM images also showed that there is a clear effect of molecular weight and tacticity on the crystal structure of the different polypropylene samples. For instance, SEM images showed that the sizes of the spherulites were decreased drastically with decreasing tacticity, also with decreasing tacticity, the spherulites showed less perfection and the sharp spherulite boundaries became more diffuse. In addition, OM indicated that the blends of two different isotactic polypropylene

samples are good miscible polymers while the blends of isotactic/syndiotactic polypropylene samples are immiscible polymers.

According to the results that were obtained from the MH testing, all the parameters that lead to an increase of crystallinity and crystallite sizes (lamellar thickness) will provide higher MH values. The crystallinity of the samples was shown to be clearly related to the molecular weight and molecular weight distribution as well as the isotacticity of the samples. Higher molecular weights, narrower molecular weight distributions, and higher isotacticities improved the crystallinity of the polypropylene samples. The molecular weight and crystallinity both show an effect on the MH, in this sense, the harder samples generally consisting of more crystalline material of a higher molecular weight. However, the most property was found to affect the MH was the isotacticity of the samples, where the samples with higher isotacticity had higher MH values. In addition, the MH test showed that the blends of two different isotactic polypropylenes presented MH values in between the two MH values of the homopolymer samples, which dependence on the type and degree of the crystallinity of the blends. Moreover, MH testing showed that syndiotactic polypropylene sample has a low MH value which is due to the low degree of crystallinity and the different type of crystals. The presence of syndiotactic polypropylene in a blend with isotactic polypropylene samples leads to decrease the MH value of the isotactic polypropylene samples. This is due to the reducing the growth and the size of isotactic polypropylene spherulites, which leads to less spherulites perfection as shown in OM and SEM results.

DMA analysis showed that the storage modulus and β-transition temperature values practically increased with increasing molecular weight and isotacticity in the temperature range measured for the different samples. This is in agreement with the results were obtained from the MH test. The reason for the increasing of the storage modulus values with increasing the molecular weight and isotacticity is due to the higher degree in the crystallinity and the presence of larger number of molecular weight entanglements per chain for the higher molecular weight polymers, in addition, an increase in the lamellar thickness as the molecular weight increases also lead to higher storage modulus values.